The role of the NF-kappaB pathway in Amyotrophic lateral sclerosis pathogenesis

Emma Charlotta KÄLLSTIG

École
polytechnique
fédérale
de Lausanne

2023

Acknowledgements

There are many people I would like to thank for their support and help during my PhD. First of all, my thesis supervisors, Dr. Bernard Schneider and Prof. Brian McCabe, for their guidance, advice, and scientific discussions. They have both helped me grow as a scientist, and I am very grateful for their support.

I would also like to thank the members of my thesis jury, Prof. Johannes Gräff, Prof. Bruno Lemaitre, Prof. Rosa Paolicelli, and Prof. Emi Nagoshi, for taking the time to evaluate and improve my thesis.

A big thank you to all the past and present members of the McCabe lab – everyone has been happy to help when I have had questions. A special thank you to Wei, who taught me everything from fly pushing to what the Imd pathway is, and read this thesis. Evelyne, who always takes the time to help and who has been with me and advised me through all the cloning problems imaginable. Marine and Greta, research and coffee breaks are much more fun when we do it together in our ALS team. Thank you for all the help and support. Sam, thanks for all of the science and life talks in our corner of the lab and for taking the time to read this thesis.

I would also like to express my gratitude to the current and past members of the LEN/PTBTG lab. I really appreciate the fact that everyone in the lab is always open to answer questions and help out. In particular I would like to thank Philippe, who has taught me everything about mouse handling, ICV injections, and behavioral experiments, and who has had a French-English tandem with me.

A big thank you to all my friends who have supported me throughout my PhD, both in Switzerland and Sweden. Alina and Eleanor, thanks for sharing the PhD ups and downs. Thank you to Evelyne and Wei for inviting me to join the climbing group, and to everyone else in it. I would also like to thank Scott and Mirren, for our Gloomhaven (and soon Frosthaven) days, which have been a perfect PhD distraction. Thank you to Hanna, who has supported me from home, and my friends from Lund: Johanna, Julia, Frida, Emelie, and Turid. And of course, thank you to Alex, who has taken the time to learn more about the NF-κB pathway than I think he ever wanted to know.

Finally, thank you to my family for their love and support. My sister, who is always there for me, and my parents, who continue to encourage me and support any idea I may have. Jag älskar er!

Summary

Amyotrophic lateral sclerosis (ALS) is a neurodegenerative motor disorder, which results in death within a few years of diagnosis. While the cause of most cases of ALS is unknown, 10% of cases are familial (fALS), and associated with mutations in one of over 25 genes (Renton et al., 2014). Several lines of evidence suggest alterations of neuroinflammatory factors in both ALS patients and animal models (Henkel et al., 2006; Kuhle et al., 2009; Mishra et al., 2016). Among these altered factors are the nuclear factor kappa-light-chain enhancer of activated B cells (NF-κB) proteins, which becomes progressively activated in cells such as astrocytes and microglia (Crosio et al., 2011; Frakes et al., 2014).

This thesis describes the generation of novel genome engineered fALS animal models and utilization of these models to interrogate the connection between the NF-κB pathway and ALS pathogenesis. We generate gene replacement 'humanized' fALS *Drosophila melanogaster* models by introducing either human TAR DNA-binding protein 43 (hTDP-43) or human Fused in Sarcoma (hFUS), with or without ALS-associated mutations, into the *Drosophila* genome, removing and replacing the respective *Drosophila* homologous coding regions while maintaining host regulatory sequences. We find that gene replacement with hFUS wild-type or TDP-43 wild-type sequences can fully rescue development deficits of orthologous *Drosophila* gene knockouts, and allows longevity, motor behavior, and synapse morphology similar to controls. Surprisingly, we also observe no or very modest motor phenotypes in models where hFUS and hTDP-43 sequences including ALS mutations. We speculate that these ALS-associated mutations create a predisposition to disease that requires additional environmental factors to develop ALS pathology.

To identify these factors, we utilized loss-of-function alleles of *Drosophila* TDP-43 or FUS to examine potential interactions between FUS, TDP-43 and NF-κB signaling. We observe a significant rescue of adult survival of TDP-43-/- and FUS-/- mutant *Drosophila* by reducing the gene dosage of NF-κB components. Building on the hypothesis that excessive activation of the NF-κB pathway in ALS-associated mutants could induce disease pathology, we investigated if bacterial infection, which activates the NF-κB pathway, could trigger disease in our models. However, we observed that hTDP-43 and hFUS ALS mutant longevity and motor behavior were not more susceptible to infection than controls. We conclude that peripheral bacterial infection is not sufficient to induce ALS-like symptoms in our humanized models.

To interrogate the potential of NF-κB as a therapeutic target in rodent ALS models, we expressed NF-κB inhibitors using viral vectors in the SOD1^{G93A} ALS mouse model. Unfortunately, we observed no improvements in motor behavior or electromyographical measurements by this treatment. However, we did observe increased CNS resident macrophages in ALS mouse models compared to controls, which we speculate may be necessary to target. In sum, our results identify a potent interaction between FUS, TDP-43 and NF-κB signaling, that support the potential of this pathway as an ALS therapeutic target, but also caution that the relationship is complex and involves the intersection of several CNS cell types.

Key words: Amyotrophic lateral sclerosis, NF-κB, Fused in Sarcoma, TAR DNA-binding protein 43, Superoxide dismutase-1

Résumé

La sclérose latérale amyotrophique (SLA) est une maladie neurodégénérative dévastatrice, provoquant la mort dans les quelques années suivant le diagnostic, et l'incidence de la SLA devrait augmenter dans le futur (Arthur et al., 2016). Bien que la cause soit inconnue, 10% des cas sont héréditaires et attribués à des mutations dans l'un des plus de 25 gènes liés à la SLA familiale (fALS) (Renton et al., 2014). Des facteurs neuroinflammatoires sont ont été découverts chez les patients atteints de SLA, ainsi que dans les modèles animaux (Henkel et al., 2006 ; Kuhle et al., 2009 ; Mishra et al., 2016). Parmi ces derniers figurent les protéines de la voie métabolique the nuclear factor kappa-light-chain enhancer of activated B cells (NF-κB), qui sont graduellement activées dans les astrocytes et la microglie les patients, comme dans les modèles animaux (Crosio et al., 2011 ; Frakes et al., 2014). Cette thèse se concentre sur la création de nouveaux modèles de la SLA et sur la comprhéension des méchanismes qui lient la voie immunitaire NF-κB à la maladie de la SLA.

Dans les deux premiers chapitres de cette thèse, nous générons des modèles de SLA chez *Drosophila melanogaster* exprimant soit la protéine humaine TAR DNA-binding protein 43 (hTDP-43), soit la protéine humaine Fused in Sarcoma (hFUS), avec ou sans mutations pathogènes liées à la SLA, remplaçant ainsi leurs orthologues respectifs. Les précédents modèles de la SLA à base de TDP-43 et de FUS étaient basés sur l'hypothèse d'une perte ou d'un gain de fonction, cependant nous avons voulu exprimer les protéines en utilisant le promoteur endogène afin de refléter plus fidèlement la condition des patients. Nous constatons que l'expression endogène de hFUS ou hTDP-43 de type sauvage peut contrer les déficits de développement. La longévité, la motricité ainsi que la morphologie des jonctions neuromusculaires, restent comparables au contrôle. De manière surprenante, nous observons des phénotypes de la SLA légers ou inexistants chez les mutants hFUS et hTDP-43, suggérant qu'un déclencheur supplémentaire peut être nécessaire pour induire la pathologie de la SLA.

Comme nous émettons l'hypothèse qu'une voie NF-κB hyperactive peut causer la SLA, nous avons cherché à savoir si l'activation de la réponse immunitaire NF-κB chez les mouches humanisées FUS et TDP-43 par une infection bactérienne pouvait servir de déclencheur. Cependant, nous observons que la longévité et le comportement moteur des mutants hTDP-43 et hFUS ALS ne sont pas plus sensibles à l'infection que les témoins.

Afin d'étudier davantage le potentiel de NF-κB comme cible thérapeutique, nous avons

injecté des vecteurs AAV exprimant des inhibiteurs de NF-κB dans le modèle de souris surexprimant SOD1^{G93A} précédemment établi et avons évalué leurs effets sur la pathologie de la SLA. Malheureusement, nous n'avons observé aucune amélioration du comportement moteur ou du potentiel d'action musculaire combiné. Cependant, nous avons pu détecter la présence de macrophages activés dans la moelle épinière SOD1^{G93A} non traitée mais étant absents des contrôles. Nous supposons qu'il s'agit de macrophages résidents du SNC. Pour les traitements futurs, nous pensons qu'il pourrait être judicieux de cibler la voie NF-κB dans ces cellules.

Mots clés : Sclérose latérale amyotrophique, NF-κB, Fused in Sarcoma, TAR DNA-binding protein 43, Superoxide dismutase-1

Contents

List of Figures

Abbreviations

AAV	Adeno-associated virus
AMP	Antimicrobial peptide
BMAA	Beta-Methylamino-L-alanine
c9orf72	Chromosome 9 Open Reading Frame 72
Caz	Cabeza
CBA	Chicken beta actin
CMAP	Compound muscle action potential
DIF	Dorsal-related immunity factor
ECC15	*Erwinia carotovora carotovora* 15
fALS	Familial ALS
FUS	Fused in Sarcoma
hSyn1	Human synapsin 1
IκBα	Nuclear factor of kappa light polypeptide gene enhancer in B-cells inhibitor, alpha
IFNγ	Interferon gamma
IKK complex	IkappaB kinase complex
Imd pathway	Immune deficiency pathway
Key	Kenny
LPS	Lipopolysaccharide
MHC-II	Major histocompatibility complex class II
NEMO	NF-κB regulatory modifier
NF-κB	Nuclear factor kappa-light-chain enhancer of activated B cells
NLS	Nuclear localization signal
OPTN	Optineurin
PGRP-LC	Peptidoglycan recognition protein LC
Rel	Relish
RIPK1	Receptor-interacting serine/threonine-protein kinase 1
sALS	Sporadic ALS
SOD1	Superoxide Dismutase 1
SR	Superrepressor
TAK1	TGF-beta activated kinase 1
TBK1	TANK-binding kinase 1

TBPH	TAR DNA-binding protein-43 homolog
TDP-43	TAR DNA-binding protein 43
TNFα	Tumor necrosis factor alpha
VGLUT	Vesicular glutamate transporter

1

Chapter 1 - Introduction

- -
This chapter borrows from the review article:

Källstig, E., McCabe, B.D., Schneider, B.L., 2021. The Links between ALS and NF-κB. International Journal of Molecular Sciences 22, 3875. https://doi.org/10.3390/ijms22083875

1.1 ALS

Amyotrophic lateral sclerosis (ALS), also known as Lou Gehrig's disease, Charcot disease or sometimes Motor Neuron Disease (MND), is a neurodegenerative disorder described in 1874 by French neurologist Jean-Martin Charcot (Kumar et al., 2011). It affects the motor system and leads to degeneration of motor neurons in the cerebral motor cortex, in addition to the brainstem and spinal cord (Rowland and Shneider, 2001). The consequent disruption of communication between the nervous system and skeletal muscles initially results in a characteristic pattern of muscular weakness and spasticity (Wijesekera and Leigh, 2009). As the denervation of muscles advances, patients develop paralysis and a majority will die due to respiratory failure within 3-5 years of diagnosis.

Today, the annual incidence of ALS in a general European population is measured as 2.16 cases per 100 000 people, and is projected to increase in the future (Arthur et al., 2016; Logroscino et al., 2010). Approximately 10% of ALS cases are attributed to inherited familial mutations in more than 25 different genes including: Chromosome 9 Open Reading Frame 72 (c9orf72), Superoxide Dismutase 1 (SOD1), TAR DNA-binding protein 43 (TDP-43), Fused in Sarcoma (FUS), Optineurin (OPTN), and TANK-binding kinase 1 (TBK1) (Renton et al., 2014). The remaining majority of cases are considered as 'sporadic' and their etiology is still poorly defined.

1.1.1 Neuroinflammation in ALS

Neuroinflammation has become an increasingly important factor underlying the cell-specific neurodegeneration observed in many diseases of the central nervous system (CNS), including ALS. Elevated levels of proinflammatory cytokines as well as activation of microglia and astrocytes have been observed in Alzheimer's disease, Parkinson's disease and Multiple Sclerosis, to name a few (Fakhoury, 2018; Ponath et al., 2018; Suescun et al., 2019). While neuroinflammation has mostly been investigated in disease context, it is important to note that it is a process that when transient and properly modulated can be beneficial, for example it can aid recovery of CNS injuries (DiSabato et al., 2016). However, when the inflammation becomes chronic and/or at a very high level, it can have negative consequences, as is suggested in the case of ALS. Several studies have proven the presence of inflammation in ALS patients, an observation also made early in the disease process in ALS animal models, suggesting that it could be a chronic condition (Henkel et al., 2006; Kuhle et al., 2009; Mishra et al., 2016). Moreover, levels of the inflammatory factors correlate with the severity of the disease (Jin et al., 2020). Both astrocytes and microglia are known to be the main sources of the inflammatory mediators that control immune responses in the CNS. Therefore, these cell types have been put under particular scrutiny. In the high-copy SOD1^{G93A} mouse model of ALS, disease symptoms onset at around 3-4 months and progress until death occurs at age of 5-6 months (Gurney et al., 1994). In this model, microglial activation has been observed from 80 days of age up to end stage. Astroglial activation has been observed from day 100 with differing results found for the activation level at 120 days (Alexianu et al., 2001; Hall et al., 1998). In diverse studies of ALS models and patients, astrocytes and microglia have both been shown to have an increase in activation of the nuclear factor kappa-light-chain enhancer of activated B cells (NF-κB) (Crosio et al., 2011; Frakes et al., 2014). The NF-κB signaling pathway has an important role in the induction of pro-inflammatory gene expression, this further supporting a role for neuroinflammation.

1.2 NF-κB Signaling in Mammals

1.2.1 NF-κB Mechanism of Action

NF-κB was discovered by Sen and Baltimore in 1986, as a protein present in activated B lymphocytes that binds to a specific, conserved DNA sequence (Sen and Baltimore, 1986). Subsequently, NF-κB has been shown to be part of a highly conserved protein family, present

in organisms as diverse as *Drosophila melanogaster* (Steward, 1987), mice and humans (Gilmore and Wolenski, 2012). NF-κB members act as constituents of related protein complexes (Oeckinghaus and Ghosh, 2009). The family has five members: p50, p52, p65/RelA, c-Rel, and RelB, which all share the presence of a Rel homology domain adjacent to a nuclear localization signal. The Rel homology domain enables DNA binding, interactions with IκB inhibitory proteins, and dimerization. The NF-κB pathway must be activated to recruit the NF-κB proteins in functional complexes and induce transcription. There are two main pathways to NF-κB activation: the canonical and the non-canonical (Sun, 2017). The canonical pathway responds to several different immune receptors, predominantly resulting in the activation of NF-κB proteins p65/RelA, p50, and c-Rel. The non-canonical pathway, on the other hand, is triggered primarily by a certain subset of receptors from the tumor necrosis factor receptor (TNFR) superfamily, causing induction of p52 and RelB. Below, we will discuss further the differences between the two pathways, as well as their diverse activities. It is however worth noting that the canonical and non-canonical pathways are not mutually exclusive. For example, canonical p65/p50 dimers can be induced by the non-canonical pathway (Shih et al., 2011). In addition, the p65/p50 dimer itself can also regulate parts of the non-canonical pathway. The full extent of this interdependency is not yet completely understood.

Canonical Pathway

The canonical pathway (hereafter known as the NF-κB pathway) responds to immediate infectious threats and pro-inflammatory signals (Sun, 2017, 2011). In the absence of such activating threats, the NF-κB proteins p65, p50 and c-Rel are located in the cytoplasm. There, they are bound to Inhibitor of κB (IκB) proteins or the IκB-like p50 precursor protein, p105. These inhibitors prevent nuclear translocation of the NF-κB proteins by masking their nucleus localization signal. When an infection or pro-inflammatory stimulus reaches the cell, many different receptors can serve as activators of the pathway including pattern-recognition receptors, TNF receptor superfamily members, T-cell receptors, B-cell receptors in addition to several cytokine receptors (T. Liu et al., 2017). Activation of these receptors initiates a cascade of intracellular proteins that induces the formation of the IκB kinase (IKK) complex. The IKK complex contains a regulatory subunit called NF-κB regulatory modifier (NEMO) that tethers the two other subunits, the kinases IKKα and IKKβ. The IKK complex phosphorylates the inhibitory IκB proteins and p105, which leads to their degradation or processing by the

proteasome. With the NF-κB protein dimers now freed from inhibition, they transfer to the nucleus where they activate or repress inflammatory gene transcription.

Non-Canonical Pathway

The non-canonical pathway is regulated via a different protein complex and relies on protein synthesis (Zarnegar et al., 2008). Hence, its activation is typically much slower, and plays roles during immune cell differentiation and development . Much like the canonical pathway, in absence of activation the non-canonical pathway NF-κB proteins RelB and p52 precursor p100 are bound to each other in the cytoplasm. In this situation, p100 functions similarly to an IκB protein by inhibiting the nuclear translocation of RelB. In the presence of non-canonical receptor stimulation (through certain TNF receptor superfamily members such as CD40, lymphotoxin β receptor, B-cell activating factor receptor, etc.), the NF-κB-inducing kinase (NIK) activates downstream IKKα dimers, which in turn phosphorylate p100 and mark it for proteasome processing. Processed p100, also known as p52, no longer inhibits the nuclear localization of RelB. The RelB/p52 heterodimer translocates to the nucleus where it regulates gene expression.

Figure 1-1. Illustration of the NF-κB pathway
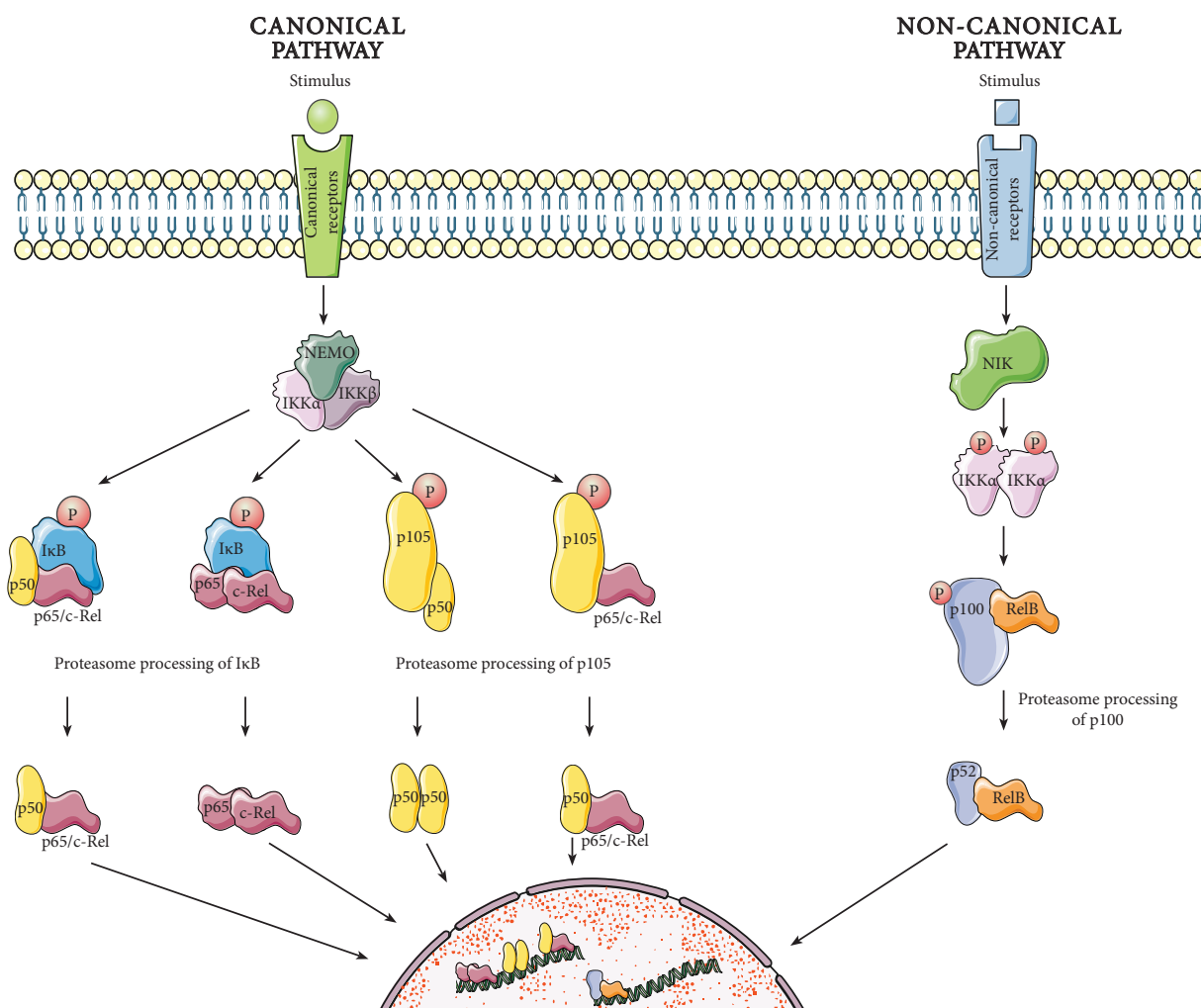
Figure 1: Simplified illustration of the canonical and non-canonical versions of the NF-κB pathway. When a stimulus activates a canonical pathway receptor, the IκB kinase (IKK) complex forms. The IKK complex phosphorylates the inhibitory IκB protein and the p50 precursor protein p105, inducing their degradation and processing, and enabling the translocation of the NF-κB dimers into the nucleus for gene expression regulation. Upon activation of the non-canonical pathway, NF-κB-inducing kinase (NIK) activates the IKKα dimer, leading to phosphorylation and proteasome processing of p100. This results in production of p52, which together with RelB translocates to the nucleus and regulates transcription. The dimers presented in this figure are not the only possible combinations.

1.2.2 Functions of NF-κB

The NF-κB pathway is firmly established for its critical role in the immune system. Upon their initial discovery, NF-κB proteins were viewed as inducers of B cell development and

activation, but have since then also been shown to be immediate activators of the innate immune system at the sites of an infection or wound (Q. Zhang et al., 2017). In the case of an extensive inflammation, the NF-κB proteins will also contribute to the activation of the adaptive immune system to keep the infection at bay.

In addition to its essential functions in the immune system, the NF-κB pathway is also critically involved in CNS function. Several NF-κB transcription factors are expressed in neurons, including the p50-p65 heterodimer and the p50-p50 homodimer. These NF-κB proteins can mediate transcriptional response to synaptic activity and play key roles in learning and memory (Meffert et al., 2003). Furthermore, NF-κB proteins have been found not only in the neuronal soma, but also in neuronal processes and synapses, where the p50-p65 heterodimer has been singularly observed. In p65-deficient mice, NF-κB dimers were no longer found in synapses whereas other NF-κB proteins were still present in the cell bodies, implying a particular role for the p65-p50 dimers in synapses. In a similar way to activation in the periphery, in the CNS the NF-κB pathway can be triggered by cytokines, interleukins, viral infections, and oxidative stress (Meffert and Baltimore, 2005). However, these inducers may not induce the same activity in the CNS as in the periphery. For example, the cytokine tumor necrosis factor α (TNFα) is well-known to be involved in the tissue injury response in peripheral tissues. However, in the CNS, in absence of inflammation, it can also mediate neural plasticity in the hippocampus (Albensi and Mattson, 2000). Similarly, the free radical nitric oxide regulates synaptic efficacy in the CNS, while in the peripheral immune system it has a role in cell death (Schuman and Madison, 1994). Given the many roles of the NF-κB pathway in both the nervous system and the immune system, disentangling how these many functions could impact the progression of neurodegenerative diseases including ALS remains a serious challenge.

1.3 NF-κB Signaling in *Drosophila melanogaster*

The NF-κB signaling pathway is very conserved between human, mouse, and *Drosophila melanogaster*. However, there are a few differences worth noting. While five NF-κB proteins exist in mammals, *Drosophila* have three: Dorsal, DIF, and Relish. Instead of canonical and non-canonical signaling, the *Drosophila* NF-κB pathway is split into the Imd and the Toll pathways (see figure 2) (Hetru and Hoffmann, 2009). The Toll pathway activates NF-κB proteins Dorsal and DIF, which share 45% homology with mammalian RelB, c-Rel, and p65, when recognizing the presence of gram-positive bacteria and/or fungi. The Imd pathway

induces Relish, which is similar to the mammalian p50 and p52 proteins, when the animal is exposed to gram-negative bacteria. Unlike mammals, *Drosophila* do not have an adaptive immune system, and rely solely on innate immunity, with the Toll and Imd pathways being responsible for inducing this (Salminen and Vale, 2020).

1.3.1 The Imd pathway

The Imd receptor Peptidoglycan-recognition protein LC (PGRP-LC) is activated by direct binding to gram-negative bacterial peptidoglycans (Hetru and Hoffmann, 2009). PGRP-LC then induces the interaction between the Immune deficiency (Imd) protein and proteins Fas-associated death domain protein (Fadd) and Death related ced-3/Nedd2-like caspase (Dredd), triggering the kinase TGF-β activated kinase 1 (TAK1). TAK1 subsequently forms a complex with TAK1- associated binding protein 2 (Tab2), which activates the *Drosophila* version of the IKK complex, consisting of proteins Immune response deficient 5 (Ird5) and Kenny (Key). Once activated, the IKK complex phosphorylates Relish leading to its cleavage most likely by Dredd (Kim et al., 2014), and Rel-68 translocates to the nucleus to alter gene expression and induce antimicrobial peptide (AMP) production as well as expression of other immune-related genes.

1.3.2 The Toll pathway

Unlike the Imd pathway receptor PGRP-LC, the Toll receptors do not directly bind to microbe components. During a fungal infection or gram-positive bacterial infection, circulating PGRP proteins and Glucan binding proteins (GNBP) instead bind to the microbes, activating proteolytic cascades that induce the cleavage of the cytokine Spätzle (Hetru and Hoffmann, 2009). Spätzle interacts with the Toll receptor resulting in interaction between MyD88, Tube, and Pelle. Pelle causes an unknown kinase to phosphorylate Cactus, which is the closest homolog to mammalian IκB and which inhibits DIF and Dorsal by keeping them in the cytoplasm. As Cactus is degraded by the proteasome, DIF and Dorsal can translocate to the nucleus to induce expression of several immune-related genes, including AMPs.

Figure 1-2. A schematic of the *Drosophila* NF-κB pathway
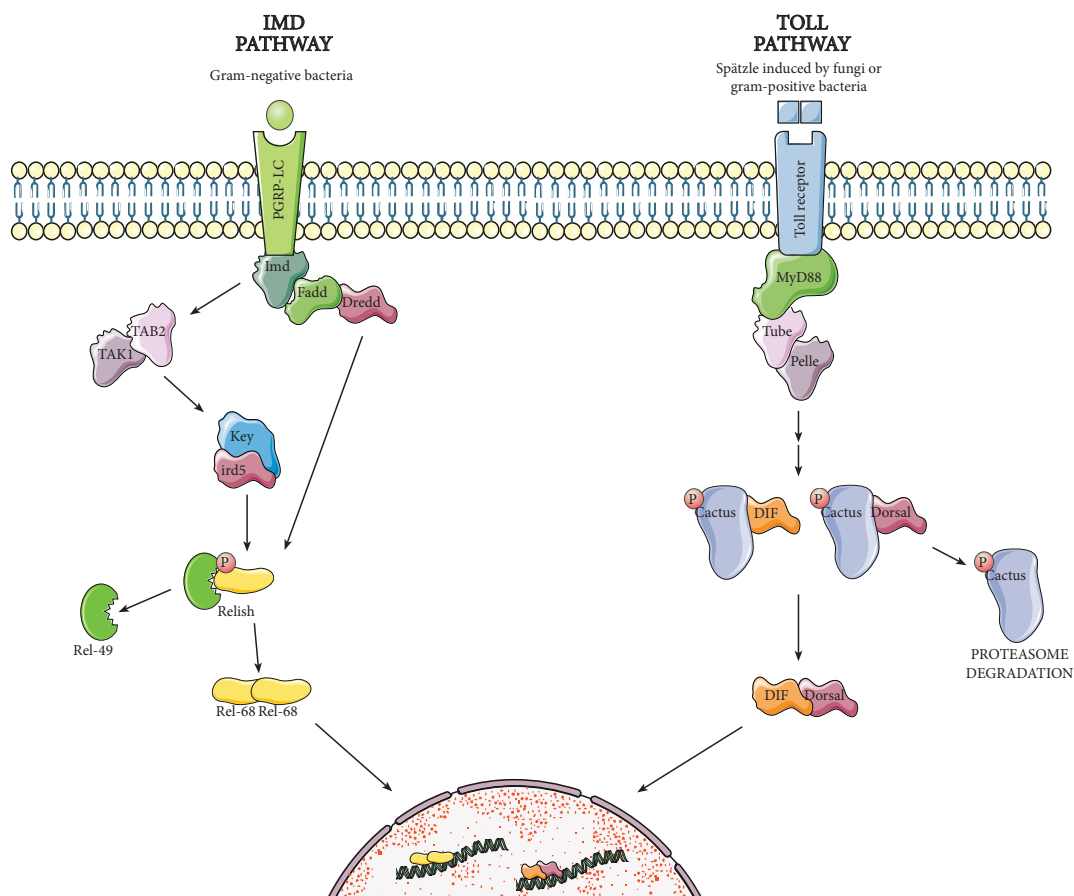
Figure 2: A schematic showing the activation of the two branches of the *Drosophila* NF-κB pathway: the Imd and the Toll pathways. The *Drosophila* NF-κB signaling pathway consists of two responses: the Imd and the Toll pathways, each responding to gram-negative bacteria or fungi and gram-positive bacteria. When activated, the Imd pathway induces the ird5-Key complex causing phosphorylation and cleavage of Relish, which subsequently translocates to the nucleus to enhance AMP gene expression. The Toll pathway uses phosphorylation and degradation of the inhibitory protein Cactus to free DIF and Dorsal, and enable their translocation to the nucleus. There are several more combinations of NF-κB homo- and heterodimers that can be combined than what is represented in this schematic, both within each pathway and between the pathways.

1.3.3 Functions of the NF-κB pathways in *Drosophila*

The Toll immune pathway is most commonly known to illicit an immune response when faced with gram-positive or fungal infections (Valanne et al., 2011). The most studied function of the Imd pathway is, similarly, its activation in following gram-negative bacterial infection. Both pathways have also been associated with response to different viral infections. Toll mutants show altered sensitivity to Drosophila X virus infection (Zambon et al., 2005),

and Relish deletion mutants infected with Sindbis virus show an increased viral load compared to controls (Avadhanula et al., 2009).

While precise functions of the pathways in neurons have not yet been completely studied, there are studies associating them with neurodegeneration. Pan-neuronal activation of either pathway causes shortened lifespan, for example (Khor and Cai, 2020). Deletion of the Toll receptor can also suppress the pathology produced by an Aβ42 overexpression *Drosophila* Alzehimer's disease model. However, dysregulation of Imd pathway activation has been even more commonly associated with neuronal loss than the Toll pathway. For example, mutations in Imd negative regulators induces toxic AMP levels and causes neurodegeneration, shortened lifespan, and locomotor defects, an effect that could be rescued through glial Imd inhibition (Kounatidis et al., 2017). In addition, gram-negative bacterial infection accelerated the disease model progression by recruiting hemocytes to the brain, causing neurodegeneration (Wu et al., 2017). It has also been observed that the Imd pathway, but not the Toll pathway, can mediate invasion of macrophages across the blood-brain barrier (BBB) in *Drosophila* pupae (Winkler et al., 2021). Injection of bacteria into the brain through the eye as well as genetic activation of the Imd pathway both lead to neurodegeneration via AMP toxicity (Cao et al., 2013). Indeed, many hypothesize that the Imd pathway in particular can be an inducer of neuronal loss, though it is not completely established what the exact mechanism of this would be.

1.4 fALS in the context of neuroinflammation and NF-κB

Besides the NF-κB pathway upregulation that has been observed in patients and ALS animal models, there are several genes associated with fALS that also influence neuroinflammation and NF-κB activation. Below, I will discuss a selection of some of the over 25 genes which have a genetic link to ALS, focusing on those with a potential connection to neuroinflammation and NF-κB activity (figure 3). In addition to this selected subset, it should be noted that several other familial ALS genes have a connection to NF-κB and inflammation, such as Ubiquilin-2 (Picher-Martel et al., 2015) and Sequestosome 1 (Rolland et al., 2007).

1.4.1 c9orf72

Expansion of a GGGGCC hexanucleotide repeat in the first intron of the c9orf72 gene is the most common genetic defect associated with familial ALS (fALS), causing 39% of fALS cases

and 7% of sporadic ALS (sALS) cases with European ancestry (Morgan and Orrell, 2016). In non-diseased individuals, the first intron of the c9orf72 gene contains ≤11 hexanucleotide repeats, but in the case of ALS patients, these repeats are expanded, ranging from hundreds to thousands of repeats (Bennion Callister and Pickering-Brown, 2014; Vanneste et al., 2019). It has been suggested that these repeats could cause disease via bidirectional transcription into RNAs which form unusual secondary structures (Balendra and Isaacs, 2018). Another potential pathogenic effect of the repeats is non-ATG (RAN) translation into dipeptide repeats which accumulate in diseased cells (Green et al., 2016). An additional and perhaps not mutually exclusive mechanism that could contribute to disease, is that the presence of the hexanucleotide repeats in the c9orf72 intron leads to reduced expression of the c9orf72 protein itself. To investigate the possibility that a loss-of-function of c9orf72 contributes to disease, several *c9orf72* null mutant mouse strains have been developed. These mutants show mild or no motor phenotypes, but instead have increased immune response activation (Atanasio et al., 2016; Burberry et al., 2016). For example, in a study by O'Rourke et al., c9orf72 -/- mice showed progressive accumulation of macrophage-like cells (O'Rourke et al., 2016). Moreover, the expression of c9orf72 was found to be highest in myeloid cells, and its removal leads to altered immune responses in macrophages and microglia. Additionally, the animals show age-related neuroinflammation. These studies suggest that c9orf72 plays an important role in normal myeloid cell function. Consistently, it was observed that knocking out c9orf72 solely in myeloid cells could mimic the phenotype seen in mice with complete *c9orf72* knockout (McCauley et al., 2020). Myeloid cells depleted of c9orf72 are also hyperresponsive to activators of the innate immune response regulator stimulator of interferon genes (STING), and display reduced degradation of STING through the autolysosomal pathway. Furthermore, the systemic inflammation and autoimmunity of *c9orf72* mutant mice can be reduced when housed in an environment with less immune-stimulating bacteria, further supporting the importance of c9orf72 function in regulating the immune response (Burberry et al., 2020). Knock-down of c9orf72 activates the NF-κB pathway in particular in a U87 glioblastoma cell model (Fomin et al., 2018), revealing the possibility that NF-κB takes part in c9orf72-dependent immune responses. Altogether, this data supports an important role for c9orf72 in innate immune regulation which potentially could contribute to ALS progression.

1.4.2 SOD1

The first gene to be discovered as an ALS-associated gene encodes Superoxide Dismutase 1 (SOD1). Over 170 ALS-causing mutations have been found in *SOD1* (Kaur et al., 2016), and SOD1 aggregation has been observed in both fALS and sALS cases. The normal function of the SOD1 dimeric enzyme is to catalyse the breakdown of superoxide into oxygen and hydrogen peroxide, in order to protect the cell from the toxicity of these reactive oxygen species (Chattopadhyay and Valentine, 2009). Although this process might be disrupted in some of the mutant versions of the gene (Kaur et al., 2016), most experimental evidence supports a gain of toxic activity in SOD1-related ALS pathology. Mutant SOD1 aggregates observed in fALS are, for example, believed to cause neurotoxicity (Chattopadhyay and Valentine, 2009). This is bolstered by the fact that mouse models of ALS based on high-copy overexpression of mutant SOD1 develop a disease very similar to human ALS (Gurney et al., 1994). As with most neurodegenerative diseases, presence of aggregated proteins has been hypothesized to induce neuroinflammation. Indeed, both microglial and astroglial activation has been observed in SOD1^{G93A} mice (Hall et al., 1998). Moreover, AAV-mediated silencing of astrocytic SOD1^{G93A} in the SOD1^{G93A} mouse model leads to late stage rescue of neuromuscular junction (NMJ) occupancy and improved motor behavior (Rochat et al., 2021). Likewise, diminishing the expression of mutant SOD1 solely in microglia using Cre-dependent transgene inactivation in floxed SOD1^{G37R} mice, slows down late disease progression (Boillée et al., 2006). In addition, SOD1^{G93A} mice lacking myeloid and lymphoid cells have a similar disease progression as SOD1^{G93A} mice, but when given a wild-type bone marrow transplant disease progression significantly slows down (Beers et al., 2006). *In vitro*, it has also been observed that SOD1^{G93A} microglia release more neurotoxic factors compared to wild-type microglia (Beers et al., 2006). When co-cultured with SOD1^{G93A} motor neurons, SOD1^{G93A} microglia induce significantly higher motor neuron death than wild-type microglia. Pro-inflammatory factors such as IL-1α, TNFα and C1qa can be released by neuroinflammatory activated microglia and induce neurotoxicity via changes in astrocyte activity. Indeed, SOD1^{G93A} mice with a triple knockout of IL-1α, TNFα and C1qa show over 50% prolongation of survival and improved motor abilities (Guttenplan et al., 2020). These effects are likely to be related to changes in neuroinflammation and thereby could be due to, or lead to, changes in NF-κB activity. Along these lines, NF-κB is activated mainly in microglia in SOD1^{G93A} mice, and deletion of NF-κB signaling in microglia prolongs mouse survival (Frakes et al., 2014). Similarly, expression of

SOD1^{G93A} and SOD1^{G85R} in cell lines is sufficient to trigger activation of NF-κB (Nivon et al., 2016), further suggesting that aggregated SOD1 may lead to immune response activation. Mutated SOD1 also leads to ER stress and activation of the unfolded protein response (UPR), which in turn can activate NF-κB (Prell et al., 2014), suggesting a possible mechanism for NF-κB activation in ALS.

1.4.3 TDP-43

Approximately 5% of fALS patients have mutations in the *TDP-43* gene, mostly inherited in an autosomal dominant manner (Morgan and Orrell, 2016). However, up to 97% of ALS patients present with TDP-43 protein aggregation independently of TDP-43 mutations (Nguyen et al., 2018), showing the importance of this protein in ALS. Normally, TDP-43 functions as an RNA- and DNA-binding protein regulating transcription, mRNA splicing, transport, and stability. It is predominantly a nuclear protein, but in case of ALS TDP-43 is often found to re-localize to the cytoplasm where the protein is found in dynamic stress granules as well as in protein inclusions (Ederle et al., 2018; Khalfallah et al., 2018). It is likely that these inclusions can lead to a toxic gain-of-function as they interact with cellular components, but the loss of TDP-43's nuclear functions may also be a source of neuronal toxicity. Studies by Swarup et al. of human ALS spinal cords has further illuminated the pathological role of the protein. In this study, TDP-43 and p65 were observed to co-localize and interact in glial cells and neurons, indicating potential interactions of TDP-43 with the NF-κB pathway (Swarup et al., 2011). In addition, electrophoretic mobility shift assay (EMSA) revealed that interaction between p65 and DNA is significantly increased when co-transfected with TDP-43 wild-type or TDP-43 G348C, suggesting that TDP-43 could act as a co-activator of p65. Overexpression of TDP-43 in neuronal cell lines exposed to glutamate toxicity also leads to cell death that can be reduced by inhibition of NF-κB activity (Swarup et al., 2011). It has also been suggested that mutated TDP-43 enters the mitochondria, triggering release of mitochondrial DNA, and thereby causes activation of the NF-κB-activating cGAS/STING pathway, resulting in inflammation (Yu et al., 2020). Crossing a mouse model overexpressing human TDP-43 A315T to mice deficient in innate immune response regulator STING results in a 40% lifespan prolongation and improves motor abilities, despite not leading to a decrease in TDP-43 expression. Expression of a STING inhibitor in the TDP-43 A315T model also l improved motor behavior, reduced neuronal death, and decreased expression of NF-κB-induced genes in cortex and spinal cord.

In addition, activated microglia and astrocytes have been observed in the motor cortex of both ALS patient samples with TDP-43 pathology and a TDP-43 mouse model, suggesting an inflammatory response in this area (Jara et al., 2019). Primary mouse astrocytes transfected with TDP-43 also show increased inflammatory response (Lee et al., 2020). In mice with AAV9-mediated neuronal TDP-43 expression, low-dose lipopolysaccharides (LPS) were continually introduced to induce a chronic inflammatory response. These studies show increased permeability of the blood brain barrier (BBB) in TDP-43-expressing mice, leading to an LPS-induced inflammatory response in the CNS. TDP-43 mice without LPS treatment also displayed infiltration of CD3+, CD4+ T cells, and immunoglobulin G (IgG) through the BBB pointing to a regulatory role of TDP-43 in the immune system (Zamudio et al., 2020). Moreover, cultured microglia and astrocytes expressing either TDP-43 wild-type or TDP-43 A315T and exposed to LPS display increased TDP-43 expression in both genotypes. In addition, both TDP-43 wild-type and TDP-43 A315T are mislocalized to the cytoplasm after LPS treatment, mimicking the cytoplasmic presence of TDP-43 in ALS. TDP-43-containing puncta were observed in the cytoplasm, at a higher level in TDP-43 A315T than in TDP-43 wild-type cells (Correia et al., 2015). In summary, these results suggest a role of TDP-43 in the immune system potentially involving changes in NF-κB activity and suggest resulting inflammatory response could induce TDP-43 mislocalization.

1.4.4 FUS

FUS is an RNA and DNA binding nuclear protein that can regulate mRNA splicing and gene expression. In around 5% of the fALS cases, mutations are observed in the *FUS* gene (Morgan and Orrell, 2016), many of them disrupting the nuclear localization signal of the protein and causing accumulation of FUS in the cytoplasm (Vance et al., 2013). Again, it is unclear whether a gain- or loss-of-function of FUS causes the pathology. FUS wild-type overexpression in *Drosophila*, mice and rats all led to neurotoxicity (Nakaya and Maragkakis, 2018). Moreover, mice expressing near endogenous levels of mutant FUS also display ALS-like pathology (López-Erauskin et al., 2018). However, in *Drosophila melanogaster*, it has also been seen that deletion of the FUS ortholog *Caz* leads to severe ALS-like phenotype, suggesting that the cause of the pathology may involve loss-of-function (Wang et al., 2011). Similar to TDP-43, the function of FUS has been further explored in the context of NF-κB signaling as the FUS protein also interacts with p65. FUS may act as a co-activator of p65 as it is able to enhance the NF-

κB response to stimuli such as TNFα, interleukin-1β (IL1β), and overexpression of NF-κB-inducing kinase (Uranishi et al., 2001). In cell lines, it has also been discovered that treatment with immune response protein type I interferon (IFN) promotes FUS mRNA stability leading to FUS accumulation (Shelkovnikova et al., 2019). When overexpressing FUS *in vitro* in mouse and human astrocytes derived from neural progenitors, the FUS-expressing astrocytes were found to have a higher pro-inflammatory response than controls when stimulated with IL1β (Ajmone-Cat et al., 2019). Medium from these astrocytes also promoted microglial activation and neuronal cell death *in vitro*. Therefore, FUS may regulate the immune response and, when mutated in ALS, may also promote neuroinflammation via NF-κB activity.

1.4.5 OPTN

ALS-causing *OPTN* mutations are most frequent in Japanese and Chinese patients where they are responsible for 3% of the fALS cases, compared to 1% of Caucasian fALS cases (Markovinovic et al., 2017). The OPTN protein has many functions: induction of autophagy, structural maintenance of the Golgi complex, regulation of post-Golgi protein trafficking, as well as inhibition of the NF-κB pathway (Ryan and Tumbarello, 2018). To inhibit NF-κB, OPTN competes with NEMO for binding to the ubiquitinated receptor-interacting protein kinase 1 (RIPK1). Without binding NEMO, RIPK1 is unable to activate the IKK complex, which prevents NF-κB activation (Slowicka and van Loo, 2018). In ALS patients, OPTN has been observed in protein inclusions, co-localizing with SOD1, TDP-43, or FUS (Akizuki et al., 2013). Interestingly, the *OPTN* mutations associated with ALS lead to autosomal recessive inheritance of the disease, which supports loss-of-function as the most likely pathogenic mechanism (Kamada et al., 2014). The expression pattern of p65 has been analyzed in patients with sALS or fALS with *OPTN* mutations (Sako et al., 2012). p65 was found to be increased in microglia and absent from neuronal nuclei suggesting that neuroinflammation is present and that microglia are activated. Following knock down of OPTN in a neuronal cell line, NF-κB expression and neuronal cell death are increased (Akizuki et al., 2013). The neuronal cell death can be hindered by the NF-κB inhibitor withaferin A. While *Optn* deficient mice develop and breed normally (Markovinovic et al., 2017), they develop motor axon degeneration and progressive demyelination through CNS cell necroptosis and neuroinflammation (Ito et al., 2016). This phenotype can be rescued by blocking cell death via inhibition of the protein RIPK1's regulation of inflammation. In ALS, mutated OPTN seems to have neurodegenerative

effects via loss-of-function possibly leading to dysregulated NF-κB activity, although it is still unclear whether this happens directly in neurons or through non-cell autonomous mechanisms.

1.4.6 TBK1

TBK1 is a tightly regulated kinase, which is involved in many different pathways such as autophagy, cell proliferation, and insulin signaling (de Diego and Rodríguez-Gallego, 2014). It also plays an important role in immunity as a response to viral infection, phosphorylating Interferon regulatory factor 3 (IRF3), which can induce an antiviral gene expression response (Sweeney et al., 2007). Additionally, as its name suggests (TANK-binding kinase 1), it binds and activates the NF-κB regulator TANK (TRAF family member-associated NF-kappa-B activator), thereby regulating the non-canonical NF-κB response (Pomerantz and Baltimore, 1999). Furthermore, TBK1 binds to and interacts with the previously mentioned NF-κB-inhibitor OPTN (Ying and Yue, 2012). Numerous fALS-associated nonsense mutations have been discovered in TBK1, suggesting haploinsufficiency as the most likely disease mechanism (de Majo et al., 2018). In addition, several missense mutations have been found, which appear to eliminate TBK1 activity by preventing its homodimerization, and abolish its ability to interact with OPTN and Interferon regulatory factor 3 (IRF3). These results suggest a loss-of-function mechanism for TBK1 in ALS pathology, although not all mutations have been characterized yet. Moreover, whereas Tbk1 knockout selectively in motor neurons does not cause any neurodegenerative phenotype *per se*, it was found to worsen motor behavior, accelerate denervation of neuromuscular junctions and disease onset when these mice were crossed with SOD1^{G93A}-expressing mice (Gerbino et al., 2020). Mice with knock-in of ALS-related TBK1 loss-of-function mutations, in combination with SOD1^{G93A} expression, display decreased levels of interferon-inducible genes in glia, accelerated disease onset, but extended lifespan (Gerbino et al., 2020). Similar results have been seen when introducing a heterozygous *Tbk1* deletion in SOD1^{G93A} mice, which leads to accelerated onset of disease but decreases microglial neuroinflammation and prolongs survival at later disease stages (Brenner et al., 2019). These results highlight the importance of cell type specificity and timing in future treatments as responses may differ as a function of disease stages and targeted cell types.

Figure 1-3. ALS genetic risk factors may affect the NF-κB pathway
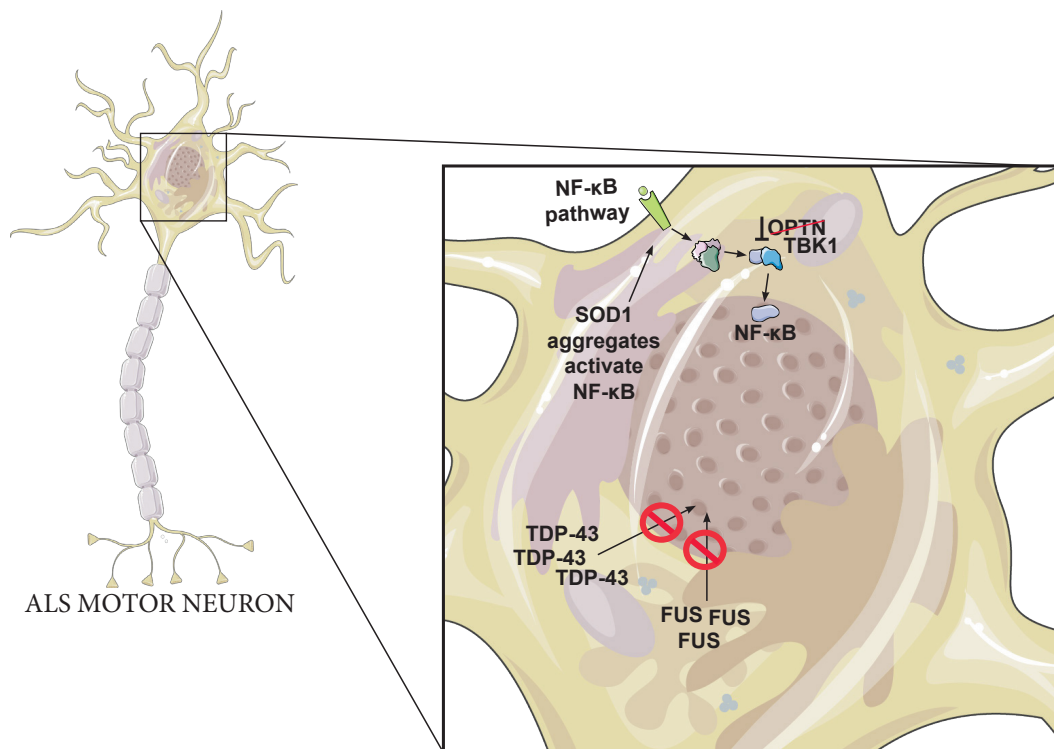
Figure 3: Schematic representation of a motor neuron showing how major genetic risk factors linked to amyotrophic lateral sclerosis (ALS) may affect the NF-κB pathway. The NF-κB pathway can be activated by either SOD1 protein aggregation or other stimuli. OPTN has limited ability to inhibit the NF-κB pathway when carrying loss-of-function ALS mutations. Mutated TBK1 is unable to bind to OPTN but may still be regulating the NF-κB pathway. Both TDP-43 and FUS, which usually bind to NF-κB in the nucleus, accumulate in the cytoplasm and may fail to maintain their nuclear activity in conditions leading to ALS.

1.5 ALS Environmental Factors

While fALS cases can give important clues about ALS molecular mechanisms, it is also important to study environmental factors that could contribute to ALS. Tobacco smoking, for example, has been shown to increase the risk of ALS in several studies, in particular for women (Alonso et al., 2010; Wang et al., 2011). Physical head trauma is another ALS risk factor (Seelen et al., 2014). However, head trauma can also lead to neurodegeneration in absence of ALS, such as in the case of chronic traumatic encephalopathy (CTE) (McCambridge and Stinson, 2020). It is also worth noting that it is not certain if the physical trauma itself is a cause of the disease in the case of ALS, or if head trauma could be an early symptom of muscle weakness in as yet undiagnosed ALS patients (Oskarsson et al., 2015). Physical exercise may also increase the risk of ALS, but not in a dose-dependent manner (Huisman et al., 2013).

Therefore, it has been suggested that exercise itself may not cause disease, but that perhaps a genetic predisposition to exercise is somehow linked to a genetic predisposition to ALS. Furthermore, exposure to metals such as lead have been suggested to be a risk factor. In a study by Fang et al., an association was found between lead levels in the blood and ALS (Fang et al., 2010). While none of the above-mentioned risk factors are linked directly to an increasing CNS NF-κB response, they all may expose the body to some type of stress. The consequences of this are not yet completely understood, but it is known that different types of stress can cause inflammation (Y.-Z. Liu et al., 2017).

However, other environmental ALS risk factors have more direct links to neuroinflammation and NF-κB signaling. Several pesticides, for example, have shown an association with ALS. One of these, organophosphates, can cause neurological damage, oxidative stress, and mitochondrial dysfunction (Bozzoni et al., 2016). Acute organophosphate intoxication leads to an increase in microglial and astroglial activation, causing a release of pro-inflammatory cytokines (Banks and Lein, 2012).

In addition, dietary choices can have an influence on the risk of ALS. Increased intake of antioxidants has been associated with decreased risk of disease, suggesting that oxidative stress may play an important role in disease development (Ascherio et al., 2005). NF-κB signaling has indeed been demonstrated to be activated by oxidative stress, and antioxidant treatment can block this activation (Wang et al., 2002). Indeed, inflammatory stimulation induces NF-κB activity in primary culture cortical astrocytes, a change that can be prevented by antioxidant treatment (Martorana et al., 2019). In primary cortical neurons exposed to the pro-inflammatory astrocyte medium, NF-κB binding to DNA decreased. This, too, could be averted through exposure to antioxidants. Similar results have been observed in primary cultures of rat neuronal cultures (Kratsovnik et al., 2005). The neurons were exposed to injury via chemical ischemia, resulting in an increased NF-κB activation that could be prevented by administration of antioxidants or an NF-κB inhibitor. These results point to a connection between oxidative stress and NF-κB that could affect inflammation.

Another risk factor of ALS is the neurotoxin β-N-methylamino-L-alanine (BMAA) (Delzor et al., 2014). BMAA was first linked to ALS when it was discovered in the diet of patients in the Pacific island of Guam, which had a significantly higher incidence of ALS than the rest of the world in the 1950s. BMAA has since been proven to activate the glutamate receptors NMDA and AMPA. This in turn disrupts mitochondrial function, increases reactive oxygen species

(ROS) production, and causes apoptosis. A study by Silva et al., proposes a novel mechanism for BMAA in Alzheimer's disease where the mitochondrial toxicity of BMAA activates Toll-like receptors (TLRs) causing the activation of p65 NF-κB (Silva et al., 2020). Indeed, in primary cortical neurons subjected to BMAA, an increase of cell surface TLR4 is observed. A decrease in IκBα causing a translocation of p65 NF-κB to the nucleus is also seen. This causes and increase in the transcription of pro-inflammatory Nod-like receptor 3 (NLRP3) as well as Interleukin 1 beta (IL-1β) precursor pro-IL-1β in the neurons. A similar mechanism could be plausible for BMAA-induced ALS cases. Next, we delve further into another environmental factor that is present in numerous ALS cases and that is known to activate both NF-κB and inflammation - bacterial infection.

1.5.1 Bacterial Infections in ALS

Bacterial DNA and prokaryotic cells have been observed in CNS tissue of ALS patients (Alonso et al., 2019). In several cases of ALS bacterial infection has been shown to be present in patients. All but one of the Gulf War veterans that were diagnosed with ALS, for example, had systemic *Mycoplasma fermentas* infections (Nicolson et al., 2002). In a cohort of non-military American, Canadian, and British ALS patients, 80% had infections with *M. penetrans, M. fermentans* (59%), *M. hominis*, or *M. pneumoniae*. In addition, studies have shown that the spirochete bacteria, *Borrelia burgdorferi*, is present in a significant proportion of ALS patients (Halperin et al., 1990; Hänsel et al., 1995). Moreover, spirochete bacteria in general have been observed in cases of both ALS and Alzheimer's disease (Allen, 2016; Nicolson, 2008). Mycoplasmas identify neither as gram-negative nor as gram-positive, due to their lack of cell wall structure, preventing a gram's stain (Kashyap and Sarkar, 2010). However, the aforementioned Mycoplasma strains all activate the NF-κB pathway, as do spirochete bacteria (Borchsenius et al., 2019; Ebnet et al., 1997; Logunov et al., 2009; Sacht et al., 1998).

Some researchers explain this connection between bacterial infection and ALS by the so-called endotoxin theory, suggesting that gram-negative bacteria, in particular, are contributors to neurodegeneration via exposure to the lipopolysaccharide (LPS) endotoxin, the main component of the gram-negative bacterial outer membrane (Brown, 2019). Normally, the endotoxin levels in blood plasma are low, but they could be increased during the course of neurodegenerative diseases (Zhang et al., 2009). When wild-type rodents are injected with high levels of endotoxins, this induces microglial activation, memory deficits and neuronal loss (Qin

et al., 2007; Zakaria et al., 2017). One puzzle is how endotoxin can influence the brain. It has been suggested that LPS may activate cells at the level of the blood-brain barrier, resulting in a release of pro-inflammatory cytokines and recruiting immune cells in the brain (Brown, 2019). Another possibility is that LPS activates the brain's immune response through the circumventricular organs. When the CNS is reached, endotoxin causes an inflammatory response by activating Toll-like receptor 4 (TLR4), leading to activation of the NF-κB pathway. The NF-κB pathway in turn induces expression of many pro-inflammatory genes, activating the immune system to clear the bacterial infection and the LPS from the body. However, if LPS is not properly cleared from the blood, this leads to a state of chronic inflammation (Morris et al., 2015). When the immune system of the brain is activated, there are several mechanisms that could lead to neurodegeneration, for example via activation of microglial cells which can result in phagocytosis of neurons, including healthy neurons (Brown, 2019).

1.6 The Effect of NF-κB Activation in Different CNS Cell Types During ALS

As has been highlighted above, there are several connections between neuroinflammation, in particular involving NF-κB, and ALS. However, there is still the question of how NF-κB activation and inflammation could lead to motor neuron death. Here, we will focus on exploring the role of NF-κB in neurons, astrocytes, and microglia during ALS and how it has been associated with neurodegeneration.

1.6.1 Neurons

In addition to its function in inflammation, the NF-κB signaling pathway has many other important roles including in neurons. Several studies have made a link between NF-κB and regulation of cognitive behaviors such as learning and memory (Ahn et al., 2008; Kassed and Herkenham, 2004; Oikawa et al., 2012). When activated in mouse excitatory glutamatergic neurons, NF-κB has also been observed to stimulate excitatory synapse formation (Boersma et al., 2011). This effect was also seen to be reversed when NF-κB signaling was decreased; resulting in reduced dendritic spine size and density, both during development as well as in mature neurons in conditions where there is increased demand for new synapses. NF-κB has also been observed to be activated by excitatory neurotransmitters in mouse cerebellar development (Guerrini et al., 1997). Given these important functions of transient NF-κB

activation in synaptic plasticity, development, and neuronal activity (Dresselhaus and Meffert, 2019), it is not implausible to suggest that conditions producing chronic NF-κB activation could instead lead to neurodegeneration. As NF-κB has been shown to be upregulated in the spinal cord of ALS patients (Swarup et al., 2011), it is possible that the activity of this pathway in neurons could contribute to the disease in different ways. For example, a study by Dutta et al. demonstrated that inhibition of the NF-κB pathway through neuron-specific expression of a super-repressor form of IκBα in both TDP-43^{A315T} and TDP-43^{G348C} transgenic mice showed improvements of motor and cognitive functions and reduction of motor neuron loss (Dutta et al., 2020). In SOD1^{G93A} mice, the same NF-κB inhibitory approach showed increased lifespan and a decrease of misfolded SOD1 accumulation. Collectively, these studies point to an important role of NF-κB in neuronal development and function, and highlight the possibility that chronic NF-κB activation contributes to neuronal degeneration in ALS.

1.6.2 Microglia

Microglia normally exist in the brain in a resting state, but they become activated when subjected to an immune challenge or injury (Dresselhaus and Meffert, 2019). Studies by Kyrargyri et al. looked into the function of NF-κB in microglia when they are not subjected to an immune stimulus (Kyrargyri et al., 2015). They used mice with partial microglial depletion of IKKβ, and thereby decreased NF-κB activity, and showed that they have problems with hippocampal-dependent learning. This suggests microglial NF-κB is not only important in inflammation. Still, NF-κB activity in microglia is most commonly studied in response to an immune challenge, where their activation induces expression of pro-inflammatory mediators (Dresselhaus and Meffert, 2019). Such microglial activation has, as previously mentioned, been observed in SOD1^{G93A} mice after day 80. In addition, it has been observed in the brains of sporadic ALS patients through positron emission tomography (PET), between 10-44 months after first disease symptoms (Turner et al., 2004). There exist two types of activated microglia: M1 and M2 (Geloso et al., 2017). When M1 microglia are stimulated by pathogenic or pro-inflammatory molecules, this induces release of several pro-inflammatory mediators. M2 microglia, on the other hand, are induced by anti-inflammatory cytokines and typically suppress inflammation and promote neuronal survival. In older mice, CNS microglia have more prominent M1 microglia while younger mice have more M2 microglia (Crain et al., 2013). In SOD1^{G93A} mice, several of the toxic M1 microglial factor levels are increased (Appel

et al., 2011), and it is noteworthy that M1 microglial activation can be induced by exposure to LPS or pro-inflammatory cytokines (Henkel et al., 2009). Chronic activation of NF-κB has also been shown to promote the M1 microglial activation and can lead to motor neuron death (Frakes et al., 2014). *In vitro,* SOD1^{G93A} microglia have been demonstrated to induce axonal damage and motor neuron death, as well as performing phagocytosis of leftover neuronal debris. This neuronal death can be rescued by depletion of microglial NF-κB signaling and the survival of ALS model mice can be prolonged due to the decrease of inflammatory microglial activation (Frakes et al., 2014).

1.6.3 Astrocytes

The normal role of NF-κB signaling in healthy astrocytes remains understudied. For example, astrocytic NF-κB upregulation in the hypothalamus leads to glucose intolerance, blood pressure rise, and body weight increase, suggesting a role of NF-κB in the astrocytic control of these factors (Y. Zhang et al., 2017). With respect to ALS, it is interesting to note that astrocyte-mediated clearing of glutamate from the synaptic cleft is dependent on astrocytic NF-κB activation, a process controlled by neurons (Ghosh et al., 2011).

However, the most explored function of NF-κB in astrocytes is related to disease conditions. In particular, exposure of these cells to pathogens leads to increased expression of pro-inflammatory genes to combat infections (Giovannoni and Quintana, 2020). This pro-inflammatory astrocyte phenotype is suggested to be induced by NF-κB (Liddelow and Barres, 2017) and leads to failure of many astrocytic neuroprotective qualities, such as promotion of neuronal survival and synaptogenesis (Liddelow et al., 2017). Co-culturing of pro-inflammatory astrocytes with spinal motor neurons produces greatly reduced neuronal viability, an effect that has been attributed to the possible release of a neurotoxin that remains to be characterized. This pro-inflammatory astrocytic phenotype can be activated by microglia, but astrocytic NF-κB activation can also itself in turn be an activator of microglia (Ouali Alami et al., 2018).

In ALS, the interplay between astrocytes and microglia could affect disease progression. For example, diminishing the expression of mutant SOD1^{G37R} selectively in astrocytes delays microglial activation and slows late disease progression in a mouse model of ALS, suggesting that astrocytes take part in regulation of microglial activation (Yamanaka et al., 2008). In SOD1^{G93A} mice, astrocytes with activated NF-κB pathway are able to induce neuroprotective

microglial proliferation at pre-symptomatic stages, leading to decreased neuronal SOD1 aggregation, retarded NMJ denervation, and thereby deceleration of early disease progression (Ouali Alami et al., 2018). However, in later stages of the disease, the astrocytic NF-κB pathway activates M1-like microglia, which accelerates the disease progression. These results point to the complex roles of glial cells with differing effects depending upon disease stage. Disappointingly however, in two separate studies, inhibition of the NF-κB pathway selectively in astrocytes has not led to any improvement in the pathology of SOD1^{G93A} mice (Crosio et al., 2011; Frakes et al., 2014). This may suggest that any possible astrocytic NF-κB-regulating therapeutic for ALS may not only require precise timing of its activity but perhaps also require co-manipulation of microglia.

Figure 1-4. Interactions between microglia, astrocytes, and neurons in ALS
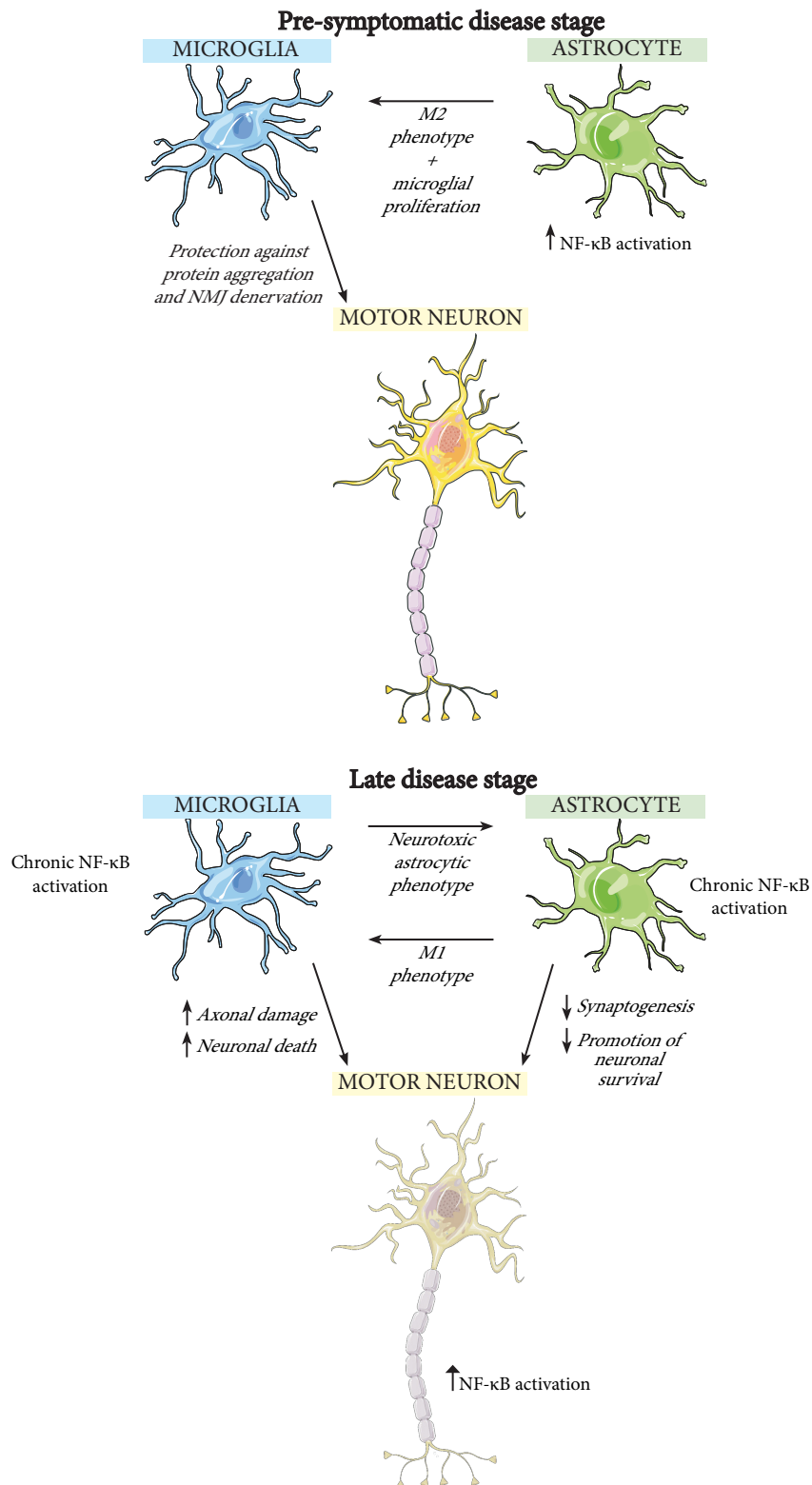
Figure 4: Illustration of the possible interactions between microglia, astrocytes, and neurons, during early and late stage ALS. The NF-κB pathway is activated in both astrocytes and microglia in ALS, but its effects

differ between the stages of the disease. Pre-symptomatically, astrocytes with activated NF-κB promote neuroprotective M2-type microglial proliferation, while at a later stage a neurotoxic M1-type microglial phenotype is induced. Subsequently, M1 microglia cause axonal damage and promote motor neuron death. In addition, M1 microglia induce a neurotoxic astrocytic phenotype, leading astrocytes to decrease their synaptogenesis and promotion of neuronal survival.

1.7 NF-κB Activation in Peripheral Cell Types During ALS

Many studies have suggested numerous cell types may be involve in ALS motor neuron death, which may not all be CNS resident cells. Indeed, several peripheral immune system cells, such as T lymphocytes and monocytes, show abnormal levels in ALS patient blood samples (McCombe et al., 2020). Here, we will focus on the T lymphocytes and peripheral macrophages, but it should be noted that there are many other peripheral immune cells that could influence the CNS as well as ALS disease progression.

1.7.1 T lymphocytes

In healthy circumstances, the CNS is almost completely secluded from the peripheral immune system. However, it is known that some peripheral immune cells, such as T lymphocytes, are able to sporadically enter the CNS to surveil the immune status (Hickey, 1991). During ALS, however, it seems that this infiltration turns from sporadic to constant, as infiltrating T lymphocytes, both CD4+ and CD8+, have been observed in ALS patient spinal cords in higher levels than in controls (Engelhardt et al., 1993; Troost et al., 1989). Deletion of CD8+ T lymphocytes in SOD1^{G93A} mice significantly decreases spinal motor neuron loss, suggesting that the T lymphocytes take part in neurodegeneration (Coque et al., 2019). While the triggering of the NF-κB pathway in T lymphocytes in the context of ALS has not been widely studied, it is known that T lymphocyte activation induces NF-κB signaling, and NF-κB is essential to several of the lymphocytes' immune responses (Gerondakis and Siebenlist, 2010; Liu et al., 2016).

1.7.2 Peripheral macrophages

Like the T lymphocytes, peripheral macrophages have been found infiltrated in the spinal cord of ALS patients (Troost et al., 1989). Characterization of peripheral macrophages in SOD1^{G93A} as well as SOD1^{G85R} mice has revealed pre-symptomatic peripheral macrophage activation that progressively infiltrates peripheral nerves (Chiu et al., 2009). Another study

using the SOD1^{G93A} model similarly observed pre-symptomatic peripheral nerve macrophage infiltration, but also revealed that at disease end-stage the peripheral macrophages had entered the spinal cord (Shiraishi et al., 2021). In SOD1^{G93A} mice, modifying peripheral macrophages was able to turn activated microglia to a more anti-inflammatory state, delay disease symptoms, and increase survival (Chiot et al., 2020). Macrophages have also been associated with another fALS associated gene, c9orf72. Deletion of c9orf72 in mice changes the immune response of macrophages and microglia and results in neuroinflammation (O'Rourke et al., 2016b). In the same way that NF-κB signaling is known to be important in T lymphocyte activation and response, the signaling pathway is also known to be a vital part of macrophage immune response (Q. Zhang et al., 2017). In a *Drosophila melanogaster* Alzheimer's disease model, Imd/NF-κB-inducing gram-negative bacterial infection causes macrophage recruitment to the brain, leading to neurodegeneration. In addition, Imd/NF-κB can mediate macrophage CNS invasion in *Drosophila* pupae. Still, the role of the NF-κB pathway in macrophages in the context of ALS has not been completely characterized, and warrants further study.

1.8 ALS animal models

ALS has been modeled by means of *in vitro* cell lines as well as for example *C. elegans*, *Drosophila melanogaster*, mouse, and rat animal models. In this thesis I will focus on some of the most commonly used *Drosophila* and mouse models, which I will present below.

1.8.1 *Drosophila* as a model animal

The fruit fly *Drosophila* has become a common model animal used to study biology and genetics, ever since it was used to prove chromosomal theory of inheritance by Thomas Hunt Morgan (Morgan, 1910). Through the creation of the balancer chromosome, the maintenance of genetic mutations in heterozygous stocks over generations was made possible. Since then, many *Drosophila* assays have been developed, and they can be used to study everything from behavior to protein interactions. As the techniques have evolved, fruit flies have become increasingly popular as model organisms, especially due to their cheap maintenance and short lifespan (Tolwinski, 2017). Yet another reason that *Drosophila* have become such a popular genetic tool is that the animal has only 4 chromosomes, and its genome is one of the most well-characterized (Kaufman, 2017).

Studying ALS using the fruit fly as a model presents both advantages and challenges. While the ease of genetic manipulation and short lifespan are useful factors, the orthologs of ALS-related proteins are not always present. OPTN, for example, does not have a *Drosophila* ortholog, making it impossible to introduce endogenous ALS mutations or perform a deletion of the gene. For the fALS associated protein FUS, TDP-43 and SOD1, however, several genetic models have been created, some of which I will present below.

SOD1

Unlike in the common SOD1^{G93A} mouse model, overexpression of mutant SOD1 has not been as effective for replicating several aspects of the ALS pathology in *Drosophila*. For example, a model overexpressing SOD1 mutant proteins in motor neurons using the Gal4 system causes climbing deficits, but no neuronal loss (Watson et al., 2008). Instead, one of the most representative SOD1 models is a recently made fly line incorporating ALS mutations in the endogenous *Drosophila* SOD1. SOD1 mutants G85R, H48R, and H71Y all caused shortened lifespan, neurodegeneration and locomotor deficits, effects that were however not seen with the SOD1 G37R mutation (Şahin et al., 2017).

FUS

In ALS cases with FUS mutations, it has not been completely established whether the pathology is based on loss- or gain-of-function. In *Drosophila*, both overexpression of FUS as well as deletion of the *Drosophila* FUS have been studied. When overexpressing FUS mutants R518K, R521C and R521H in the eye using the Gal4 system, neurodegeneration was observed. Expressing mutant FUS in adult fly neurons caused both shortened lifespan and decreased climbing ability (Lanson et al., 2011). The Caz[1] model, created by Wang et al (Wang et al., 2011), is on the other hand based on the deletion of the *Drosophila* FUS ortholog; Caz. When characterized, several ALS-like symptoms were observed in the fly strain. Caz[1] *Drosophila* has decreased eclosion, locomotor speed, and lifespan compared to control flies, and these phenotypes could be rescued by wild-type human FUS but not by ALS-associated mutant FUS.

TDP-43

Much like for FUS ALS cases, it is unclear whether TDP-43-based ALS is caused by loss-or gain-of-function mechanisms. Overexpression of human TDP-43 wild-type in different

neuronal subpopulations such as the mushroom bodies and the eyes already causes severe neurodegeneration, even in the absence of any ALS mutations (Li et al., 2010). In fact, when comparing overexpression of TDP-43 wild-type and TDP-43 ALS mutant A315T, TDP-43 wild-type gives more severe neuronal loss and shortened survival than A315T (Estes et al., 2011). Still, deletion of the *Drosophila* TDP-43 ortholog TBPH causes impaired eclosion and locomotion, as well as shortened lifespan (Diaper et al., 2013). Decrease in both frequency and amplitude of miniature excitatory junction potentials (mEJPs) can also be observed in these *Drosophila*. In addition to these loss- and gain-of-function models, Chang et al. have produced a model inserting the human TDP-43 gene with or without ALS mutations in place of the fruit fly *tbph* gene (Jer-Cherng Chang, David B. Morton*, 2017). The human TDP-43 wild-type completely rescues the absence of TBPH. Surprisingly, the ALS mutant lines also completely rescue the TBPH deletion, and show no defects in lifespan or development. The only defects observed in mutants is a slightly faster decline in negative geotaxis with age, and increased phosphorylated-TDP-43 staining in the case of the M337V mutant. All in all, the authors believe that additional environmental or genetic factors are needed to trigger additional disease-like phenotypes in these flies.

1.8.2 Mouse models of ALS

The creation of the first transgenic mouse at Massachusetts Institute of Technology in 1974 opened up many possibilities in mimicking and studying diseases (Vandamme, 2014). As is well known, using mice as model organisms of disease has many benefits. There is a strong conservation of genes and physiological systems between mice and humans (Dowell, 2011). In addition, compared to other mammals, mice have a short generation time and are convenient to keep (Phifer-Rixey and Nachman, 2015). Since the beginning of ALS research, many mouse ALS models have been created. However, completely imitating ALS has proved a challenge as many of the ALS-associated mutations discovered in patients do not result in similar symptoms in mice. As stated previously, for example, loss of function mutations in the OPTN protein are associated with fALS, but neither expression of mutant OPTN nor OPTN deficiency lead to any motor behavior phenotype in mice (Markovinovic et al., 2017). Below I will present a few of the ALS mouse models based on SOD1, FUS and TDP-43-associated ALS mutations.

SOD1

The most successful protein used in ALS mouse modeling has been the SOD1, and the first model based on overexpression of this protein is the SOD1^{G93A} mouse model. SOD1^{G93A} mice have a high overexpression of the human SOD1 protein with the G93A ALS mutation, leading them to develop a pathology that is very similar to the disease. It is one of the most famous and well-used ALS mouse models. Histopathologically, a selective loss of vulnerable motor neuron populations as well as neuroinflammation is observed. In addition, the oculomotor muscles that remain intact in human patients are also unaffected in the SOD1^{G93A} mouse model (Comley et al., 2016). Symptomatically, the mice experience a progressive muscle paralysis similar to that of patients (Gurney et al., 1994). At P60 a decrease is seen in the electrical signal detected in the *triceps surae* with sciatic nerve stimulation, suggesting a decreased neuromuscular function in the animals. In addition, motor neurons in all sections of the spinal cord significantly decrease during the lifespan of the mice. Behaviorally, this decrease takes effect at around P80 when the SOD1^{G93A} mice take significantly longer time to swim to a 1 meter distant platform than wild-type (Dirren et al., 2015). The clinical disease onset begins at P90 days, at which significant decrease of limb muscle innervation has already taken place. At the end stage, measured at approximately P135 days, up to 50% of cervical and lumbar motor neurons have been lost. At this point, the humane endpoint has been reached, meaning that the animals are not able to right themselves when placed on their backs (Chiu et al., 1995). Since the development of the SOD1^{G93A} model in 1994, models with mutations in G37R (Wong et al., 1995) and G85R (Bruijn et al., 1997) have been established, both showing similar pathology as G93A in overexpression models. Still, it should be noted that the pathology has not been consistent for all SOD1 ALS mutations. SOD1^{A4V}, for example, results in an aggressive form of ALS in humans, with patients surviving only around 2 years after disease onset (Saeed et al., 2009). However, when the human mutant protein is overexpressed in mice, the pathology is non-existent (Deng et al., 2006).

FUS

While not as well-known as the SOD1 mouse models, several FUS-based ALS mouse models have been developed, with varying similarities to the human disease. Deletion of FUS in mice results in frontotemporal lobar degeneration (FTLD) and hyperactivity that can be observed after 2 years of age, but no ALS-like pathology (Kino et al., 2015). However, when replacing

exon 15 of mouse FUS (mFUS) with human exon 15 FUS (hFUS) with a frameshift mutation, progressive motor neuron loss and longevity decrease after 22 months was found (Devoy et al., 2017). When using a murine prion promoter (PrP) to express human FUS^{R521C}, mice develop motor deficits and die within 4-6 weeks after disease onset (Qiu et al., 2014). Overexpression of wild-type hFUS using the PrP promoter also leads to a severe ALS-like phenotype with early motor symptoms and death withing 3 months (Mitchell et al., 2013). Indeed, it has been difficult to establish the basis of FUS-related ALS through these models as none of them depict the disease as closely as, for example, the SOD1^{G93A} model.

TDP-43

In the TDP-43 models that have been produced, overexpression of either wild-type or mutant protein gave very early neurological phenotypes, uncharacteristic of ALS. The highest overexpression led to death within the first few weeks, and the ALS-typical TDP-43 aggregation was absent (Lutz, 2018). When knocking out TDP-43 completely, you instead see embryonic lethality (Liu et al., 2013). Mice expressing hTDP-43 at close to endogenous levels using the CNS-specific PrP have been created with and without ALS mutations (Arnold et al., 2013). The mice start showing the first significant motor impairment around 10 months of age, and electrophysiological analysis indicated neuromuscular denervation. Similar strains have been created with TDP-43 wild-type or ALS mutants, and using different CNS-specific promoters such as PrP and the Thy1 promoter, all causing different levels of ALS-like symptoms (Hatzipetros et al., 2014; Stallings et al., 2013; Wils et al., 2010; Xu et al., 2011, 2010). However, these mouse strains all still have presence of mouse TDP-43 (mTDP-43) in addition to the expression of hTDP-43, which could lead to unforeseen effects. It has also been observed that TDP-43 itself can autoregulate its own synthesis, something that has to be taken into account when drawing conclusions from any model expressing TDP-43 at non-endogenous levels (Polymenidou et al., 2011). One mouse strain, however, has been created using CRISPR/Cas9 technology inserting an equivalent of the human ALS mutation Q331K in the mTDP-43. This strain is therefore expressing mutated mTDP-43 at completely endogenous levels. Interestingly, these mice showed no significant motor impairment and instead showed weakened memory (White et al., 2018). This could suggest that an additional trigger is needed to induce severe ALS-like phenotypes.

1.8.3 Expression levels and disease modeling

In the models that I have presented above, both in *Drosophila* and mice, it has become clear that inducing any sort of severe ALS phenotype seems to require either overexpression or deletion of an ALS associated protein. While SOD1-based ALS is well depicted in the mouse overexpression models, suggesting a gain-of-function mechanism, the same cannot be said for FUS and TDP-43-based models. In many cases, FUS and TDP-43 deletion and overexpression can both lead to very similar ALS-like pathologies. This calls into question how to interpret the results we get when treating an ALS model, as we are not sure whether we are accurately depicting the disease to begin with.

It also raises the question of how we can model ALS in the way that is most similar to what happens in patients. It has been observed that endogenous expression levels of ALS related genetic mutations have not been able to induce severe disease in mice or *Drosophila*. However, this does not necessarily mean that humans have evolved to be more penetrant to theses mutations, but perhaps that the genetic mutations we have found are not the sole triggers of disease. This goes in line with papers suggesting that for some ALS-related genes, genetic mutations need to be triggered to induce disease, whether this be by an environmental stimulus or other genetic interactions (Jer-Cherng Chang, David B. Morton*, 2017; Yu and Pamphlett, 2017).

1.9 Current ALS treatments

Currently, there is not cure for ALS, but there are some potentially life-extending treatments and several drugs that are being tested. The most common drug used is Riluzole, which blocks glutamate release and can prolong the lives of patients by a few months (Mejzini et al., 2019). Recently, the antioxidative drug Edaravone has been approved in a few countries, as it can moderately decrease the functional loss in patients. The new drug Relyvrio, has just approved by the FDA, and will soon start to be used in patients. It is meant to relieve mitochondrial dysfunction and endoplasmatic reticulum stress (Paganoni et al., 2020). A potential future therapeutic is the SOD1 antisense oligonucleotide Tofersen, which decreases SOD1 expression in fALS SOD1 patients. While the phase 3 clinical trial was not able to show improvements within the 28 week primary endpoint, after the 52 week extension phase, there were symptom improvements in the patients that had been administered Tofersen (Miller et al., 2022).

As the studies of neuroinflammation and its effect on ALS progression have increased, so have the clinical trials testing different anti-inflammatory drug options in patients. For example, an inhibitor of known pro-inflammatory protein TNFα, which has been a successful therapeutic target in ALS mouse studies, has been tried in patients. However, the TNFα inhibitor, named Thalidomide, showed no improvement and induced several side-effects (Stommel et al., 2009). In a similar way, a pilot study using an IL-1 blocker was able to decrease levels of an inflammatory marker but did not lead to any reduction in disease progression (Maier et al., 2015). A drug that blocks the IL-6 receptor to decrease neuroinflammation is also being tested (Liu and Wang, 2017; Mizwicki et al., 2012). An inhibitor of NF-κB signaling specifically in macrophages and monocytes, named NP001, has also recently been tried in ALS patients. The drug was not able to reduce the general progression of disease, but in the subset of patients with a higher systemic inflammation baseline, progression of disease slowed down (Miller et al., 2015). All in all, anti-inflammatory drugs have so far failed to produce a slowed progression of ALS in patients. However, this could be due to many reasons. For example, not high enough dose, incorrect means of administration, or not targeting the relevant cells. All of these theories need to be further studied to be able to say if anti-inflammatory drugs could one day provide useful treatment for ALS patients.

1.10 Aims of the thesis

ALS is a neurodegenerative disorder in which neuroinflammation and the activation of the NF-κB pathway has been observed. In this thesis, I used both *Drosophila melanogaster* and mice to model ALS and investigate the link between NF-κB and disease pathology.

The first and second aims of this thesis was to generate FUS and TDP-43 based *Drosophila* ALS models that replace the fly genes with the human gene orthologs, with or without ALS mutations, expressing the proteins at an endogenous level and pattern. The majority of current models existing are based on either loss or gain of function, which does not replicate the conditions in patients. Therefore, we used CRISPR/Cas9 technology to generated humanized FUS and TDP-43 *Drosophila*, and characterized them through assessing their eclosion rate, longevity, subcellular protein localization, motor behavior, and neuromuscular junctions.

In the third chapter, we use previously created fly models containing deletions of the *Drosophila* FUS and TDP-43 orthologs, Caz and TBPH, to assess the effect of inhibiting the immune NF-κB pathway on their ALS-like phenotypes.

In the fourth chapter, we use gram-negative bacterial infection in the humanized ALS models created in chapters one and two, to trigger the NF-κB pathway in these *Drosophila*. We predict that activation of NF-κB could further increase ALS phenotypes through inducing neuroinflammation.

The final aim of this thesis was to investigate the therapeutic potential of NF-κB inhibition in an ALS mouse model, through the use of AAV vectors. We create two different vectors, each inhibiting NF-κB with different promoters, and measure the behavioral changes and compound muscle action potential of the mice, as well as analyze the spinal cord tissue using immunohistochemistry after sacrifice.

2

Chapter 2 – Expression of human FUS in place of *Drosophila* ortholog rescues *Drosophila* FUS deletion phenotype, while ALS mutant FUS expression causes only mild ALS pathology

- -

Emma Källstig, Evelyne Ruchti, Bernard Schneider, Brian McCabe

Creation of the hFUS wild-type and mutant Drosophila by Emma Källstig and Evelyne Ruchti; all other experiments performed by Emma Källstig.

2.1 Abstract

FUS, a mostly nuclear protein involved in mRNA splicing, gene expression, and DNA repair, has been linked to 5% of familial ALS cases. Here, we used CRISPR/Cas9 genome engineering to create humanized FUS *Drosophila melanogaster*, in which replace the *Drosophila* FUS ortholog is replaced with human FUS, wild-type or one of three ALS mutants (R495X, R521H, and R522G). Hence, human FUS is expressed at endogenous level and pattern. We find that expression of wild-type hFUS rescues Caz-/- development deficits. The only difference observed between hFUS wild-type and control is a slight motor behavior deficit, whereas longevity, fertility and neuromuscular junction (NMJ) morphology are comparable to control. Only one of the three humanized ALS mutants, R495X, has a mildly decreased longevity and a significant motor deficit, while the two other ALS mutants (R521H and R522G) do not. We also observed that mutants R495X and R522G partly mislocalize to the cytoplasm in neurons, whereas R521H does not. None of the ALS mutants show any observable effects on NMJ structure, and we hypothesize that an additional genetic or environmental trigger is necessary to induce a more severe ALS-like phenotype in this model.

2.2 Introduction

In 2009, mutations in the FUS gene were first reported to be linked to about 5% of fALS cases (Lanson and Pandey, 2012). The majority of these patients develop an aggressive disease course with a younger than average disease onset (Nolan et al., 2016).

FUS encodes a 526 amino acid long protein containing 15 exons, that includes an N-terminal transcriptional activation QGSY-rich domain, three nucleic acid binding RGG domains, as well as a Zinc finger domain, an RNA recognition motif, and a C-terminal nuclear localization signal (NLS) (Deng et al., 2014). Normally, the NLS causes the FUS protein to be mostly present in the nucleus. There, it is thought to be involved in regulating both mRNA splicing and gene expression, as well as being involved in DNA repair, although all of its functions are not yet elucidated (Morgan and Orrell, 2016). In ALS, over 50 mutations in FUS have so far been reported, with a majority being characterized by autosomal dominant inheritance (Nolan et al., 2016). The mutations have been observed in several regions of the protein, but many mutations, including one of the most common FUS mutations observed in humans, R521H, are localized to the C-terminus NLS. These mutations cause cytoplasmic accumulation and aggregation of FUS, as well as changes in the dynamics of stress granules (Vance et al., 2013).

Some have theorized that the cytoplasmic localization, aggregation, and toxic disruption of stress granule dynamics causes a toxic gain-of-function, leading to pathology. For example, a study has shown that FUS ALS mutants, but not FUS wild-type assemble into perinuclear stress granules proportionally to their cytoplasmic expression level (Bosco et al., 2010). The observed changes in subcellular FUS localization caused by mutations also suggest that loss-of-function mechanisms may lead to ALS motor neuron degeneration, through the impairment of its normal nuclear functions including splicing, transcription, and DNA repair, which in turn could affect genes linked to neuronal survival (Ishigaki and Sobue, 2018). Several FUS-based ALS animal models have been created, and the observed phenotypes support both the loss- and gain-of-function theories. In *Drosophila,* for example, eye-specific overexpression of FUS mutants R518K, R521C and R521H cause neurodegeneration (Lanson et al., 2011). Likewise, neuronal expression of these mutants led to decreased lifespan and climbing ability. A mouse model overexpressing human FUS (hFUS) wild-type also causes aggressive ALS symptoms such as hind limb paralysis and severely reduced lifespan (Mitchell et al., 2013). Still, loss-of-function models have also showed phenotypes reminiscent of ALS. In zebrafish, knockdown of FUS expression causes a motor phenotype

that can be rescued by wild-type, but not ALS mutant, FUS (Kabashi et al., 2011). Similarly, in *Drosophila melanogaster*, deletion of the *Drosophila* FUS ortholog, Caz, also leads to severe phenotypes including a dramatic decrease in the eclosion rate, shortened lifespan, and reduced locomotor speed (Wang et al., 2011). FUS wild-type can rescue these phenotypes, unlike ALS mutant FUS. However, mice with a knockout of the mouse FUS ortholog do not display any ALS phenotypes, but instead showed early behavioral defects such as hyperactivity and reduction of anxious behavior related to frontotemporal lobar degeneration (FTLD) (Kino et al., 2015).

As becomes evident from these studies, it is still unclear by which mechanisms FUS mutants lead to the pathology observed in familial ALS. Importantly, none of these animal models are completely recapitulating the genetic conditions of ALS patients, where the FUS protein itself is neither overexpressed nor fully inhibited. The animal model with the closest depiction of the patient genetic makeup thus far is the FUSDelta14 mouse model, where the mouse FUS exon 15 is replaced by the human version of the exon including a frameshift mutation. This model results in a significant lifespan difference observed only after 22 months, and while progressive spinal motor neuron loss was observed, no FUS aggregation was found (Devoy et al., 2017).

Our aim was to create a *Drosophila* FUS-based ALS model that as closely as possible mimics the genetic conditions seen in patients, conserving the level and pattern of FUS protein expression observed in this organism, and that can be used to study the mechanisms behind FUS pathology. To do this, we used CRISPR/Cas9 technology to generate a humanized FUS model, expressing human FUS (hFUS) from the endogenous *Drosophila caz* locus. In addition, we made three other versions of this line, each containing a different FUS C-terminal ALS mutation (R495X, R521H, and R522G). We found that expression of hFUS in place of Caz can fully rescue the decreased eclosion rate in Caz-/- *Drosophila*. Longevity, fertility, and neuromuscular junction (NMJ) morphology are also comparable to control, and the only difference observed between control and hFUS wild-type is a slight motor deficit. In the R495X and R521H FUS mutants, we observed a mild decrease in lifespan compared to FUS wild-type control, and slightly declined motor abilities in the R495X. The R522G and R495X mutants also show partly cytoplasmic mislocalization in neurons. Interestingly, we do not see any difference between FUS mutants' NMJs compared to control. These modified *Drosophila* can be used to explore additional genetic or environmental triggers of a more severe ALS phenotype.

2.3 Results

2.3.1 Generation of FUS knock-in *Drosophila*

In order to investigate the effects of endogenous expression of hFUS wild-type and hFUS ALS mutant protein in *Drosophila,* we aimed to create hFUS knock-in flies by replacing the expression of the endogenous *Drosophila* FUS ortholog, Caz. To this end, hFUS wild-type cDNA followed by a dsRed cassette marker, was cloned into a backbone plasmid (figure 1A). The construct also included the following additional genetic tools that could be used to further modify the fly line in the future: to enable creation of a full knockout of Caz gene expression, PiggyBac sites, which can excise the inserted sequence by mating with a fly line expressing the PiggyBac transposase, were placed on each side of the insert. PhiC31 attP sites were put in place to enable replacement of the insert with another insert of choice through plasmid injection with PhiC31 integrase. To remove the dsRed cassette, LoxP sites were added to each side of it, enabling excision when mated to a fly line expressing the Cre recombinase. In addition, two guide RNAs were cloned into pCFD3 plasmids, to be injected together with the hFUS gene into *Drosophila* embryos and enable CRISPR/Cas9-based insertion of the construct. Further information about the creation of humanized *Drosophila* can be found in the Annex.

The plasmids were injected into fly embryos by Genetivision Corportation (USA), and we received dsRed-positive fly lines of each genotype. The lines were sequenced to ascertain correct insertion, and backcrossed six generations into a w[1118] control line to ensure minimal differences in genetic background. Through western blot, we were able to confirm the expression of hFUS and the absence of the fly ortholog Caz (figure 1B). When quantifying the hFUS protein expression, we found that the relative hFUS protein expression was higher in ALS mutants R522G and R521H as compared to wild-type hFUS (figure 1C). Expression of the R495X mutant, on the other hand, was lower than hFUS wild-type expression, although this difference did not reach statistical significance. As Caz is thought to autoregulate itself, the high expression of R522G and R521H could be attributed to the mutations causing defects in autoregulation (Jäckel et al., 2015). As for the R495X mutation, on the other hand, it is possible that the fact that the mutation causes a premature stop codon could play a role in the decreased protein expression. Early stop codons are known to be able to cause destabilized mRNA, which in turn would lead to lower levels of protein translation (Gorgoni et al., 2019).

Figure 2-1. CRISPR/Cas9 technology was used to create humanized FUS *Drosophila*
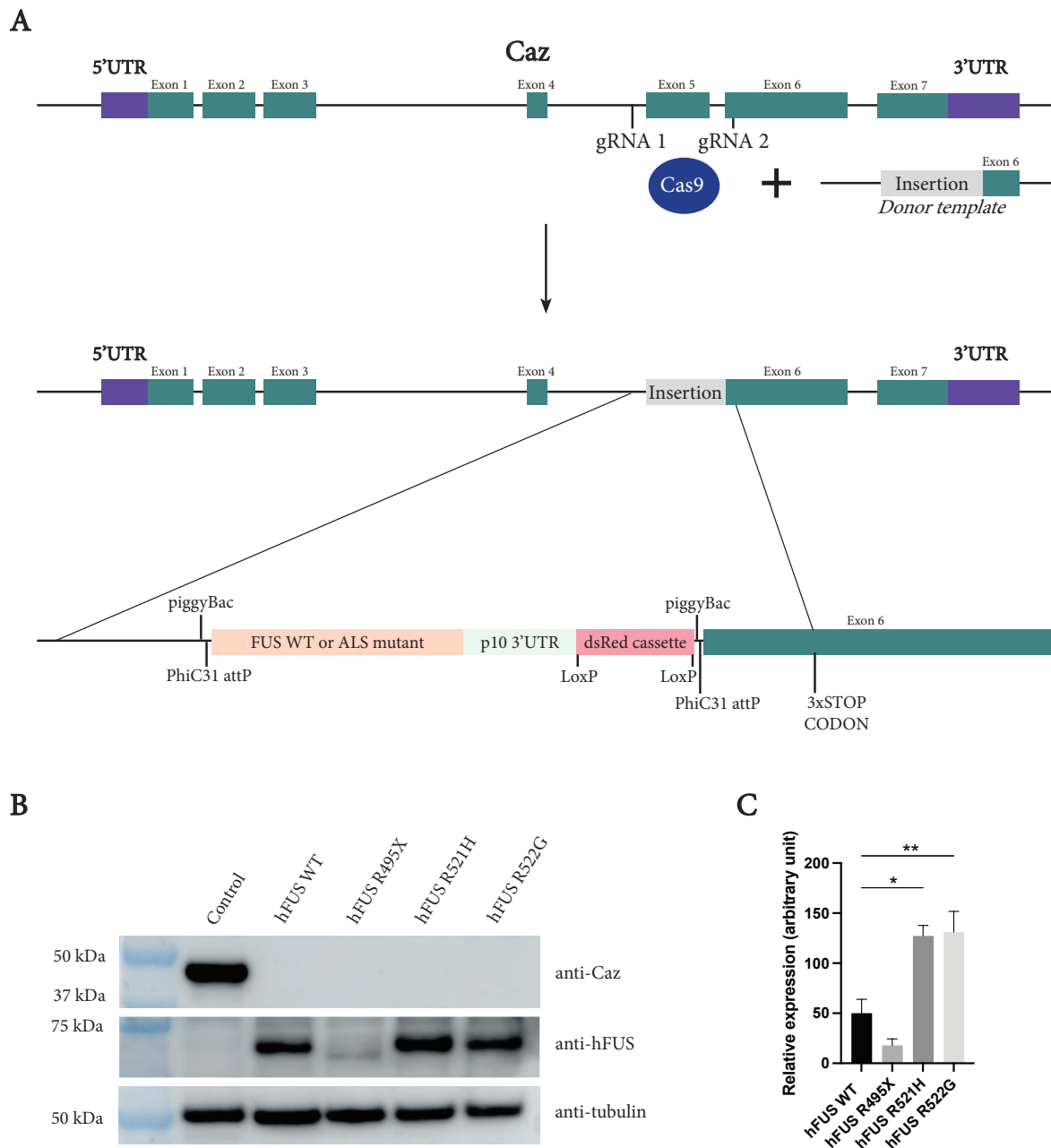
Figure 1: Using CRISPR/Cas9 technology, hFUS wild-type and hFUS ALS mutants R495X, R521H, and R522G knock-in *Drosophila* were created. (A) Two CRISPR/Cas9 guide RNAs (gRNA 1 and 2) targeting the intron before exon 5 and exon 6, respectively, were used to insert the hFUS wild-type and hFUS ALS mutants R495X, R521H, and R522G into the *caz* gene. The FUS construct includes several different genetic tools (piggyBac, PhiC31, and LoxP sites) to enable removal/substitution of different parts of the insert. The construct also includes a dsRed cassette driven by an eye-specific promoter as a marker. (B) Western blot depicting the hFUS and Caz expression levels. (C) Quantifications of hFUS relative protein expression levels in the different

hFUS knock-in lines, calculated with tubulin as reference, with mutants R521H and R522G having a significantly higher relative hFUS expression than hFUS wild-type. (n = 3). Data are presented as mean ± standard error of the mean; statistical analysis: one-way ANOVA with Dunnett's Multiple Comparisons post-hoc test comparing all genotypes to hFUS wild-type.

2.3.2 Expression of both hFUS wild-type and mutant hFUS rescues the development of Caz knock-out *Drosophila*

After confirmation of hFUS protein expression, the effects of the insertion of the human ortholog gene on *Drosophila* development were evaluated. To do this, a known number of *Drosophila* L3 larvae were placed in a fresh vial to determine the fraction of adult *Drosophila* able to eclose. The number of adult flies eclosed was then calculated as a percentage of the number of larvae originally placed in the vial, to reflect how many of the *Drosophila* that were able to develop into adults. As can be seen in figure 2A, around 80% of control larvae developed to adult flies, while if the larvae had a deletion of the *Drosophila* hFUS ortholog, Caz, only around 4% of the larvae eclosed into adults. In the *Drosophila* expressing hFUS wild-type, the eclosion was rescued to around 70%, which is not significantly different compared to control. Remarkably, all three hFUS ALS mutant lines also showed a complete rescue of eclosion rate, comparable to control. This demonstrates that there are no significant defects in eclosion ability in any of the hFUS lines, regardless of the presence of ALS mutations, suggesting that both hFUS wild-type and ALS mutants can completely rescue the role of Caz during *Drosophila* development.

2.3.3 Severe ALS FUS mutations induce sterility in male *Drosophila*

As the *Drosophila* lines were being kept over several generations, it soon became evident that the ALS mutant lines had a phenotype that is not known to be associated with ALS: complete or partial sterility (Uysal et al., 2021). In order to quantify this, we mated a single male from each line with a single control virgin female and counted the progeny. From these experiments we could clearly see that while the hFUS control and hFUS R521H both have a similar number of progenies as control, the hFUS R522G and R495X showed significant decreases in number of progeny, with R495X being completely sterile (figure 2B). We did not perform the experiments with females, as obtaining homozygous females is impossible with the completely sterile males from the R495X line. Interestingly, the degree of sterility that the male *Drosophila* show mirrors the degree of disease severity that each mutation

causes in ALS patients, with R495X causing the most aggressive form of ALS in humans as well as complete sterility in flies (Waibel et al., 2010). It is worth noting that the *caz* gene is located on the X chromosome (Stolow and Haynes, 1995). While male fertility is more commonly associated with the Y chromosome, the X chromosome as well as the autosomes also contain genes related to male fertility (Lindsley et al., 2013; Zhang et al., 2020).

2.3.4 The longevity of *Drosophila* expressing hFUS wild-type is even longer than that of control, while hFUS mutants R521H and R495X have slightly shorter lifespan

As one of the main symptoms of ALS is a severely decreased lifespan, we measured the longevity of the different fly lines (figure 2C-F). hFUS wild-type had a small but significantly increased longevity relative to wild-type control, whereas hFUS R522G remained similar to hFUS wild-type control. hFUS R521H and hFUS R495X, on the other hand, displayed a significantly shorter lifespan than hFUS wild-type. It is still noteworthy, however, that these differences are modest compared to human ALS.

Figure 2-2. The eclosion, lifespan, and fertility of the humanized FUS *Drosophila*
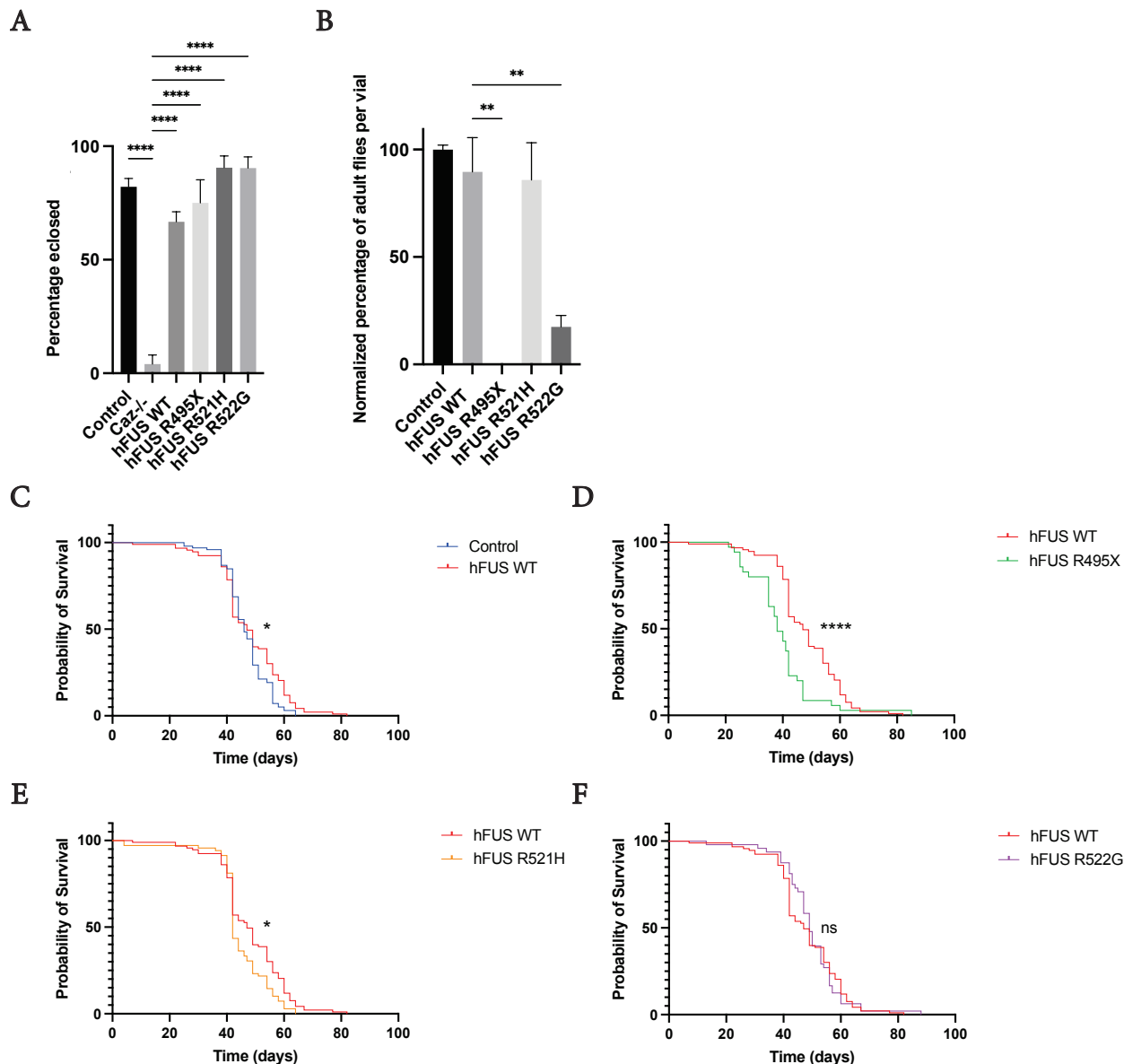
Figure 2: Humanized hFUS wild-type and ALS mutants all rescue the development of Caz-/- *Drosophila*, but in adult *Drosophila*, R495X and R521H have decreased lifespan compared to hFUS wild-type. (A) Caz-/- causes significantly decreased eclosion rate, while hFUS wild-type as well as all hFUS ALS mutants rescue this effect (n≥53 larvae per group). (B) hFUS wild-type and hFUS R521H male *Drosophila* have a similar fecundity while mutant hFUS R522G has a severely decreased fertility and hFUS R495X male *Drosophila* are completely sterile (n=3 crosses per genotype). Lifespan of the humanized FUS lines: (C) Control (blue, n=99) compared with hFUS wild-type (red, n=93) (D) hFUS wild-type compared with hFUS R495X (green, n=35) (E) hFUS wild-type compared with hFUS R521H (orange, n=78) (F) hFUS wild-type compared with hFUS R522G (magenta, n=48). The same hFUS wild-type data is used in C-F. All longevity data for the different genotypes are from the same experiment but separated into different graphs only for ease of

visualization. Data are presented as mean ± standard error of the mean; statistical analysis: one-way ANOVA with Tukey's Multiple Comparisons post-hoc test (A-B), and Mantel-Cox test (C-F).

2.3.5 hFUS R495X *Drosophila* show mild motor deficits compared to hFUS wild-type

As we observed some mild differences in lifespan when comparing the hFUS controls and mutants, we aimed to assess one of the other hallmark symptoms of ALS in humans: motor behavioral deficits. Here, we used a negative geotaxis assay. The *Drosophila* were placed in glass vials and were tapped down to the bottom of the vial. Due to an innate escape response, falling to the bottom of the vial triggers the flies to climb up the walls of the vial (Gargano et al., 2005). Through this assay, we found that the geotactic behavior of hFUS wild-type *Drosophila* was significantly worse than controls, an effect that is the most visible around 15 days, and which could be attributed to differences between Caz and hFUS (figure 3). Surprisingly, the motor phenotype of the ALS mutants hFUS R521H and hFUS R522G was nearly identical to the hFUS wild-type animals. The hFUS R495X mutant, however, showed significant climbing deficits, unlike the rest of the genotypes. Altogether, the R495X *Drosophila* showed mild phenotype characterized by shortening of lifespan and decrease of climbing abilities. However, these differences were exclusively observed in this mutant, and motor behavior deficits were remarkably absent from the other two ALS mutant lines.

Figure 2-3. Negative geotaxis behavior of the humanized FUS *Drosophila*
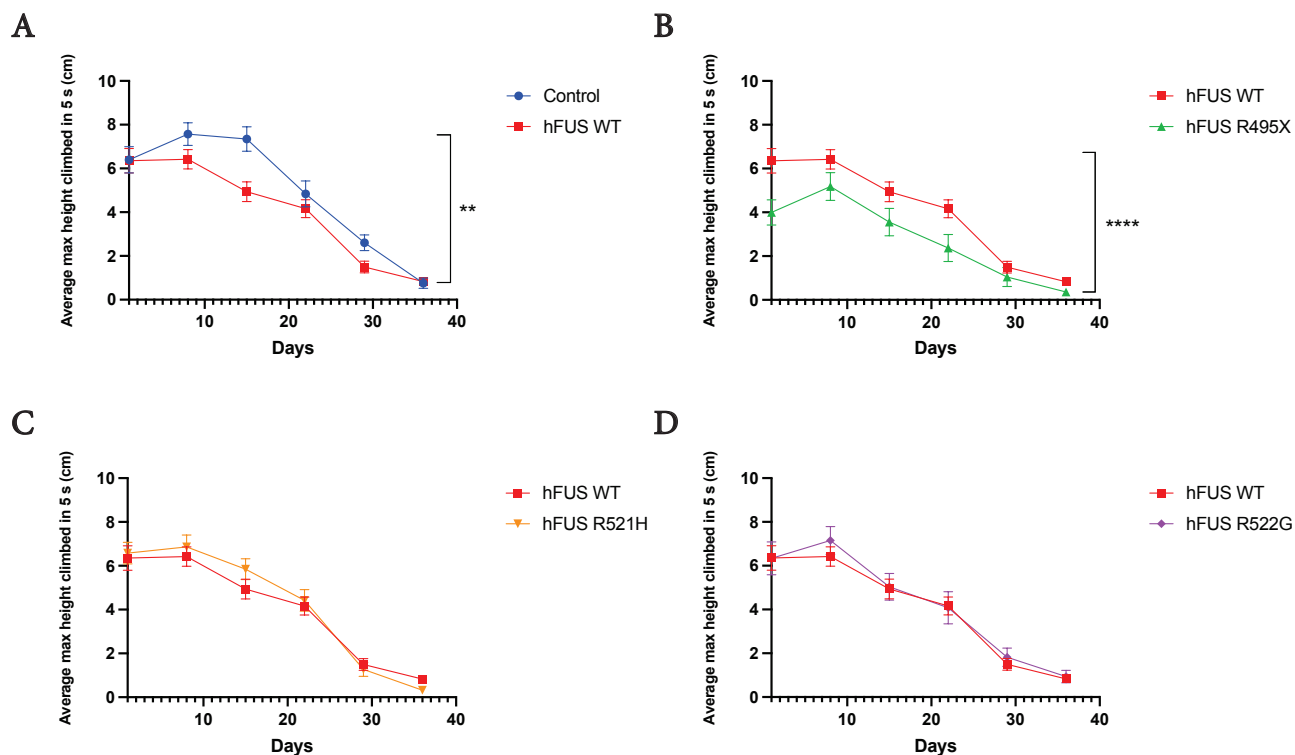
Figure 3: Negative geotactic motor behavior of humanized hFUS wild-type and mutated hFUS *Drosophila* shows mild motor deficits in *Drosophila* expressing hFUS R495X. The graphs show the average max height climbed by the flies in 5 s, as a function of their age. (A) Control (blue, n= 30 flies at day 1) compared with hFUS wild-type (red, n=30 flies at day 1). (B) hFUS wild-type compared with hFUS R495X mutant (green, n=18 flies at day 1). (C) hFUS wild-type compared with hFUS R521H mutant (orange, n=30 flies at day 1). (D) hFUS wild-type compared with hFUS R522G mutant (magenta, n=25 flies at day 1). hFUS wild-type shows a slightly decreased motor ability compared to control. The only hFUS mutant with a significant motor behavior deficit compared to hFUS wild-type is hFUS R495X. The same hFUS wild-type data is used in A-D. All negative geotaxis data for the different genotypes are from the same experiment but separated into different graphs only for ease of visualization. Data are presented as mean ± standard error of the mean; statistical analysis: two-way ANOVA with Dunnett's Multiple Comparisons post-hoc test looking at the main effect of each genotype and comparing all genotypes to hFUS wild-type.

2.3.6 Cellular localization of the hFUS protein

The *Drosophila* FUS ortholog, Caz, is known to be expressed strongly in the fly head, but we also wanted to assess the expression of hFUS in the fly spinal cord equivalent, known as the ventral nerve cord (VNC), in our newly created humanized *Drosophila* (Stolow and Haynes, 1995). Firstly, we aimed to visualize the pattern of endogenous Caz protein expression in controls, and compare it to the hFUS wild-type expression (figure 4). In the control, we also

used elav-Gal4 to drive UAS-histone-GFP, to visualize neuronal nuclei. In the hFUS wild-type fly, on the other hand, we instead used an elav antibody. As can be seen in figure 4, when comparing the control and hFUS wild-type images, the expression did not completely overlap. We suspect that this is either due to antibody affinity or differences in post-translational processing, as both hFUS and Caz share the same promoter and should be expressed in the same pattern.

To more specifically evaluate if hFUS is expressed in neurons, glia, or both, in the VNC we used anti-elav to stain neuronal nuclei, anti-repo to stain glial nuclei, and anti-hFUS to visualize the hFUS protein. We found a strong co-localization between hFUS and neurons in all the humanized genotypes. However, glial cells did not seem to express high levels of hFUS compared to neurons (figure 5). Indeed, in the VNC, neurons appeared to be the cell type most strongly expressing hFUS.

Figure 2-4. The expression pattern of hFUS is comparable to that of endogenous Caz
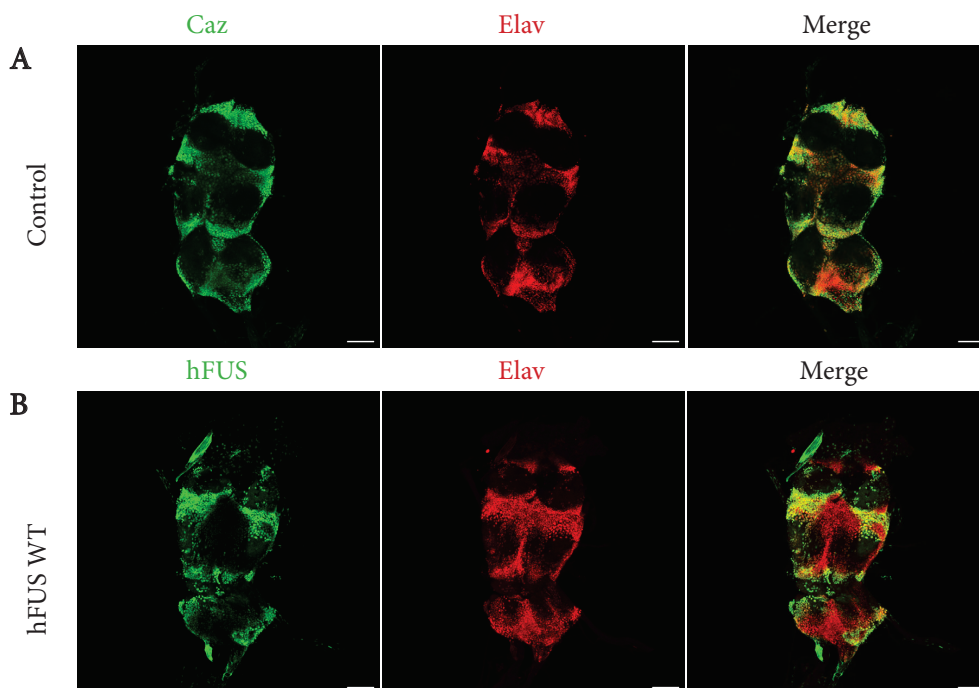
Figure 4: The expression pattern of hFUS is comparable to that of endogenous Caz. Images of full VNCs, in (A) control stained for endogenous Caz expression (green), with elav-Gal4 used to express UAS-histone-GFP (red) in neuronal nuclei and (B) hFUS wild-type stained for hFUS expression (green), with anti-elav used to stain for neuronal nuclei (red). The pattern of Caz and hFUS expression differ slightly, though this may be due to difference in antibody affinity or post-translational processing. The scale bar is 50 μm.

All three ALS mutations, that were induced into the humanized FUS *Drosophila*, cause a disruption in the protein's NLS. Based on this, we stained *Drosophila* VNCs with anti-hFUS antibody, and anti-elav to visualize neuronal nuclei, to assess the localization of the hFUS protein within the cell. We found that wild-type hFUS is mainly nuclear, similarly to what has been observed in previous studies (figure 6C) (Åman et al., 1996; Andersson et al., 2008; Dormann et al., 2010). R521H, the mutation which causes the least severe disease in patients, was also mainly localized to the cell nucleus (figure 6D). R522G, however, showed some cytoplasmic FUS, and the most severe ALS mutant R495X was clearly both nuclear and cytoplasmic (figure 6E-F).

Figure 2-5. hFUS expression in the ventral nerve cord cells
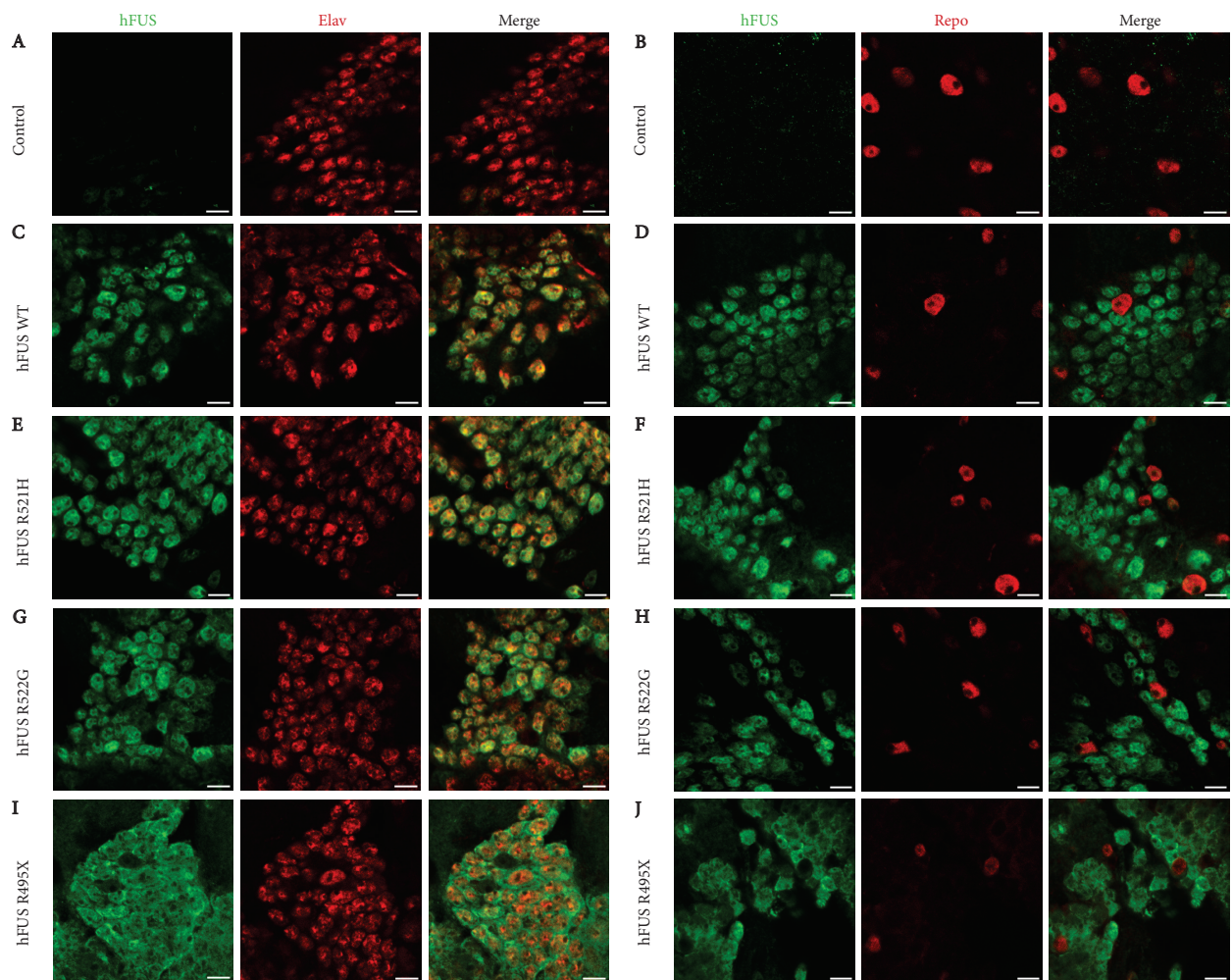
Figure 5: hFUS is expressed within neurons in the ventral nerve cord, and is only weakly expressed in glial cells. The ventral nerve cords of the different genotypes were dissected out and hFUS staining (green) was

co-stained with either anti-elav (red, A, C, E, G, I) to visualize the neuronal nuclei or anti-repo to visualize glial nuclei (red, B, D, F, H, J). (A-B) Control stained with anti-elav or anti-repo (C-D) hFUS wild-type stained with anti-elav or anti-repo (E-F) hFUS R521H stained with anti-elav or anti-repo (G-H) hFUS R522G stained with anti-elav or anti-repo (I-J) hFUS R495X stained with anti-elav or anti-repo. Note the low expression of hFUS in glial nuclei, as opposed to the strong expression of hFUS in neuronal nuclei. The scale bar is 5 μm.

Figure 2-6. Subcellular hFUS expression
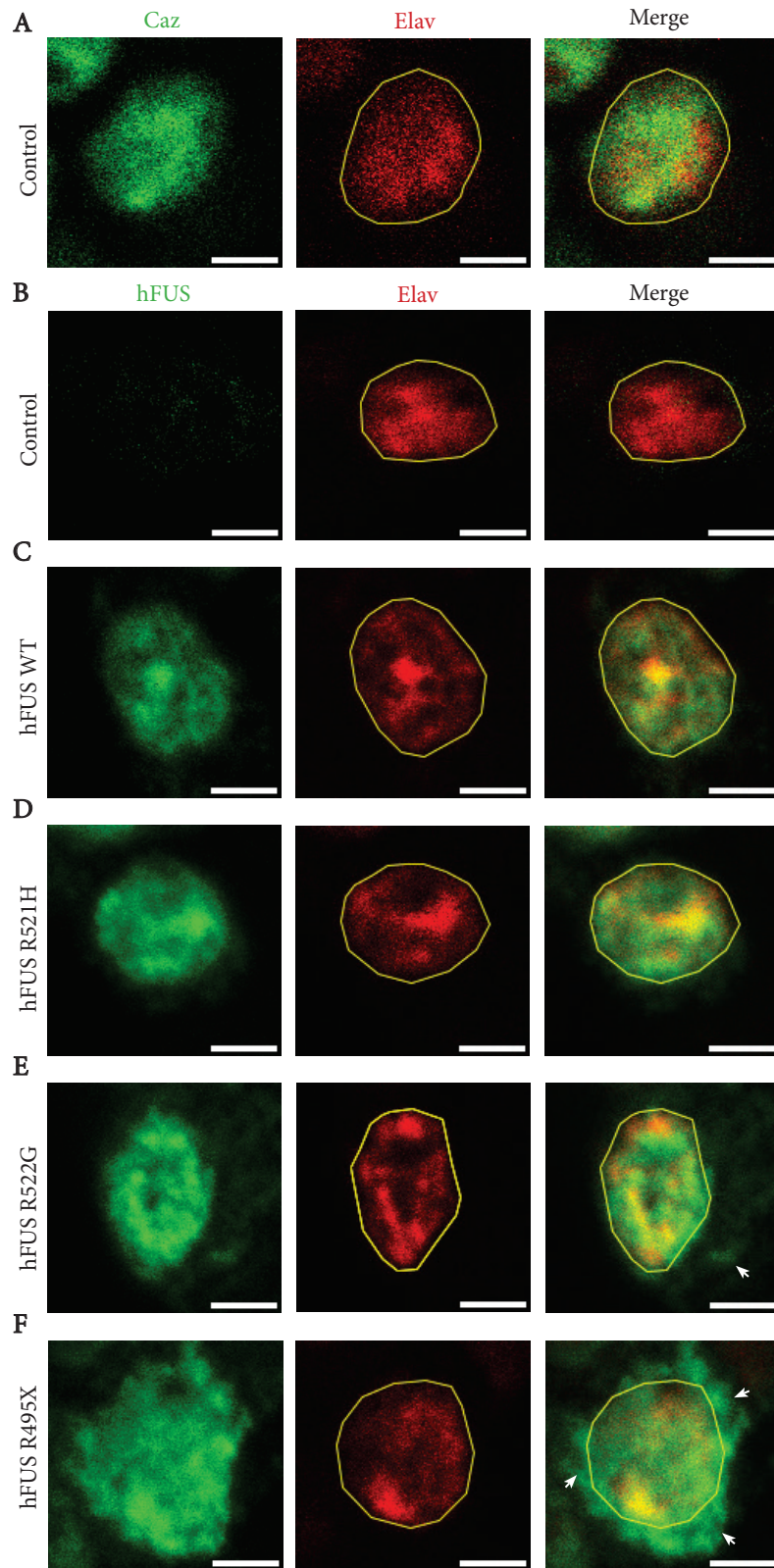
Figure 6: hFUS is nuclear in hFUS wild-type *Drosophila*, but shows some cytoplasmic localization in ALS mutants R522G and R495X. The images show individual neurons in the ventral nerve cords of the different

genotypes. (A) Endogenous Caz expression was stained using anti-Caz antibody (green), while the neuronal nuclei were visualized using expression of UAS-histone-GFP by elav-Gal4 (red). Note that Caz is mainly localized to the nucleus. (B-F) Anti-hFUS was co-stained with neuronal nuclear marker anti-elav (red) to visualize hFUS (green) localization in the neurons in control, hFUS wild-type, hFUS R521H, hFUS R522G, and hFUS R495X. hFUS wild-type is localized mainly to the nucleus, similarly to the localization of endogenous Caz. hFUS mutants R522G and R495X, on the other hand, both show some cytoplasmic localization. A yellow outline around the neuronal nuclear staining has been made in ImageJ to clarify the location of hFUS. White arrows point out locations were hFUS appears not nuclear. The scale bar is 2 μm.

2.3.7 In humanized FUS *Drosophila*, the neuromuscular junctions are similar to controls

Since ALS is characterized by the loss of neuromuscular junctions (NMJs) (Cappello and Francolini, 2017). To assess the presynaptic NMJ area and the density of active zones, we examined the bilateral terminals of motor neurons that innervate the muscles in the third abdominal segment of the flies 4-5 days post-eclosion (figure 7A-F). Since these NMJs are known to be glutamatergic, anti-VGLUT staining was used to visualize the presynaptic area, and the area of the staining was measured. We found no significant differences in NMJ presynaptic area in any genotype compared to control (figure 7I). To further characterize this, we also co-stained the NMJs with anti-Bruchpilot, which stains the active zone synaptic vesicle release site (figure 7G). As for the presynaptic area, we did not find any significant differences between mutants and controls (figure 7H). While NMJs seem comparable across conditions in young *Drosophila*, it remains possible that differences may appear during ageing.

Figure 2-7. hFUS knock-in fly neuromuscular junctions
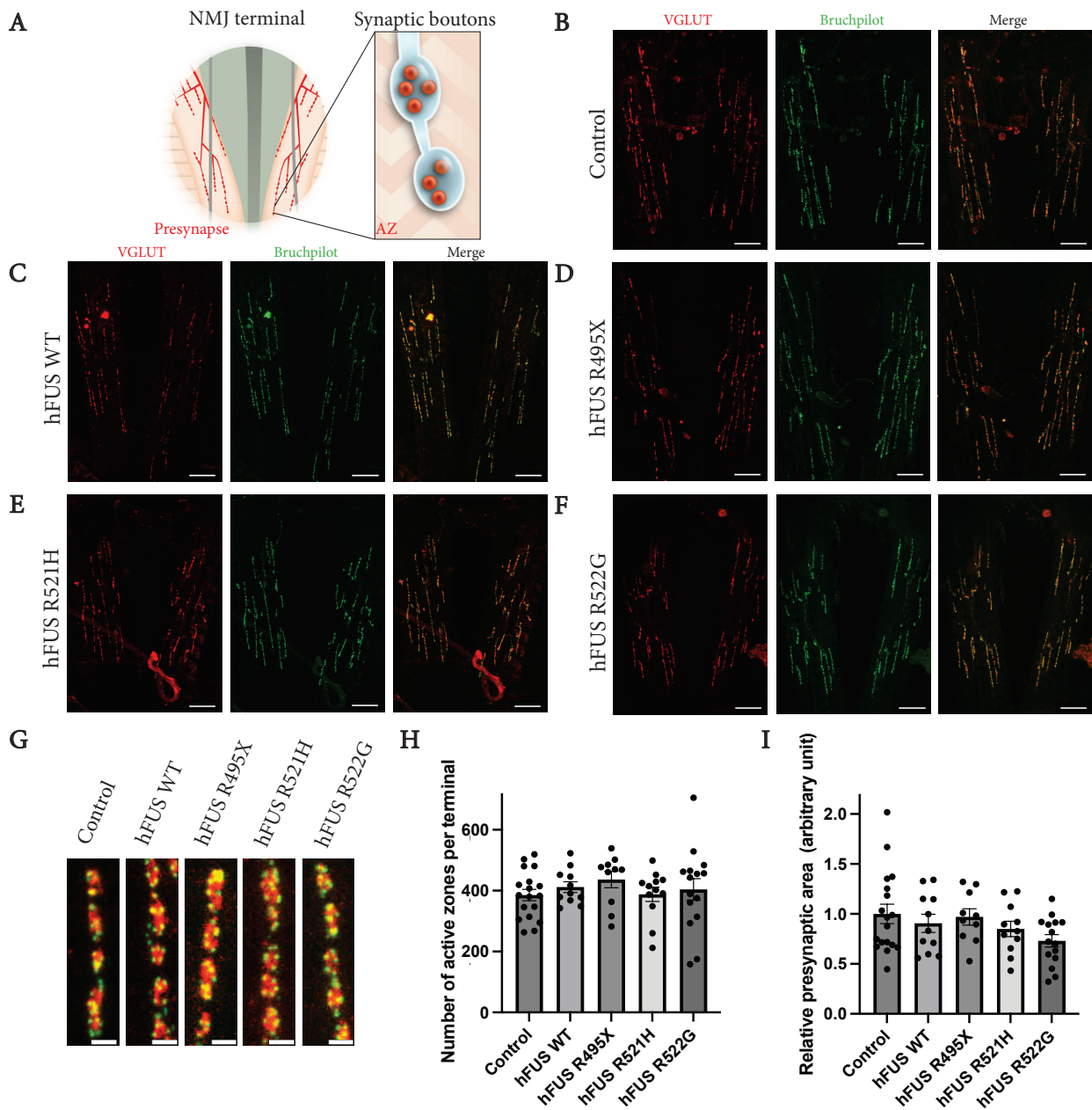
Figure 7: hFUS knock-in *Drosophila* have neuromuscular junction presynaptic areas and active zone numbers comparable to control flies. (A) Illustration of the bilateral NMJ terminal in abdominal segment 3 of a *Drosophila*, as well as a magnification of synaptic boutons with active zones (AZ) of synaptic vesicle release (both the presynaptic terminal and active zones shown in red). (B-F) Images of NMJ terminals in abdominal segment 3 stained for the presynaptic marker VGLUT (red) and the active zone (AZ) marker Bruchpilot (green) in control, hFUS wild-type, hFUS R495X, hFUS R521H, hFUS R522G. (G) Magnified images of the synaptic boutons of the different genotypes stained for VGLUT (red) and Bruchpilot (green). (H) Quantification of the number of active zones per terminal (n ≥ 10). (I) Quantification of the relative presynaptic area of the different genotypes, normalized to control (n ≥ 10). There is no significant difference in the number of active zones or the

presynaptic are between the genotypes. The scale bars are 20 μm (B-F) and 2 μm (G). Data are presented as mean ± standard error of the mean; statistical analysis: one-way ANOVA with Dunnett's Multiple Comparisons post-hoc test, comparing all groups with hFUS wild-type.

2.4 Discussion

Here, we have used CRISPR/Cas9 to create a humanized FUS-based *Drosophila melanogaster* ALS model that expresses hFUS at endogenous levels in place of the *Drosophila* ortholog, Caz. In this study, we were able to observe that hFUS wild-type completely rescues the eclosion phenotypes observed in Caz-/-. The only significant difference between control and hFUS wild-type was a slight decrease in negative geotaxis, whereas fertility, lifespan, and NMJ structure were comparable to control. It is noteworthy that hFUS is able to compensate almost completely for the lack of Caz, and it shows how well conserved the functions of these two genes are. Furthermore, we created hFUS ALS mutant *Drosophila* using the same technique. We observed no decrease in adult eclosion in mutants compared to control, but hFUS mutant adult males display levels of sterility that correlate with the severity of the disease caused by the same FUS mutations in humans. In addition, the severity of disease caused by each mutation in humans also correlates with the level of cytoplasmic localization in neurons. The ALS FUS mutant R495X also shows mild decrease in lifespan and motor ability, but none of the *Drosophila* have abnormal NMJs.

2.4.1 Each hFUS mutation's severity of disease in patients correlates with its level of cytoplasmic localization

Several previous studies in SH-SY5Y and N2a cell lines have shown that hFUS wild-type is normally localized mainly to the nucleus, while hFUS lines with mutations in the NLS are also cytoplasmic (An et al., 2019; Niu et al., 2012). In our experiment, we observe nuclear wild-type hFUS, replicating the FUS localization previously observed in other studies. In the R495X mutant, the protein is localized to both cytoplasm and nucleus, and some cytoplasmic localization of hFUS is observed in the R522G mutant. R521H, however, appears mostly nuclear in our fly line. Interestingly, the level of cytoplasmic localization in the humanized hFUS VNCs, correlates with the severity of disease the mutations cause in ALS patients, as well as with the level of sterility we observe in the male *Drosophila*.

2.4.2 The correlation between sterility and the mutations' severity of disease also correlated with the amount of hFUS present in the cytoplasm

An unexpected observation in the hFUS knock-in *Drosophila* was the fact that the ALS mutants, unlike the controls, were partially sterile. Caz-/- males that eclose into adults have previously been observed to have abnormal genitalia, suggesting that Caz may be important in male *Drosophila* genital development (Wang et al., 2011). Interestingly, in our experiments we observe that the degree of sterility of the male hFUS knock-in *Drosophila* correlates with the degree of ALS mutant disease severity, further highlighting the importance of the hFUS C terminus in particular in male fertility (Waibel et al., 2010). While both R521H and R522G are mutations within the NLS, R495X induces a stop codon that prevents NLS translation but also partially disrupts the C terminus RGG repeat region, and R495X causes the most severe cytoplasmic hFUS localization of the three mutants. It is possible that this amplifies the effect on sterility, perhaps disabling regulation of fertility-related genes. Other RNA-binding proteins, such as the protein Maca, are known to bind RNA and facilitate expression of proteins crucial to male fertility (Zhu and Fukunaga, 2021). Another possibility is that mutations in the C terminus region of hFUS may change the conformation of the protein, causing diminished interaction possibilities for several of the protein domains.

Interestingly, FUS-related male sterility is not only observed in humanized FUS flies. Male mice with a deletion of mouse FUS (mFUS) are also proven to be sterile, and it has been observed that their pre-meiotic spermatocytes have an increased number of unpaired as well as mispaired chromosomal axes, suggesting that the role of FUS in DNA pairing and recombination is crucial for male fertility (Kuroda et al., 2000). Overall, the RNA-binding, DNA pairing and recombination qualities of the FUS protein may be conserved across species and be vital for male fertility.

2.4.3 The difference in relative protein expression between mutants and hFUS wild-type may cause differing results

When quantifying the relative hFUS protein expression, compared to tubulin loading control, we observe a significant increase in the expression level of mutants R521H and R522G compared to control. Interestingly, R495X does not show this increase and trends toward a lower expression level than control. A study has previously shown that when overexpressing hFUS wild-type in *Drosophila* causes an increased nuclear level of Caz and hFUS, which in

turn leads to a decrease in endogenous Caz levels (Jäckel et al., 2015). This suggests that Caz/hFUS is able to autoregulate its expression levels. On the basis of these results, it is possible that the R521H and R522G mutants are less able to properly autoregulate their expression, and that cytoplasmic localization and/or involvement in inclusions causes the hFUS expression to increase. However, it remains unclear why this effect is not observed in the R495X mutant. It is also interesting that the R495X mutation is displaying more severely shortened lifespan and motor symptoms, compared to the other two mutations. It is possible that this is induced due to lower protein expression levels causing an augmented loss of function phenotype, while the increased expression of R521H and R522G are able to compensate for this.

2.4.4 Abdominal neuromuscular junctions are not affected in the mutants at a young age, but this may change in older *Drosophila*

ALS is known to be characterized by a loss of the NMJs (Cappello and Francolini, 2017), which is why we chose to stain and quantify the presynaptic area and active zone number in the *Drosophila* NMJs. Surprisingly, we observed no significant differences between the humanized hFUS ALS mutant flies and control, suggesting that the NMJs are not degenerating. However, our experiments were performed on young *Drosophila*, at 4-5 days old, and even though FUS ALS is known to be relatively early onset in patients it is possible that NMJ loss does not occur until an older age. It is worth noting, however, that the only significant motor phenotype differences observed between any ALS mutant and hFUS control is between hFUS wild-type and hFUS R495X, at 1 day of age. This suggests that if a degenerated NMJ was at the root of this difference, differences between mutant and control NMJ should be observed in our measurements.

Another detail worth noting is that we are assessing the abdominal neuromuscular junction. While at end stage of disease, almost all NMJs are affected and degenerating, ALS commonly starts in a particular area of the body before spreading. Usually, ALS is classified into bulbar onset and limb onset ALS, where bulbar onset begins in the muscles controlling speech, chewing, and swallowing, and limb onset starts in the limb muscles. The majority of ALS-FUS R495X patients, for example, which is the only fly genotype for which we observe motor symptoms, display bulbar or upper limb onset (Bosco et al., 2010). It is possible that the phenotype we see in the negative geotaxis assay is due to NMJ degeneration in the forelegs, and won't be visible at the abdominal NMJs.

While NMJ degeneration is a hallmark feature of ALS, it is not the only neuronal degeneration observed. Both lower and upper motor neurons are known to degenerate during disease (Menon and Vucic, 2021). It is possible that the observed phenotype in the R495X mutant is not due to NMJ degeneration, but because of upper motor neurons or premotor neuron dysfunction.

2.4.5 Is an additional trigger needed to increase the severity of pathology?

We observe very mild, if any, ALS phenotypes in our humanized hFUS *Drosophila*. Since our model is expressing hFUS, wild-type or mutant, at an endogenous level in the absence of Caz, we believe that we have created an ALS model that is mimicking the genetic condition of patients as closely as possible. With the lack of severe symptoms in these *Drosophila*, it is possible that there are additional factors, other than the FUS mutations, that need to be considered when modeling FUS-based ALS. For example, it is possible that a combination of mutations is needed, or that environmental factors are necessary to trigger pathology.

The lack of symptoms in the presence of an ALS mutation is not exclusive to our *Drosophila* model. A patient carrying the R495X mutation suffered from juvenile ALS onset, while their parent who carried the same mutation was asymptomatic at age 47, suggesting additional factors are needed to induce disease (Grassano et al., 2022). Furthermore, in multiple rodent ALS-FUS models, FUS aggregation is not observed (Devoy et al., 2017; Huang et al., 2011; Sharma et al., 2016). This has prompted many to hypothesize that an additional stressor may be needed to trigger FUS proteinopathies. While combinations of FUS mutations and other ALS-related mutations in patients have not yet been discovered, many have made connections between environmental ALS risk factors as a possible trigger to induce ALS-FUS. In *Drosophila* expressing neuronal wild-type or ALS mutant hFUS and exposed to a traumatic brain injury, hFUS ALS mutants had a higher level of mortality than control (Anderson et al., 2018). Another study has found that anti-viral immune response component type I interferon can promote FUS accumulation by stabilizing its mRNA (Shelkovnikova et al., 2019). Several viral infections have also been shown to exacerbate ALS pathology in iPSC-derived spinal neurons with FUS mutations (Bellmann et al., 2019). All in all, it is possible that a trigger is needed to induce ALS phenotypes in the humanized FUS *Drosophila*.

2.5 Conclusion

In conclusion, we have created and verified a humanized FUS-based *Drosophila* ALS model. In our model, we found that hFUS wild-type expression can almost completely rescue Caz-/-. Among the ALS mutants, we observe a mild decrease in longevity in R521H and R495X compared to hFUS control. We have also found that R495X has a deficiency in motor behavior, and cytoplasmic mislocalization. In addition, we saw that hFUS ALS mutant disease severity surprisingly correlates with level of sterility. However, no differences are observed between the genotypes at the level of the NMJ. It is possible that an additional trigger is needed to induce more severe ALS symptoms.

2.6 Materials and methods
2.6.1 Generation of FUS knock-in *Drosophila* lines
Fly embryos expressing Cas9 were injected by Genetivision (Houston, TX, USA) with three plasmids, each at the concentration 500 ng/µl. Two of the plasmids are pCFD3 vectors each expressing a separate gRNA targeting intron 4 or exon 5 (5'-GGTTTCACATCTAAGTGTCCT-3' and 5'- ACTGTCACCTACGACGACACC -3') of the *caz* gene. The gRNAs were designed using the CRISPR Optimal Target Finder (http://targetfinder.flycrispr.neuro.brown.edu) and cloned into the pCFD3 plasmid. The third plasmid contains human FUS cDNA, either wild-type, ALS mutant R522G, ALS mutant R521H, or ALS mutant R495X, followed by a p10 3'UTR and a dsRed cassette driven by the eye-specific promoter 3xP3. The dsRed cassette is removable by LoxP flanking sites. The FUS cDNA, p10 3'UTR, and dsRed cassette are also surrounded by piggyBac and PhiC31 attP sites. To ensure the knock-out of the endogenous *caz* gene, 3 consecutive stop codons were added downstream of the inserted construct. In the end, this resulted in four lines: FUS wild-type knock-in, FUS R522G knock-in, FUS R521H knock-in, and FUS R495X knock-in.

2.6.2 Immunoblotting
20 adult fly heads were collected per group and kept on ice before homogenization in RIPA lysis buffer (140 mM NaCl, 1 mM EDTA, 1% Triton X-100, 0.5 mM EGTA, 10 mM Tris-Cl pH 8, 0.1% SDS). The samples were sonicated for 5 s and centrifuged for 1 min at 12 000 x g. The supernatant was collected, and part of it was used for measuring the protein concentration with a Micro BCA Protein Assay kit (Thermo Scientific) while the rest was

mixed with 4x Laemmli buffer and heated for 2 min at 85˚C. 30 μg of protein was loaded in a 4-12% Tris-Glycine gel (Invitrogen). The protein bands were transferred to a nitrocellulose membrane and submerged in blocking solution for 1 h. Primary antibodies were incubated in blocking solution overnight (anti-FUS, HPA008784, Sigma Aldrich, 1:1000) (anti-Caz, gift from X, 1:30) (anti-tubulin, T6199, Sigma, 1:10 000). Protein bands were imaged after 1 h of secondary antibody incubation (goat anti-rabbit, 111-035-003, Jackson ImmunoResearch, 1:10 000) (goat anti-mouse 115-035-003, Jackson ImmunoResearch, 1:10 000) and addition of chemiluminescent substrate (WesternBright Sirius, Advansta). The membrane was stripped for 10 min at 37˚C (Restore Western Blot Stripping Buffer, Thermo Scientific), re-blocked, and stained with a loading control antibody.

2.6.3 Eclosion

Around 25 male larvae of the correct genotype were transferred into a fresh vial. The number of adult *Drosophila* that eclosed in the vial were counted and compared to the total number of larvae originally placed in the vial.

2.6.4 Fecundity

One male fly of each genotype was mated with one w^{1118} control virgin fly each. After 7 days together, the parental *Drosophila* were removed, and the offspring counted when eclosed. The experiment was repeated three times for each genotype, and the results were normalized to the average amount of offspring in the w^{1118} control.

2.6.5 Lifespan

The *Drosophila* were collected and kept in food vials with 10 flies or less in each. The vials were kept in at 25°C, and flipped to a new vial every other day. At these timepoints the number of dead *Drosophila* were recorded.

2.6.6 Negative geotaxis

The negative geotaxis assay on the hFUS knock-in *Drosophila* were performed using a climbing set-up, including glass vials attached to a metal rod. The flies were placed in glass vials and tapped down to the bottom of the vial three times, after which they climbed up the walls of the vials. The experiments were filmed using a Raspberry Pi Camera. Using ImageJ, the maximum height climbed by each fly during 5 s was measured and averaged.

2.6.7 Immunohistochemistry

For the neuromuscular junctions, 4-5 day old *Drosophila* reared at 29°C were dissected in cold PBS to expose the abdominal muscles. The preparations were then fixed in Bouin's fixative for 7 minutes. After four 30 minutes washes in 1xPBS, 0.3% Triton-X the tissue was blocked in 2% Normal Goat Serum diluted in 1xPBS, 0.3% Triton-X. The primary antibody was incubated in blocking overnight, and after four additional 30 minutes washes the secondary antibodies were added for 2 h at room temperature. After several washes, the preparations were mounted in Prolong Diamond antifade mounting medium (Invitrogen) and imaged using a Zeiss 700 inverted confocal microscope. Primary antibodies used were mouse anti-nc82 (DSHB, 1:100) and chicken anti-VGLUT (Eurogentec, custom made, 1:150), and the secondary antibodies used were anti-mouse Alexa Fluor 488 (Lifetech, 1:400) and anti-chicken Alexa Fluor 555 (Lifetech, 1:400). NMJ images were analyzed using a macro in ImageJ, counting the Bruchpilot spots and the area of VGLUT staining.

The ventral nerve cords of 4-5 day old *Drosophila*, kept at 29°C, were dissected in cold PBS and fixed with 4% PFA for 40 minutes. The preparations were washed three times during a total of one h with 1xPBS, 0.4% Triton-X, before they were blocked in 5% Normal Goat Serum diluted in 1xPBS, 0.4% Triton-X. After overnight incubation with the primary antibody in blocking solution, the samples were washed three times during 1 h and then incubated for 1 h with secondary antibodies. After 2 h of repeated washing, the samples were mounted in Prolong Diamond antifade mounting medium (Invitrogen). The primary antibodies used were anti-elav (DSHB, 1:50), anti-repo (DSHB, 1:25), anti-hFUS (Sigma Aldrich, 1:100). The secondary antibodies used were anti-mouse Alexa Fluor 546 (Lifetech, 1:400) and anti-rabbit Alexa Fluor 488 (Lifetech, 1:400).

2.6.8 Statistics

Data are presented as mean ± standard error of the mean. p-values for all survival curves were analyzed using the Mantel-Cox test. For the negative geotaxis assay two-way ANOVA with Dunnett's Multiple Comparisons post-hoc test assessing the main effect of each genotype was used. To test relative protein expression, sterility, NMJ analysis, and eclosion, one-way ANOVA with either Dunnett's or Tukey's Multiple comparisons post-hoc tests were used.

3

Chapter 3 – Human TDP-43 expression completely rescues the absence of the *Drosophila* ortholog TBPH, while ALS mutant TDP-43 expression only leads to mild phenotypes

- -

Emma Källstig, Evelyne Ruchti, Bernard Schneider, Brian McCabe

Creation of the hTDP-43 wild-type and mutant Drosophila by Emma Källstig and Evelyne Ruchti; all other experiments performed by Emma Källstig.

3.1 Abstract

As a gene linked to 5% of fALS cases and a protein that forms pathological aggregates in 97% of all ALS cases, TDP-43 has become a common target of research. Here, we used CRISPR/Cas9 genome engineering to create humanized TDP-43 *Drosophila* by replacing the fly TDP-43 ortholog, *tbph*, with human *TARDBP*, resulting in human TDP-43 (hTDP-43) expression at levels similar to the endogenous protein. Wild-type hTDP-43 expression completely rescues the decreased eclosion rate observed in *Drosophila* TBPH knockouts. Adult hTDP-43 *Drosophila* also show lifespan, motor behavior, and NMJ morphology comparable to controls. In addition, we generated five different hTDP-43 ALS mutant lines (A90V, G287S, G294A, A315T and M337V) using the same technology. We further characterized the lifespan and motor abilities of these fly lines and find that the M337V and G294A hTDP-43 ALS mutants have a mildly decreased lifespan, while the hTDP-43 M337V, hTDP-43 G287S, and hTDP-43 A315T all display a significant motor deficit. Interestingly, the final ALS mutant we created, hTDP-43 A90V, shows no deficits in lifespan or motor behavior. Moreover, none of the ALS mutants exhibit degenerated neuromuscular junctions. These results suggest that an additional trigger may be needed to provoke a more severe ALS pathology in *Drosophila*.

3.2 Introduction

TDP-43 is one of the most well-known genes linked to fALS, causing approximately 5% of fALS cases (Morgan and Orrell, 2016). Interestingly, TDP-43 is not only linked to fALS, but TDP-43 aggregates are also found in 97% of all cases, sporadic cases included, highlighting the importance of this protein in pathology (Nguyen et al., 2018).

hTDP-43 is a member of the heteronuclear ribonucleotide binding protein family. The TARDBP gene consists of six exons, which can be assembled into five known isoforms (François-Moutal et al., 2019; Shenouda et al., 2022). The hTDP-43 protein comprises an N-terminal domain, followed by an NLS, and two RNA recognition motifs that are required for nucleic acid binding. Finally, a C-terminal glycine-rich region which can interact with several protein partners and is the site of the majority of the ALS-associated mutations (Chiang et al., 2016). TDP-43 normally functions as a DNA- and RNA-binding protein that regulates transcription, mRNA splicing, transport, and stability (Ederle et al., 2018). While the hTDP-43 protein is localized mainly to the nucleus, it also shuttles back and forth from the cytoplasm and can be found in the mitochondria, but when it aggregates in disease it often mislocalizes to the cytoplasm (Suk and Rousseaux, 2020). The mechanisms of TDP-43 aggregate formation are yet to be understood, although one theory dictates that improperly controlled formation of stress granules may be a starting point for aggregation (Streit et al., 2022). TDP-43 is known to take part in the regulation of stress granules, which are suspected to have a role in ALS pathology when their dynamics are dysregulated (Ding et al., 2021; Khalfallah et al., 2018). Indeed, studies have observed colocalization of TDP-43 and stress granule markers, suggesting that chronic stress may be a cause of pathology, by inducing an imbalance in stress granule dynamics (Colombrita et al., 2009; Liu-Yesucevitz et al., 2010). Still, it remains unclear if the mechanisms behind TDP-43 pathology in ALS involve gain of function due to aggregation and chronic stress granules, loss of the nuclear function of the protein, a dominant negative effect, or another alternative hypothesis (Floare and Allen, 2020).

In order to investigate these different theories, researchers have created animal models based on TDP-43 ALS-linked mutations to attempt to replicate disease phenotypes. However, there have been a few challenges. When overexpressing TDP-43 in mice, both wild-type and ALS mutant cause death within weeks (Lutz, 2018). Similar results have been found in *Drosophila melanogaster* models of TDP-43-based ALS. Overexpression of hTDP-43 wild-type or hTDP-43 A315T ALS mutant both cause neurodegeneration and shortened survival, with

TDP-43 wild-type actually leading to more severe phenotypes than A315T (Estes et al., 2011). However, deletion of mouse TDP-43 leads to embryonic lethality, and deletion of the *Drosophila* TDP-43 ortholog, TBPH, also leads to impaired eclosion, decreased motor behavior abilities, and shortened lifespan (Diaper et al., 2013; Liu et al., 2013). The severe phenotypes observed in both deletion and overexpression models illustrate the challenges of generating animal models which accurately replicate the course of disease in ALS patients. To address this problem, Chang and Morton have created a humanized TDP-43 *Drosophila* model, expressing hTDP-43 wild-type or ALS mutant in place of TBPH at endogenous levels (Chang and Morton, 2017). Surprisingly, hTDP-43 wild-type and ALS mutant lines hTDP-43 G294A and hTDP-43 M337V show no defects in lifespan or development, and the mutants have only mild deficits in motor behavior as they age. The authors speculated that an additional trigger could be absent that is required to induce more severe ALS symptoms. In this study, we measured the longevity of Chang and Morton's humanized TDP-43 *Drosophila* model, but were not able to replicate their results. Therefore, we aimed to create our own humanized TDP-43 *Drosophila* model, including five TDP-43 ALS mutant fly lines: A90V, G287S, G294A, A315T, and M337V, using CRISPR/Cas9. In these *Drosophila*, we observe that hTDP-43 wild-type can completely rescue the eclosion impairment caused by the deletion of the endogenous TBPH. Humanized TDP-43 *Drosophila* also show motor behavior, lifespan, and NMJ morphology comparable to controls. In the ALS mutant flies, we found a mild decrease in lifespan in only in hTDP-43 M337V and hTDP-43 G294A compared to hTDP-43 wild-type, while all other mutants show longevity comparable to hTDP-43 wild-type. The M337V, G287S and A315T mutants also have deficits in motor abilities, revealed in the negative geotaxis assay. However, no significant differences between mutants and control can be observed at the level of the NMJ. Much like Chang and Morton, we hypothesize that these *Drosophila* can be used to investigate the effects that an additional genetic or environmental trigger may have on ALS phenotypes.

3.3 Results

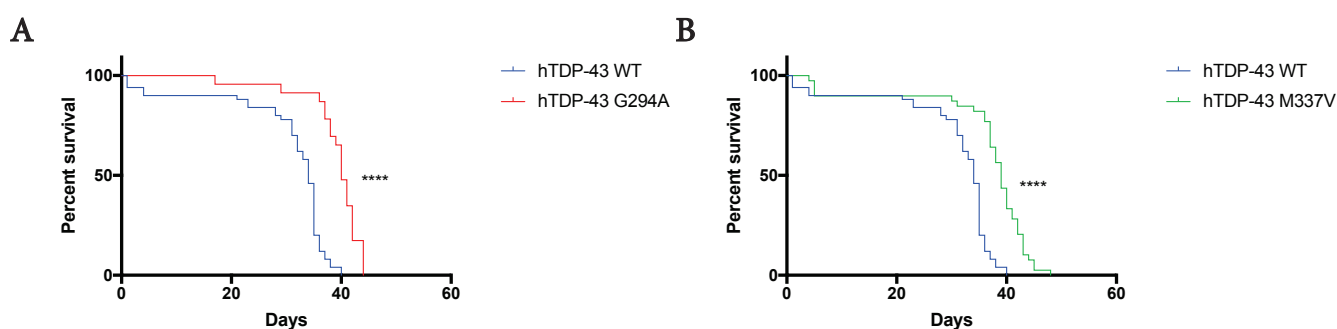### 3.3.1 Chang and Morton's humanized TDP-43 ALS mutant fly lines have significantly longer lifespan than hTDP-43 wild-type

Prior to creating our own humanized fly line, we tested the fly lines previously generated by Chang and Morton. We assessed the fly lifespan of the hTDP-43 wild-type knock-in, as well as the two ALS mutant knock-in lines: G294A and M337V. In the reported results, there was

no significant difference between any of the lifespans, though the M337V mutant had a slightly, but not significantly, longer lifespan than all other fly lines. Instead, we saw a significantly shorter lifespan in the hTDP-43 wild-type *Drosophila* than in either of the mutants. Based on this observation, we decided to generate our own humanized TDP-43 fly lines. In addition to the two mutations chosen by Chang and Morton, we also aimed to generate three additional lines expressing other ALS-associated hTDP-43 mutants.

Figure 3-1. The lifespan of Chang and Morton's humanized TDP-43 *Drosophila*

Figure 1: The lifespan of Chang and Morton's humanized TDP-43 wild-type is significantly shorter than both ALS mutants. (A) The lifespan of hTDP-43 wild-type (blue, n=50) compared to hTDP-43 G294A (red, n=23). (B) The lifespan of hTDP-43 wild-type compared to hTDP-43 M337V (green, n=39). Both mutants display a significantly longer lifespan than hTDP-43 wild-type. The same hTDP-43 wild-type data is used in A and B. All longevity data for the different genotypes are from the same experiment but separated into different graphs only for ease of visualization. Statistical analysis: Mantel-Cox test.

3.3.2 Generation of hTDP-43 knock-in *Drosophila*

Using CRISPR/Cas9 technology, we replaced the *Drosophila* TDP-43 ortholog, TBPH, with hTDP-43. To this end, we cloned hTDP-43 cDNA, followed by a removable dsRed cassette flanked by piggyBac sites to facilitate identification of flies with correct transgene insertion, into a backbone plasmid (figure 2A). Two gRNAs were also cloned into pCFD3 plasmid backbones, to be injected together with the hTDP-43-dsRed plasmid into fly embryos and facilitate CRISPR/Cas9 gene integration. The gRNA target sites were placed in neighboring genes (*bgcn* and *cpes*), but were designed to not change the resulting amino acid sequence after hTDP-43 insertion. Further information about the creation of the humanized *Drosophila* can be found in the Annex.

Injection of the plasmids into fly embryos was performed by Genetivision Corporation (USA), and dsRed-positive lines of each genotype were subsequently sequenced to ensure

correct insertion and backcrossed 6 generations into a w[1118] control fly line to obtain a similar genetic background. The presence of hTDP-43 protein expression as well as the absence of TBPH expression was confirmed and quantified using western blot (figure 2B and C). While slightly higher relative protein expressions compared to tubulin control were observed in mutants G294A and M337V, the differences were not significant, showing that TDP-43 is expressed at similar levels across all genotypes.

Figure 3-2. CRISPR/Cas9 technology was used to generate humanized TDP-43 *Drosophila*
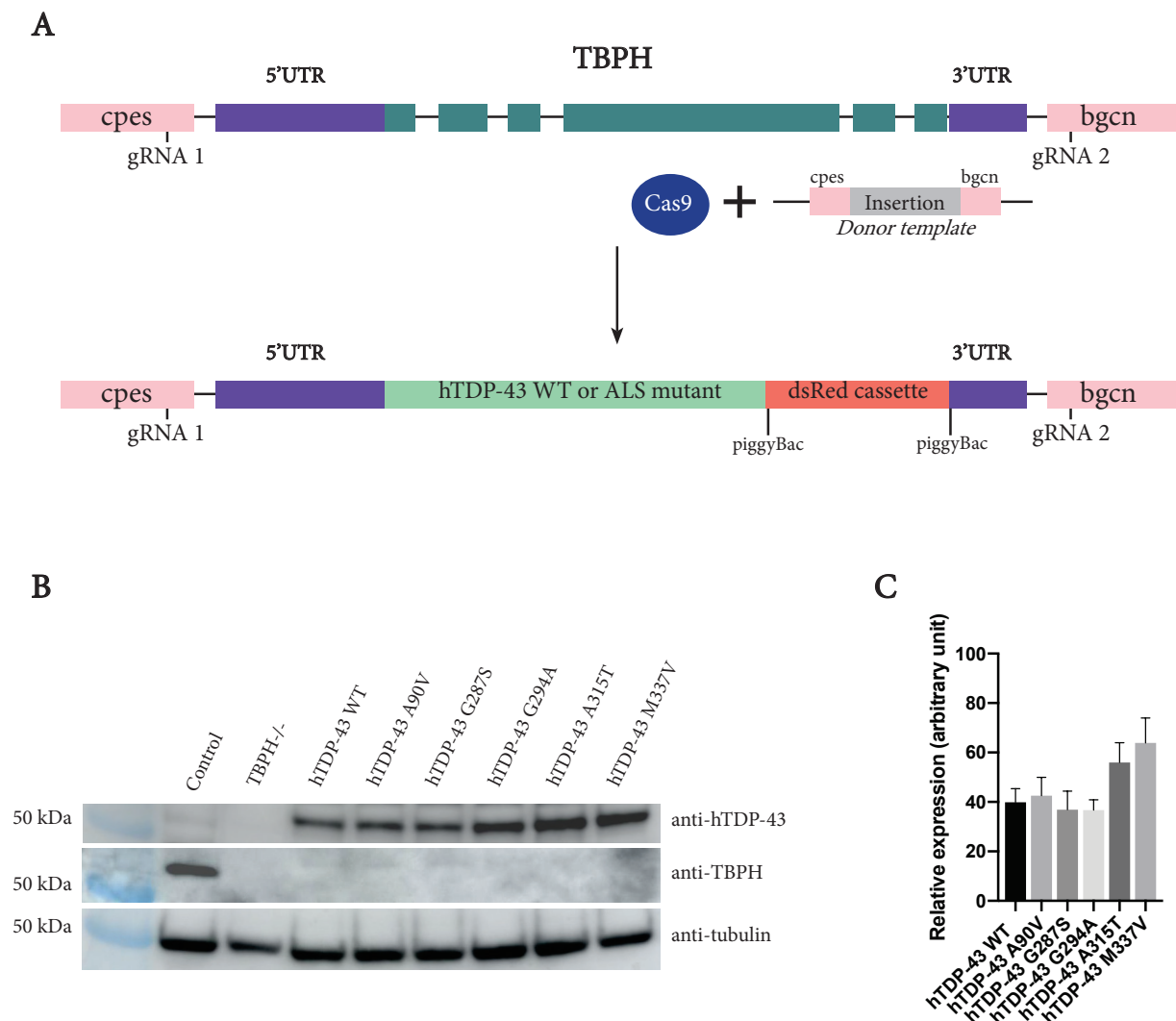
Figure 2: CRISPR/Cas9 technology was used to replace the Drosophila *tbph* gene with either hTDP-43 wild-type or hTDP-43 ALS mutants. (A) Illustration of the CRISPR/Cas9 technology and the location of the gRNAs. The *tbph* gene was completely replaced by hTDP-43, and even though the gRNAs were place in neighboring genes (*bgcn* and *cpes*) the strategy was designed not to change the resulting amino acid sequence of

those genes after *tbph* excision. A removable dsRed cassette with an eye-specific promoter was also inserted following the hTDP-43 gene, to facilitate identification of flies with the insert present. (B) Western blot showing the expression of hTDP-43 in all the wild-type and mutant knock-in *Drosophila*, as well as the absence of fly ortholog TBPH. (C) Quantification of the hTDP-43 relative protein expression in the different mutants as well as wild-type, using tubulin as a reference. There is no significant difference between the groups (n=3). Data are presented as mean ± standard error of the mean; statistical analysis: one-way ANOVA with Dunnett's Multiple Comparisons post-hoc test, where all groups were compared with hTDP-43 wild-type.

3.3.3 Expression of both hTDP-43 wild-type and hTDP-43 ALS mutants rescue the developmental defects caused by deletion of endogenous TBPH

To evaluate the effect of hTDP-43 insertion on development, we assessed ability of *Drosophila* larvae to eclose to produce adult flies. We isolated a known number of L3 larvae in fresh food vials and counted the number of adult *Drosophila* that eclosed. As can be seen in figure 1 C, around 80% of control larvae eclosed into adults, unlike flies with a deletion of the endogenous *tbph* gene in which only around 16% of larvae eclosed into adults. When deleting endogenous TBPH and inserting hTDP-43 wild-type in its place, however, this was completely rescued (figure 3A). All five hTDP-43 ALS mutants also rescued the TBPH-/- eclosion defect, suggesting that hTDP-43 ALS mutants do not affect development of larvae into adult *Drosophila*.

3.3.4 hTDP-43 wild-type longevity is comparable to control, while mutants M337V and G294A show modestly shortened lifespan

To assess if the humanized TDP-43 *Drosophila* had any difference in lifespan, we measured fly longevity (figure 3B-G). Insertion of hTDP-43 wild-type in place of the fly TBPH even led to significantly longer lifespan than control. When comparing the hTDP-43 wild-type line with the different ALS mutants, some mutants showed stronger phenotypes than others. G287S had no significant lifespan difference compared to hTDP-43 wild-type, while both A90V and A315T showed a small but significant increase in longevity. The G294A and M337V mutants, on the other hand, presented a mild decrease in lifespan compared to control, which was more severe in the M337V line. The differences in longevity between the five mutants in relation to control suggests that even mutants of the same protein domain may not cause similar phenotypes, and that the M337V may induce a more severe phenotype than the other chosen mutations. Interestingly, the average age of onset of M337V mutations in

patients is slightly younger than all the other mutants (Corrado et al., 2009; Kabashi et al., 2011; Sreedharan et al., 2008; Winton et al., 2008).

Figure 3-3. Eclosion and lifespan of humanized TDP-43 *Drosophila*
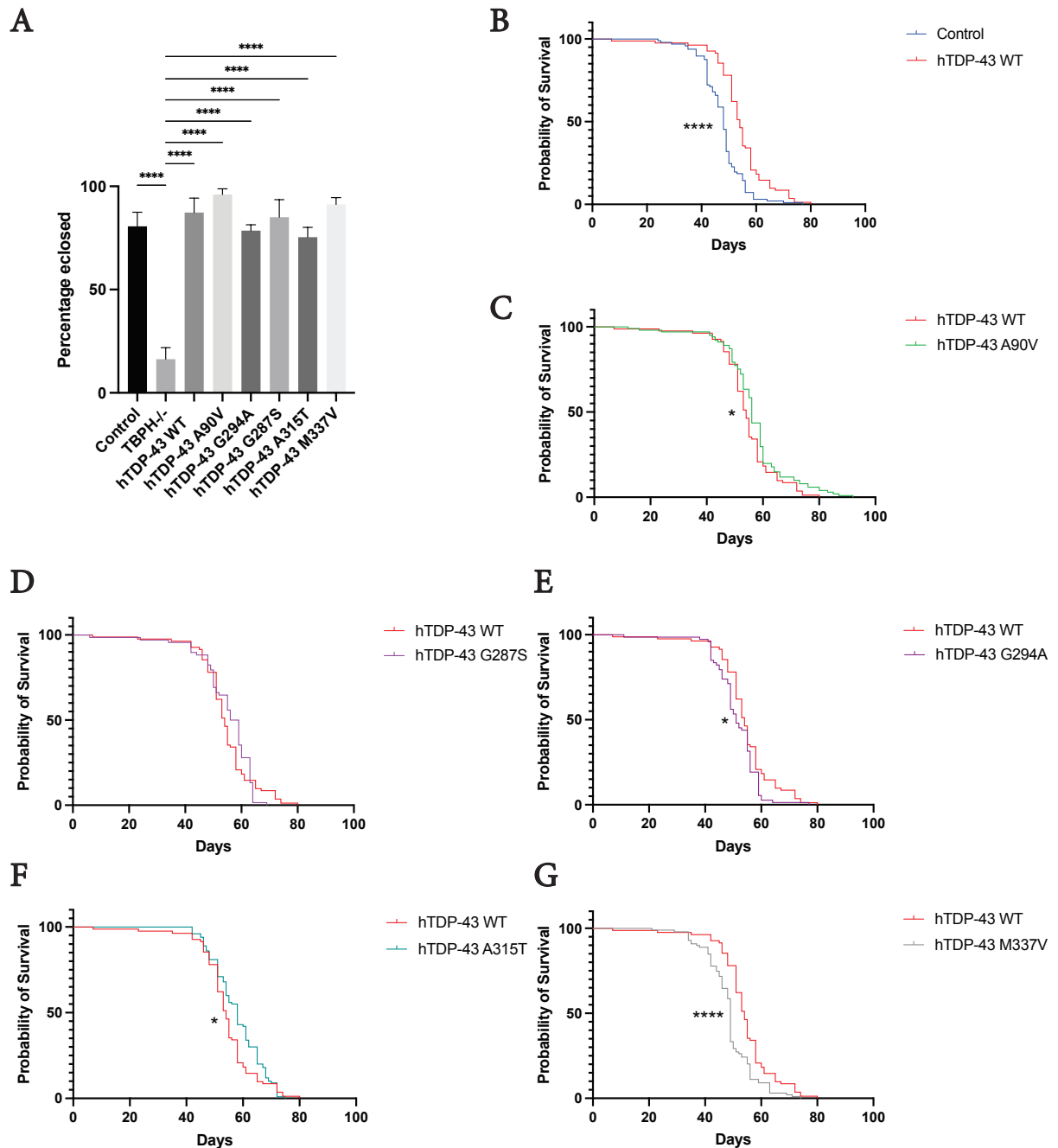
Figure 3: hTDP-43 wild-type knock-in completely rescues fly longevity and eclosion, while hTDP-43 M337V and G294A mutants have a shorter lifespan compared to hTDP-43 control. (A) TBPH-/- have significantly lower eclosion rate compared to control, an effect that can be rescued by expression of hTDP-43

wild-type as well as ALS mutants (n≥56 larvae per group). With the exception of the TBPH-/-, no significant difference is found between any of the other genotypes. Lifespan graphs of: (B) Control (blue, n=97) compared to hTDP-43 wild-type (red, n=82) (C) hTDP-43 wild-type compared to hTDP-43 A90V (green, n=101) (D) hTDP-43 wild-type compared to hTDP-43 G287S (magenta, n=68) (E) hTDP-43 wild-type compared to hTDP-43 G294A (purple, n=73) (F) hTDP-43 wild-type compared to hTDP-43 A315T (turquoise, n=100) (G) hTDP-43 wild-type compared to hTDP-43 M337V (grey, n=99). Only hTDP-43 mutants G294A and M337V show a significantly shortened lifespan compared to hTDP-43 wild-type. The same hTDP-43 wild-type data is used in B-G. All longevity data for the different genotypes are from the same experiment but separated into different graphs only for ease of visualization. Data are presented as mean ± standard error of the mean; statistical analysis: one-way ANOVA with Tukey's Multiple Comparisons post-hoc test (A), and Mantel-Cox test (B-G).

3.3.5 hTDP-43 mutants M337V, A315T and G287S are the only genotypes showing mild geotactic motor behavior deficits

To assess the motor behavior of the *Drosophila*, we used the negative geotaxis assay. Flies were tapped to the bottom of a glass vial and the average maximum height the *Drosophila* climbed in 5 s was measured. The geotactic behavior of hTDP-43 wild-type was again comparable to control, causing us to conclude that TDP-43 is well-conserved between fly and human (figure 4). When observing the motor behavior of the hTDP-43 mutants, the M337V, A315T, and G287S mutants exhibited deficits in climbing abilities. Neither of the two other ALS mutants, A90V and G294A, presented a significant motor deficit compared to hTDP-43 control.

Figure 3-4. Negative geotaxis behavior of humanized TDP-43 *Drosophila*
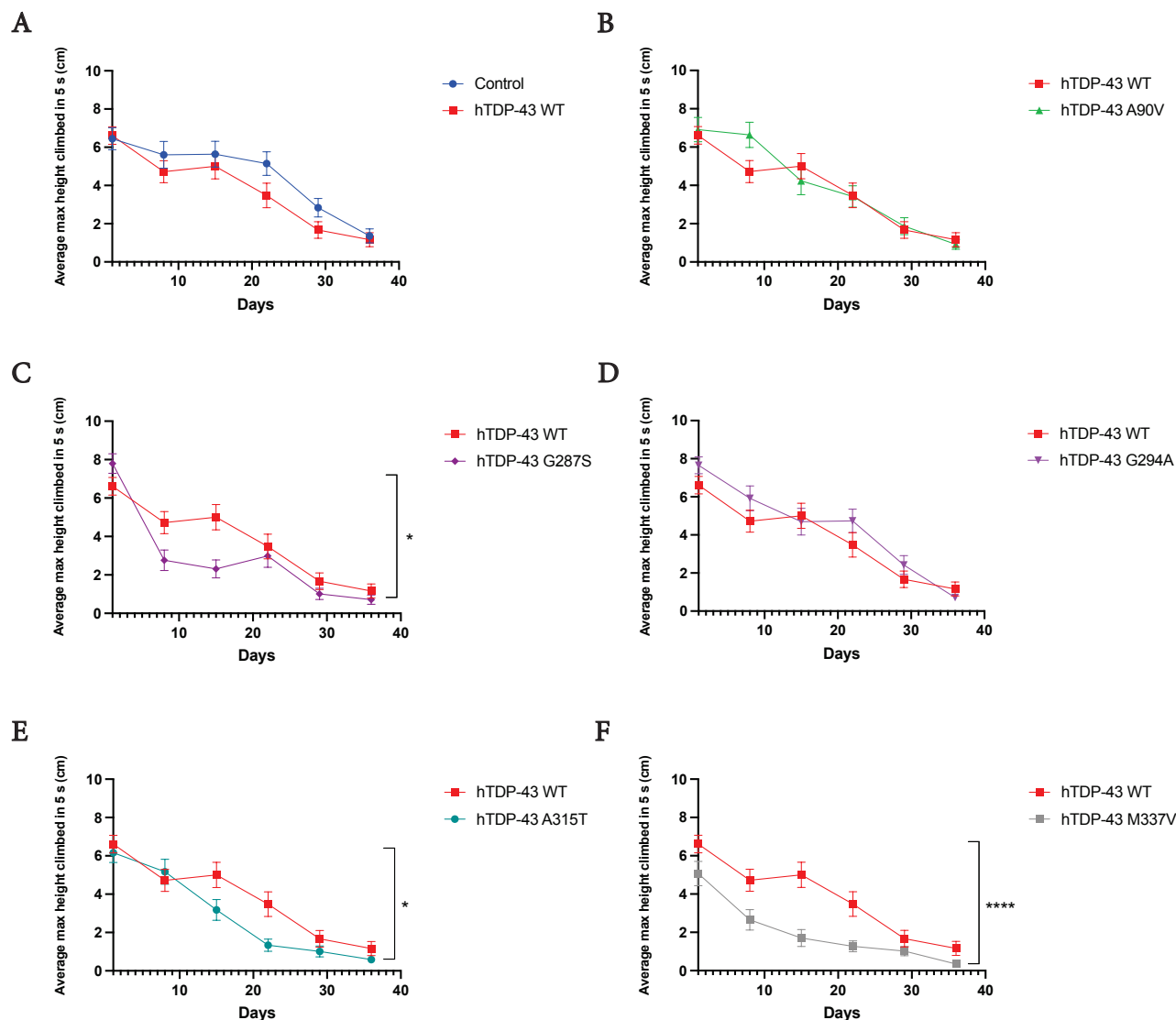
Figure 4: hTDP-43 wild-type shows motor behavior comparable to control, while hTDP-43 mutants A315T, G287S and M337V have significant motor behavior deficits in the negative geotaxis assay, unlike the other mutants. Results of the negative geotaxis assay, measuring the average max height climbed by the *Drosophila* in 5 s as a function of their age, in (A) Control (blue, n=30 flies at day 1) compared with hTDP-43 wild-type (red, n=30 flies at day 1). (B) hTDP-43 wild-type compared with hTDP-43 A90V (green, n=30 flies at day 1). (C) hTDP-43 wild-type compared with hTDP-43 G287S (purple, n=30 flies at day 1). (D) hTDP-43 wild-type compared with hTDP-43 G294A (magenta, n=30 flies at day 1). (E) hTDP-43 wild-type compared with hTDP-43 A315T (turquoise, n=30 flies at day 1). (F) hTDP-43 wild-type compared with hTDP-43 M337V (grey, n=29 flies at day 1). hTDP-43 wild-type is comparable to control, while mutants A315T, G287S and M337V show significant motor deficits. The same hTDP-43 wild-type data is used in A-F. All negative geotaxis data for the different genotypes are from the same experiment but separated into different graphs only for ease of visualization. Data are presented as mean ± standard error of the mean; statistical analysis: two-way ANOVA

with Dunnett's Multiple Comparisons post-hoc test looking at the main effect of each genotype and comparing all genotypes to hTDP-43 wild-type.

3.3.6 hTDP-43 is localized to neuronal nuclei as well as a subset of glial nuclei

The ventral nerve cord (VNC) of the different hTDP-43 mutants and wild-type were dissected out and stained to visualize the localization of hTDP-43. Firstly, hTDP-43 appeared to be strongly expressed in neuronal nuclei when co-stained with elav, a nuclear neuronal marker (figure 5A-G). When co-stained with nuclear glial marker, anti-repo, hTDP-43 appeared to be expressed in some, but not all, glial cells (figure 6A-G).

Figure 3-5. hTDP-43 expression in ventral nerve cord neurons
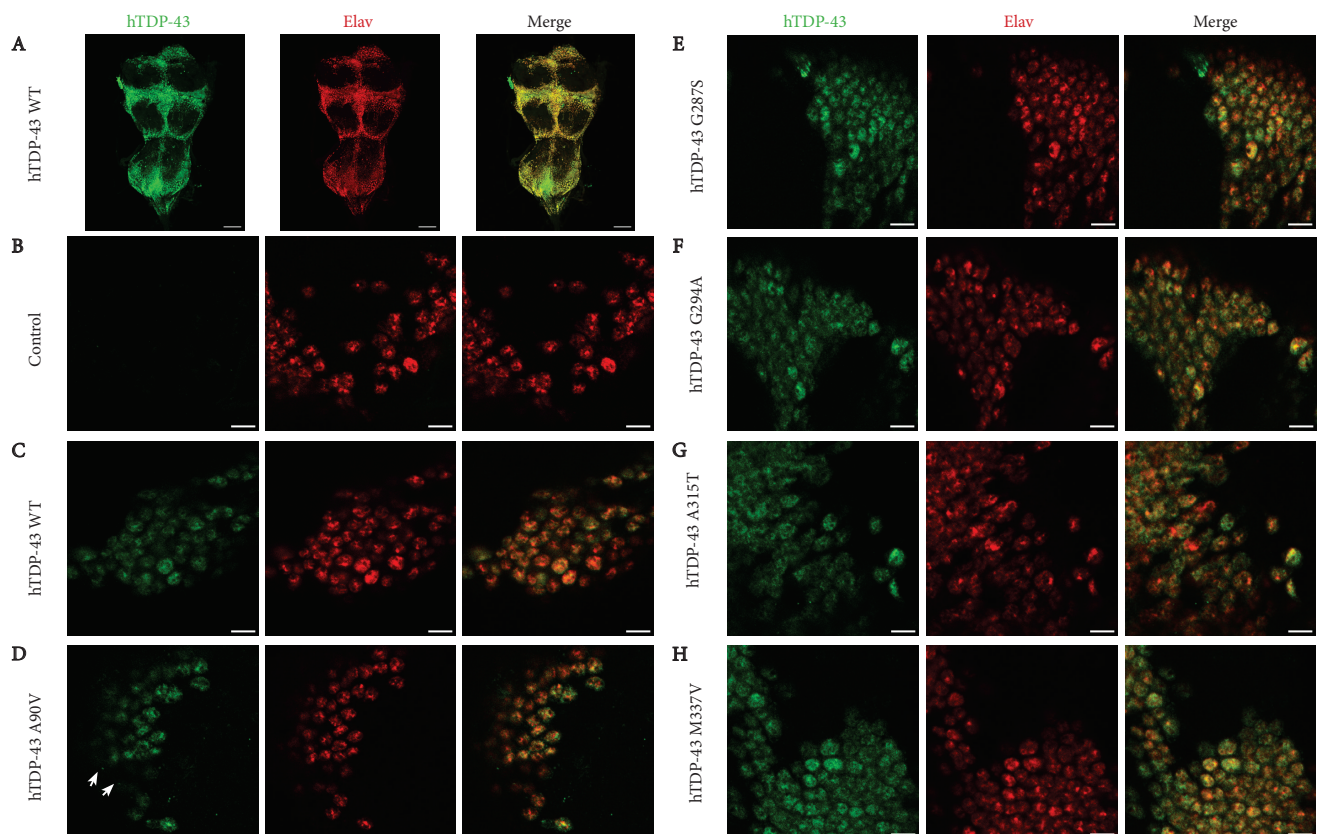
Figure 5: hTDP-43 expression colocalizes with neuronal nuclei in the *Drosophila* VNC, with some cytoplasmic puncta present only in the A90V mutant. (A) Image of the full hTDP-43 wild-type VNC co-stained for hTDP-43 (green) and neuronal nuclear marker elav (red). (B-H) Magnifications of *Drosophila* VNC neurons stained for hTDP-43 and nuclear neuronal marker elav for genotypes: control, hTDP-43 wild-type, hTDP-43 A90V, hTDP-43 G287S, hTDP-43 G294A, hTDP-43 A315T, and hTDP-43 M337V. All humanized TDP-43 lines show co-localization between neuronal nuclei and hTDP-43 expression. In the A90V mutant,

however, some cytoplasmic puncta are also observed, which are marked by white arrows in this figure. The scale bar is 50 μm (A) and 5 μm (B-H).

Figure 3-6. hTDP-43 expression in ventral nerve cord glia
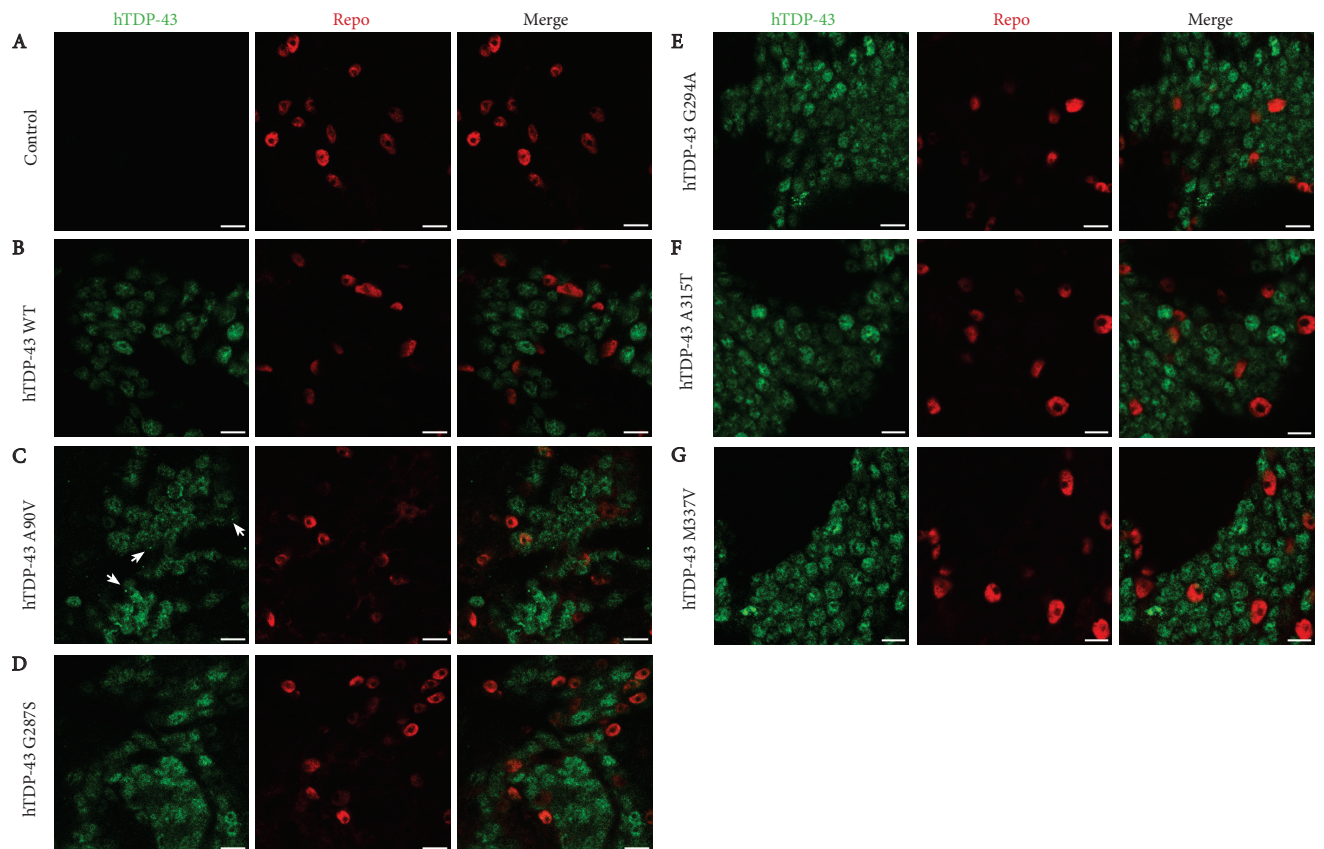
Figure 6: hTDP-43 is expressed in some, but not all, glial nuclei, and hTDP-43 puncta are present in the hTDP-43 A90V mutant. VNCs were dissected and stained for hTDP-43 (green) together with glial nuclear marker, repo (red), in (A) control, (B) hTDP-43 wild-type (C) hTDP-43 A90V (D) hTDP-43 G287S (E) hTDP-43 G294A (F) hTDP-43 A315T (G) hTDP-43 M337V. Some, but not all, glial nuclei express hTDP-43. In addition, hTDP-43 puncta are observed in the A90V mutant, which are marked by white arrows in this figure. The scale bar is 5 μm.

When increasing the magnification on the cells to better visualize the cellular localization of hTDP-43, we observed that hTDP-43 wild-type and ALS mutants all appear to be highly expressed in the neuronal nuclei, and do not appear to be strongly cytoplasmic (figure 7A-G). In the A90V mutant, however, we also observed some non-nuclear puncta, that were not as prevalent in the other genotypes, and that may be due to cytoplasmic aggregation or formation of stress granules (figure 5C, 6C and 7C).

Figure 3-7. Subcellular expression of hTDP-43
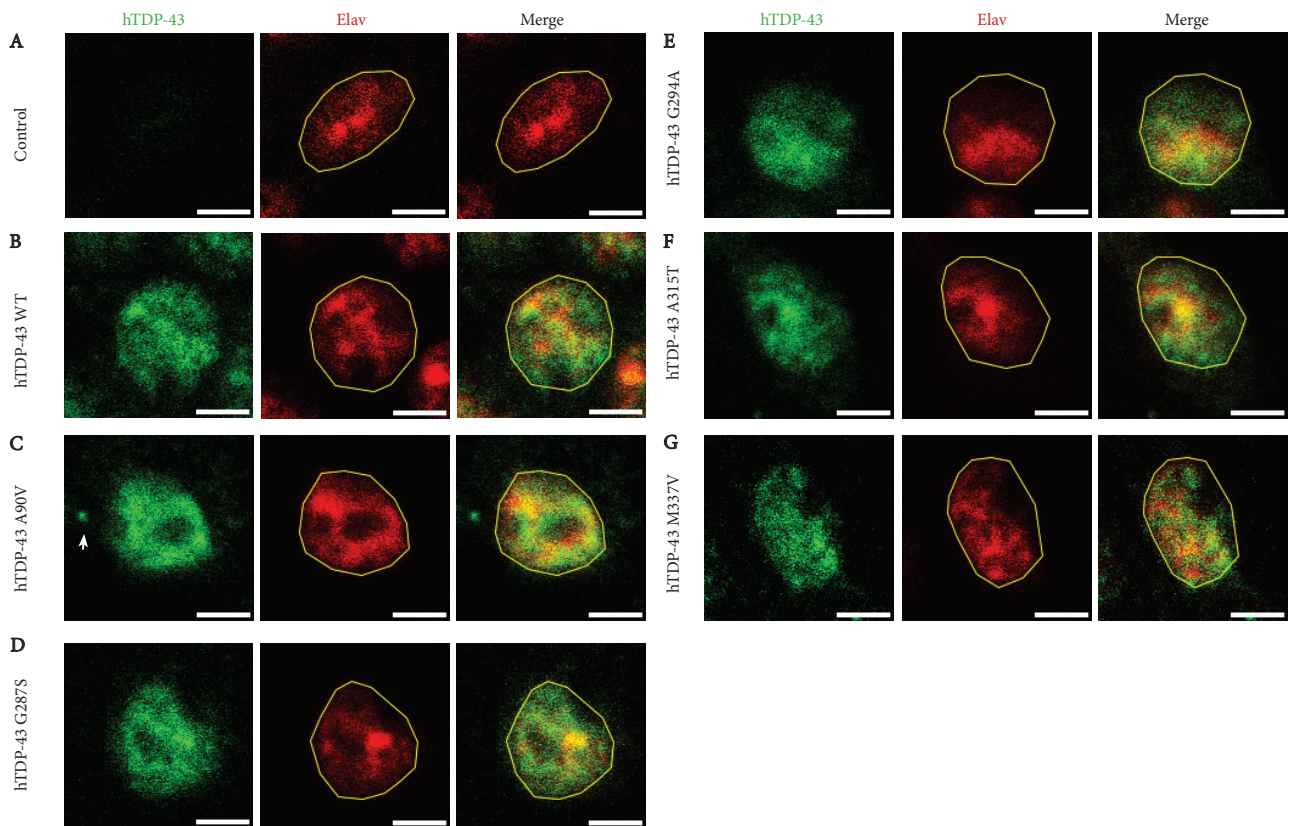
Figure 7: hTDP-43 wild-type is localized to the neuronal nucleus, but some cytoplasmic puncta are found in neuronal cell bodies expressing the A90V mutant. The VNCs of the different genotypes were dissected out and stained for nuclear neuronal elav (red) and hTDP-43 (green) in (A) control (B) hTDP-43 wild-type (C) hTDP-43 A90V (D) hTDP-43 G287S (E) hTDP-43 G294A (F) hTDP-43 A315T (G) hTDP-43 M337V. A yellow outline around the neuronal nuclei has been made in ImageJ to clarify the nuclear versus cytosolic localization of hTDP-43. In all humanized TDP-43 lines, the hTDP-43 protein is mainly localized to the nucleus. In the A90V mutant line, hTDP-43 puncta are observed in the cytoplasm (white arrow). The scale bar is 2 μm.

3.3.7 The neuromuscular junctions are comparable to control in *Drosophila* expressing hTDP-43 wild-type as well as all hTDP-43 ALS mutants

Since we observed motor deficits in three of the ALS mutants, we analyzed the morphology of bilateral NMJ terminals in the third abdominal segment of 4-5 day old *Drosophila,* as a possible early indicator of muscle denervation. The NMJs were stained with presynaptic VGLUT and the active zones with the Bruchpilot marker (figure 8A-I). The presynaptic area and the number of active zones per terminal were quantified. Unexpectedly, even with the M337V, A315T and G287S mutants, which displayed motor symptoms, we observed no

decrease in active zone number or presynaptic area compared to control (figure 8J-K). While the presynaptic area and active zone numbers were all comparable between genotypes at this age, it is possible that at a later timepoint NMJ loss may appear.

Figure 3-8. Abdominal neuromuscular junctions of humanized TDP-43 *Drosophila*
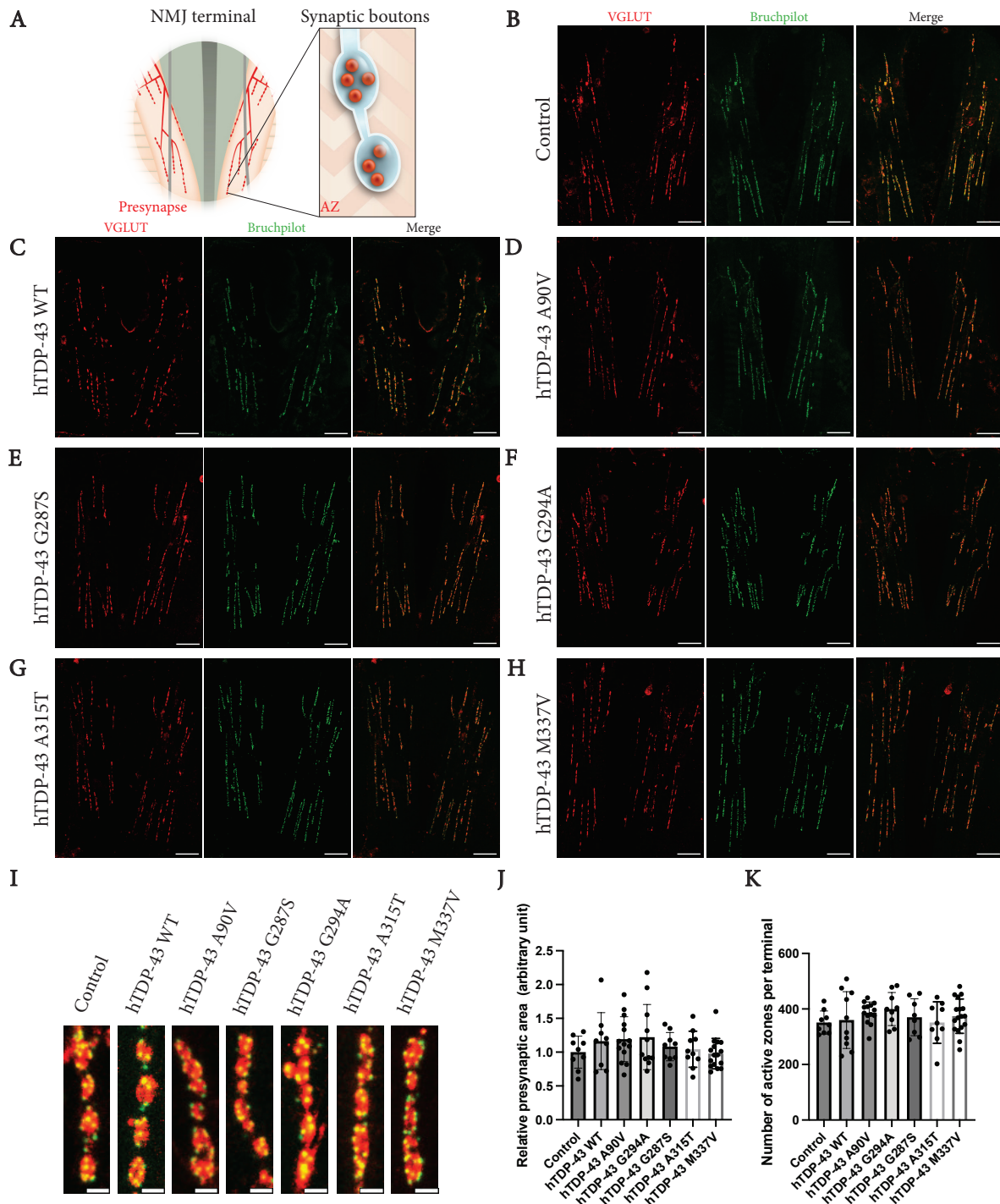
Figure 8: All hTDP-43 knock-ins have active zone numbers and presynaptic areas comparable to control *Drosophila*. (A) Illustration of the bilateral NMJ in abdominal segment 3, including magnification of synaptic

boutons. The presynapse and active zones are both shown in red. (B-H) Images of NMJ terminals in the abdominal segment 3, stained for presynaptic marker VGLUT (red) and active zone marker Bruchpilot (green) in (B) control, (C) hTDP-43 wild-type, (D) hTDP-43 A90V, (E) hTDP-43 G287S, (F) hTDP-43 G294A, (G) hTDP-43 A315T, (H) hTDP-43 M337V. (I) Magnification of the synaptic boutons of each genotype stained for VGLUT (red) and Bruchpilot (green). (J) Quantification of number of active zones per terminal in the different genotypes (n ≥ 8). (K) Quantification of the relative presynaptic area, normalized to control, for the different genotypes (n ≥ 8). No significant difference between the groups is observed with regards to presynaptic area or active zone number. The scale bars are 20 μm (B-H) and 2 μm (I). Data are presented as mean ± standard error of the mean; statistical analysis: one-way ANOVA with Dunnett's Multiple Comparisons post-hoc test, comparing all groups with hTDP-43 wild-type.

3.4 Discussion

In this study, we used CRISPR/Cas9 technology to create a humanized *TARDBP* knock-in fly line expressing hTDP-43 in place of the endogenous fly TBPH. hTDP-43 wild-type expression was able to completely rescue the eclosion deficits of TBPH-/- *Drosophila.* Adult flies also show lifespan, motor behavior, and NMJ morphology comparable to control, proving how well-conserved the functions of TDP-43 are between these two species. We also created five different ALS-associated hTDP-43 mutant fly lines, and observed that while the eclosion rate and NMJs of all mutants are comparable to hTDP-43 wild-type, mutants M337V and G294A show slightly decreased lifespan and mutants M337V, G287S, and A315T have mild motor behavior symptoms. hTDP-43 mutant A90V also displays presence of cytoplasmic TDP-43 puncta.

3.4.1 Differences between the *Drosophila* model generated by Chang and Morton and our newly made humanized TDP-43 *Drosophila*

A previous study by Chang and Morton has created and characterized humanized TDP-43 lines with M337V and G294A. They observed no significant differences in longevity between any of the genotypes, and their M337V mutant conversely trended toward a longer lifespan than TDP-43 control. However, when we repeated their study, the Chang and Morton hTDP-43 wild-type lifespan was significantly shorter than their mutant lifespans. In our newly made humanized TDP-43 model, we were conversely able to observe a decrease in the M337V lifespan compared to hTDP-43 wild-type. As with our study, Chang and Morton performed a negative geotaxis experiment, where they also saw motor deficits in M337V and G294A compared to control. While we observed motor deficits in our M337V mutant, we

were not able to reproduce the results Chang and Morton found in their G294A mutant. It is possible that the differences observed in our fly lines and those of Chang and Morton are caused by the use of differences in genetic background. Still, it is clear that in both cases the phenotypes observed in the ALS mutants are consistently surprisingly mild compared to hTDP-43 wild-type.

3.4.2 hTDP-43 wild-type is localized mainly to neuronal nuclei as well as a subset of glial nuclei, while cytoplasmic puncta are present in neurons expressing A90V mutant hTDP-43

Many previous studies have shown that TDP-43 wild-type is predominantly localized to the cell nucleus (Duan et al., 2022; Voigt et al., 2010; Zhang et al., 2009). Indeed, we also observed nuclear localization of hTDP-43 wild-type in *Drosophila* neurons and in a subset of glial cells. Interestingly, the only mutant in which we detect any cytoplasmic mislocalization of hTDP-43 is the A90V mutant, where non-nuclear puncta can be observed. A90V is also the only one, out of the five mutants, which is located in the hTDP-43 nuclear localization signal, making it perhaps the most likely to induce cytoplasmic localization (Wobst et al., 2017). A previous study, testing the cellular localization of hTDP-43 in HEK293 cells, a non-neuronal *Drosophila* cell line, and a neuronal *Drosophila* cell line, observed nuclear localization of hTDP-43 wild-type but also both G287S and A315T hTDP-43 mutants (Voigt et al., 2010). The only hTDP-43 variant in which cytoplasmic mislocalization was observed was hTDP-43ΔNLS, where the NLS was completely removed, which goes in line with what we observe in our study. The hTDP-43 A90V mutant, unlike hTDP-43 wild-type, has also been observed to localize to both cytoplasm and nucleus in a QBI-293 cell line, and the disruption of the NLS was hypothesized to be the cause of this (Winton et al., 2008). It is possible that to induce further mislocalization, it would be necessary to age the *Drosophila* longer or to expose them to an additional trigger. We also have not yet been able to discern whether the puncta observed in our A90V mutant are hTDP-43 aggregates or if they are part of stress granules, which is a question that would be beneficial to investigate further in the future.

3.4.3 Abdominal neuromuscular junctions are preserved in young adult *Drosophila*

When observing and quantifying the NMJs of the different genotypes, we did not detect any significant differences at 4-5 days of age. However, as the average age of onset of human

patients suffering from the chosen ALS-TDP-43 mutations are all mid-life, it is possible that age-related phenotypes could appear at a later stage of the fly lifespan. Additionally, as mentioned in the previous chapter, the abdominal NMJs may not be the first affected as ALS is usually confined to either bulbar or limb onset, eventually progressing to other body parts (Bosco et al., 2010). In a future experiment, it would be useful to assess, if technically possible, for example leg neurons, which are more related to the phenotype observed in patients. In addition, it is possible that the climbing deficits observed in the M337V, G287S, and A315T mutants are not due to NMJ loss, but instead caused by upper motor neuron or premotor neuron dysfunction, which is also something that should be investigated.

3.4.4 Severity of the disease in human patients partly overlaps with lifespan and motor symptoms in *Drosophila*

In our experiments, the mutant in which we observe the greatest effect, in both lifespan and motor behavior, is hTDP-43 M337V. The G287S and A315T show significant motor decline but no shortening of lifespan, and the G294A mutant displays slightly shortened lifespan but no motor phenotype compared to hTDP-43 wild-type. The final mutant, A90V, shows none of these phenotypes. When comparing these results to the severity of disease in human patients with the same mutation, M337V is indeed the most severe mutant in both humans and flies, with the lowest average age of onset and one of the shortest durations of disease (Sreedharan et al., 2008). G294A, G287S, and A315T all lead to similar age of onset and duration of disease, while A90V has a much longer disease course and may also lead to Frontotemporal lobar degeneration (FTLD) (Corrado et al., 2009; Kabashi et al., 2008; Sreedharan et al., 2008; Winton et al., 2008). It is also noteworthy that the A90V mutation is associated with sporadic ALS, and is known to exist in controls without causing disease (Winton et al., 2008).

3.4.5 TDP-43 has been linked to the inflammatory response

Both we and Chang and Morton have observed very mild ALS phenotypes in humanized TDP-43 *Drosophila* expressing TDP-43 at an endogenous level. This suggests that an additional trigger may be needed to induce pathology, be it genetic or environmental. For example, studies have shown that environmental metal exposure, a known risk factor of ALS, induces TDP-43 aggregation (Koski et al., 2021). Another known risk factor of ALS is infection (Alonso et al., 2019). Interestingly, TDP-43 has been linked to the cellular response

to infection in several studies. Enteroviruses, for example, which are known to be able to target motor neurons, can cause cytoplasmic aggregation of TDP-43 both *in vitro* and *in vivo* (Xue et al., 2018). Likewise, TDP-43 mislocalizes and forms aggregates in cultured cells infected with Theiler's virus murine encephalomyelitis (TMEV) (Masaki et al., 2019). Mitochondrial DNA release into the cytoplasm can also be triggered by TDP-43, causing activation of the cytoplasmic DNA-sensing cyclic GMP-AMP synthase (cGAS)/stimulator of interferon genes (STING) pathway, which is part of the immune response against bacterial and viral infection (Yu et al., 2020). All of these results suggest a role of TDP-43 in the immune response, something that, when mutated, could be dysfunctional and cause neuroinflammation. Therefore, it is possible that an immune trigger could take part in inducing TDP-43 pathology.

3.5 Conclusion

To summarize, we created humanized TDP-43 fly lines, both wild-type and ALS mutant, and observed that hTDP-43 wild-type *Drosophila* are comparable to control. Interestingly, so are several of the hTDP-43 ALS mutant fly lines we generated. Only in the M337V and G294A mutants were we able to observe a lifespan decrease, and in the M337V, G287S, and A315T mutants we found a mild motor behavior deficit. In addition, hTDP-43 is localized to the nucleus in all genotypes, except in the A90V mutant in which we found the presence of cytoplasmic puncta. However, we could not detect any differences between the different genotypes at the NMJ. It is possible that another trigger could be necessary to induce pathology, possibly through immune activation as several studies have connected TDP-43 with the immune response.

3.6 Materials and methods

3.6.1 Generation of TDP-43 knock-in *Drosophila* lines

Cas9-expressing fly embryos were injected by Genetivision (Houston, TX, USA) with two PCFD3 plasmid vectors expressing two different gRNAs and one plasmid expressing either hTDP-43 wild-type or one of five chosen ALS mutants (A90V, A315T, G294A, G287S, M337V) each at a concentration of 500 ng/µl. The two gRNAs (5'- GGATAATGTAACCGCTGTAC -3', 5'- GGCCGGCATCCACAAGGGTC -3') were chosen using CRISPR Optimal Target Finder (http://targetfinder.flycrispr.neuro.brown.edu) and targeted neighboring *tbph* genes *cpes* and *bgcn*, while making sure to not change the

amino acid sequence of either gene. The inserted sequence included both *tbph* 5' and 3' UTRs but with the *tbph* coding sequence replaced by a fly-codon optimized version of the human TDP-43 cDNA.

3.6.2 Immunoblotting

20 adult *Drosophila* heads were lysed in RIPA lysis buffer (140 mM NaCl, 1 mM EDTA, 1% Triton X-100, 0.5 mM EGTA, 10 mM Tris-Cl pH 8, 0.1% SDS) and sonicated for 5 s. The samples were subsequently centrifuged for 1 min at 12 000 x g, the supernatant collected, and the protein concentration measured with a Micro BCA Protein Assay kit (Thermo Scientific). Before loading 30 μg of protein into a 4-12% Tris-Glycine gel (Invitrogen), the samples were mixed with 4x Laemmli buffer and heated for 2 minutes at 85˚C. After running the gel the protein bands were transferred to a nitrocellulose membrane which was blocked for 1 h in 5% milk blocking solution. The membrane was then incubated at 4˚C overnight in a mix of blocking solution and primary antibodies. The primary antibodies used were anti-TDP-43 (H00023435-M01, Novus Biologicals, 1:500), anti-TBPH (made in the lab, 1:500), anti-tubulin (T6199, Sigma, 1:10 000). Membranes were incubated with secondary antibodies (goat anti-rabbit, 111-035-003, Jackson ImmunoResearch, 1:10 000) (goat anti-mouse 115-035-003, Jackson ImmunoResearch, 1:10 000) diluted in blocking solution for 1 h. Chemiluminescent substrate (WesternBright Sirius, Advansta) was added to enable imaging. To stain with several consecutive antibodies the membranes were stripped for 10 min at 37˚C (Restore Western Blot Stripping Buffer, Thermo Scientific) and re-blocked.

3.6.3 Eclosion

25 larvae were collected and transferred into a new vial. By quantifying the number of adult flies that eclosed compared to the original number of larvae placed in the vial, the eclosion percentage was determined.

3.6.4 Lifespan

In all lifespan assays *Drosophila* were kept at 25˚C, except for the lifespan assay of the Chang and Morton *Drosophila* model, in which the flies were kept at 29˚C. *Drosophila* were placed in food vials with 10 flies per vial, and were flipped to fresh food every other day. At these timepoints the number of dead flies were recorded.

3.6.5 Negative geotaxis

The negative geotaxis assay was performed using glass vials attached to a rod filmed by a Raspberry Pi Camera. The *Drosophila* are placed in the glass vials and tapped down together using gravity to ensure less variable force. The height climbed by each fly during 5 s was measured and average in ImageJ.

3.6.6 Immunohistochemistry

The abdominal muscles of 4-5 day old *Drosophila* kept at 29°C were dissected out and the neuromuscular junctions exposed. The tissue was fixed in Bouin's fixative for 7 minutes and was then washed for four 30-minute intervals in 1xPBS, 0.3% Triton-X. After blocking in 2% Normal Goat Serum diluted in 1xPBS, 0.3% Triton-X, the preparations were incubated with the primary antibody overnight and then washed for 2 more h before 2 h incubation with secondary antibodies. Finally, the samples were washed 2 more h and then mounted in Prolong Diamond antifate mounting medium (Invitrogen). The primary antibodies used were mouse anti-nc82 (DSHB, 1:100) and chicken anti-VGLUT (Eurogentec, custom made, 1:150), and the secondary antibodies used were anti-mouse Alexa Fluor 488 (Lifetech, 1:400) and anti-chicken Alexa Fluor 555 (Lifetech, 1:400). NMJ images were analyzed using a macro in ImageJ, counting the Bruchpilot spots and the area of VGLUT staining.
Ventral nerve cords were dissected out from 4-5 day old *Drosophila*, reared at 29°C, in cold PBS and fixed in 4% PFA. After three washes during a total of one h in 1xPBS, 0.4% Triton-X, samples were blocked in 5% Normal Goat Serum diluted in 1xPBS, 0.4% Triton-X. Subsequently, they were incubated overnight with primary antibodies diluted in blocking solution. The next day, the samples were washed three times during a total of 1 h, and then incubated 1 h with the secondary antibodies. After 2 h of repeated washes, the VNCs were then mounted in Prolong Diamond antifade mounting medium (Invitrogen). Primary antibodies used were anti-elav (DSHB, 1:50), anti-repo (DSHB, 1:25), anti-hTDP-43, and anti-phospho-hTDP-43 (Ser409, Ser410) (Invitrogen, 1:50).

3.6.7 Statistics

Data are presented as mean ± standard error of the mean. The p-values were calculated with a one-way ANOVA with either Dunnett's or Tukey's Multiple Comparisons post-hoc test or, for the negative geotaxis assay, a two-way ANOVA with Dunnett's Multiple Comparisons

post-hoc test assessing the main effect of each genotype. For survival curves, the Mantel-Cox test was used. Results with a p-value < 0.05 were considered significant.

4

Chapter 4 – *Drosophila* FUS and TDP-43 deletion models can be partly rescued through reducing the NF-κB signaling pathway

- -

Emma Källstig, Wei Jiao, Marine Van Campenhoudt, Bernard Schneider, Brian McCabe

Caz-/- eclosion experiments with heterozygous Imd mutants or hOPTN overexpression performed by Wei Jiao; Caz-/- negative geotaxis and lifespan experiments with heterozygous Imd mutants performed by Emma Källstig; TBPH-/- eclosion and lifespan experiments with heterozygous Imd mutants performed by Marine Van Campenhoudt.

4.1 Abstract

Optineurin (OPTN) is one of the many genes that have been associated with familial ALS, but one of the only genes to be linked to the disease through autosomal recessive inheritance. Since OPTN is a known inhibitor of the pro-inflammatory NF-κB pathway, we decided to investigate the effect of OPTN expression as well as NF-κB inhibition in two *Drosophila* ALS model based on the deletion of the *Drosophila* FUS ortholog Caz and the *Drosophila* TDP-43 ortholog *tbph*. We observed that wild-type OPTN expression, but not ALS mutant OPTN expression, can partly rescue Caz-/- eclosion rate. In addition, heterozygous mutants of several NF-κB pathway components significantly improved eclosion rate, longevity and motor abilities in the fly models. Together, these results point to aberrant NF-κB activation as a possible consequence of loss-of-function of the orthologs of FUS and TDP-43, two genes implicated in ALS in humans.

4.2 Introduction

There are over 25 genes linked to fALS, with a variety of different functions in the cell (Renton et al., 2014). Optineurin (OPTN) is one of the only genes whose ALS-associated mutations are known to be inherited in an autosomal recessive manner. This mode of inheritance supports a loss-of-function hypothesis in OPTN-based ALS, leading us to be able to more easily investigate its mechanisms (Kamada et al., 2014).

OPTN is a protein with many different functions. It contributes to autophagy induction, Golgi complex maintenance, regulation of post-Golgi protein trafficking, and inhibition of the pro-inflammatory NF-κB pathway (Ryan and Tumbarello, 2018). Interestingly, OPTN is not the only gene linked to fALS that has also been known to bind to or regulate the NF-κB pathway. Both TDP-43 and FUS, for example, have been observed to physically interact with and possibly regulate the pro-inflammatory NF-κB protein p65 (Swarup et al., 2011; Uranishi et al., 2001). Since inflammatory markers, among them NF-κB proteins, have been observed in both ALS patients and animal models, this suggest chronic neuroinflammation due to NF-κB dysregulation as a possible mechanism of disease (Crosio et al., 2011; Frakes et al., 2014; Henkel et al., 2006; Jin et al., 2020; Kuhle et al., 2009; Mishra et al., 2016).

The NF-κB pathway is commonly activated by different types of infection, and the protein cascade induces translocation of the NF-κB proteins to the nucleus where they regulate pro-inflammatory gene expression. In *Drosophila*, the NF-κB pathway acts through the Imd and Toll innate immunity signaling pathways. Activation of the Imd pathway in particular, which responds to gram-negative bacterial infection and induces nuclear translocation of one of the *Drosophila* NF-κB proteins, Relish (Rel), has been associated with neurodegeneration in several *Drosophila* studies (Cao et al., 2013; Kounatidis et al., 2017; Wu et al., 2017). In the context of ALS, TDP-43-based *Drosophila* neurodegeneration has also been associated with the Imd pathway (Zhan et al., 2015). While motor neuron-specific overexpression of TDP-43 wild-type induces significantly decreased longevity, heterozygous deletion of *Drosophila* NF-κB protein Relish rescues the shortened lifespan by ~20%.

The aim of this study was to investigate the effect of OPTN overexpression on ALS-like pathology, and to evaluate if the effect was due to its function as an NF-κB inhibitor by using mutants of the Imd pathway. We assessed this in previously established *Drosophila* models containing a deletion of *Drosophila* FUS and TDP-43 orthologs, Caz and TBPH. These models are known for their severe phenotypes in eclosion, lifespan, and motor behavior. We

observed that overexpression of human OPTN in the Caz-/- model significantly increases the eclosion rate of the *Drosophila*. Using both Caz-/- and TBPH-/-, we were also able to detect that a heterozygous Imd pathway component mutants rescue the rate of eclosion and, in the case of the Caz-/- *Drosophila*, increased lifespan and improved motor behavior. This suggests that the NF-κB-inhibitory function of OPTN may contribute to ALS pathology, and highlights the NF-κB pathway as a possible therapeutic target.

4.3 Results

4.3.1 Overexpression of hOPTN, but not ALS mutant hOPTN Q398X, rescues Caz-/- eclosion

The Caz1 model made by Wang et al., hereafter referred to as Caz-/-, has removed 58% of the *caz* gene causing a full deletion of Caz protein expression (Wang et al., 2011). Caz-/- *Drosophila* have previously been established to have severe problems with decreased locomotion, lifespan, and adult viability. To assay the effect of OPTN in this model, we used human OPTN (hOPTN) as OPTN does not have a *Drosophila* ortholog. In mammals, OPTN inhibits NF-κB through binding to the IKK complex, whose ortholog in *Drosophila* would be the ird5-Key complex, and we hypothesize that hOPTN may interact with this complex (figure 1A) (Tusco et al., 2017). We overexpressed wild-type hOPTN, and the hOPTN ALS mutant Q398X, ubiquitously in the animals. As can be seen in figure 1B, wild-type hOPTN expression, but not ALS mutant hOPTN expression, partly rescued Caz-/- eclosion.

Figure 4-1. hOPTN overexpression partially rescues Caz-/- eclosion
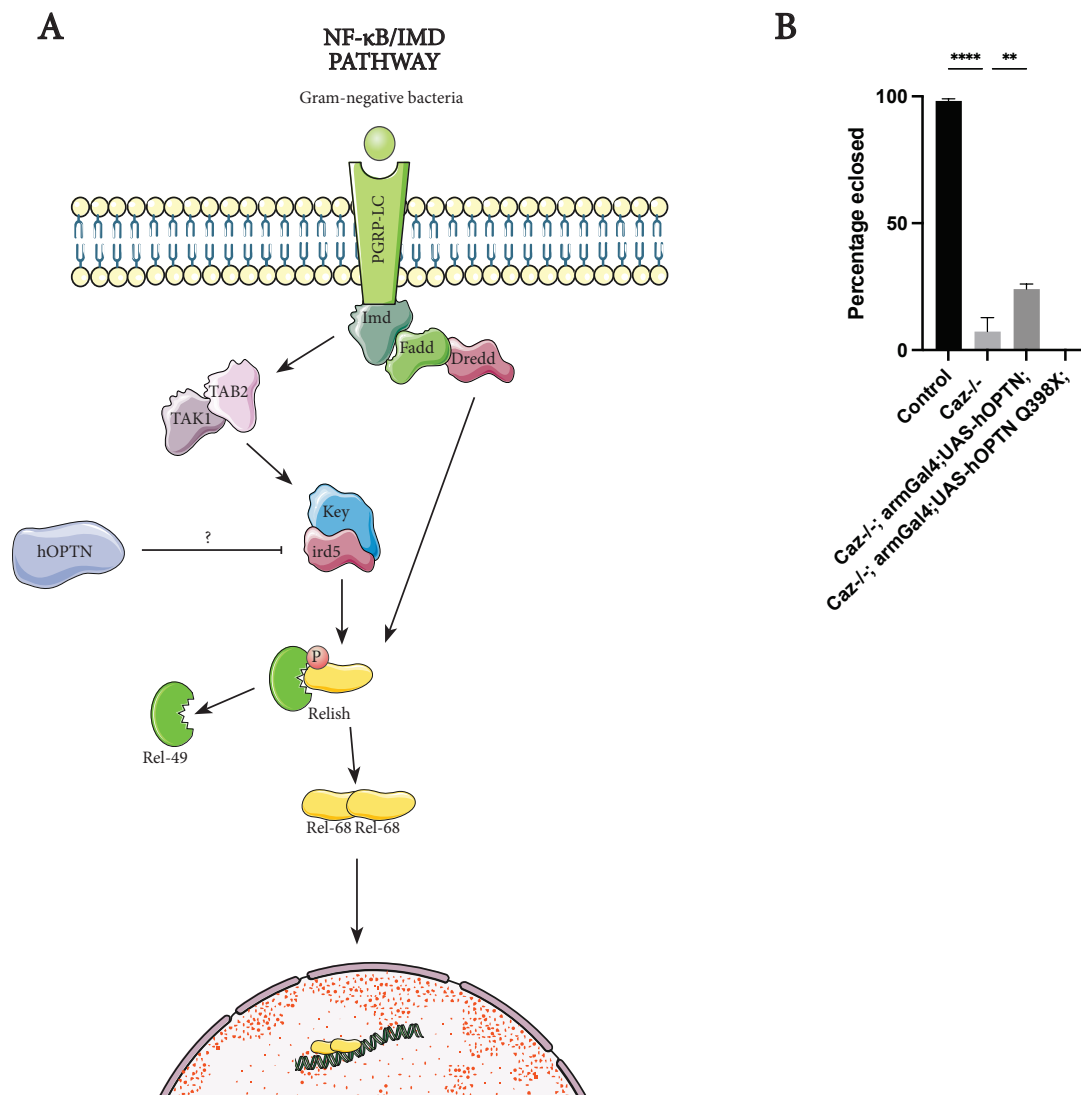
Figure 1: hOPTN overexpression partially rescues Caz-/- eclosion. (A) An illustration of the components in the *Drosophila* Imd pathway. Also included, a possible interaction partner for hOPTN based on homology with the human protein, as *Drosophila* do not have an OPTN ortholog. (B) The ubiquitously expressed Arm-Gal4 was used to overexpress UAS-hOPTN or ALS mutant UAS-hOPTN Q398X in the Caz-/- background, with hOPTN overexpression significantly increasing the eclosion rate (n ≥ 15 larvae per group). Data are presented as mean ± standard error of the mean; statistical analysis: one-way ANOVA with Dunnett's Multiple Comparisons post-hoc test, with all groups compared with Caz-/-.

4.3.2 Caz-/- eclosion can be partially rescued by heterozygous mutations of Imd pathway components

As OPTN is a known inhibitor of the NF-κB pathway and OPTN mutants are associated to ALS in a loss-of-function manner, we aimed to assess the effects of heterozygous mutants of

Imd pathway components Kenny (Key), Relish (Rel) or Peptidoglycan recognition protein LC (PGRP-LC) in the Caz-/- model (Kamada et al., 2014; Ryan and Tumbarello, 2018). We observed that the percentage of eclosion was significantly increased with mutations in PGRP-LC and Rel, but not Key (figure 2A). The results with decreased PGRP-LC and Rel expression suggest that the Imd pathway may be regulated by Caz, and that overactivation of the pathway could cause part of the eclosion phenotype. It remains unclear, however, why the same rescue was not observed with the heterozygous Key mutant. It is possible that rescue of the phenotype requires a very specific level of decrease in the Imd pathway, which could not be reached with heterozygous Key mutation.

Figure 4-2. Caz-/- eclosion rate, motor behavior, and lifespan with heterozygous Imd mutations
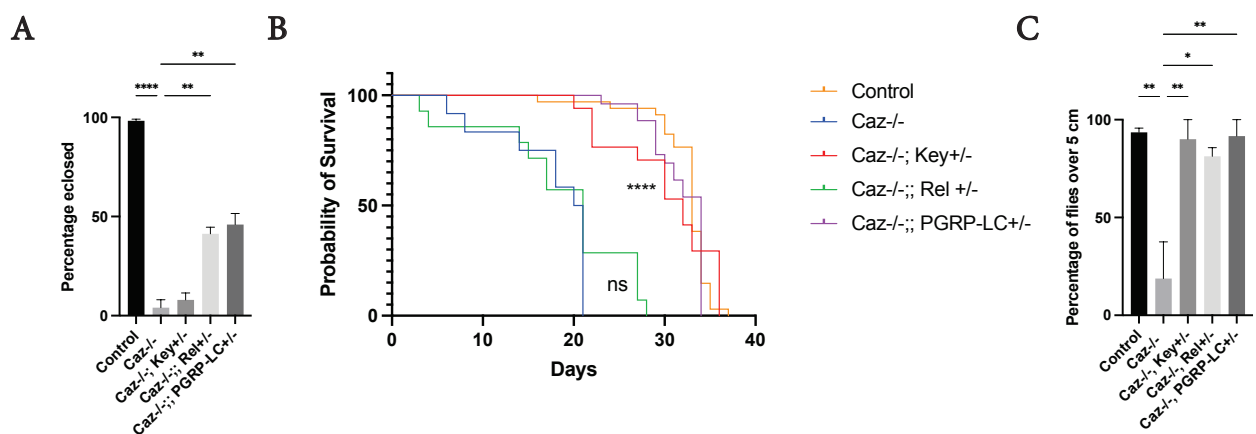
Figure 2: Caz-/- fly eclosion rate, motor behavior, and lifespan can be rescued by heterozygous mutations in certain Imd pathway components. (A) The Caz-/- level of eclosion is significantly rescued through heterozygous mutations in Rel and PGRP-LC, but not Key (n ≥ 52 larvae per group). (B) Lifespan curve of control (orange, n=34), Caz-/- (blue, n=12), Caz-/-;Key+/- (red, n=17), Caz-/-;;Rel+/- (green, n=14), Caz-/-;;PGRP-LC+/- (magenta, n=26). Caz-/- longevity increases with heterozygous mutations of Key and PGRP-LC, but not Rel. (C) Negative geotaxis test, measuring the percentage of flies that have climbed over 5 cm in 10 s. Heterozygous mutations of Rel, PGRP-LC, and Key all rescue the motor skills in the Caz-/- *Drosophila* (n ≥ 24). Data are presented as mean ± standard error of the mean; statistical analysis: one-way ANOVA with Dunnett's Multiple Comparisons post-hoc test (A and C), comparing all genotypes with Caz-/-, and Mantel Cox test (B).

4.3.3 Caz-/- lifespan can be increased by heterozygous Key and PGRP-LC but not Rel mutations

As we observed an increased eclosion with decreased levels of Imd components, we wanted to see if this rescue was reflected in adult fly lifespan. Indeed, we found that the lifespan of the Caz-/- *Drosophila* was significantly increased with heterozygous mutation of PGRP-LC or Key (figure 2B). Heterozygous Rel mutants, however, did not give the same effect. Interestingly, heterozygous Key mutation was sufficient to rescue adult lifespan but not eclosion, and in the case of Rel the opposite was observed. It may be that these proteins play other important roles in the fly that are specific to the age and point in development.

4.3.4 The motor phenotype of Caz-/- *Drosophila* is severely perturbed, but partly rescued through decrease of Imd pathway components

Subsequently, the motor behavior of the adult *Drosophila* was assessed using the negative geotaxis assay. The flies were tapped down to the bottom of a glass vial and their ability to climb up the walls of the vial was measured. We quantified the percentage of *Drosophila* that are able to climb over 5 cm of height within 10 s after the start of the assay. In this experiment we observed that Rel, Key, and PGRP-LC heterozygous mutants all significantly rescued the climbing ability of the Caz-/- *Drosophila* (figure 2C).

4.3.5 TBPH-/- aberrant development can be partly rescued by heterozygous mutants of Imd pathway components

Since we observed significant rescue through decreasing the expression of Imd pathway components in the Caz-/- *Drosophila*, we decided to further investigate a similar approach in TBPH knockout *Drosophila*. The TBPHΔ96 model, hereafter mentioned as TBPH-/-, was previously produced by Diaper et al (Diaper et al., 2013). These genetically modified *Drosophila* revealed that deletion of TBPH causes significant developmental problems shown by low levels of pupal eclosion, as well as a severely shortened longevity. To investigate if the rescue effects of modifying the Imd pathway in the Caz model could be replicated in TBPH-/- *Drosophila*, we induced heterozygous mutants of Rel and PGRP-LC in the TBPH-/- background. As is shown in figure 3A, the heterozygous Rel and PGRP-LC mutants resulted in a significant increase and partial rescue of the TBPH-/- eclosion rate, pointing to Imd pathway dysregulation contributing to the severe developmental phenotypes observed in TBPH-/- *Drosophila*.

Figure 4-3 Eclosion and lifespan of TBPH-/- with heterozygous Imd mutants
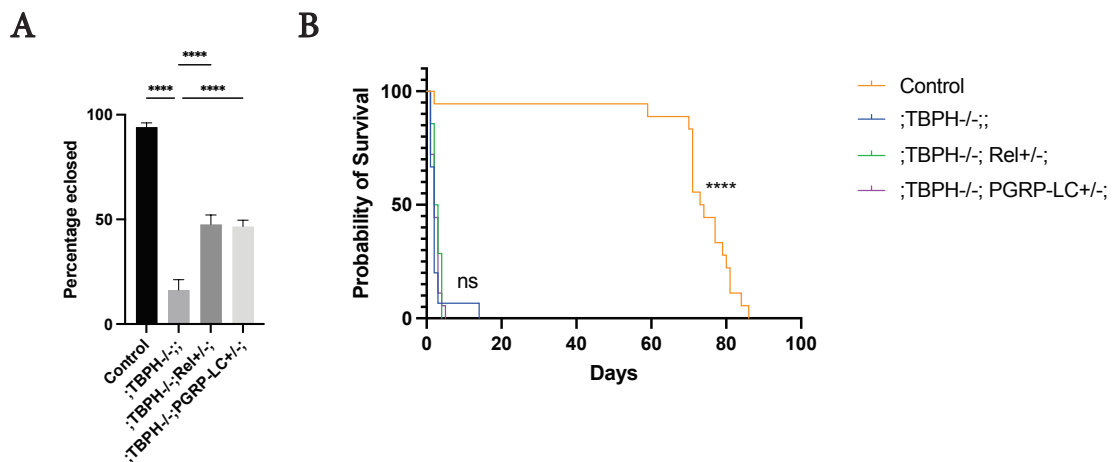
Figure 3: Heterozygous mutations in Imd pathway components rescue TBPH-/-fly eclosion rate but not lifespan. (A) The severely reduced eclosion rate caused by TBPH deletion is rescued by heterozygous Rel and PGRP-LC mutants (n ≥ 105). (B) Lifespan curve showing control (orange, n=18) TBPH-/- (n=15), ;TBPH-/-;Rel+/-; (green, n=14), and ;TBPH-/-;PGRP-LC+/-; (magenta, n=18). The decreased lifespan of TBPH-/- compared to control cannot be rescued by heterozygous Rel and PGRP-LC mutants (n ≥ 14). Data are presented as mean ± standard error of the mean; statistical analysis: one-way ANOVA with Dunnett's Multiple Comparisons post-hoc test comparing all genotypes with TBPH-/- (A), and Mantel Cox test (B).

4.3.6 The shortened lifespan of TBPH-/- *Drosophila* cannot be rescued by heterozygous Imd pathway mutations

As with the Caz-/- *Drosophila*, we also measured TBPH-/- lifespan with and without a decreased Imd pathway component expression. Unlike in the Caz-/- *Drosophila*, we observed that the reduced Rel and PGRP-LC does not influence the longevity of the TBPH-/- flies (figure 3B). This could be due to several factors. For example, the heterozygous mutations in Imd pathway components may not be enough to rescue the lifespan, and we may need a more severe decrease in the proteins to induce a longevity increase. However, it is noteworthy that both for the Caz-/- and TBPH-/-, homozygous Imd mutations do not survive to adulthood, further emphasizing the importance of the level of Imd pathway activation. It is also possible that the lack of longevity rescue in the TBPH-/- *Drosophila* is due to different Imd protein levels being optimal during development and adulthood. Likewise, in the Caz-/- experiments, heterozygous Key mutant caused an increase in lifespan but did not rescue eclosion. A similar mechanism could be at play for the TBPH-/-, where the Imd decrease appears to

rescue eclosion during developmental stage, but is not sufficient to prolong lifespan during adulthood.

4.4 Discussion

Here, we have shown that the known NF-κB inhibitor OPTN can rescue the eclosion rate in a Caz-/- model. Furthermore, several heterozygous mutants of components in the *Drosophila* Imd pathway can also rescue eclosion, and in some cases adult lifespan and motor behavior, in Caz-/- or TBPH-/- *Drosophila*. Together, this suggests that OPTN is rescuing Caz-/- eclosion through its NF-κB inhibitory function. Our data also point to a connection between Caz, TBPH and Imd, and highlight chronic neuroinflammation through aberrant NF-κB pathway activation as a possible pathologic mechanism in ALS.

4.4.1 TBPH and Caz have been shown to be in a common pathway, possibly regulating Imd

In mammalian cells, FUS and TDP-43 have been observed to form a complex when expressed at endogenous levels, suggesting that the two proteins may take part in common pathways in the cell (Kim et al., 2010). In *Drosophila*, it has also been shown in a coimmunoprecipitation assay that Caz and TBPH physically interact in neurons (Wang et al., 2011). The study also revealed that Caz overexpression in TBPH-/- *Drosophila* can rescue both eclosion and longevity, pointing to Caz acting downstream of TBPH in a common pathway. As we here show that both TBPH-/- and Caz-/- eclosion can be rescued by heterozygous mutants in Imd pathway components, it is possible that Caz and TBPH have a function in immunity, and that they take part in downregulation of the Imd pathway. An increase of the Imd pathway in Caz-/- and TBPH-/- could then be rescued through Imd heterozygous mutants. In addition, in mice, the NF-κB protein p65 interacts with both FUS and TDP-43, suggesting that this possible function could be conserved between species (Swarup et al., 2011; Uranishi et al., 2001).

4.4.2 Different Imd pathway components can rescue different parts of the fly development

In our experiments we observed that not all heterozygous mutants of Imd pathway components can rescue both fly development and adult lifespan. In the Caz-/- *Drosophila*,

Key+/- rescued lifespan but not eclosion, and Rel+/- conversely rescued eclosion but not lifespan. In the TBPH-/- *Drosophila*, heterozygous PGRP-LC and Rel mutants rescued eclosion but neither of them improved longevity. It is therefore possible that very specific levels of each of these proteins is required for rescued eclosion and longevity, and the required levels may differ between development and adulthood. The Toll pathway, for example, is known to be vital during embryonic development, and it is possible that immune genes from the Imd pathway have yet to be discovered roles in development and adulthood as well (Valanne et al., 2011).

4.4.3 Inhibition of NF-kB pathway as a potential target for therapeutic development

With several heterozygous Imd mutants we can observe increased eclosion rate, prolonged lifespan, and improved motor abilities in our Caz and TBPH knockout fly models of ALS. In addition, the known NF-κB inhibitor OPTN can significantly increase the eclosion rate of Caz-/- *Drosophila*. Therefore, we hypothesize that the NF-κB pathway is aberrantly activated in ALS, which may cause chronic neuroinflammation, and that inhibiting this pathway could be a possible treatment for the disease. Indeed, the NF-κB pathway has been shown to be upregulated in ALS patient spinal cord tissue (Swarup et al., 2011). Several other studies have also pointed to the connection between ALS and NF-κB (Crosio et al., 2011; Frakes et al., 2014), and neuronal inhibition of the pathway in both TDP-43[A315T] and TDP-43[G348C] transgenic mice reduces motor neuron loss and improves cognitive and motor functions (Dutta et al., 2020). Microglial depletion of NF-κB in SOD1[G93A] ALS mice also increases mouse survival, again highlighting NF-κB inhibition as a possible therapeutic approach for ALS (Frakes et al., 2014).

4.5 Conclusion

In conclusion, we were able to observe improvement in eclosion, lifespan and/or motor abilities of TBPH-/- and Caz-/- *Drosophila* through heterozygous mutations in Imd pathway components. In addition, overexpression of ALS-associated NF-κB inhibitor OPTN, but not ALS mutant OPTN Q398X, significantly increases Caz-/- eclosion rate. Together, this highlights the possibility of NF-κB overactivation as a pathogenic mechanism in ALS, as well as NF-κB inhibition as a possible therapeutic strategy.

4.6 Materials and methods

4.6.1 *Drosophila* lines

w^{1118}, caz1;;, ;TBPHΔ96;;, ;;UAS-OPTN;, ;;UAS-OPTN Q398X;, ;armadillo-Gal4;;, ;;PGRP-LCΔexon5;, ;KeyC02831;;, ;;Rele20;.

4.6.2 Eclosion

15 male larvae of the chosen genotype were moved to a new food vial. The adult flies that eclosed from said vial were counted and compared to the original number of larvae in the vial. At least 100 larvae were used for each genotype.

4.6.3 Lifespan

The *Drosophila* were collected and placed in vials with a maximum of 10 flies per vial. The flies were flipped into fresh food vials every other day, and at each point of flipping the number of dead *Drosophila* was counted. For the Caz-/- lifespan experiments, the *Drosophila* were kept at 29°C, while for all other lifespan experiments, they were kept at 25°C.

4.6.4 Negative geotaxis

The negative geotaxis assay on the Caz-/- *Drosophila* was performed on 4-day old flies at 29°C. The *Drosophila* were placed in a glass vial and manually tapped down to the bottom. The percentage of flies that were able to climb over 5 cm up the tube in 10 s was measured. Two trials with a 2-minute resting period in between were averaged.

4.6.5 Statistics

Data are presented as mean ± standard error of the mean, and p-values were calculated using one-way ANOVA with Dunnett's Multiple Comparison post-hoc test in and Mantel-Cox test in Prism. Results with a p-value < 0.05 were considered significant.

5

Chapter 5 – Humanized FUS and TDP-43 ALS mutants are not more susceptible to gram-negative bacterial infection than controls

- -

Emma Källstig, Marine Van Campenhoudt, Bernard Schneider, Brian McCabe

Experiment with images of TBPH-LexA driving a nuclear fluorescent protein performed by Marine Van Campenhoudt; all other experiments performed by Emma Källstig

5.1 Abstract

In chapters one and two of this thesis, as well as in a previous study by Chang and Morton (Chang and Morton, 2017), it has been found that humanized *Drosophila* models expressing wild-type TDP-43 or FUS at the endogenous levels can rescue the phenotypes caused by the absence of the fly ortholog genes *tbph* and *caz,* respectively. However, ALS mutations in these humanized models do not replicate the severity of the motor symptoms that characterize ALS. In the third chapter of this thesis, we have shown that the loss of Caz or TBPH functions leads to severe ALS-like phenotypes which can be partly rescued through heterozygous mutations of components of the NF-κB pathway. Based on those findings, we hypothesize that if the NF-κB pathway is triggered by a stimulus, ALS mutant FUS and TDP-43 fly lines may improperly regulate NF-κB activity, leading to more severe ALS pathology. To explore this possibility, we sought to expose the *Drosophila* models to NF-κB-inducing stimuli. We used septic injury bacterial infection with the gram-negative bacterium *Erwinia carotovora carotovora* 15 (*ECC*15) in the humanized FUS and TDP-43 mutants and wild-type, to assess the effects of induction of the Imd immune pathway. However, we did not observe a difference in susceptibility to infection in any of the ALS mutants, which showed very similar motor activity and survival to humanized wild-type controls following exposure to *ECC*15. On the other hand, we observed severe deficits in motor behavior and a

dramatically decreased survival when genetically activating the Imd pathway exclusively in glial cells in wild-type *Drosophila*, and to a lesser extent in neuronal cells, in the absence of any bacterial infection. Although the response to peripheral infection does not appear to be modified in *Drosophila* carrying FUS and TDP-43 ALS mutations, these results indicate that Imd activation directed to glial cells may have severe consequences, a question which will need to be addressed in the context of the humanized FUS and TDP-43 *Drosophila* lines.

5.2 Introduction

The humanized FUS and TDP-43 *Drosophila* models generated in the first chapters of this thesis did not show any severe phenotypes when carrying ALS mutations. This suggests that another trigger may be required to induce pathology. Since we were able to partly rescue ALS loss-of-function *Drosophila* models in chapter three through heterozygous mutation of NF-κB-pathway components, we hypothesize that NF-κB-pathway activation could be a possible trigger of ALS pathology in the humanized FUS and TDP-43 models.

Several environmental risk factors that could act as an immune challenge have been associated with ALS, including both bacterial and viral infections. For example, several viral infections worsen ALS phenotypes in a FUS mutation model of iPSC-derived spinal neurons (Bellmann et al., 2019), and enteroviruses can cause cytoplasmic aggregation of TDP-43 *in vitro* and *in vivo* (Xue et al., 2018). TDP-43 can also induce the release of mitochondrial DNA into the cytoplasm, leading to activation of the cGAS/STING pathway which takes part in the immune response against bacterial and viral infection (Yu et al., 2020). Bacterial infections have been revealed to be present in many ALS patients, including all but one of the Gulf War veterans that were diagnosed with ALS (Nicolson et al., 2002). 80% of non-military American, Canadian, and British ALS patients also had infections with *M. penetrans, M. fermentans, M. hominis*, or *M. pneumoniae*. Likewise, *Borrelia burgdorferi* infection is observed in a significant amount of ALS patients (Halperin et al., 1990; Hänsel et al., 1995). All aforementioned bacterial infections are known to activate the NF-κB pathway (Borchsenius et al., 2019; Ebnet et al., 1997; Logunov et al., 2009; Sacht et al., 1998).

In *Drosophila,* the NF-κB pathway corresponds to the two innate immune pathways: Imd and Toll. Overactivation of the Imd pathway and its NF-κB protein Relish (Rel) has been linked with neurodegeneration in several studies. For example, creating mutations in negative regulators of the Imd pathway leads to toxic antimicrobial peptide (AMP) levels and

neurodegeneration, decreased longevity, and locomotor defects (Kounatidis et al., 2017). Another study has observed that gram-negative bacterial infection, activating the Imd pathway, causes recruitment of hemocytes to the brain causing neurodegeneration in an Alzheimer's disease model (Wu et al., 2017). In a *Drosophila* ALS model overexpressing TDP-43 in motor neurons, heterozygous deletion of Relish can also rescue the decreased lifespan by ∼20% (Zhan et al., 2015).

Here, we aim to investigate if gram-negative bacterial infection can act as a trigger of pathology in our previously generated humanized FUS and TDP-43 fly lines. Both the humanized FUS and TDP-43 lines with ALS mutations show no or very mild ALS-like symptoms, perhaps due to the absence of an external trigger. However, after septic injury infection with gram-negative bacterium *Erwinia carotovora carotovora 15* (*ECC*15) we did not observe any significant differences in lifespan or motor behavior in the *Drosophila*. On the other hand, in otherwise wild-type flies, activation of the Imd pathway in glial cells induced severe motor behavior deficits and longevity decrease. This suggests that to induce pathology in the humanized ALS *Drosophila*, glial Imd pathway activation may be required.

5.3 Results

5.3.1 hFUS, but not hTDP-43, is expressed in the fat body

Firstly, we aimed to assess if hFUS or hTDP-43 is expressed in the cells of the main *Drosophila* immune organ: the fat body. This was to confirm if any effect that may be observed when activating the fly Imd pathway could be due to the fat body immune response. To facilitate this, we dissected out the *Drosophila* fat body and labelled it. In the case of hFUS, we used an hFUS antibody to assess the presence of the protein in the fat body of hFUS wild-type *Drosophila*, and as can be seen in figure 1A and 1B, hFUS was indeed present in the fat body cell nuclei. When we stained hTDP-43 wild-type *Drosophila* for the presence of hTDP-43, on the other hand, we observed no expression of the protein in the *Drosophila* fat body (figure 1C,D). To confirm this, we used a fly line containing a LexA driver driven by the endogenous TBPH promoter, and crossed it with a fly containing a LexOP-histone-Cherry. The progeny expressed fluorescent proteins in the nuclei of cells that normally express TBPH. After dissecting these flies, we did not observe any nuclear Cherry in the fat body (figure 1E), causing us to conclude that TBPH and hTDP-43 are indeed not expressed by the fat body. These results highlight the difference in expression pattern between FUS and TDP-43.

Figure 5-1. hFUS is expressed in the *Drosophila* fat body while hTDP-43 is not
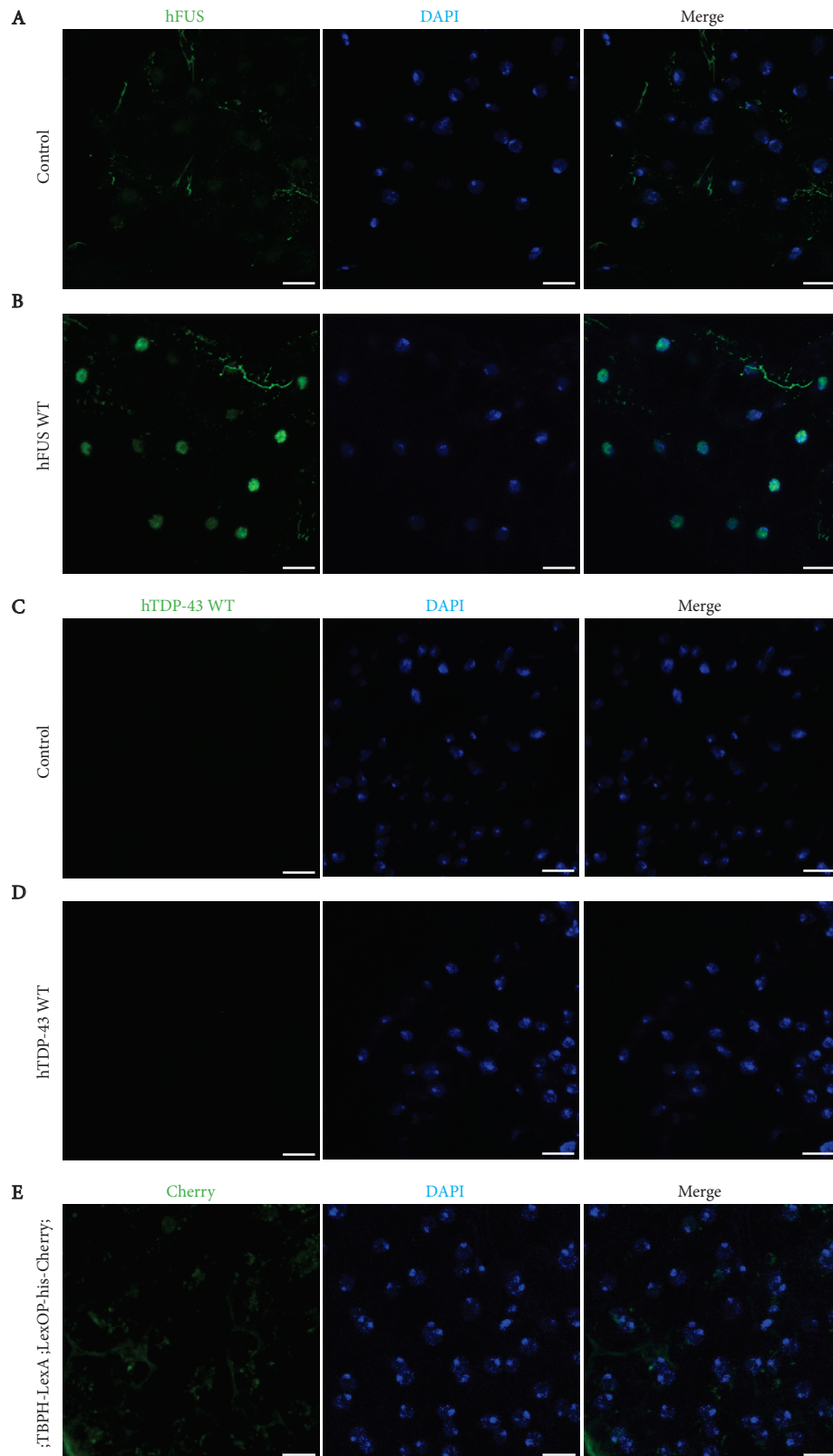
Figure 1: hFUS is expressed in the *Drosophila* fat body while hTDP-43 is not. The *Drosophila* fat body was dissected out and stained to assess for the presence of hFUS and hTDP-43. (A) Control fly fat body co-stained for hFUS (green) and DAPI (blue). (B) hFUS wild-type flies stained for hFUS and DAPI, note the presence of the protein in the nuclei in the fat body cells. (C) Control flies stained for hTDP-43 (green) and DAPI (blue). (D) hTDP-43 wild-type flies stained for hTDP-43 and DAPI, note that hTDP-43 is not expressed in the fat body. (E) A control fly containing a LexA driver in the endogenous *tbph* gene was crossed with a LexOP line expressing histone-Cherry. The fat body of the progeny was subsequently dissected out, stained with DAPI (blue), and imaged to assess the expression pattern of endogenous TBPH (green). This image confirms that TBPH is indeed not expressed in the fat body of the *Drosophila*. The scale bar is 10 μm.

5.3.2 hFUS ALS mutant longevity is not more susceptible to bacterial infection than controls

In order to assess the effect of gram-negative infection on ALS mutant *Drosophila*, we used *ECC*15 bacteria. *ECC*15 is part of the gram-negative Enterobacteriaceae family, and it is known to cause potato blackleg disease (Basset et al., 2000). *Drosophila* carrying *ECC*15 are commonly found in potato fields, acting as vectors of the bacteria and carrying it to nearby potato plants. In *Drosophila* research, it has been used both through septic injury and oral administration to induce an immune response.

3-4 day old male humanized FUS *Drosophila*, both ALS mutant and wild-type, were infected with *ECC*15 by pricking them in the thorax with a needle dipped in *ECC*15 bacteria concentrated at an OD_{600} of 100. In addition, we infected Rel-/- *Drosophila*, who have a deficient Imd pathway, to ascertain that the infection worked efficiently. To control for other unwanted infections and the septic injury itself, we pricked the *Drosophila* with a needle dipped in the PBS that was used to dilute the bacteria (this control is named sham). In the sham control, we observed a significant but very mild difference in lifespan between hFUS wild-type and the R521H mutant (figure 2A), confirming the effects of this FUS mutant previously observed in *Drosophila* without septic injury. When infecting the flies with *ECC*15, Rel-/- mutants died within the first day, showing that the infection has been efficient (figure 2B). Humanized FUS wild-type and ALS mutants, however, showed no significant difference in their lifespan compared to each other or control, suggesting that ALS mutants are not more susceptible to gram-negative infection than wild-type (figure 2C, D).

To assess the microbial load in each fly of the different genotypes, we quantified the colony-forming units 24 h post-infection. In control as well has all humanized FUS *Drosophila*, including the ALS mutants, the microbial load remained comparable. As a positive control,

we included flies with a deletion of Imd pathway component Key, which had a significantly higher bacterial load than control (figure 2E).

Figure 5-2. hFUS *Drosophila* infected with *ECC*15
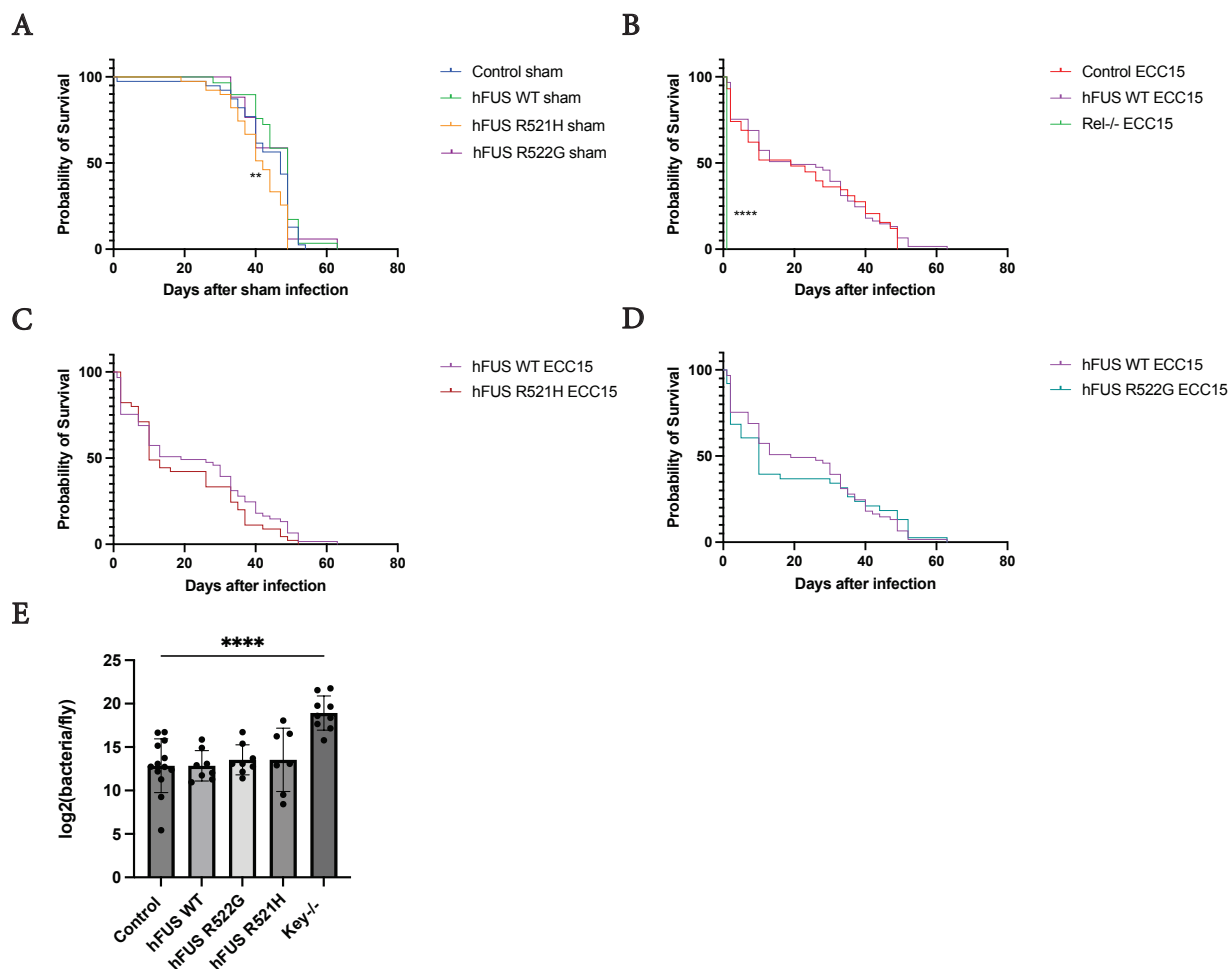
Figure 2: Infection of the *Drosophila* with *ECC*15 bacteria at $OD_{600}=100$ does not significantly decrease hFUS ALS mutant lifespan compared to controls. Flies were infected with *ECC*15 ($OD_{600}=100$) through a septic needle injury in the thorax at 3-4 days of age, and the lifespan was recorded for (A) All sham control genotypes, pricked with a needle dipped in PBS instead of *ECC*15. The genotypes are control (blue, n=39), hFUS wild-type (green, n=29), hFUS R521H (orange, n=39), hFUS R522G (purple, n=17). The significance is between hFUS wild-type and hFUS R521H. (B) Control (red, n=58) compared to hFUS wild-type (magenta, n=61), as well as an immunodeficient Rel-/- (green, n=10) control infected with *ECC*15. The significance is between Rel-/- and control. (C) hFUS wild-type compared to hFUS R521H infected with *ECC*15 (brown, n=56). (D) hFUS wild-type compared to hFUS R522G infected with *ECC*15 (turquoise, n=38). The same hFUS wild-type *ECC*15 data is used in B-D. All longevity data for the different genotypes are from the same experiment but separated into different graphs only for ease of visualization. (E) Colony-forming unit measurements presented as log2(), showing the bacterial load of the different genotypes compared to an immunodeficient Key

knockout fly line 24 h after infection (n $\geq$ 7). Data are presented as mean $\pm$ standard error of the mean; statistical analysis: Mantel-Cox test (A-D), one-way ANOVA with Dunnett's Multiple Comparisons post-hoc test (E), with all genotypes compared to control.

5.3.3 No difference in motor behavior is observed between ECC15-infected hFUS wild-type and ALS mutants

Though no significant longevity differences were observed between ALS mutants and the humanized control, we also wanted to assess potential differences in motor abilities, as motor behavior deficit is a major ALS phenotype. Therefore, we used the negative geotaxis assay to measure the average max height climbed by the *Drosophila* in 5 s, as they age, after infection with sham control or *ECC*15. In the sham control experiment, no genotype showed infection susceptibility compared to controls (figure 3A-C). After infection with *ECC*15, the results were similar, with no infection susceptibility seen in the FUS ALS mutants compared to control (figure 4A-C). We conclude that humanized FUS ALS mutants are not more susceptible to *ECC*15 infection than control.

Figure 5-3. hFUS *Drosophila* with sham infection
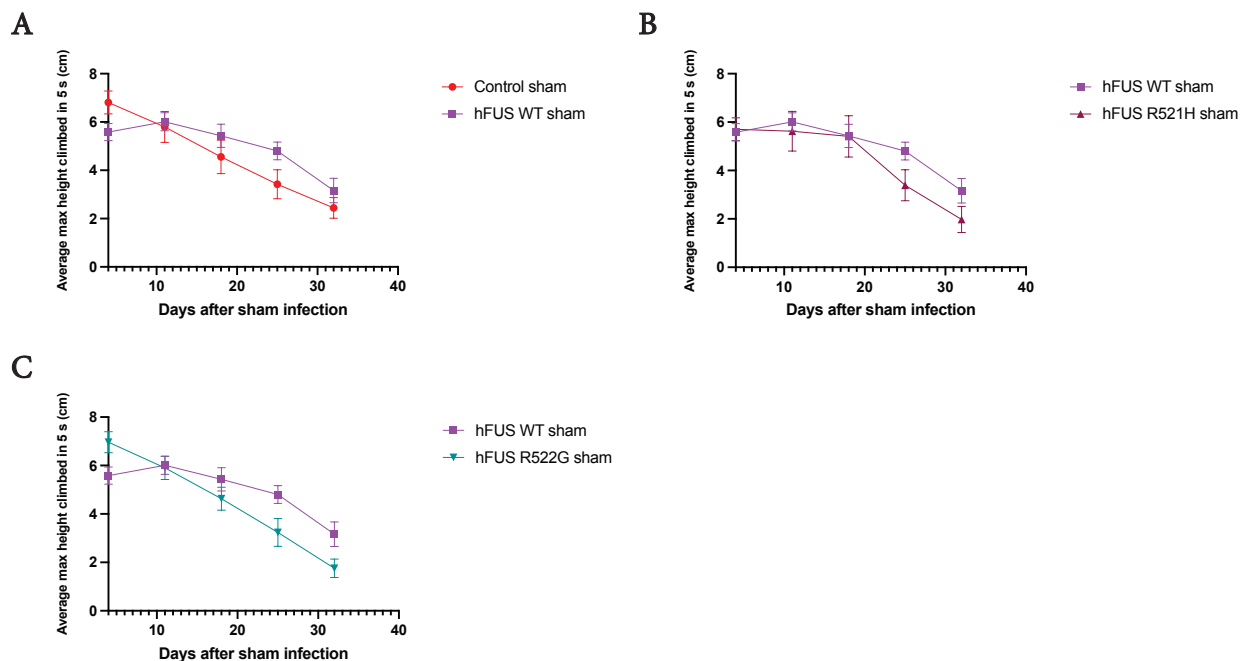
Figure 3: Sham infection does not cause any significant difference in motor behavior between hFUS fly lines. The flies were sham pricked with a needle dipped in PBS and then their motor ability was tested using the negative geotaxis assay as they aged. The average max height climbed in 5 s is presented for: (A) Control (red, n=28 flies at first timepoint) compared to hFUS wild-type (magenta, n=29 flies at first timepoint) (B) hFUS

wild-type compared to hFUS R521H (maroon, n=30 flies at first timepoint) (C) hFUS wild-type compared to hFUS R522G (turquoise, n=20 flies at first timepoint). There was no significant difference in motor behavior after sham infection, between any of the groups compared to hFUS wild-type. The same hFUS wild-type sham data is used in A-C. All negative geotaxis data for the different genotypes are from the same experiment but separated into different graphs only for ease of visualization. Data are presented as mean ± standard error of the mean; statistical analysis: two-way ANOVA with Dunnett's Multiple Comparisons post-hoc test looking at the main effect of each genotype and comparing all genotypes to hFUS wild-type.

Figure 5-4. Negative geotaxis of infected hFUS *Drosophila*
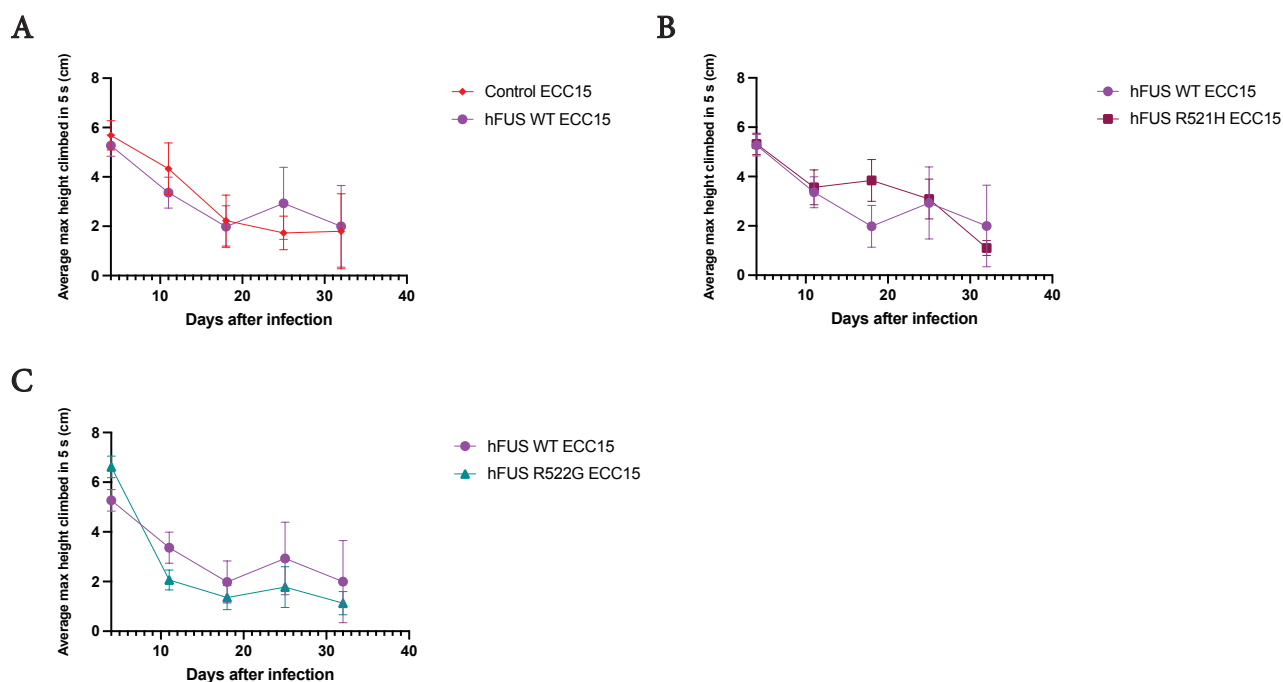
Figure 4: Gram-negative *ECC*15 infection does not decrease the motor behavior ability of hFUS ALS mutant *Drosophila* compared to the hFUS wild-type control. After *ECC*15 infection of the flies, negative geotaxis assay results presented as the average max height climbed in 5 s for: (A) Control (red, n=20 flies at first timepoint) compared to hFUS wild-type (magenta, n=30 flies at first timepoint) (B) hFUS wild-type compared to hFUS R521H (maroon, n=30 at first timepoint) (C) hFUS wild-type compared to hFUS R522G (turquoise, n=29 flies at first timepoint). There is no significant difference between any of the genotypes compared to hFUS wild-type. The same hFUS wild-type *ECC*15 data is used in A-C. All negative geotaxis data for the different genotypes are from the same experiment but separated into different graphs only for ease of visualization. Data are presented as mean ± standard error of the mean; statistical analysis: two-way ANOVA with Dunnett's Multiple Comparisons post-hoc test looking at the main effect of each genotype and comparing all genotypes to hFUS wild-type.

5.3.4 Chang and Morton's humanized TDP-43 M337V mutant is more susceptible to infection than control

Prior to the finalization of the creation of our own humanized TDP-43 *Drosophila*, we used the hTDP-43 lines previously created by Chang and Morton to assess the susceptibility of TDP-43 ALS mutant M337V to gram-negative infection (Chang and Morton, 2017). As stated in Chapter two, we observed that Chang and Morton's hTDP-43 wild-type line's lifespan was significantly shorter than their ALS mutant lines. Due to these discrepancies, we chose to compare Chang and Morton's M337V line to a non-humanized wild-type control fly in these experiments. As can be observed in figure 5A, when pricking the flies with a needle dipped in PBS, no significant difference was seen between hTDP-43 M337V and control. When the needle is dipped in *ECC*15, however, there was a significant shortening of the M337V lifespan compared to control, indicating an infection susceptibility specific to the ALS mutant. The efficiency of the infection is assured through the rapid death of Rel-/- mutants when infected.

Figure 5-5. Chang and Morton's hTDP-43 *Drosophila* infected with *ECC*15
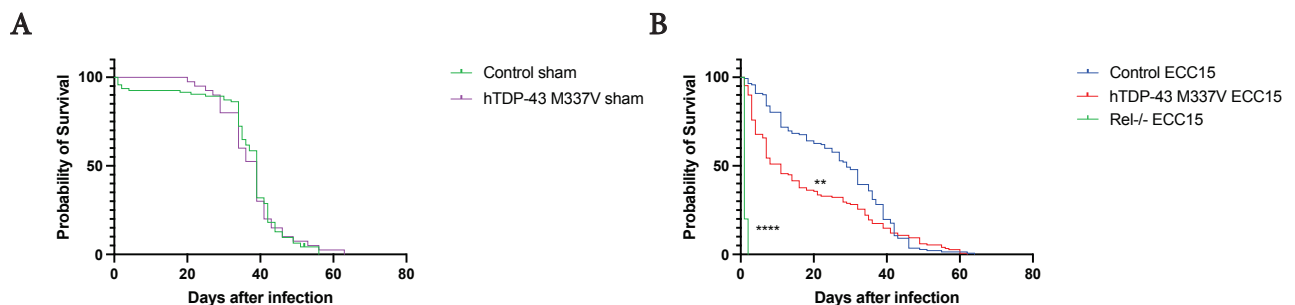
Figure 5: Chang and Morton's hTDP-43 M337V is more susceptible to *ECC*15 infection than control with regards to its longevity. (A) Sham infected *Drosophila*, pricked with a needle dipped in PBS instead of *ECC*15, for control (green, n=91) and Chang and Morton's hTDP-43 M337V (magenta, n=40). (B) *Drosophila* infected with *ECC*15, for control (blue, n=142) and hTDP-43 M337V (red, n=149). Included is also an immunodeficient Rel-/- control (green, n=10) infected with *ECC*15. Statistical analysis: Mantel-Cox test.

5.3.5 hTDP-43 ALS mutant *Drosophila* are not more susceptible to bacterial infection than control

After finalizing the creation of our own humanized TDP-43 *Drosophila*, we wanted to ascertain if we could replicate the infection susceptibility of ALS mutant M337V, which we previously observed in the Chang and Morton humanized TDP-43 *Drosophila* model. We

again included Rel-/-, infected with *ECC*15, as a positive control. The Rel-/- flies die within the first 2 days, showing that they were efficiently infected with gram-negative bacteria. The septic injury itself did not seem to cause differences between the sham control groups, as the only significant longevity difference was between hTDP-43 wild-type and hTDP-43 M337V, a difference which was already present before sham infection (figure 6A). Unlike with Chang and Morton's humanized TDP-43 *Drosophila*, we did not observe any difference in infection susceptibility in our humanized TDP-43 ALS mutants compared to hTDP-43 wild-type control (figure 6B-G). We further assessed the microbial load in the different genotypes 24 h after infection by measuring the colony-forming units, compared to a Key-/- control which is deficient in the Imd pathway and should have a high number of bacteria per fly. Indeed, we observed a significantly higher microbial load in Key-/- compared to control, but no significant differences in any of the hTDP-43 *Drosophila* compared to control, suggesting no difference in Imd activation at this time (figure 6H).

Figure 5-6. hTDP-43 *Drosophila* infected with *ECC*15
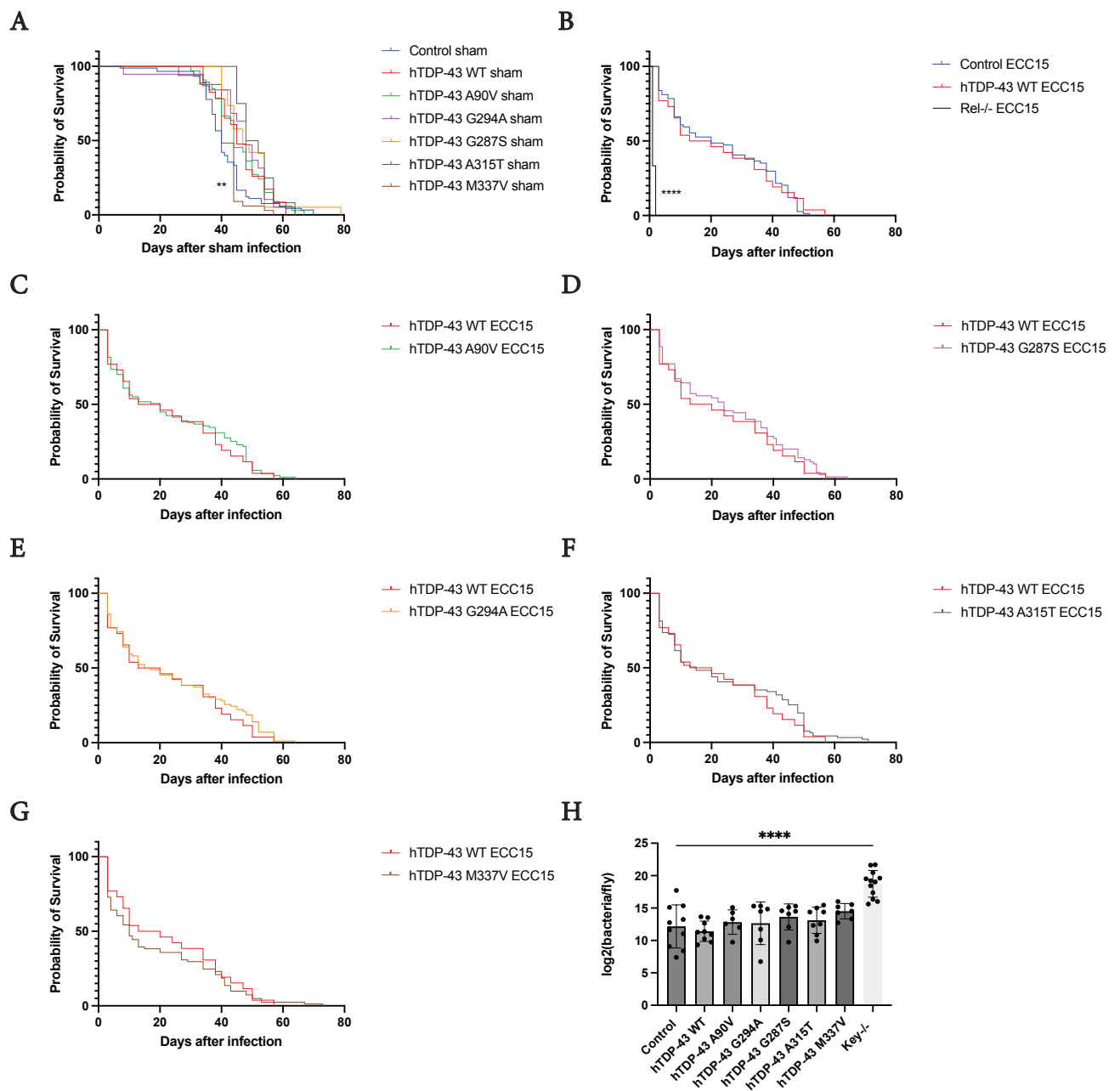
Figure 6: Infection of the *Drosophila* with *ECC*15 bacteria does not significantly decrease hTDP-43 ALS mutant lifespan compared to controls. Flies were infected with *ECC*15 through a septic needle injury at 3-4 days of age, and the lifespan was recorded for (A) Sham control flies, pricked with a needle dipped in PBS, for control (blue, n=90), hTDP-43 wild-type (red, n=23), hTDP-43 A90V (green, n=33), hTDP-43 G294A (magenta, n=19), hTDP-43 G287S (orange, n=19), hTDP-43 A315T (grey, n=12), hTDP-43 M337V (brown, n=33). The only significant difference observed, and which is indicated in the graph is between hTDP-43 wild-type and hTDP-43 M337V. (B) Control (blue, n=74) compared to hTDP-43 wild-type (red, n=26), as well as an immunodeficient Rel-/- control infected with *ECC*15 (black, n=10). (C) hTDP-43 wild-type compared to hTDP-

43 A90V (green, n=87) infected with *ECC*15. (D) hTDP-43 wild-type compared to hTDP-43 G287S (magenta, n=70) infected with *ECC*15. (E) hTDP-43 wild-type compared to hTDP-43 G294A (orange, n=86) infected with *ECC*15. (F) hTDP-43 wild-type compared to hTDP-43 A315T (black, n=91) infected with *ECC*15. The data shows that hTDP-43 ALS mutants are not more susceptible to *ECC*15 infection than hTDP-43 wild-type. The same hTDP-43 wild-type *ECC*15 data is used in B-F. All longevity data for the different genotypes are from the same experiment but separated into different graphs only for ease of visualization. (G) Colony-forming unit measurements presented as log2(), showing the bacterial load of the different genotypes compared to an immunodeficient Key knockout fly line 24 h after infection (n ≥ 6). Data are presented as mean ± standard error of the mean; statistical analysis: one-way ANOVA with Dunnett's Multiple Comparisons post-hoc test, comparing all genotypes to control (H), and Mantel-Cox test (A-G).

5.3.6 No infection-dependent difference in motor behavior is seen between hTDP-43 ALS mutants and control

As infection susceptibility may not be visible through longevity differences but may still cause motor behavior changes, we used the negative geotaxis assay to measure the climbing abilities of the hTDP-43 *Drosophila* after *ECC*15 infection. After sham infection, hTDP-43 wild-type shows a slight decline in motor behavior compared to control, and hTDP-43 M337V has a motor deficit compared to hTDP-43 wild-type (figure 7). The difference between hTDP-43 M337V and hTDP-43 wild-type was, however, already observed without sham infection (see chapter three). When infecting the flies with *ECC*15, the only genotype which showed a significant difference compared to hTDP-43 wild-type is, again, the hTDP-43 M337V mutant (figure 8). However, as can be observed in the sham infected *Drosophila*, the hTDP-43 M337V mutant already has a significant motor deficit without infection. All in all, this points to no infection susceptibility of our humanized TDP-43 ALS mutants compared to control.

Figure 5-7. Negative geotaxis of hTDP-43 *Drosophila* with sham infection
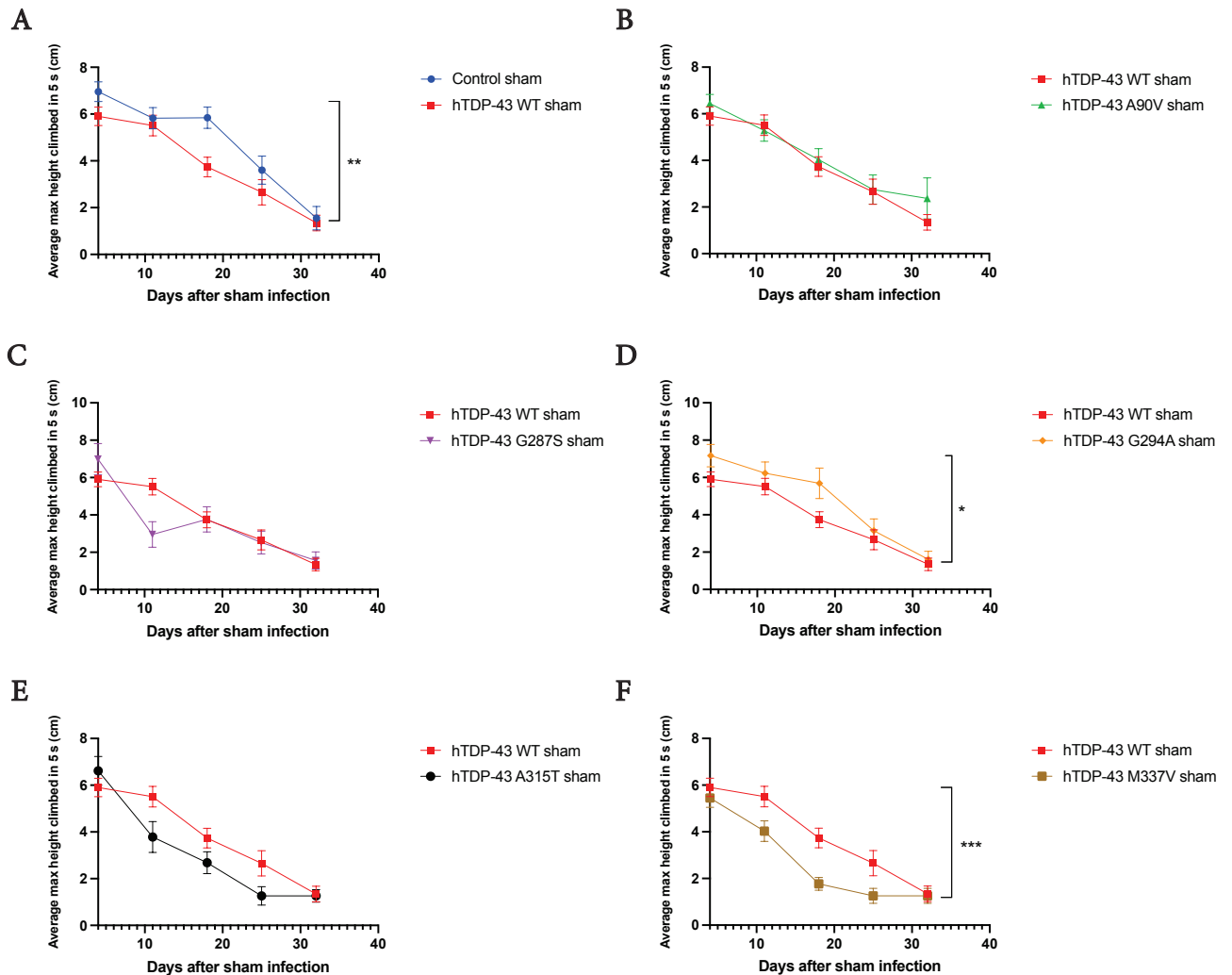
Figure 7: Sham infection with a needle dipped in PBS controls causes some motor behavior deficits only in hTDP-43 wild-type. The *Drosophila* were sham pricked with a needle dipped in PBS and then their motor ability was tested using the negative geotaxis assay as they aged. The average max height climbed in 5 s is presented for: (A) Control (blue, n=60 flies at first timepoint) compared to hTDP-43 wild-type (red, n=59 flies at first timepoint) (B) hTDP-43 wild-type compared to hTDP-43 A90V (green, n=57 flies at first timepoint) (C) hTDP-43 wild-type compared to hTDP-43 G287S (magenta, n=27 flies at first timepoint) (D) hTDP-43 wild-type compared to hTDP-43 G294A (orange, n=30 flies at first timepoint) (E) hTDP-43 wild-type compared to hTDP-43 A315T (black, n=29 flies at first timepoint) (F) hTDP-43 wild-type compared to hTDP-43 M337V (brown, n =60 flies at first timepoint). Sham control injury causes a small deficit in motor behavior in hTDP-43 wild-type, compared to control. In addition, hTDP-43 M337V displays motor deficit, however this was already present in this mutant before sham infection (see chapter three). The same hTDP-43 wild-type sham data is used in A-F. All negative geotaxis data for the different genotypes are from the same experiment but separated into different graphs only for ease of visualization. Data are presented as mean ± standard error of the mean;

statistical analysis: two-way ANOVA with Dunnett's Multiple Comparisons post-hoc test looking at the main effect of each genotype and comparing all genotypes to hTDP-43 wild-type.

Figure 5-8. Negative geotaxis assay of infected hTDP-43 *Drosophila*
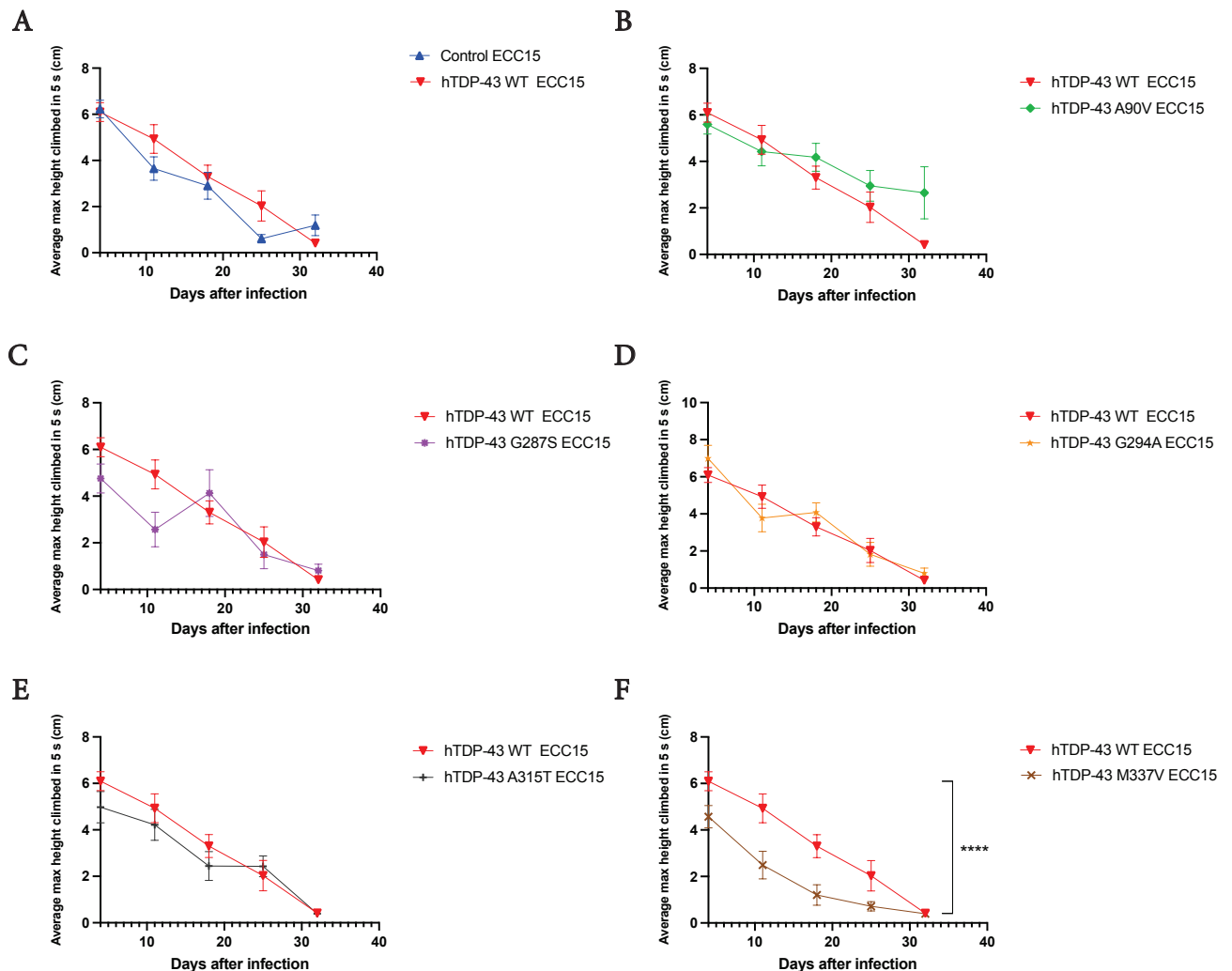
Figure 8: After gram-negative *ECC*15 infection, hTDP-43 ALS mutants do not show significantly different motor behavior compared to hTDP-43 wild-type. Flies were infected with *ECC*15, and then the negative geotaxis assay was performed as the flies aged. The average max height climbed in 5 s is presented for: (A) Control (blue, n=59 flies at first timepoint) compared to hTDP-43 wild-type (red, n=58 flies at first timepoint) (B) hTDP-43 wild-type compared to hTDP-43 A90V (green, n=58 flies at first timepoint) (C) hTDP-43 wild-type compared to hTDP-43 G287S (magenta, n=30 flies at first timepoint) (D) hTDP-43 wild-type compared to hTDP-43 G294A (orange, n=28 flies at first timepoint) (E) hTDP-43 wild-type compared to hTDP-43 A315T (black, n=28 flies at first timepoint) (F) hTDP-43 wild-type compared to hTDP-43 M337V (brown, n=60 flies at first timepoint). The only significant negative geotaxis deficit observed is in the hTDP-43 M337V mutant compared to hTDP-43 wild-type. This difference was already observed before infection, see figure 7. The same hTDP-43 wild-type *ECC*15 data is used in A-F. All negative geotaxis data for the different genotypes

are from the same experiment but separated into different graphs only for ease of visualization. Data are presented as mean ± standard error of the mean; statistical analysis: two-way ANOVA with Dunnett's Multiple Comparisons post-hoc test looking at the main effect of each genotype and comparing all genotypes to hTDP-43 wild-type.

5.3.7 The Imd pathway may need to be activated within the CNS to induce ALS pathology

We observe no susceptibility to gram-negative bacterial infection in either hFUS or hTDP-43 ALS mutant *Drosophila*. The infection that we have applied to the flies is a septic peripheral infection, in which bacteria should normally not be able to enter the CNS. A previous study has shown that mutated Imd pathway regulators can cause neurodegeneration which can be rescued by glial Imd inhibition (Kounatidis et al., 2017). Based on this, we hypothesize that Imd activation needs to be CNS-specific to cause decreased lifespan and motor deficits, and that the peripheral infection the humanized FUS and TDP-43 flies have been subjected to is not sufficient to induce more severe ALS pathology as it is not able to enter the CNS. To investigate the consequence of Imd activation in glia and neurons, we used the Gal4 system to express the Imd pathway receptor, PGRP-LC, exclusively in either glia or neurons in wild-type *Drosophila*. To bypass the effects this may have on fly development, we used the temperature-sensitive Gal80 system to induce the expression only once the *Drosophila* adults have eclosed. As can be seen in figure 9, we observe a significant decrease in fly longevity when the PGRP-LC is exclusively expressed in glia, while we only observe a non-significant trend toward decreased fly longevity when PGRP-LC is neuronally expressed. In addition, we used the negative geotaxis assay to measure the motor behavior of the *Drosophila*, one day after starting the expression of UAS-PGRP-LC. The flies expressing PGRP-LC have a significantly decreased climbing ability, compared to controls. This suggests that *Drosophila* are specifically vulnerable to Imd pathway activation in glial cells, and this may be the cell type in which Imd should be upregulated to induce symptoms in the humanized FUS and TDP-43 ALS mutants, as well.

Figure 5-9. Lifespan and negative geotaxis of wild-type *Drosophila* overexpressing PGRP-LC in different cell types
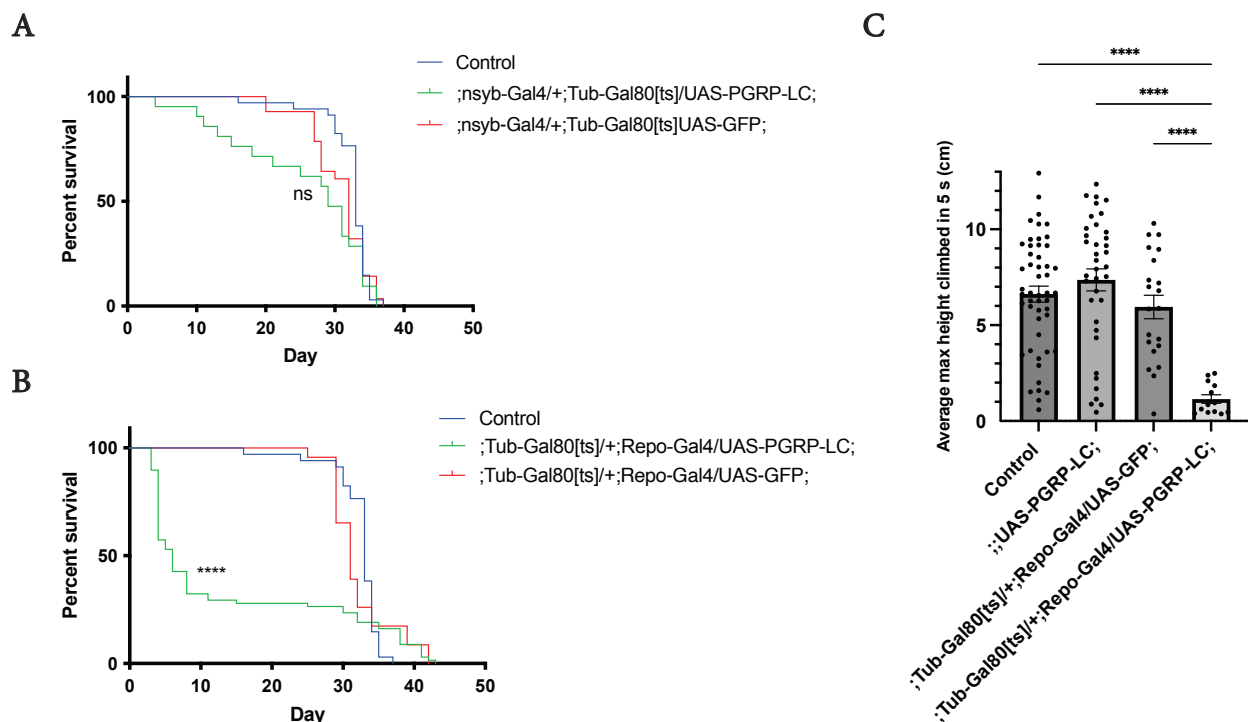
Figure 9: Wild-type *Drosophila* expressing PGRP-LC in glia have significantly decreased lifespan, in contrast to neuronal expression. (A) Lifespan of wild-type flies expressing PGRP-LC specifically in neurons using a neuronal Gal4 driver (nsyb-Gal4) exclusively after development through the use of temperature-sensitive Gal80[ts] (green, n=21). Also included are flies expressing UAS-GFP instead of UAS-PGRP-LC, as a control (, red, n=28), as well as wild-type control flies (blue, n=34). (B) Lifespan of wild-type flies also expressing temperature-controlled PGRP-LC after development, but specifically in glia using the Repo-Gal4 driver (green, n=68). Control flies expressing UAS-GFP instead of UAS-PGRP-LC are also included (red, n =23), as well as wild-type control flies (blue, n=34). (C) Negative geotaxis of flies expressing glial UAS-PGRP-LC (n=13), as well as control flies expressing UAS-GFP (n=21), control flies containing UAS-PGRP-LC without driver (n=37), and regular control flies (n=50), at one day of age. The same control data is used in A and B. All longevity data for the different genotypes are from the same experiment but separated into different graphs only for ease of visualization. Data are presented as mean ± standard error of the mean; statistical analysis: Gehan-Breslow-Wilcoxon test (A-B) and one-way ANOVA with a Dunnett's Multiple Comparisons post-hoc test (C).

5.4 Discussion

Here, we aimed to assess if a more severe ALS phenotype could be induced in the humanized TDP-43 and FUS ALS mutant *Drosophila* through challenging them with a bacterial infection. We measured the longevity and motor behavior of the *Drosophila* after a septic

injury infection with gram-negative bacteria *ECC*15. However, we did not observe any differences in susceptibility to infection between the ALS mutants and control. We conclude that a transient infection is not sufficient to induce ALS pathology, and that an upregulation of the immune system may need to be directed to the CNS. Indeed, we observe that upregulation of the Imd pathway exclusively in glia can cause decreased longevity and impaired locomotion in wild-type *Drosophila*, showing the importance of strict Imd regulation in this cell type.

5.4.1 Infection susceptibility varies between the Chang and Morton humanized TDP-43 *Drosophila* model and our humanized TDP-43 fly lines

When we first assessed the infection susceptibility of humanized TDP-43 ALS mutant *Drosophila*, we did so using the fly lines previously generated by Chang and Morton (Chang and Morton, 2017). When compared to our control line, we observed a significant infection susceptibility in the M337V mutant. However, we were not able to replicate this in the humanized TDP-43 *Drosophila* we later created. A possible explanation for the differences in results could be attributed to genetic background. There exist several *Drosophila* wild-type control strains, all with small differences in their genetic backgrounds, which may affect their resistance to infection. In our experiments, we compared Chang and Morton's hTDP-43 M337V line to a control line from our lab named w[1118], which is the same background strain that Chang and Morton backcrossed their newly generated lines into. However, it is possible that the w[1118] strain from Chang and Morton's lab and the w[1118] strain from our lab have evolved differently over time, and may contain some variances in genetic background, causing infection susceptibility. In support of this, another study has performed infection experiments comparing several different background strains, including for example w[1118], Oregon, and Canton-S, and observe varied susceptibility to different infections both evident in the longevity and the level of AMPs produced (Eleftherianos et al., 2014). From this we can conclude that ensuring a common genetic background between the genotypes in infection experiments is vital to interpreting the experimental outcome.

5.4.2 hFUS, but not hTDP-43, is expressed in the fat body, highlighting the different functions of the two proteins

We also assessed the expression of hFUS and hTDP-43 in the main *Drosophila* immune organ: the fat body. Interestingly, hFUS is found in fat body cell nuclei, while hTDP-43 is not

expressed. It is possible that hFUS takes part in the fat body immune response, but that the ALS mutations we introduced do not affect the protein's ability to perform its immune functions. It is also possible that hFUS has a non-immune related role in fat body tissue, as the fat body is also important in, for example, energy storage and metabolism (Zheng et al., 2016). In fact, a previous study has shown that hFUS interacts with several proteins involved in energy metabolism in HEK293T cells. The difference in fat body expression between hTDP-43 and hFUS is also noteworthy, highlighting the differences in function of these two proteins and the possibility that their roles in ALS may happen through different mechanisms, something that should be further characterized in the future.

5.4.3 Peripheral infection is not be sufficient to trigger ALS phenotypes

Based on the very mild symptoms observed in our humanized ALS model *Drosophila* lines, we hypothesized that an additional immune challenge may be required to induce ALS pathology in hFUS and hTDP-43 ALS mutant *Drosophila*. To this end, we infected hFUS and hTDP-43 lines, including both controls and ALS mutants, with gram-negative *ECC*15 to cause Imd pathway activation. However, we did not observe any differences in bacterial susceptibility between ALS mutants and controls with regards to the two main phenotypes affected by ALS: longevity and motor behavior. It is important to note, however, that the bacterial infection through septic injury that the *Drosophila* are exposed to in our experiments is known to induce a systemic immune response, but should not be able to reach the nervous system through the blood-brain barrier (BBB), and therefore should not cause Imd activation in neurons or glia in normal cases (Buchon et al., 2009). The *Drosophila* BBB is made up of glial cells and separates the hemolymph from the nervous system (Schirmeier and Klämbt, 2015). During peripheral bacterial infection, the BBB protects the CNS from being affected, as immune activation within the nervous system can cause unwanted consequences. Such consequences have previously been exemplified by a study showing that mutations in Imd negative regulators causes toxic AMP levels and neurodegeneration which can be rescued through glial Imd inhibition, suggesting that the glial immune activation was the source of the degenerative phenotype (Kounatidis et al., 2017). Another study has shown that if there is glial activation of the Imd pathway during pupal stages, this can attract peripheral macrophages causing them to cross the BBB. The macrophages can then phagocytose synapses and cause deficiencies in motor behavior and shortened longevity (Winkler et al., 2021). Altogether, this demonstrates that activation of the Imd pathway

within the CNS, and particularly in glia, can cause degenerative phenotypes. Indeed, we find that overexpression of PGRP-LC exclusively in adult glia causes severe motor behavior deficits and shortened lifespan. It is plausible that to induce an ALS phenotype in the humanized FUS and TDP-43 ALS mutants, a peripheral immune response is not sufficient as it does not reach the CNS, and a glial Imd pathway activation may be required.

5.4.4 Glial expression of hFUS and hTDP-43 may be key to inducing an ALS phenotype

In chapters one and two, when creating and characterizing the humanized FUS and TDP-43 *Drosophila* lines, we observed high expression of both hFUS and hTDP-43 in neurons. hFUS was not expressed in all glia, however, and in the glial cells where it was present, it seemed to be expressed at lower levels than in neurons. hTDP-43 was highly expressed in some, but not all, glia, suggesting it is expressed in a glial subtype. As we observe here that glial, but not neuronal, expression of PGRP-LC in control *Drosophila* causes a significant decrease in lifespan, it is possible that the Imd pathway would need to be induced in the glial subtypes that express hTDP-43 and hFUS, respectively, to trigger ALS symptoms in the humanized FUS and TDP-43 *Drosophila* models. In future experiments, it would be interesting to further assess if hFUS and hTDP-43 are expressed within the same or different glial subtypes.

5.5 Conclusion

In conclusion, here we have tested the infection susceptibility of the humanized FUS and TDP-43 fly lines created in chapters one and two. We have used gram-negative *ECC*15 bacteria in order to induce an Imd pathway immune response that was aimed to cause aberrant Imd activation. The ALS mutants, however, show no decrease in lifespan or deficits in motor behavior as a response to infection, compared to hFUS and hTDP-43 wild-type controls. When activating the Imd pathway exclusively in glia in wild-type *Drosophila*, on the other hand, we observe both decreased longevity and motor behavior deficits. We conclude that in the future, activating the Imd pathway in glia may prove more effective to invoke ALS pathology in the humanized FUS and TDP-43 fly lines.

5.6 Materials and methods

5.6.1 Immunohistochemistry

The abdominal fat bodies of 4-5 day old *Drosophila* reared at 29°C were dissected out and fixed in 4% PFA. After fixation, the preparations were washed three times during a total of

one h in 1xPBS, 0.4% Triton-X, and blocked in 5% Normal Goat Serum diluted in the washing solution. The samples were then incubated overnight with the primary antibodies, and subsequently washed for one h before incubation with the secondary antibodies. After an additional two h of washing, the samples were mounted in ProLong Diamond antifade mounting medium (Invitrogen). The primary antibodies used are anti-hFUS (Sigma Aldrich, 1:100), anti-hTDP-43 (Huabio, 1:100), and DAPI (Biotium Chem.Brunschwig, 1:5000). The secondary antibodies used were anti-mouse Alexa Fluor 546 (Lifetech, 1:400), and anti-rabbit Alexa Fluor 488 (Lifetech, 1:400).

5.6.2 Lifespan

Drosophila were kept in food vials and were moved to fresh vials every two days, at which point the number of dead flies in each vial was counted. A maximum of 10 *Drosophila* were housed in each vial, and the longevity test was performed at 25°C.

5.6.3 Negative geotaxis

Negative geotaxis was performed using a set-up with glass vials attached to a metal rod using gravity to tap down the *Drosophila* with a less variable force. The flies were tapped down three times, and the maximum height climbed by each fly in 5 s was measured. The assay was filmed with a Raspberry Pi Camera the results were analyzed in ImageJ.

5.6.4 Bacterial infection experiments

Erwinia carotovora carotovora 15 (*ECC*15) were grown in LB broth overnight, in a 29°C incubator shaking at 200 rpm. The bacteria were then centrifuged, and the pellet was diluted in PBS to an Optical density at 600 nm (OD) of 100. 3 to 4-day old adult male *Drosophila* were pricked in the thorax with a pin (tip diameter 0.0175 mm and rod diameter 0.15 mm) (Fine Science, 26002-15) dipped in the bacterial solution. The *Drosophila* were then kept at 25 °C, with a maximum of 10 flies per food vial.

5.6.5 Bacterial load

Drosophila were infected with *ECC*15 bacteria at an OD_{600} of 100. 24 h post-infection, three replicates of 10 flies per genotype were anesthetized with CO_2 and washed in 70% ethanol. The ethanol was removed and the flies were washed twice in sterile PBS. Subsequently, the flies were homogenized in 200 µl of PBS using a pestle, and the homogenized flies were

centrifuged at 8000 rpm for 3 minutes. The supernatants were recovered and serially diluted several times before drops of 7 μl were pipetted onto LB agar plates and incubated overnight at 29 °C. The next day, the colony-forming units were manually counted.

5.6.6 Statistics

Data are presented as mean ± standard error of the mean. The p-values were calculated with a one-way ANOVA with Dunnett's Multiple Comparisons post-hoc test or, for the negative geotaxis assay, a two-way ANOVA with Dunnett's post-hoc test assessing the main effect of each genotype. For survival curves, the Mantel-Cox test or the Gehan-Breslow-Wilcoxon test was used. Results with a p-value < 0.05 were considered significant.

6

Chapter 6 - Inhibiting the NF-κB pathway rescues motor neuron death *in vitro* but does not ameliorate symptoms in an ALS mouse model

- -

Emma Källstig, Philippe Colin, Greta Limoni, Roxane Crabé, Cédric Raoul, Brian McCabe, Bernard Schneider

In vitro primary cell line experiments performed by Roxane Crabé and Cédric Raoul; intracerebroventricular injections, mouse perfusions and spinal cord dissections performed by Emma Källstig and Philippe Colin; all stainings shown in the discussion performed by Greta Limoni; all other experiments performed by Emma Källstig.

6.1 Abstract

In ALS patients and animal models, neuroinflammation and NF-κB upregulation has been observed in the spinal cord. We used two different AAV vectors expressing NF-κB inhibitors (Superrepressor and Optineurin) to inhibit NF-κB activation in IFNγ and TNFα based *in vitro* models as well as the SOD1^{G93A} ALS mouse model. In IFNγ and TNFα based *in vitro* models, NF-κB inhibition rescues motor neuron degeneration. In the *in vivo* SOD1^{G93A} mouse model, however, motor behavior and electromyographical symptoms cannot be improved by ICV injection of NF-κB-inhibiting AAVs. Through immunohistochemistry we detected an increased density of MHC-II positive immune cells in the spinal cords of SOD1^{G93A} mice compared to wild-type, and hypothesize that further work is needed to investigate the role of these immune cells in ALS pathology.

6.2 Introduction

The first gene discovered to be associated with fALS is the *SOD1* gene (Zarei et al., 2015). This genetic link between fALS and SOD1 is the basis of several ALS animal models, such as overexpression of SOD1^{G37R}, SOD1^{G86R}, or SOD1^{G85R} in mice, and SOD1^{G93A} overexpression in rats (Bruijn et al., 2004; Ripps et al., 1995; Wong et al., 1995). Among these models is also a high-copy overexpression of SOD1^{G93A} in C57BL/6 mice. Around 3-4 months of age SOD1^{G93A} mice develop several ALS-like symptoms, including loss of spinal motor neurons, limb weakness leading to paralysis, and concluding in death by age 5-6 months (Gurney et al., 1994).

The SOD1^{G93A} overexpression mouse model has contributed to several advances in ALS research, including observations regarding the role of neuroinflammation in ALS. For example, the main inflammatory-mediating CNS cell types, microglia and astrocytes, are activated in SOD1^{G93A} mice from day 80 and 100, respectively, and they contribute to disease progression (Alexianu et al., 2001; Hall et al., 1998). Through *in vitro* studies, SOD1^{G93A} microglia have been observed to release more neurotoxic factors and promote higher motor neuron death when co-cultured with SOD1^{G93A} motor neurons than wild-type microglia (Beers et al., 2006). Likewise, SOD1^{G93A}-expressing astrocytes co-cultured with motor neurons that do not express SOD1^{G93A} cause selective motor neuron toxicity (Valbuena et al., 2017).

The presence of inflammation has also been observed in ALS patients, where pro-inflammatory chemokines are present in the cerebrospinal fluid (CSF) (Kuhle et al., 2009). The NF-κB proteins are major regulators of such pro-inflammatory signals. Indeed, in several ALS mouse and patient studies, increased activation of NF-κB has been detected (Crosio et al., 2011; Frakes et al., 2014). The NF-κB proteins are normally located in the cytoplasm, where they are bound to the inhibitory IκB proteins. When the NF-κB signaling pathway is activated by an inflammatory stimulus, the IKK complex is formed and causes phosphorylation of IκB, marking it for degradation. This frees the NF-κB proteins, allowing them to translocate to the nucleus and regulate gene expression, advancing an inflammatory response (Sun, 2017).

In addition to the observed presence of activated NF-κB in ALS animal models and patients, there are also genetic links between the signaling pathway and the disease. Several proteins, including TDP-43, FUS, TBK1, SQSTM1, and UBQLN2, that are associated to familial ALS

through mutations, also regulate or interact with NF-κB (Källstig et al., 2021). In particular, Optineurin (OPTN), which is linked to fALS through loss-of-function mutations, is also a negative regulator of NF-κB (Kamada et al., 2014). Due to their important role in the induction of pro-inflammatory gene expression, as well as their observed activation in ALS patients and genetic connection to fALS, dysregulation of the NF-κB proteins has been hypothesized to mediate motor neuron death in ALS.

In this study, our aim was to explore the effects of inhibiting the NF-κB pathway on the pathology of ALS in SOD1^{G93A} mice and IFNγ and TNFα ALS primary cell line models. To do this, we created AAV vectors overexpressing NF-κB inhibitors in different CNS cell types. The first vector was designed to overexpress OPTN, as OPTN mutations possibly leading to the loss of NF-kB regulatory activity cause familial forms of ALS with autosomal recessive inheritance, and since we observed a rescue in eclosion by overexpressing OPTN in a Caz-/- model in Chapter three of this thesis. However, OPTN also has other functions besides its role regulating NF-κB. For example, OPTN takes part in autophagy induction, Golgi structural maintenance, and post-Golgi protein trafficking regulation (Markovinovic et al., 2017). To facilitate a more specific inhibition of the NF-κB pathway, we therefore chose to also overexpress the Superrepressor (SR) protein. SR is an engineered form of IκBα, which contains serine-to-alanine mutations at amino acids 32 and 36, preventing the SR-IκBα from its phosphorylation and degradation, and thereby precluding nuclear translocation of the NF-κB proteins (Hellerbrand et al., 1998). For the administration of SR, we chose expressing with the neuronal Synapsin promoter, to primarily target neurons. NF-κB proteins have important roles in maintenance of neurons, for example activation in mouse excitatory glutamatergic neurons stimulates synapse formation, an effect which is reversed when NF-κB signaling is downregulated (Boersma et al., 2011). This, in combination with the fact that motor neurons are the main cell type degenerating during disease, caused us to aim to inhibit NF-κB signaling neuronally.

When administering AAV6-CBA:OPTN and AAV6-hSyn1:SR in IFNγ and TNFα *in vitro* ALS models, we observed rescued motor neuron death with both NF-κB inhibitors. When administered through intracerebroventricular (ICV) injection in SOD1^{G93A} mice, however, we did not observe any significant improvement in motor behavior or electromyographical measurements. Altogether, we suspect that the lack of symptom improvement *in vivo* could be caused by targeting of the incorrect CNS cell type. Through immunohistochemistry, we

observed and increased density of MHC-II-positive immune cells in the spinal cord of SOD1^{G93A} mice compared to wild-type controls, whose role in ALS pathology should be further investigated.

6.3 Results

6.3.1 Viral plasmids express proteins-of-interest in HEK293 cells

OPTN and SR cDNA as well as EGFP cDNA controls were cloned into AAV plasmids containing the ubiquitous CBA promoter and the neuronal hSyn1 promoter, respectively. To assess the expression of the proteins-of-interest by the AAV plasmids, we transfected the plasmids into HEK293 cells and performed western blots. As can be seen in figure 1, all plasmids were expressing their protein-of-interest. The plasmids were subsequently used to produce suspensions of vectors. For expression of SR, we used AAV serotype 6 (AAV6), as AAV6 injected ICV with a ubiquitous promoter already favors spinal motor neuron transduction (Dirren et al., 2014). To make sure that neurons were the only targeted cell type, we combined the AAV6 serotype with the neuronal hSyn1 promoter. AAV serotype 9 (AAV9) is an efficient transducer of many different tissue types, and in combination with intracerebroventricular (ICV) injection and an astrocyte-specific promoter it has already been observed to significantly transduce astrocytes (Dirren et al., 2014). As we were aiming for a more general transduction of several CNS cell types *in vivo*, we combined the AAV9 vector with a CBA promoter to express OPTN. However, as AAV6 is a more efficient transducer of primary cell lines than AAV9, we also produced an AAV6 version of the CBA-OPTN vector to be used in the *in vitro* experiments (Ellis et al., 2013).

Figure 6-1. AAV-mediated expression of NF-κB inhibitors OPTN and SR
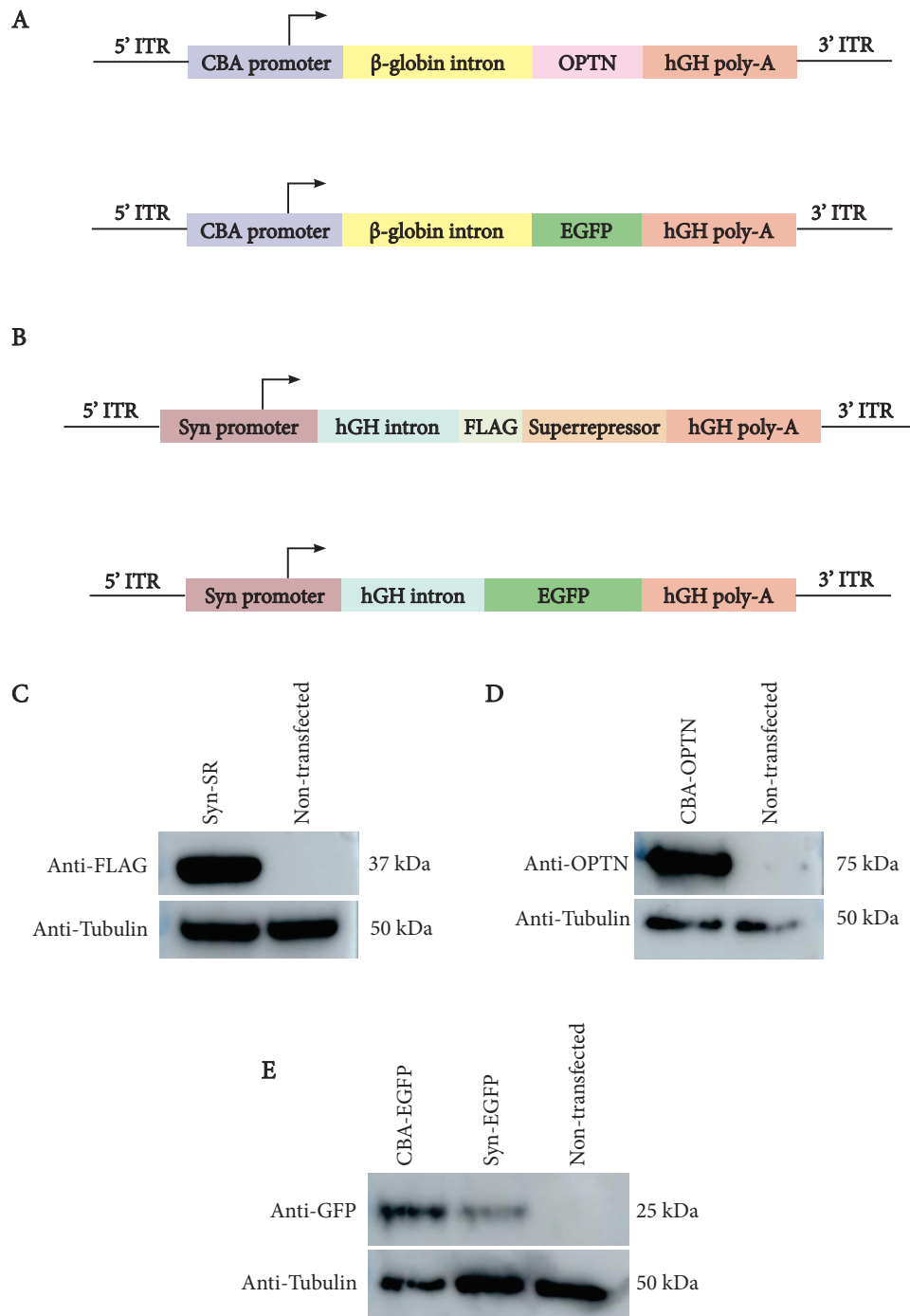
Figure 1: Reducing the activity of the NF-κB pathway by AAV-mediated expression of NF-κB inhibitors OPTN and SR. Experimental design for overexpression of NF-κB inhibitors (A) OPTN and (B) SR, as well as their EGFP-expressing controls, ubiquitously or selectively in neurons, respectively. (C-E) Western blots depicting SR, OPTN, and GFP expression in HEK293 cell lysate post-transfection of pAAV-hSyn1:FLAG:SR,

pAAV-CBA:OPTN, pAAV-hSyn1:EGFP or pAAV-CBA:EGFP, as well as non-transfected controls. Anti-α-tubulin was used as a loading control.

### 6.3.2 AAV vectors expressing NF-κB inhibitors rescue motor neuron death in IFNγ and TNFα in vitro ALS models

Before testing the viruses *in vivo,* we wanted to verify that they could be neuroprotective in primary cell ALS models. It has previously been observed that the pro-inflammatory cytokine IFNγ can selectively stimulate motor neuron death, and induce neurotoxicity via astrocytes in primary cell lines expressing SOD1^{G93A} (Otsmane et al., 2014). In addition, exposure to a neutralizing IFNγ antibody in the CSF of SOD1^{G93A} mice delays motor function deterioration. In a similar way, lack of astrocytic and neuronal TNFα receptor TNFR2 in SOD1^{G93A} mice partially protects spinal motor neurons from degeneration (Tortarolo et al., 2015). Moreover, the CSF and serum levels of IFNγ and TNFα, respectively, are elevated in ALS patients (Liu et al., 2015; Poloni et al., 2000). Based on this, primary motor neuron cell line ALS model protocols have been established where treatment with IFNγ or TNFα causes motor neuron death (Aebischer et al., 2011; Ugolini et al., 2003). In accordance with these protocols, we treated primary motor neurons with IFNγ or TNFα for 48 h and quantified the surviving neurons, with and without transduction with the NF-κB-inhibiting AAV vectors. We observed a significant decrease in motor neuron survival after both IFNγ and TNFα treatment, as previously described. The same effects of IFNγ and TNFα were also seen in neurons transduced with the control vectors AAV6-CBA:EGFP or AAV6-hSyn1:EGFP, in either condition. When the cell culture was exposed to AAV6-CBA:OPTN or AAV6-hSyn1:SR, however, the loss of motor neuron survival was significantly rescued (figure 2). Firstly, this suggests that the viruses themselves are producing their intended protein (OPTN or SR). Secondly, it shows the ability of NF-κB inhibitor overexpression to rescue motor neuron death induced by TNFα or IFNγ, both of which have been hypothesized to play roles in ALS pathology.

Figure 6-2. Inhibition of the NF-κB pathway *in vitro* in primary cell lines
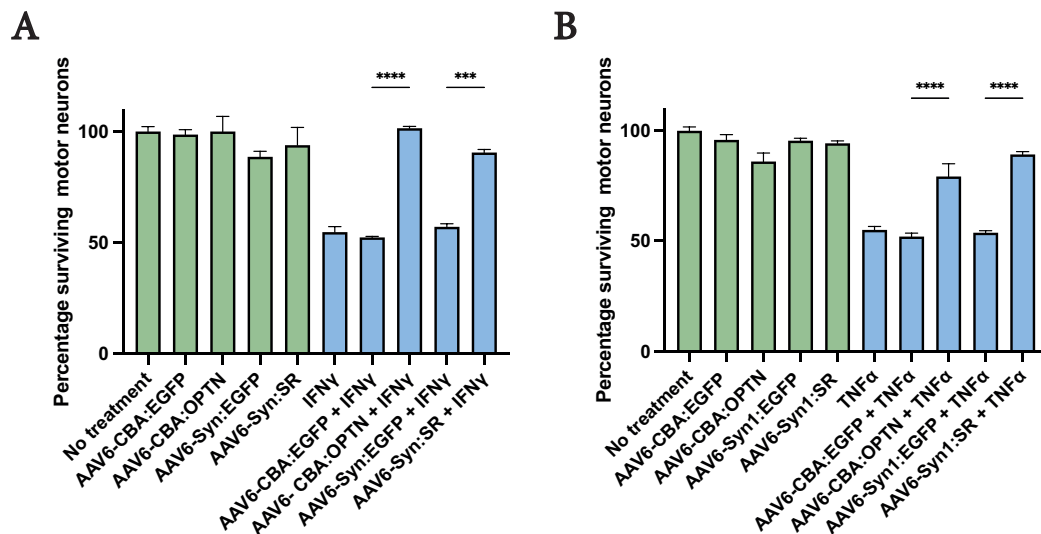
Figure 2: Inhibition of the NF-κB pathway through administration of AAV9-CBA:OPTN or AAV6-CBA:SR rescues motor neuron death in IFNγ and TNFα ALS models. Compared to EGFP-expressing controls, AAV9-CBA:OPTN and AAV6-hSyn1-SR significantly rescue motor neuron death in (A) IFNγ-treated cells and (n = 3 experiment repeats) (B) TNFα-treated cells (n = 3 experiment repeats). The green bars were not treated with IFNγ or TNFα, while the blue bars were treated with IFNγ or TNFα. Data are presented as mean ± standard error of the mean; statistical analysis: one-way ANOVA with Tukey's Multiple Comparisons post-hoc test.

6.3.3 Ubiquitously expressed OPTN delivered via AAV9 vector does not ameliorate electromyographical ALS phenotypes in SOD1^{G93A} mice

To further test the effect of NF-κB inhibition *in vivo,* we used the well characterized SOD1^{G93A} overexpression mouse model. We began by testing the efficiency of OPTN overexpression, as OPTN loss-of-function is observed in ALS cases. At P1-2, pups were injected with AAV9-CBA:OPTN, or controls, through ICV injection, ensuring spreading of the viruses in brain and spinal cord, as previously shown (Dirren et al., 2014). Throughout their lifespan up until sacrifice at 130 days of age, electromyographical recordings were performed on the mice, with the purpose of assessing neuromuscular function using compound muscle action potential (CMAP) measurements. The sciatic nerve was stimulated through an electrode above the lumbar spinal cord and action potentials were recorded in the gastrocnemius muscle. SOD1^{G93A} mice showed a significant decrease in CMAP amplitude, as compared to wild-type PBS injected mice (figure 3A). Ubiquitous OPTN expression, however did not rescue CMAP amplitudes of transgenic SOD1^{G93A} mice. At all timepoints,

CMAP amplitudes of the AAV9-treated mice remained very similar to the amplitudes measured in both the PBS and the AAV9-EGFP injected SOD1^{G93A} mice.

6.3.4 OPTN overexpression does not result in a significant improvement in SOD1^{G93A} motor phenotypes

To observe if OPTN overexpression had any effect on motor behavior, two different tests were performed: the rotarod test and the swimming test. In the rotarod test, the mice run on an accelerating rotating rod, thereby measuring their muscle coordination and endurance. If they have not fallen off the rod within 180 s, they are removed from the rod and placed back in their cages. When transduced with viral vectors expressing OPTN, the treatment did not improve the motor abilities of the mice in the rotarod assay (figure 3B).

The swimming test was used to measure the overall motor abilities of the mice. It measures the time for the mice to swim a distance of 0.8 meter to a visible platform, (figure 3C). Alike the results of the rotarod test, no significant difference was observed between control transgenic mice and OPTN treated. In summary, it seems that AAV9 treatment ubiquitously expressing OPTN leads to no rescue of SOD1^{G93A} behavioral or electromyographical phenotypes.

Figure 6-3. Motor behavior of SOD1^{G93A} mice treated with AAV9-CBA:OPTN
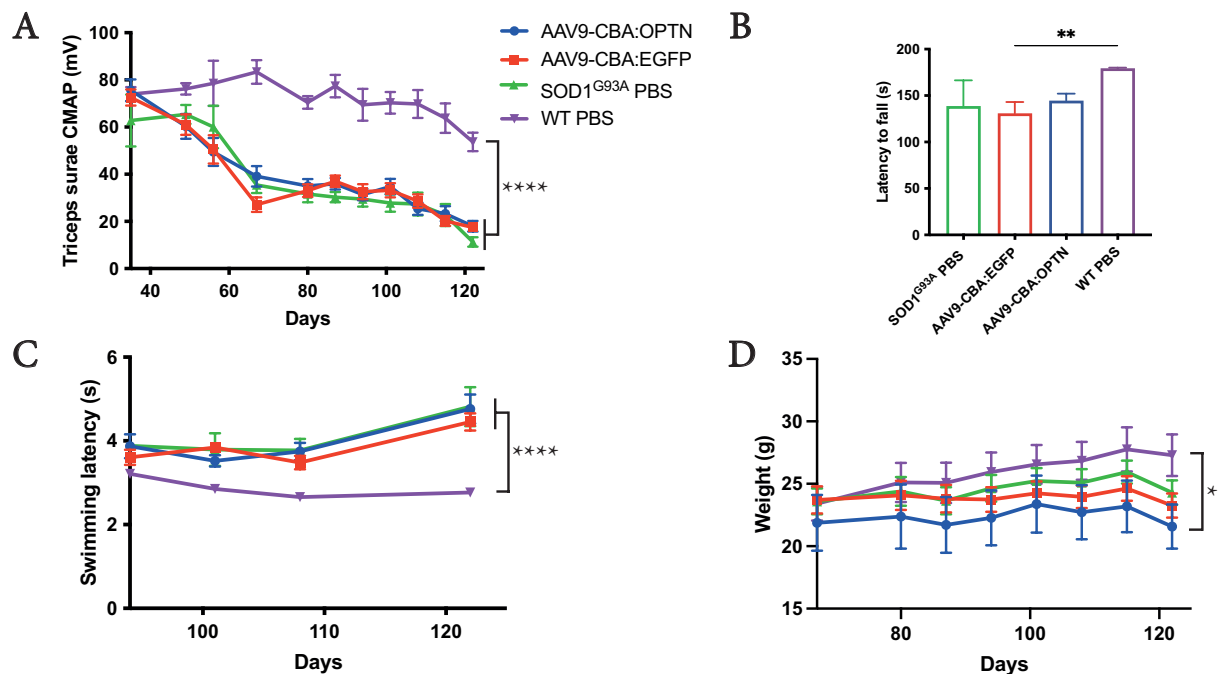
Figure 3: SOD1^{G93A} mice treated with AAV9-CBA:OPTN do not display any significant improvement in motor behavior or CMAP. Behavioral and electromyographical tests in wild-type injected with PBS in magenta (n=9), SOD1^{G93A} injected with PBS in green (n=4), SOD1^{G93A} injected with AAV9-CBA:EGFP in red (n=10), and SOD1^{G93A} injected with AAV9-CBA:OPTN in blue (n=8). (A) Recorded amplitude of the evoked compound muscle action potential (CMAP) in the *triceps surae*. (B) Rotarod test showing the latency of the mice to fall from an accelerating rotating rod, as a measurement of motor coordination, at day 122. (C) The swimming test evaluating the latency for the mice to swim to a 0.8-meter distant platform in a plexiglass pool, used to quantify the overall motor abilities of the mice. (D) The weight evolution of the mice during the experiment. The only significant differences observed in these tests were between the transgenic SOD1^{G93A} mice and the wild-type mice, while no differences were seen in response to the treatment. Data are presented as mean ± standard error of the mean; statistical analysis: for CMAP, swimming test, and weight, two-way ANOVA with Tukey's Multiple Comparisons post-hoc test. For the rotarod, one-way ANOVA with Tukey's Multiple Comparisons post-hoc test.

6.3.5 OPTN expression is mostly detected in GFAP-positive astrocytes

After perfusion at disease end stage, the spinal cords of the animals were dissected out and stained for the proteins of interest. In the case of AAV9-CBA:OPTN, the EGFP-expressing control was stained to confirm expression as it is the OPTN construct did not have a tag. Through this staining, it was confirmed that the AAV vector was indeed expressing EGFP

(figure 4). Interestingly, the expression was mainly localized to astrocytes positive for GFAP, even though the constitutively active CBA promoter should enable expression in all CNS cell types, including neurons. This could be due to the late stage of disease in which the tissue was collected. By 130 days, the mice are severely sick and have lost most of their neurons, possibly including neurons that were previously expressing OPTN as a result of AAV9-mediated transduction.

Figure 6-4. AAV9-CBA:EGFP successfully expresses EGFP
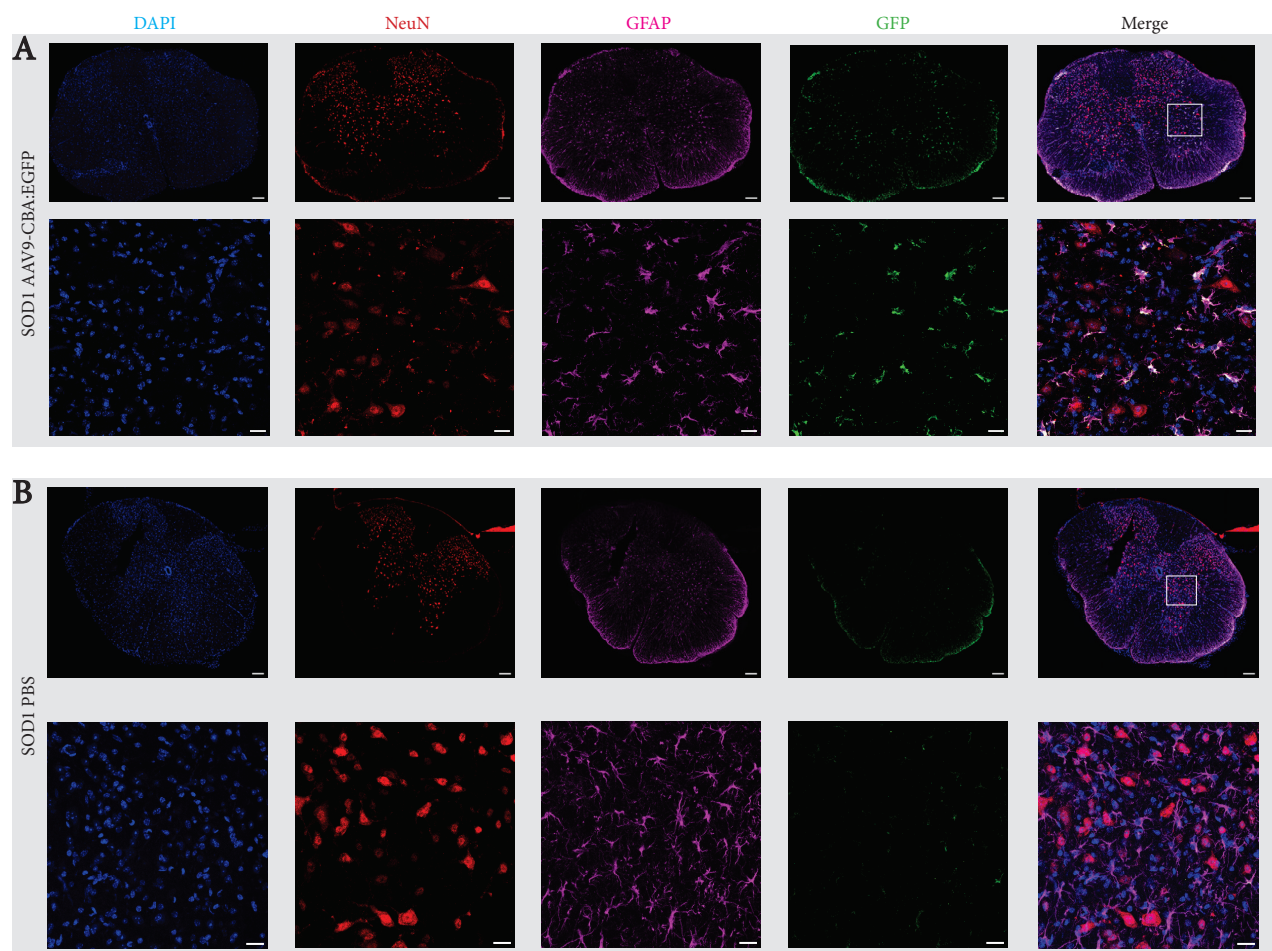
Figure 4: AAV9-CBA:EGFP successfully expresses EGFP, mostly in GFAP+ cells. (A) Spinal cord section of AAV9-CBA:EGFP transduced mice at end stage, including a picture of the full spinal cord section and a magnification of the area marked by a white square. EGFP expression is co-localizing with GFAP in the magnified images. (B) Control staining of EGFP in SOD1 PBS mice. PBS-injected SOD1[G93A] mice do not show presence of EGFP. In both (A) and (B), images showing the full spinal cord section have a scale bar of 100 μm, and the magnified images have a scale bar of 20 μm.

6.3.6 OPTN overexpression may cause side effects detectable in the gallbladder and eyes

While performing the swimming tank test, one of the mice treated with AAV9-CBA:OPTN started displaying symptoms suggesting visual problems in the left eye. The mouse repeatedly touched the left wall of the tank during swimming, as if she was not able to see the left edge of the tank. While these symptoms were clearly observable in just one mouse, it is worth noting as mutations in OPTN are known to be associated with glaucoma, which causes blindness (Bansal et al., 2015). At 130 days of age, the animals were sacrificed and perfused with 4% PFA. During perfusion, it became visible that half of the mice treated with AAV9-CBA:OPTN had enlarged gallbladders compared to the other mice (see figure 5). As ICV injection of AAV9 is known to cause high levels of liver cell transduction, it is possible that CBA-driven OPTN expression in liver cells leads to enlarged gallbladders (Mathiesen et al., 2020). Loss of OPTN function has been linked to cancer in several studies (Du et al., 2021; Salvagno and Cubillos-Ruiz, 2021). While in our experiments we induce overexpression, it is possible that this dysregulation results in gallbladder cancer manifesting as enlarged gallbladders, however, this remains unconfirmed.

Figure 6-5. Several mice transduced with AAV9-CBA-OPTN showed enlarged gallbladders
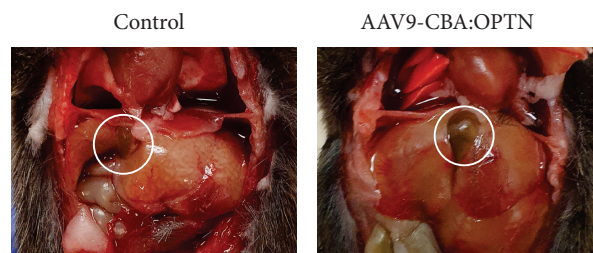
Figure 5: Several mice transduced with AAV9-CBA-OPTN showed enlarged gallbladders during dissection. An example of a control wild-type mouse injected with PBS, as well as a SOD1 PBS mouse injected with AAV9-CBA:OPTN. The gallbladders are encircled in white.

6.3.7 Neuronal SR expression does not improve the CMAP recordings of SOD1^{G93A} mice

While ubiquitous OPTN overexpression did not rescue SOD1^{G93A} mouse pathology, this does not mean that NF-κB inhibition, in general, cannot lead to improvement of ALS phenotypes. Expression of OPTN in several different cell types may have caused dysregulation of the NF-κB pathway through cell-to-cell interaction. The many different functions of OPTN may also

be the cause of side-effects observed when administering OPTN overexpression in our study. To rectify this, we aimed to restrict the NF-κB inhibition to neurons in particular, as it is the cell type which degenerates in human patients, and to use expression of SR protein to eliminate side effects, as its only function is NF-κB inhibition.

We administered AAV6-hSyn1:SR through ICV at P1-2 in SOD1^{G93A} pups. As with the OPTN experiment, the CMAP in the gastrocnemius muscle, induced by stimulation in the lumbar spinal cord, was measured. However, we did not observe any improvement in the group treated with AAV6-hSyn1:SR compared to controls (figure 6A).

6.3.8 Motor behavior is not rescued through administration of neuronal SR

To further assess the effect of neuronal SR expression, we also evaluated the motor behavior of the mice regularly after viral treatment. When measuring the ability of the mice to run on an accelerating rod in the rotarod test, no difference between the SOD1^{G93A} treated and control groups was observed (figure 6B). The only significant difference observed was between any group of SOD1^{G93A} genotype and the wild-type group treated with PBS. Similar results were observed in the swimming test, where the overall motor abilities of the mice were measured by forcing them to swim to a platform (figure 6C). From this we conclude that AAV6-mediated expression of NF-κB inhibitor SR exclusively in neurons is not enough to rescue SOD1^{G93A} mouse pathology, and that perhaps a different cell type needs to be targeted.

Figure 6-6. Motor behavior of SOD1^{G93A} mice treated with AAV6-hSyn1:SR
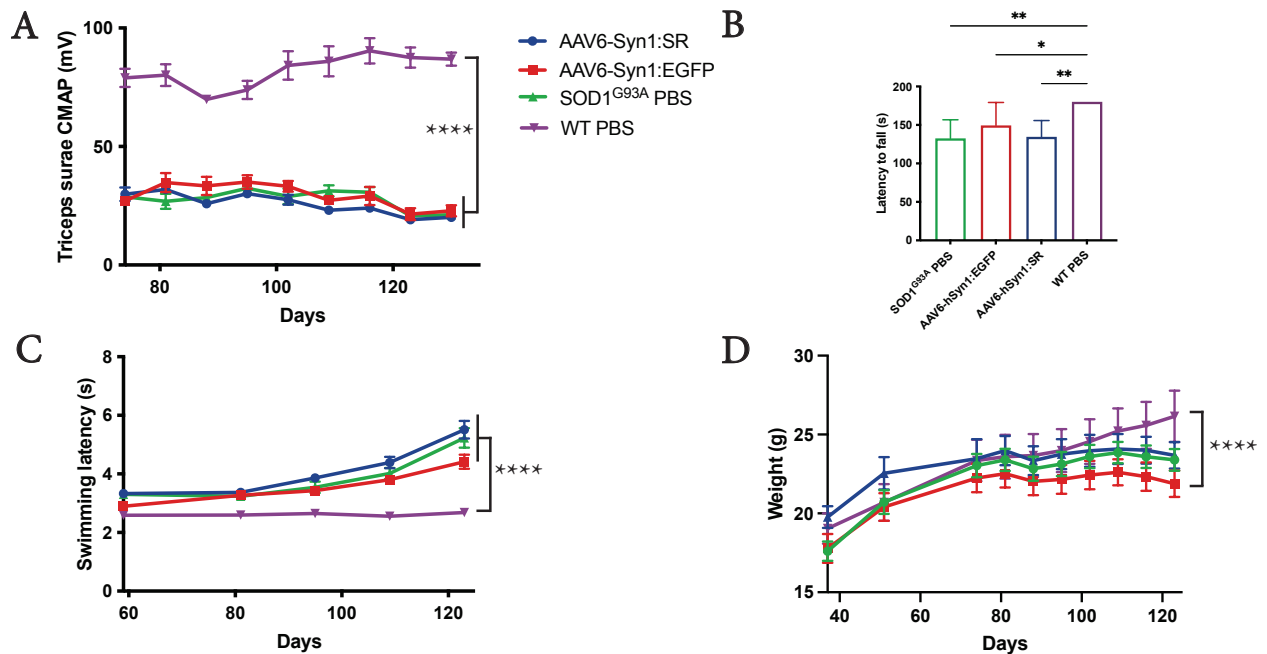
Figure 6: Administration of AAV6-hSyn1:SR does not significantly rescue the ALS phenotypes of SOD1^{G93A} mice. Behavioral and electromyographical tests in wild-type injected with PBS (n=8) in magenta, SOD1^{G93A} injected with PBS in green (n=7), SOD1^{G93A} injected with AAV6-hSyn1:EGFP in red (n=9), and SOD1^{G93A} injected with AAV6-hSyn1:SR in blue (n=9) (A) Amplitude of evoked compound muscle action potential (CMAP), recorded in the *triceps surae*. (B) Rotarod measuring the motor coordination of the mice on an accelerating rotating rod at day 123. (C) Measuring the overall motor abilities of the mice through their latency when swimming to a 0.8-meter distant platform. (D) The weight gain and loss of the mice throughout the experiment. In all tests, no significant improvement was seen due to the AAV treatment. The only significance found was between wild-type mice and SOD1^{G93A} mice. Data are presented as mean ± standard error of the mean; statistical analysis: for CMAP, swimming test, and weight, two-way ANOVA with Tukey's Multiple Comparisons post-hoc test. For the rotarod, one-way ANOVA with Tukey's Multiple Comparisons post-hoc test.

6.3.9 The SR protein is expressed in ventral horn neurons

In the spinal cord tissue collected from AAV6-hSyn1:SR after sacrifice, we were able to directly stain for the SR expression as the construct included a FLAG tag. It has previously been shown that ICV injection of AAV6 preferentially targets motor neurons (Dirren et al., 2014). In figure 7 it can be observed that the SR is indeed expressed in the ventral horn where

the motor neurons are situated, albeit in few neurons. Alike for the OPTN virus, the small number of neurons can be attributed to the collection of the samples at disease end stage.

Figure 6-7. SR is expressed in ventral horn neurons
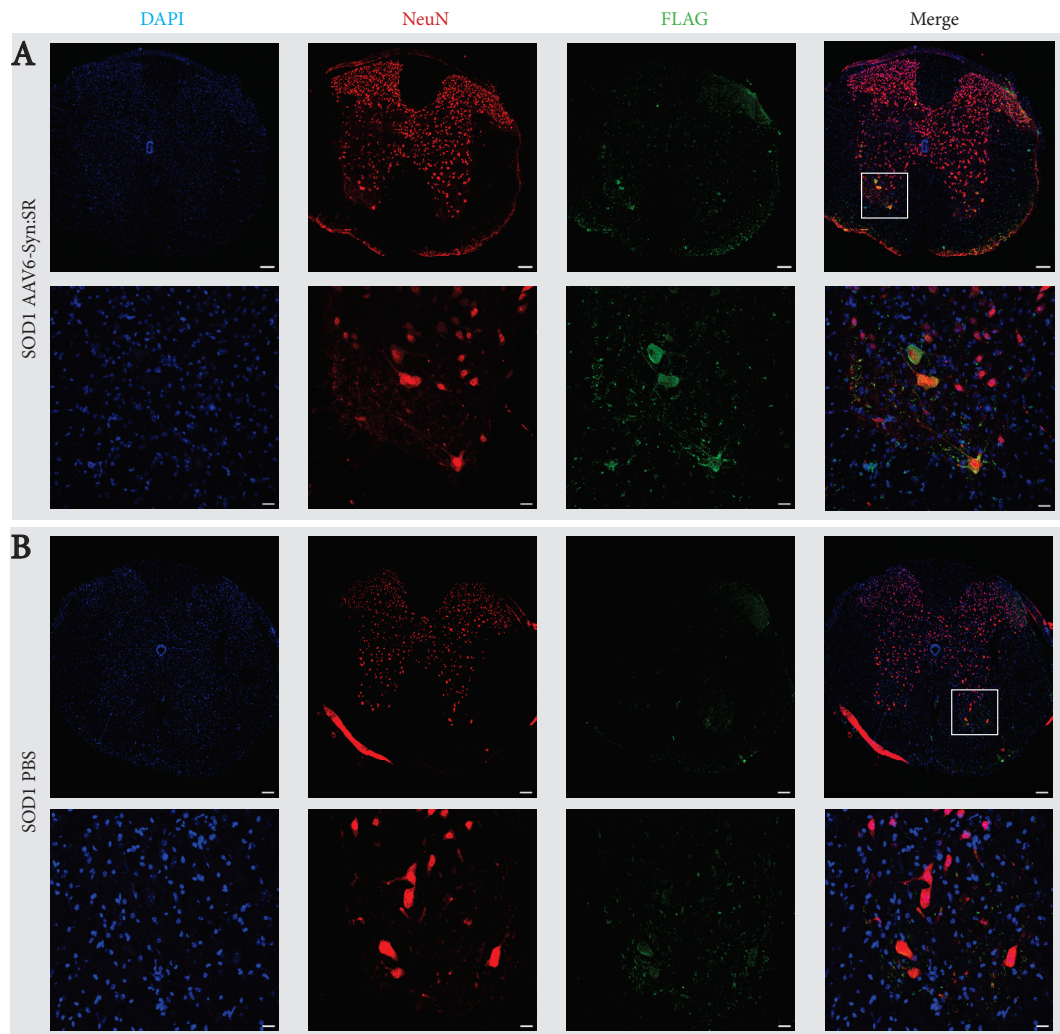
Figure 7: SR is expressed in ventral horn neurons of AAV6-hSyn1:SR injected mice. (A) AAV6-hSyn1-SR spinal cord section stained with anti-FLAG to visualize SR expression, including a picture of the full spinal cord section and a magnification of the area marked by a white square. Anti-FLAG colocalizes with NeuN in the ventral horn. (B) Control staining of FLAG in PBS-injected SOD1^{G93A} mice. The scale bars of the images showing full spinal cord section are 100 μm, and the scale bars of the magnified images are 20 μm.

6.4 Discussion

Here, we have shown that AAV-based inhibition of the NF-κB pathway is effective in reducing motor neuron loss in both IFNγ and TNFα-based ALS primary cell models. However, when the viruses expressing OPTN and SR were injected into a SOD1^{G93A} mouse

model, they did not lead to any improvement in the behavior or electromyographical measurements of the mice. We conclude that expression of NF-κB inhibitors may need to be induced in a different cell type than what was done in this study.

6.4.1 The difference in effectiveness of NF-κB inhibition in IFNγ- and TNFα-models compared to the SOD1^{G93A} model

We observed a clear difference in efficiency between the administration of the viruses in IFNγ/TNFα-based primary motor neuron *in vitro* models compared to the SOD1^{G93A} *in vivo* mouse model. IFNγ and TNFα, while not having been genetically linked to ALS, are both upregulated in patients and are known to cause motor neuron death *in vitro* (Liu et al., 2015; Poloni et al., 2000). Their potential role in ALS is unknown and it is not clear if their increased levels are a cause or consequence of disease. It is known, however, that both IFNγ and TNFα can induce the NF-κB pathway (Lin et al., 2012; Pozniak et al., 2014). As TNFα neurotoxicity through prevention of glutamate uptake can be rescued by inhibiting NF-κB (Zou and Crews, 2005), it is not unlikely that the TNFα-induced toxicity in our primary cell line model is at least partly through activation of NF-κB, which is then reversed with the application of the AAVs. A similar process could be hypothesized in the case of IFNγ.

6.4.2 The many functions of OPTN requires its expression to be more restricted

In the experiments overexpressing OPTN using a ubiquitous promoter, it is important to consider that while we are focusing on OPTNs function as a NF-κB inhibitor, it also plays many other roles in the cell (Toth and Atkin, 2018). For example, it is well-known for its importance in autophagy induction, the loss of which has been theorized to have significance in ALS pathogenesis (Markovinovic et al., 2017). Moreover, the combination of its different functions together, such as the combination of effects on neuroinflammation and autophagy, could be of importance in the disease mechanism.

The reason we chose to express OPTN in our AAV, was that the OPTN mutations involved in ALS are known to be loss-of-function. Therefore, adding OPTN was intended to increase its capacity to perform its function, that when lost causes disease. However, we observed several possible side effects of the treatment due to our ubiquitous overexpression of the protein, such as possible loss of vision and enlarged gallbladders. OPTN may still be a viable option for treatment, but would most probably have to be severely restricted to a specific cell

type in order to have only the intended effect instead of being overexpressed ubiquitously as we did in this study.

6.4.3 SR treatment may need to be administered at a higher titer to show effect

In ALS, motor neurons are observed to degenerate. As we hypothesized that aberrant NF-κB pathway activation is the cause of this neurotoxicity, we wanted to try to restrict the NF-κB inhibitory treatment to neurons. Therefore, we administered the AAV6-hSyn1-SR vector. However, as can be observed in our results, this did not seem to produce an efficient treatment of the ALS-like symptoms. In a similar study by Dutta et al., where transgenic mice with neuronal expression of SR were crossed to SOD1^{G93A} mice, an increased lifespan and improved behavior was observed (Dutta et al., 2020). This could be due to a higher level of SR production which cannot be replicated with an AAV vector. Thereby the mechanism of action may be correct, but the virus itself would need to be administered at a higher titer.

6.4.4 The efficiency of treatment can vary with the stage of disease

In our experiments we administered the viruses at P1-2 and expression of the proteins continued through the lifespan of the mice, theoretically causing constant inhibition of NF-κB signaling. However, the level of NF-κB activation and its helpfulness in combating the pathology may vary during the course of the disease. In fact, astrocytic NF-κB activation in SOD1^{G93A} mice causes microglial proliferation and leukocyte infiltration that prolongs the pre-symptomatic phase (Ouali Alami et al., 2018). However, in the symptomatic phase the response becomes damaging and causes an acceleration of the disease development, theorized to be due to a shift in the microglial phenotype from the anti-inflammatory M2 phenotype to the pro-inflammatory M1 phenotype. In the presymptomatic phase, NF-κB-dependent microglial activation would induce more anti-inflammatory microglia which would serve to be neuroprotective, while the symptomatic stage pro-inflammatory microglia may accelerate inflammation and motor neuron degeneration. Based on this, it may have been more appropriate to inject the AAV viruses at a symptomatic stage in our experiments, to maintain the NF-κB-related anti-inflammatory effects that can be observed pre-symptomatically. Indeed, this would also reflect the most likely timing of intervention in patients.

6.4.5 Cell type specificity of AAV vector treatment could play a crucial role in efficiency

While it is possible that our experiments did not show the hypothesized effect due to off-target functions of the proteins, timing of treatment, or because of too low titers of virus, another variable that could be playing a role is the cell type specificity. In the OPTN-expressing experiment, our aim was to express the protein in several different cell types, as we were unsure which would be the most effective or if it was needed in several cell types simultaneously. For the SR experiment, we wanted to specifically target neurons, and a majority of motor neurons, as they are the cell type which degenerate during the course of ALS. However, it is very possible that non-cell autonomous interaction of NF-κB signaling between several cell types, for example, causes disease, or that a NF-κB signaling is activated in a cell type which we could not target with our treatment. It has been established, for example, that all AAV vectors have very low transduction efficiency in microglia, and that microglial-specific NF-κB inhibition in SOD1^{G93A} mice improves ALS phenotypes (Maes et al., 2019) (Frakes et al., 2014).

To further assess the presence of NF-κB signaling in SOD1^{G93A} mice, and in which cell type it may be activated, we stained SOD1^{G93A} spinal cord tissue from 130-day old mice with an antibody targeting the NF-κB protein p65 (figure 8A). We observed the presence of p65-positive cells in both wild-type and SOD1^{G93A} grey matter, but in the SOD1^{G93A} mice we also saw presence of p65-expressing cells in the white matter. In addition, in the wild-type mice p65 appeared to be cytoplasmic, indicating a non-activated NF-κB pathway, while in the SOD1 mice the p65 staining appeared more nuclear (figure 8B). This implies that NF-κB signaling is activated in a cell type present in both white and grey matter during SOD1^{G93A} pathogenesis, unlike in wild-type control.

Figure 6-8. Localization of NF-κB protein p65 in SOD1^{G93A} mouse spinal cords
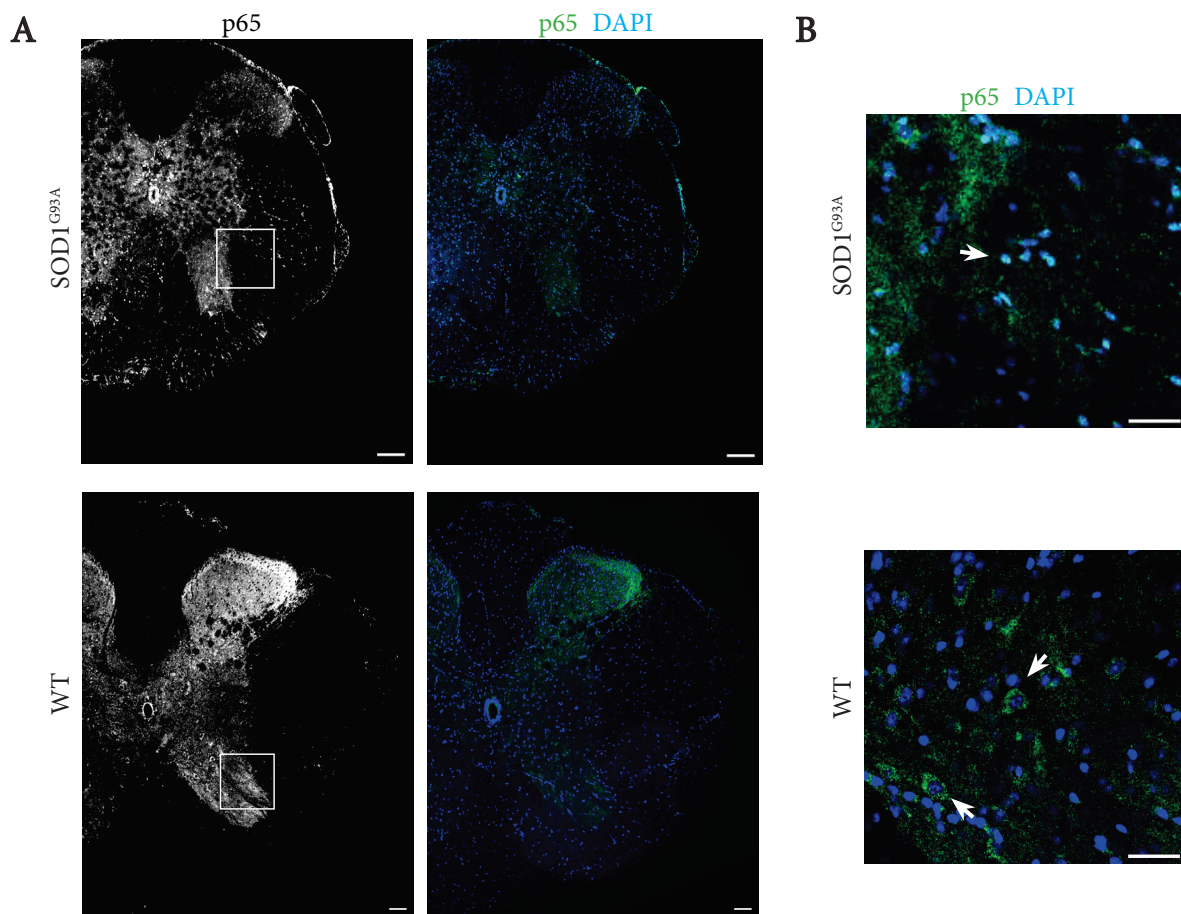
Figure 8: The NF-κB protein p65 is localized to the nucleus in both grey and white matter cells of SOD1^{G93A} mice, unlike wild-type control where the expressed p65 appears cytoplasmic. (A) Anti-p65 staining (green) and DAPI staining (blue) in SOD1^{G93A} mice as well as wild-type control, at 130 days of age. (B) Magnification of the p65 and DAPI staining highlighted by a white square in figure A. The arrows point to examples of cells with nuclear p65 expression (in the SOD1^{G93A} image) and cytoplasmic p65 expression (in the wild-type image). Scale bars are 100 μm, except in magnified images where scale bars are 30 μm.

We hypothesized that the cell type nuclearizing p65, and thereby activating the NF-κB pathway, was an immune cell, as the role of the NF-κB pathway in the immune response is well known. To further assess the identity of these cells, we co-stained anti-p65 together with anti-Iba1, a known macrophage marker which is most famous for its labelling of microglia, but which can also label peripheral macrophages that infiltrate the brain (Amici et al., 2017; Jurga et al., 2020). We observed p65 expression in Iba1-positive macrophages in the SOD1^{G93A} spinal cord, seemingly throughout the whole cell bodies, suggesting activation of

the NF-κB pathway in these cells (figure 9). We conclude that NF-κB is indeed activated in either CNS-resident macrophages or macrophages of peripheral origin.

Figure 6-9. Iba1-positive cells with nuclear p65 present in SOD1^{G93A} mouse spinal cord
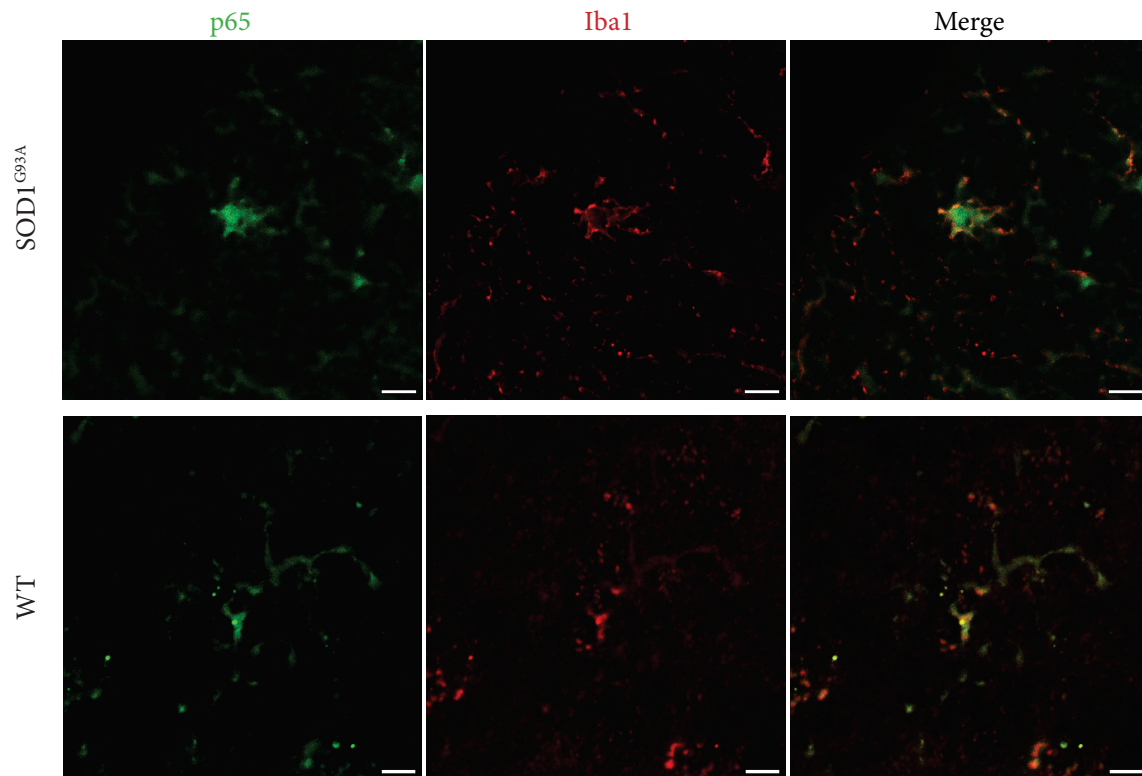
Figure 9: Iba1-positive cells with nuclear p65 present in SOD1^{G93A} mouse spinal cord. Magnified images of examples of Iba1 (red) and p65 (green) positive cells in the SOD1^{G93A} and wild-type spinal cord. The scale bar is 10 μm.

There is a lot of intrinsic heterogeneity among both microglia and macrophages in terms of morphology, density of cells, and the markers expressed in pathology and homeostasis which may differ depending on CNS region (Jurga et al., 2020). We decided to assess the presence of marker MHC-II in the SOD1^{G93A} spinal cord tissue. MHC-II is normally present on antigen-presenting immune cells, such as peripheral immune cells like dendritic cells and macrophages (D'Agostino et al., 2012; Roche and Furuta, 2015). Previous studies also show that microglia can begin expressing MHC-II in the CNS in an inflammatory context, possibly to present antigens to potential T lymphocytes (Wolf et al., 2018). To assess the presence of MHC-II in SOD1^{G93A} mice during ageing, we sacrificed spinal cord tissue from SOD1^{G93A} and wild-type mice aged 75, 100, 125, and 150 days and stained with anti-MHC-II and

nuclear DAPI. The density of MHC-II-positive cells in the grey and white matter were quantified, and we could observe a significant increase of cells expressing MHC-II in SOD1^{G93A} mice compared to wild-type (figure 10).

Figure 6-10. MHC-II positive cells are more prevalent in SOD1^{G93A} mouse spinal cords
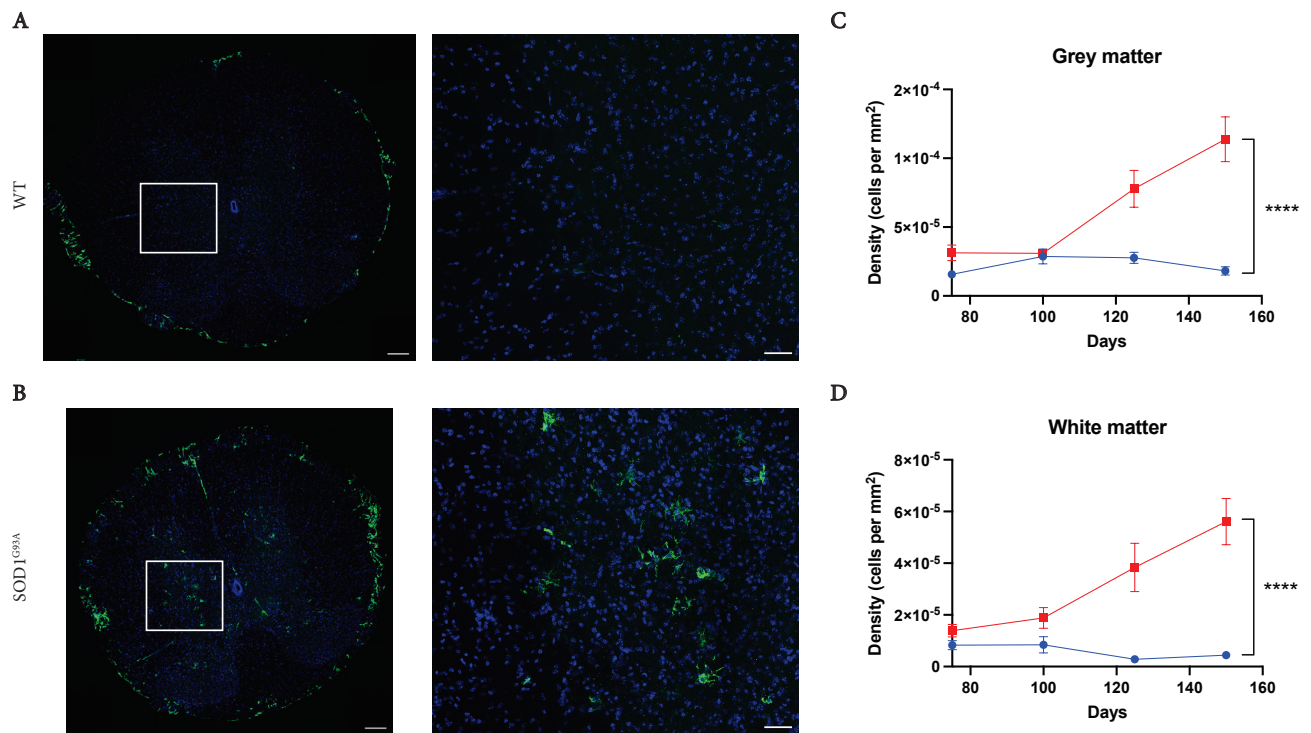
Figure 10: MHC-II positive cells are more prevalent in SOD1^{G93A} mouse spinal cords compared to wild-type control spinal cords. (A-B) Images of MHC-II (green) co-stained with DAPI (blue) in wild-type control and SOD1^{G93A} mouse spinal cords at age 150. (C) Quantification of the density of cells expressing MHC-II in the grey matter of wild-type and SOD1^{G93A} spinal cords, from 75 to 150 days of age. (D) Quantification of the density of cells, displayed as number of cells per mm^2, expressing MHC-II in the white matter of wild-type and SOD1^{G93A} spinal cords, from 75 to 150 days of age. Cells expressing MHC-II are significantly more prevalent in both grey and white matter of SOD1^{G93A} spinal cords than grey and white matter of wild-type spinal cords as the mice age. Scale bars of images showing the full spinal cord section are 100 μm, and the magnified areas have a scale bar of 40 μm. Data are presented as mean ± standard error of the mean; statistical analysis: two-way ANOVA looking at the main effect the genotypes.

To further evaluate the identity of the MHC-II$^+$ cells we also stained SOD1^{G93A} and wild-type spinal cord tissue for MHC-II and Iba1, and observed expression of both proteins in the same cells in both SOD1^{G93A} and wild-type (figure 11). We hypothesize that it may be these Iba1 and MHC-II expressing cells that have an upregulated NF-κB pathway. The cells could be a

type of resident microglia, that are stimulated to expand in numbers in the presence of SOD1^{G93A} pathology, or peripheral macrophages that have increasingly infiltrated the CNS. The identity of these cells and their influence on disease progression remains to be further studied.

Figure 6-11. MHC-II staining colocalizes with Iba1 staining
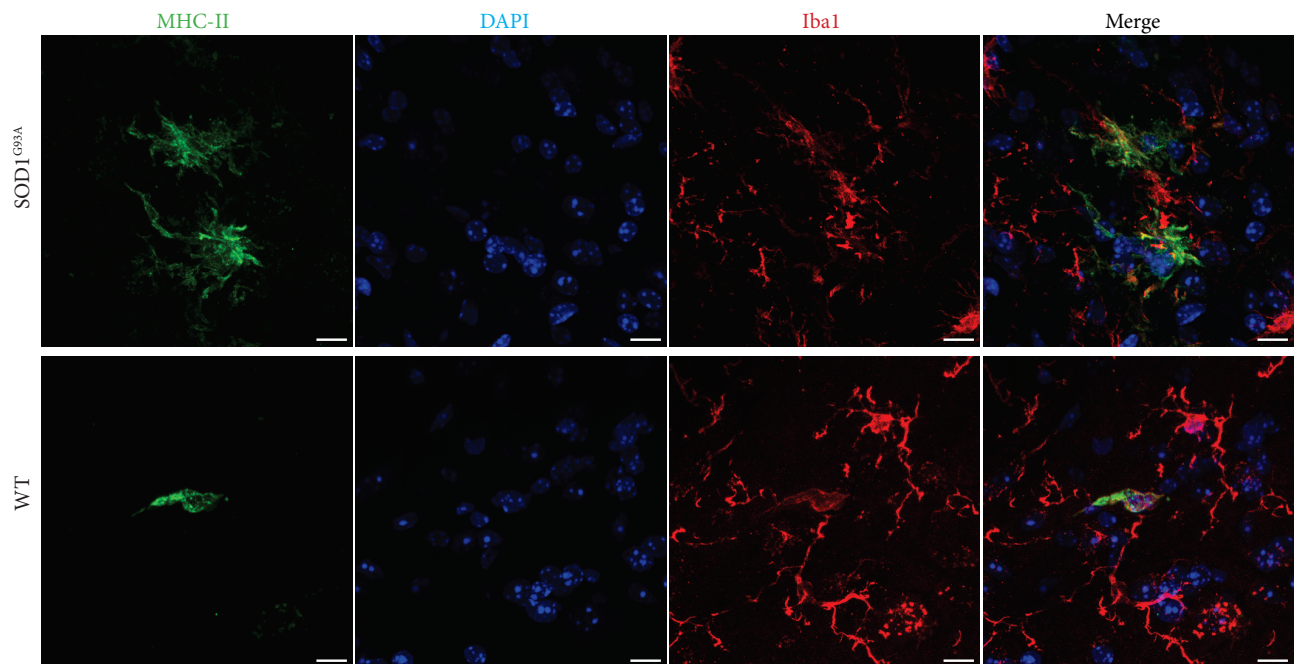
Figure 11: MHC-II staining colocalizes with Iba1 staining in SOD1^{G93A} mouse spinal cord. Magnified images of Iba1 (green), MHC-II (red), and DAPI (blue) positive cells in the SOD1^{G93A} and wild-type control spinal cords. The scale bar is 10 μm.

6.5 Conclusion

Here, we have demonstrated that AAV viruses aimed to inhibit NF-κB signaling can rescue motor neuron death in IFNγ and TNFα-based *in vitro* models. However, the same viruses could not rescue the behavioral and electromyographical symptoms in the SOD1^{G93A} mouse model. The difference could be due to the change in genetic basis of ALS model, or the titer of the virus. It could also be due to the viruses affecting an incorrect cell type, and the role of the macrophages expressing MHC-II that we observed at an increased density in the spinal cord of SOD1^{G93A} mice in ALS pathology needs to be further explored.

6.6 Materials and methods

6.6.1 Cloning of pAAVs and determination of pAAV protein production

The OPTN and EGFP were separately cloned into the pAAV-CBA plasmid. The SR attached to a FLAG tag (Addgene, 22504) and EGFP were separately cloned into the pAAV-hSyn1 plasmid. Lipofectamin and plasmid in Opti-MEM medium were used to transfect HEK293T cells with the pAAV-CBA:OPTN, pAAV-CBA:EGFP, pAAV-hSyn1:SR, and pAAV-hSyn1:EGFP plasmids, separately. After 48 h, cells were lysed in a lysis buffer (0.5% Triton X-100, 50 mM Tris/HCl pH 7.4, 175 mM NaCl, 5 mM EDTA pH 8.0, 1% protease inhibitor mixture), and the protein concentration was determined using a Micro BCA Protein Assay kit (Thermo Scientific). 25 μg of protein was loaded in a 4-12% Tris-Glycine gel (Invitrogen, XP04120BOX). Following protein separation, the proteins were transferred to a nitrocellulose membrane, and subsequent to 1 h of blocking, primary antibodies were incubated overnight (anti-Optineurin, Abcam 151240, concentration 1:1000) (anti-GFP, Roche 11814460001, concentration 1:5000) (anti-Flag, Sigma F7425, 1:5000). After 2 hrs incubation with secondary antibody (goat anti-rabbit 111-035-003, Jackson ImmunoResearch) (goat anti-mouse 115-035-003, Jackson ImmunoResearch), protein bands were detected. The membrane was stripped for 10 minutes at 37 °C (Restore Western Blot Stripping Buffer, Thermo Scientific), and, after washing, re-blocked and stained with anti-α-tubulin as loading control (mouse anti-α-tubulin T6199, Sigma Aldrich).

6.6.2 Viral production

The pAAV-CBA:OPTN, pAAV-CBA:EGFP, pAAV-hSyn1:SR, and pAAV-hSyn1:EGFP plasmids were co-transfected with helper plasmids into HEK293-AAV cells. 48 h after transfection, cells were lysed and the viral particles purified using iodixanol step gradient and ion exchange chromatography. TaqMan qPCR (Invitrogen) using primers recognizing the β-globin intron and albumin was performed to measure the amount of viral genome copies.

6.6.3 Motor neuron cell culture

CD-1 mouse spinal cords were dissected at E12.5 and motor neurons were isolated using immunoaffinity purification against a p75 antibody as described by Arce et al. (Arce et al., 1999) and modified by Raoul et al. (Raoul et al., 2002). The motor neurons were subsequently plated on poly-ornithine/laminin-treated wells. To induce IFNγ-related

neurotoxicity, the neurons were treated with 250 ng/ml of IFNγ for 48 h, either with or without treatment with each AAV virus at a titer of 15 TU/ml. After said 48 h, the surviving motor neurons were counted and quantified. To compare values from the different groups, the average value of the untreated (without IFNγ or viruses) was set as 100% survival. The same experiment was performed but with the neurons being treated with TNFα to induce neurotoxicity in combination with the different AAV viruses.

6.6.4 Animals and administration of vector

Animal work was performed according to Swiss legislation for the care and use of laboratory animals. B6.Cg-Tg(SOD1*G93A)dl1Gur/J males were bred with C57BL/6J females (Charles River Laboratories), and at P1-2, biopsies of the pups' tails were taken. Primers against human SOD1 as well as control primers against housekeeping gene IL2 were used in a PCR to verify the genotype of the pups. The same day, ICV injections were performed on the pups. 20 minutes prior to injection, analgesic Eutectic Mixture of Local Anesthetics (EMLA) cream was administered on the pups' heads in order to minimize discomfort. During the injection, mice are immobilized using surgical tape at the neck and nose. A small cube of polysterene (1 mm x 1 mm x 1 mm) is placed through the needle to ensure the appropriate depth of injection, and 4 μl of the virus or PBS solution was injected into the right lateral ventricle using a 29G insulin syringe (B. Braun, Hessen, Germany). After the short procedure, the pups were returned to the cages of their mothers.

6.6.5 Behavioral experiments and electromyography

When the pups reached 4 weeks of age they were weaned, and at 5 weeks the first Compound muscle action potential (CMAP) test was performed. The mice were anesthetized using isoflurane and an electrode placed over the lumbar spinal cord stimulated the sciatic nerve, as the action potentials were recorded in the gastrocnemius muscle. Subsequently, CMAP was measured every 2 weeks until sacrifice. At 6 weeks, the first rotarod test was performed, which continued every 4 weeks until sacrifice. The mice were placed on an accelerating rod and allowed to run on it for a maximum of 180 s. When they fell, or they for repeated rounds held onto the rod instead of running on it, the time was recorded. Similarly, the swimming tank test was first performed at 8 weeks, and continued every 4 weeks until sacrifice. The mice were put in a narrow plexiglass pool with a 0.8-meter distance to a visible platform. The time taken for the mice to swim to the platform was measured.

6.6.6 Immunohistochemistry

For the experiments using viral vectors, the mice were sacrificed at 130 days of age, while for the experiments quantifying MHC-II$^+$ cells and staining for the presence of p65 and Iba1, mice were sacrificed at 75, 100, 125, and 150 days of age. The sacrifice was performed through intraperitoneal injection of pentobarbital and were subsequently perfused with 4% PFA. The spinal cord was dissected, kept in 4% PFA overnight, and then transferred to 25% sucrose solution. Subsequently, the spinal cords were frozen in cryomatrix and sliced into 50 µm thick sections on a microtome.

The sections were washed in PBS 0.03% Triton X-100 azide, and blocked in 2% NHS for an h. The primary antibodies were diluted in 2% NHS and incubated over 3 nights before washing with PBS 0.03% Triton-X 100. The secondary antibodies were diluted in PBS 0.03% Triton-X 100 and incubated for 2 h. The sections were washed in 0.1 M PBS 7.4 pH, and mounted in Mowiol. The primary antibodies used were rabbit anti-GFP (Invitrogen, 1:500) rabbit anti-FLAG (Sigma, 1:200), rabbit anti-GFAP (Dako, 1:500), mouse anti-NeuN (Millipore, 1:1000), anti-MHC II (Invitrogen, 1:100), anti-p65 (Cell Signaling, 1:400), anti-P2Y12 (Invitrogen, 1:200), anti-Iba1 (Invitrogen, 1:250), and DAPI (Biotium Chem.Brunschwig, 1:5000). The secondary antibodies used were, anti-mouse Alexa Fluor 546 (Lifetech, 1:500), anti-rabbit Alexa Fluor 647 (Lifetech, 1:500), anti-rabbit Alexa Fluor 488 (Lifetech, 1:500).

6.6.7 Quantifications of cells expressing MHC-II

Analysis was performed manually using Fiji (ImageJ), with cell counting plugin. The gray and white matter areas of the spinal cord were defined with DAPI density. Density of MHC-II$^+$ cells was then calculated as number of MHC-II$^+$ cells divided by the area of the region (in mm^2). Data are presented as spinal cord averages calculated from three slices (bilaterally) along the torso-lumbar axis per animal.

6.6.7 Statistics

Data are presented as mean ± standard error of the mean, and p-values were calculated using a two-way ANOVA with Tukey's Multiple Comparisons post-hoc test assessing the main effect of the genotypes for CMAP, swimming test, weight and quantification of cells expression MHC-II. Rotarod p-values were calculated using a one-way ANOVA with

Tukey's Multiple Comparisons post-hoc test. Results with a p-value < 0.05 were considered significant.

7

Chapter 7 - General Conclusions and Discussion

- -

7.1 Links between ALS and the NF-κB pathway

Chronic neuroinflammation has been a long-standing theory in neurodegenerative research, including ALS. Inflammation is observed in both ALS patients and animal models, and the level of inflammatory factors correlates with disease severity (Henkel et al., 2006; Jin et al., 2020; Kuhle et al., 2009; Mishra et al., 2016). In addition, in ALS models and patients, microglia and astrocytes display upregulation of the pro-inflammatory NF-κB proteins (Crosio et al., 2011; Frakes et al., 2014). Several different studies have genetically engineered mice to produce the super-repressor form of IκBα (SR) to inhibit the NF-κB pathway activation in neurons, microglia, and astrocytes in different studies using SOD1^{G93A} mice (Crosio et al., 2011; Dutta et al., 2020; Frakes et al., 2014). In both neurons and microglia, but not astrocytes, the SR expression increased the lifespan of the mice.

It is important to note that the links between ALS and NF-κB are not only observed in SOD1 ALS animal models, but in several models based on different familial variants of the disease. For example, knock-down of the most common gene linked to fALS, c9orf72, in a glioblastoma cell model leads to activation of the NF-κB pathway (Fomin et al., 2018). TDP-43 ALS mutant transgenic mice also improve motor and cognitive function as well as decrease motor neuron loss when genetically engineered to produce the SR neuronally (Dutta et al., 2020).

In the third chapter of this thesis, we investigated the effect of heterozygous mutations of proteins in the *Drosophila* NF-κB pathway on FUS and TDP-43 knock-out ALS models. We were able to observe that in both the FUS and TDP-43 models, the adult eclosion rate increased with heterozygous mutations of several members of the fly NF-κB pathway, and in

the case of the FUS model, improvement of the motor behavior and longevity was also observed. Alike the previous studies, this reinforces the evidence showing connections between ALS-related genes and the NF-κB pathway, in particular studies showing that decrease of the pathway can improve symptoms. In general, it seems that inhibition of NF-κB can be beneficial in ALS models.

7.2 Humanized TDP-43 and FUS Drosophila ALS models have only mild ALS phenotypes that cannot be further triggered by peripheral bacterial infection

In the first two chapters of this thesis, we created humanized FUS and TDP-43 ALS models which express the human protein and cause a deletion of the *Drosophila* ortholog. Interestingly, while wild-type hFUS and hTDP-43 were able to completely rescue knockout phenotypes, we found very mild ALS-like phenotypes in hFUS and hTDP-43 ALS-associated mutant *Drosophila*. We decided to attempt to induce a more severe ALS phenotype in the humanized fly models using peripheral gram-negative bacterial infection. However, we did not observe any differences in infection susceptibility between the ALS mutants and wild-type controls, suggesting that a septic injury bacterial infection cannot provoke ALS pathology in these *Drosophila*. As peripheral infection, activating the Imd pathway in peripheral macrophages, did not successfully induce ALS phenotypes, we hypothesize that Imd activation may in fact be required in CNS-resident glial immune cells. Indeed, when we overexpressed an activated version of Imd pathway receptor PGRP-LC in the glia of control flies, we induced severely shortened lifespan and deficits in motor behavior. This highlights the possibility of the Imd pathway needing to be activated in resident CNS glial cells, and in the future inducing glial Imd activation in the humanized FUS and TDP-43 ALS mutants may induce more severe disease phenotypes.

7.3 Advantages and disadvantages of humanizing *Drosophila* genes

In designing our humanized FUS and TDP-43 *Drosophila* models, the aim was to remove and replace the orthologous *Drosophila* coding sequences with the human gene coding sequence, allowing expression of the human protein under the regulation of endogenous regulatory sequences. This CRISPR/Cas9-based humanization technique has the advantage of reflecting the genetics observed in ALS patients more accurately than ALS models based on overexpression of human transgenes or deletion of the *Drosophila* ortholog, and is potentially extendable to allow creation of novel animal models for many other genetic disorders.

However, the during the process of this genome editing, we experienced some unexpected challenges (explained in more detail in the Annex). Most troublesome, in ~ 20% of the humanized TDP-43 *Drosophila* lines that were selected for successful genome editing based marker dsRed eye marker and had correctly inserted and expressed the human gene, the *Drosophila* ortholog gene *tbph* was still present and still producing *Drosophila* TBPH protein. We speculate that double-stranded DNA breaks induced by CRISPR/Cas9 enabled a reinsertion or duplication of the *tbph* locus, however the precise mechanisms through which this occurs and the location of the gene remains unclear. The high occurrence of these events emphasizes the importance of verifying the expression of the gene-of-interest and the absence of the unedited *Drosophila* gene during 'humanizing' and potentially other many gene editing modifications.

7.4 Cell type specificity can change the course of ALS treatments

When attempting to inhibit the NF-κB pathway using AAV vectors in mice, we chose to express NF-κB inhibitor and ALS-associated protein OPTN ubiquitously, and the NF-κB inhibitor SR neuronally, and saw no improvement of the ALS-like phenotypes with either virus. In the OPTN experiments, several factors could have caused the lack of effect. For example, OPTN has many functions, and while NF-κB inhibition is thought to be one of them, it could be that its functions in for example autophagy are the more relevant target for ALS treatment. It is also possible that in a different ALS model, that is not based on SOD1 ALS, it could have been more efficient as it is not known if the same mechanism is involved in all ALS cases. Although previous studies have observed improvements in pathology through neuronal SR expression, it is important to note that those studies used genetically engineered expression of SR. In our case, using AAV vectors, the expression may not be as high as in those experiments, which may account for the lack of effect. However, and some of our evidence supports this (see below), it is distinctly possible in retrospect that we were targeting the wrong cell types in our experiments.

7.5 CNS-resident macrophages may play a role in ALS pathology

In our SOD1^{G93A} mouse study, we observed Iba1-expressing cells with an activated NF-κB pathway as shown by nuclearized p65. We also observed MHC-II and Iba1-positive cells in the SOD1^{G93A} spinal cord, with MHC-II expression being characteristic of antigen-presenting cells, which suggests that the MHC-II-positive cells could be antigen-presenting cells from

the periphery which have infiltrated the CNS (D'Agostino et al., 2012; Roche and Furuta, 2015). The CNS contains several types of myeloid cells, including the parenchymal microglia, meningeal macrophages, choroid plexus macrophages, and perivascular cells, but when responding to an immune challenge these are not the only immune cells present in the CNS (Yin et al., 2017). Upon persistent lymphocytic choriomeningitis virus (LCMV) infection in mice, for example, T cells can infiltrate the CNS without causing BBB breakdown and induce proliferation of microglia as well as their conversion into antigen-presenting cells (Herz et al., 2015). During certain CNS disorders, including inflammatory diseases, the BBB is also known to be able to be disrupted causing peripheral immune cells to enter (Prinz and Priller, 2017). Altogether, this points to a peripheral immune activation possibly acting as an inducer of, or accelerating the progression, of ALS.

However, when we infected humanized FUS or TDP-43 *Drosophila* with gram-negative bacteria to induce a peripheral immune response, we observed no difference in susceptibility between ALS mutants and controls. This causes us to hypothesize that the macrophages we observe in the SOD1^{G93A} mice are not peripheral, but instead resident CNS macrophages. The NF-κB pathway is known to be activated in microglia, for example, as a response to an immune challenge, causing upregulated expression of pro-inflammatory genes (Dresselhaus and Meffert, 2019). Inhibition of NF-κB activation in microglia also improves ALS phenotypes in a SOD1^{G93A} model (Frakes et al., 2014).

7.6 What could be the trigger of NF-κB activation in the CNS?

As we conclude that peripheral infection is not able to trigger ALS in genetically predisposed *Drosophila* and instead activation of the immune system within the CNS could be needed, the question becomes: what could be the trigger? There are several possibilities that may induce immune system activation in the CNS, such as viral infections, but also traumatic brain injury and stress. In *Drosophila*, the Zika virus has been shown to infect the brain and induce Imd pathway activation which in turn activates STING (Liu et al., 2018). Epstein-Barr virus (EBV), which is known to be able to infect both periphery and brain and which has been associated with Multiple Sclerosis (MS), is also an activator of the Imd pathway in flies (Hassani et al., 2018; Sherri et al., 2018). In mice and humans, several viruses can also infect the brain, such as Herpes Simplex virus, which also causes nuclear translocation of NF-κB (Bookstaver et al., 2017; Hill et al., 2009). In addition to viral infections, other means may cause upregulation of NF-κB in the brain. Traumatic brain injury, for example, increases NF-

κB activation in rats, mice and *Drosophila* (Mettang et al., 2018; Nonaka et al., 1999; Swanson et al., 2020). Moreover, long-term stress, as well as aging, can cause increased neuroinflammation (DiSabato et al., 2016). It is possible that one, or a combination of, these factors function as a trigger in genetically predisposed individuals, triggering ALS. This is something that can be further tested using the humanized FUS and TDP-43 models.

7.7 Future perspectives

The MHC-II-positive macrophages we observed in the SOD1^{G93A} mouse model, in combination with the lack of symptoms induced in our humanized FUS and TDP-43 fly lines in response to peripheral immune activation, causes us to hypothesize that NF-κB-based activation of microglia or other CNS-resident macrophages take part in ALS motor neuron degeneration. However, should this be the case, the challenge is to be able to target the CNS macrophages and decrease their activation at a high enough level and early enough in the disease to make a difference for patients. Several NF-κB inhibitory drugs are available on the market, including drugs that can penetrate the BBB, but as these drugs are not cell type specific the wide NF-κB inhibition may cause many unwanted peripheral side effects (Miller et al., 2010; Uddin et al., 2021). AAV vector technology, on the other hand, has the advantage of being able to be cell type specific, but microglia are unfortunately not readily transduced by AAVs (Maes et al., 2019). To combat this, it is possible to use AAV vectors targeted to a CNS-resident cell type such as, for example, astrocytes, and induce it to express anti-inflammatory molecules. While this is not completely targeted only to microglia, it can still aid in avoiding NF-κB inhibition in peripheral cell types. All in all, we theorize that future experiments inhibiting the NF-κB pathway should be targeted to CNS resident immune cells, and that this could be achieved through CNS-centric expression of anti-inflammatory factors via AAV vectors.

8

Chapter 8 – References

- -

Aebischer, J., Cassina, P., Otsmane, B., Moumen, A., Seilhean, D., Meininger, V., Barbeito, L., Pettmann, B., Raoul, C., 2011. IFN γ triggers a LIGHT-dependent selective death of motoneurons contributing to the non-cell-autonomous effects of mutant SOD1. Cell Death Differ 18, 754–768. https://doi.org/10.1038/cdd.2010.143

Ahn, H.J., Hernandez, C.M., Levenson, J.M., Lubin, F.D., Liou, H.-C., Sweatt, J.D., 2008. c-Rel, an NF-κB family transcription factor, is required for hippocampal long-term synaptic plasticity and memory formation. Learn. Mem. 15, 539–549. https://doi.org/10.1101/lm.866408

Ajmone-Cat, M.A., Onori, A., Toselli, C., Stronati, E., Morlando, M., Bozzoni, I., Monni, E., Kokaia, Z., Lupo, G., Minghetti, L., Biagioni, S., Cacci, E., 2019. Increased FUS levels in astrocytes leads to astrocyte and microglia activation and neuronal death. Scientific Reports 9, 4572. https://doi.org/10.1038/s41598-019-41040-4

Akizuki, M., Yamashita, H., Uemura, K., Maruyama, H., Kawakami, H., Ito, H., Takahashi, R., 2013. Optineurin suppression causes neuronal cell death via NF-κB pathway. Journal of Neurochemistry 126, 699–704. https://doi.org/10.1111/jnc.12326

Albensi, B.C., Mattson, M.P., 2000. Evidence for the involvement of TNF and NF-kappaB in hippocampal synaptic plasticity. Synapse 35, 151–159. https://doi.org/10.1002/(SICI)1098-2396(200002)35:2<151::AID-SYN8>3.0.CO;2-P

Alexianu, M.E., Kozovska, M., Appel, S.H., 2001. Immune reactivity in a mouse model of familial ALS correlates with disease progression. Neurology 57, 1282–1289. https://doi.org/10.1212/wnl.57.7.1282

Allen, H.B., 2016. Alzheimer's Disease: Assessing the Role of Spirochetes, Biofilms, the Immune System, and Amyloid-β with Regard to Potential Treatment and Prevention. J Alzheimers Dis 53, 1271–1276. https://doi.org/10.3233/JAD-160388

Alonso, A., Logroscino, G., Hernán, M.A., 2010. Smoking and the risk of amyotrophic lateral sclerosis: a systematic review and meta-analysis. J. Neurol. Neurosurg. Psychiatry 81, 1249–1252. https://doi.org/10.1136/jnnp.2009.180232

Alonso, R., Pisa, D., Carrasco, L., 2019. Searching for Bacteria in Neural Tissue From Amyotrophic Lateral Sclerosis. Front. Neurosci. 13. https://doi.org/10.3389/fnins.2019.00171

Åman, P., Panagopoulos, I., Lassen, C., Fioretos, T., Mencinger, M., Toresson, H., Höglund, M., Forster, A., Rabbitts, T.H., Ron, D., Mandahl, N., Mitelman, F., 1996. Expression Patterns of the Human Sarcoma-Associated GenesFUSandEWSand the Genomic Structure ofFUS. Genomics 37, 1–8. https://doi.org/10.1006/geno.1996.0513

Amici, S.A., Dong, J., Guerau-de-Arellano, M., 2017. Molecular Mechanisms Modulating the Phenotype of Macrophages and Microglia. Frontiers in Immunology 8.

An, H., Skelt, L., Notaro, A., Highley, J.R., Fox, A.H., La Bella, V., Buchman, V.L., Shelkovnikova, T.A., 2019. ALS-linked FUS mutations confer loss and gain of function in the nucleus by promoting excessive formation of dysfunctional paraspeckles. Acta Neuropathologica Communications 7, 7. https://doi.org/10.1186/s40478-019-0658-x

Anderson, E.N., Gochenaur, L., Singh, A., Grant, R., Patel, K., Watkins, S., Wu, J.Y., Pandey, U.B., 2018. Traumatic injury induces stress granule formation and enhances motor dysfunctions in ALS/FTD models. Hum Mol Genet 27, 1366–1381. https://doi.org/10.1093/hmg/ddy047

Andersson, M.K., Ståhlberg, A., Arvidsson, Y., Olofsson, A., Semb, H., Stenman, G., Nilsson, O., Åman, P., 2008. The multifunctional FUS, EWS and TAF15 proto-oncoproteins show cell type-specific expression patterns and involvement in cell spreading and stress response. BMC Cell Biology 9, 37. https://doi.org/10.1186/1471-2121-9-37

Appel, S.H., Zhao, W., Beers, D.R., Henkel, J.S., 2011. The Microglial-Motoneuron dialogue in ALS. Acta Myologica 30, 4.

Arce, V., Garces, A., Bovis, B. de, Filippi, P., Henderson, C., Pettmann, B., deLapeyrière, O., 1999. Cardiotrophin-1 requires LIFRβ to promote survival of mouse motoneurons

purified by a novel technique. Journal of Neuroscience Research 55, 119–126. https://doi.org/10.1002/(SICI)1097-4547(19990101)55:1<119::AID-JNR13>3.0.CO;2-6

Arnold, E.S., Ling, S.-C., Huelga, S.C., Lagier-Tourenne, C., Polymenidou, M., Ditsworth, D., Kordasiewicz, H.B., McAlonis-Downes, M., Platoshyn, O., Parone, P.A., Da Cruz, S., Clutario, K.M., Swing, D., Tessarollo, L., Marsala, M., Shaw, C.E., Yeo, G.W., Cleveland, D.W., 2013. ALS-linked TDP-43 mutations produce aberrant RNA splicing and adult-onset motor neuron disease without aggregation or loss of nuclear TDP-43. Proceedings of the National Academy of Sciences 110, E736–E745. https://doi.org/10.1073/pnas.1222809110

Arthur, K.C., Calvo, A., Price, T.R., Geiger, J.T., Chiò, A., Traynor, B.J., 2016. Projected increase in amyotrophic lateral sclerosis from 2015 to 2040. Nature Communications 7. https://doi.org/10.1038/ncomms12408

Ascherio, A., Weisskopf, M.G., O'reilly, E.J., Jacobs, E.J., McCullough, M.L., Calle, E.E., Cudkowicz, M., Thun, M.J., 2005. Vitamin E intake and risk of amyotrophic lateral sclerosis. Ann. Neurol. 57, 104–110. https://doi.org/10.1002/ana.20316

Atanasio, A., Decman, V., White, D., Ramos, M., Ikiz, B., Lee, H.-C., Siao, C.-J., Brydges, S., LaRosa, E., Bai, Y., Fury, W., Burfeind, P., Zamfirova, R., Warshaw, G., Orengo, J., Oyejide, A., Fralish, M., Auerbach, W., Poueymirou, W., Freudenberg, J., Gong, G., Zambrowicz, B., Valenzuela, D., Yancopoulos, G., Murphy, A., Thurston, G., Lai, K.-M.V., 2016. C9orf72 ablation causes immune dysregulation characterized by leukocyte expansion, autoantibody production, and glomerulonephropathy in mice. Sci Rep 6, 23204. https://doi.org/10.1038/srep23204

Avadhanula, V., Weasner, B.P., Hardy, G.G., Kumar, J.P., Hardy, R.W., 2009. A novel system for the launch of alphavirus RNA synthesis reveals a role for the Imd pathway in arthropod antiviral response. PLoS Pathog 5, e1000582. https://doi.org/10.1371/journal.ppat.1000582

Balendra, R., Isaacs, A.M., 2018. C9orf72-mediated ALS and FTD: multiple pathways to disease. Nat Rev Neurol 14, 544–558. https://doi.org/10.1038/s41582-018-0047-2

Banks, C.N., Lein, P.J., 2012. A Review of Experimental Evidence Linking Neurotoxic Organophosphorus Compounds and Inflammation. Neurotoxicology 33, 575–584. https://doi.org/10.1016/j.neuro.2012.02.002

Bansal, M., Swarup, G., Balasubramanian, D., 2015. Functional analysis of optineurin and some of its disease-associated mutants. IUBMB Life 67, 120–128. https://doi.org/10.1002/iub.1355

Basset, A., Khush, R.S., Braun, A., Gardan, L., Boccard, F., Hoffmann, J.A., Lemaitre, B., 2000. The phytopathogenic bacteria Erwinia carotovora infects Drosophila and activates an immune response. Proceedings of the National Academy of Sciences 97, 3376–3381. https://doi.org/10.1073/pnas.97.7.3376

Beers, D.R., Henkel, J.S., Xiao, Q., Zhao, W., Wang, J., Yen, A.A., Siklos, L., McKercher, S.R., Appel, S.H., 2006. Wild-type microglia extend survival in PU.1 knockout mice with familial amyotrophic lateral sclerosis. PNAS 103, 16021–16026. https://doi.org/10.1073/pnas.0607423103

Bellmann, J., Monette, A., Tripathy, V., Sójka, A., Abo-Rady, M., Janosh, A., Bhatnagar, R., Bickle, M., Mouland, A.J., Sterneckert, J., 2019. Viral Infections Exacerbate FUS-ALS Phenotypes in iPSC-Derived Spinal Neurons in a Virus Species-Specific Manner. Frontiers in Cellular Neuroscience 13.

Bennion Callister, J., Pickering-Brown, S.M., 2014. Pathogenesis/genetics of frontotemporal dementia and how it relates to ALS. Exp. Neurol. 262 Pt B, 84–90. https://doi.org/10.1016/j.expneurol.2014.06.001

Boersma, M.C.H., Dresselhaus, E.C., Biase, L.M.D., Mihalas, A.B., Bergles, D.E., Meffert, M.K., 2011. A Requirement for Nuclear Factor-κB in Developmental and Plasticity-Associated Synaptogenesis. J. Neurosci. 31, 5414–5425. https://doi.org/10.1523/JNEUROSCI.2456-10.2011

Boillée, S., Yamanaka, K., Lobsiger, C.S., Copeland, N.G., Jenkins, N.A., Kassiotis, G., Kollias, G., Cleveland, D.W., 2006. Onset and Progression in Inherited ALS Determined by Motor Neurons and Microglia. Science 312, 1389–1392. https://doi.org/10.1126/science.1123511

Bookstaver, P.B., Mohorn, P.L., Shah, A., Tesh, L.D., Quidley, A.M., Kothari, R., Bland, C.M., Weissman, S., 2017. Management of Viral Central Nervous System Infections: A Primer for Clinicians. J Cent Nerv Syst Dis 9, 1179573517703342. https://doi.org/10.1177/1179573517703342

Borchsenius, S.N., Daks, A., Fedorova, O., Chernova, O., Barlev, N.A., 2019. Effects of mycoplasma infection on the host organism response via p53/NF-κB signaling. Journal of Cellular Physiology 234, 171–180. https://doi.org/10.1002/jcp.26781

Bosco, D.A., Lemay, N., Ko, H.K., Zhou, H., Burke, C., Kwiatkowski, T.J., Jr, Sapp, P., McKenna-Yasek, D., Brown, R.H., Jr, Hayward, L.J., 2010. Mutant FUS proteins that cause amyotrophic lateral sclerosis incorporate into stress granules. Human Molecular Genetics 19, 4160–4175. https://doi.org/10.1093/hmg/ddq335

Bozzoni, V., Pansarasa, O., Diamanti, L., Nosari, G., Cereda, C., Ceroni, M., 2016. Amyotrophic lateral sclerosis and environmental factors. Funct Neurol 31, 7–19. https://doi.org/10.11138/FNeur/2016.31.1.007

Brenner, D., Sieverding, K., Bruno, C., Lüningschrör, P., Buck, E., Mungwa, S., Fischer, L., Brockmann, S.J., Ulmer, J., Bliederhäuser, C., Philibert, C.E., Satoh, T., Akira, S., Boillée, S., Mayer, B., Sendtner, M., Ludolph, A.C., Danzer, K.M., Lobsiger, C.S., Freischmidt, A., Weishaupt, J.H., 2019. Heterozygous Tbk1 loss has opposing effects in early and late stages of ALS in mice. Journal of Experimental Medicine 216, 267–278. https://doi.org/10.1084/jem.20180729

Brown, G.C., 2019. The endotoxin hypothesis of neurodegeneration. J Neuroinflammation 16, 180. https://doi.org/10.1186/s12974-019-1564-7

Bruijn, L.I., Becher, M.W., Lee, M.K., Anderson, K.L., Jenkins, N.A., Copeland, N.G., Sisodia, S.S., Rothstein, J.D., Borchelt, D.R., Price, D.L., Cleveland, D.W., 1997. ALS-linked SOD1 mutant G85R mediates damage to astrocytes and promotes rapidly progressive disease with SOD1-containing inclusions. Neuron 18, 327–338. https://doi.org/10.1016/s0896-6273(00)80272-x

Bruijn, L.I., Miller, T.M., Cleveland, D.W., 2004. Unraveling the Mechanisms Involved in Motor Neuron Degeneration in Als. Annual Review of Neuroscience 27, 723–749. https://doi.org/10.1146/annurev.neuro.27.070203.144244

Buchon, N., Broderick, N.A., Poidevin, M., Pradervand, S., Lemaitre, B., 2009. Drosophila intestinal response to bacterial infection: activation of host defense and stem cell proliferation. Cell Host Microbe 5, 200–211. https://doi.org/10.1016/j.chom.2009.01.003

Burberry, A., Suzuki, N., Wang, J.-Y., Moccia, R., Mordes, D.A., Stewart, M.H., Suzuki-Uematsu, S., Ghosh, S., Singh, A., Merkle, F.T., Koszka, K., Li, Q.-Z., Zon, L., Rossi, D.J., Trowbridge, J.J., Notarangelo, L.D., Eggan, K., 2016. Loss-of-function mutations in the C9ORF72 mouse ortholog cause fatal autoimmune disease. Sci Transl Med 8, 347ra93. https://doi.org/10.1126/scitranslmed.aaf6038

Burberry, A., Wells, M.F., Limone, F., Couto, A., Smith, K.S., Keaney, J., Gillet, G., van Gastel, N., Wang, J.-Y., Pietilainen, O., Qian, M., Eggan, P., Cantrell, C., Mok, J., Kadiu, I., Scadden, D.T., Eggan, K., 2020. C9orf72 suppresses systemic and neural inflammation induced by gut bacteria. Nature 582, 89–94. https://doi.org/10.1038/s41586-020-2288-7

Cao, Y., Chtarbanova, S., Petersen, A.J., Ganetzky, B., 2013. Dnr1 mutations cause neurodegeneration in Drosophila by activating the innate immune response in the brain. Proc Natl Acad Sci U S A 110, E1752–E1760. https://doi.org/10.1073/pnas.1306220110

Cappello, V., Francolini, M., 2017. Neuromuscular Junction Dismantling in Amyotrophic Lateral Sclerosis. Int J Mol Sci 18, 2092. https://doi.org/10.3390/ijms18102092

Chang, J.-C., Morton, D.B., 2017. Drosophila lines with mutant and wild type human TDP-43 replacing the endogenous gene reveals phosphorylation and ubiquitination in mutant lines in the absence of viability or lifespan defects. PLoS ONE 12, e0180828. https://doi.org/10.1371/journal.pone.0180828

Chattopadhyay, M., Valentine, J.S., 2009. Aggregation of copper-zinc superoxide dismutase in familial and sporadic ALS. Antioxid. Redox Signal. 11, 1603–1614. https://doi.org/10.1089/ars.2009.2536

Chiang, C.-H., Grauffel, C., Wu, L.-S., Kuo, P.-H., Doudeva, L.G., Lim, C., Shen, C.-K.J., Yuan, H.S., 2016. Structural analysis of disease-related TDP-43 D169G mutation: linking enhanced stability and caspase cleavage efficiency to protein accumulation. Sci Rep 6, 21581. https://doi.org/10.1038/srep21581

Chiu, A.Y., Zhai, P., Dal Canto, M.C., Peters, T.M., Kwon, Y.W., Prattis, S.M., Gurney, M.E., 1995. Age-dependent penetrance of disease in a transgenic mouse model of familial amyotrophic lateral sclerosis. Mol. Cell. Neurosci. 6, 349–362. https://doi.org/10.1006/mcne.1995.1027

Colombrita, C., Zennaro, E., Fallini, C., Weber, M., Sommacal, A., Buratti, E., Silani, V., Ratti, A., 2009. TDP-43 is recruited to stress granules in conditions of oxidative insult. Journal of Neurochemistry 111, 1051–1061. https://doi.org/10.1111/j.1471-4159.2009.06383.x

Comley, L.H., Nijssen, J., Frost-Nylen, J., Hedlund, E., 2016. Cross-disease comparison of amyotrophic lateral sclerosis and spinal muscular atrophy reveals conservation of

selective vulnerability but differential neuromuscular junction pathology. Journal of Comparative Neurology 524, 1424–1442. https://doi.org/10.1002/cne.23917

Corrado, L., Ratti, A., Gellera, C., Buratti, E., Castellotti, B., Carlomagno, Y., Ticozzi, N., Mazzini, L., Testa, L., Taroni, F., Baralle, F.E., Silani, V., D'Alfonso, S., 2009. High frequency of TARDBP gene mutations in Italian patients with amyotrophic lateral sclerosis. Human Mutation 30, 688–694. https://doi.org/10.1002/humu.20950

Correia, A.S., Patel, P., Dutta, K., Julien, J.-P., 2015. Inflammation Induces TDP-43 Mislocalization and Aggregation. PLoS One 10. https://doi.org/10.1371/journal.pone.0140248

Crain, J.M., Nikodemova, M., Watters, J.J., 2013. Microglia express distinct M1 and M2 phenotypic markers in the postnatal and adult central nervous system in male and female mice. Journal of Neuroscience Research 91, 1143–1151. https://doi.org/10.1002/jnr.23242

Crosio, C., Valle, C., Casciati, A., Iaccarino, C., Carrì, M.T., 2011. Astroglial Inhibition of NF-κB Does Not Ameliorate Disease Onset and Progression in a Mouse Model for Amyotrophic Lateral Sclerosis (ALS). PLoS One 6. https://doi.org/10.1371/journal.pone.0017187

D'Agostino, P.M., Gottfried-Blackmore, A., Anandasabapathy, N., Bulloch, K., 2012. Brain dendritic cells: biology and pathology. Acta Neuropathol 124, 599–614. https://doi.org/10.1007/s00401-012-1018-0

de Diego, R.P., Rodríguez-Gallego, C., 2014. Chapter 34 - Other TLR Pathway Defects, in: Sullivan, K.E., Stiehm, E.R. (Eds.), Stiehm's Immune Deficiencies. Academic Press, Amsterdam, pp. 687–710. https://doi.org/10.1016/B978-0-12-405546-9.00034-0

de Majo, M., Topp, S.D., Smith, B.N., Nishimura, A.L., Chen, H.-J., Gkazi, A.S., Miller, J., Wong, C.H., Vance, C., Baas, F., ten Asbroek, A.L.M.A., Kenna, K.P., Ticozzi, N., Redondo, A.G., Esteban-Pérez, J., Tiloca, C., Verde, F., Duga, S., Morrison, K.E., Shaw, P.J., Kirby, J., Turner, M.R., Talbot, K., Hardiman, O., Glass, J.D., de Belleroche, J., Gellera, C., Ratti, A., Al-Chalabi, A., Brown, R.H., Silani, V., Landers, J.E., Shaw, C.E., 2018. ALS-associated missense and nonsense TBK1 mutations can both cause loss of kinase function. Neurobiology of Aging 71, 266.e1-266.e10. https://doi.org/10.1016/j.neurobiolaging.2018.06.015

Delzor, A., Couratier, P., Boumédiène, F., Nicol, M., Druet-Cabanac, M., Paraf, F., Méjean, A., Ploux, O., Leleu, J.-P., Brient, L., Lengronne, M., Pichon, V., Combès, A.,

Abdellaoui, S.E., Bonneterre, V., Lagrange, E., Besson, G., Bicout, D.J., Boutonnat, J., Camu, W., Pageot, N., Juntas-Morales, R., Rigau, V., Masseret, E., Abadie, E., Preux, P.-M., Marin, B., 2014. Searching for a link between the L-BMAA neurotoxin and amyotrophic lateral sclerosis: a study protocol of the French BMAALS programme. BMJ Open 4, e005528. https://doi.org/10.1136/bmjopen-2014-005528

Deng, H., Gao, K., Jankovic, J., 2014. The role of FUS gene variants in neurodegenerative diseases. Nat Rev Neurol 10, 337–348. https://doi.org/10.1038/nrneurol.2014.78

Deng, H.-X., Shi, Y., Furukawa, Y., Zhai, H., Fu, R., Liu, E., Gorrie, G.H., Khan, M.S., Hung, W.-Y., Bigio, E.H., Lukas, T., Dal Canto, M.C., O'Halloran, T.V., Siddique, T., 2006. Conversion to the amyotrophic lateral sclerosis phenotype is associated with intermolecular linked insoluble aggregates of SOD1 in mitochondria. Proc. Natl. Acad. Sci. U.S.A. 103, 7142–7147. https://doi.org/10.1073/pnas.0602046103

Devoy, A., Kalmar, B., Stewart, M., Park, H., Burke, B., Noy, S.J., Redhead, Y., Humphrey, J., Lo, K., Jaeger, J., Mejia Maza, A., Sivakumar, P., Bertolin, C., Soraru, G., Plagnol, V., Greensmith, L., Acevedo Arozena, A., Isaacs, A.M., Davies, B., Fratta, P., Fisher, E.M.C., 2017. Humanized mutant FUS drives progressive motor neuron degeneration without aggregation in 'FUSDelta14' knockin mice. Brain 140, 2797–2805. https://doi.org/10.1093/brain/awx248

Diaper, D.C., Adachi, Y., Sutcliffe, B., Humphrey, D.M., Elliott, C.J.H., Stepto, A., Ludlow, Z.N., Vanden Broeck, L., Callaerts, P., Dermaut, B., Al-Chalabi, A., Shaw, C.E., Robinson, I.M., Hirth, F., 2013. Loss and gain of Drosophila TDP-43 impair synaptic efficacy and motor control leading to age-related neurodegeneration by loss-of-function phenotypes. Hum. Mol. Genet. 22, 1539–1557. https://doi.org/10.1093/hmg/ddt005

Ding, Q., Chaplin, J., Morris, M.J., Hilliard, M.A., Wolvetang, E., Ng, D.C.H., Noakes, P.G., 2021. TDP-43 Mutation Affects Stress Granule Dynamics in Differentiated NSC-34 Motoneuron-Like Cells. Frontiers in Cell and Developmental Biology 9.

Dirren, E., Aebischer, J., Rochat, C., Towne, C., Schneider, B., Aebischer, P., 2015. SOD1 silencing in motoneurons or glia rescues neuromuscular function in ALS mice. Annals of Clinical and Translational Neurology 2, 167–184. https://doi.org/10.1002/acn3.162

Dirren, E., Towne, C.L., Setola, V., Redmond, D.E., Schneider, B.L., Aebischer, P., 2014. Intracerebroventricular Injection of Adeno-Associated Virus 6 and 9 Vectors for Cell

Type–Specific Transgene Expression in the Spinal Cord. Human Gene Therapy 25, 109–120. https://doi.org/10.1089/hum.2013.021

DiSabato, D., Quan, N., Godbout, J.P., 2016. Neuroinflammation: The Devil is in the Details. J Neurochem 139, 136–153. https://doi.org/10.1111/jnc.13607

Dormann, D., Rodde, R., Edbauer, D., Bentmann, E., Fischer, I., Hruscha, A., Than, M.E., Mackenzie, I.R.A., Capell, A., Schmid, B., Neumann, M., Haass, C., 2010. ALS-associated fused in sarcoma (FUS) mutations disrupt Transportin-mediated nuclear import. The EMBO Journal 29, 2841–2857. https://doi.org/10.1038/emboj.2010.143

Dowell, R.D., 2011. The similarity of gene expression between human and mouse tissues. Genome Biology 12, 101. https://doi.org/10.1186/gb-2011-12-1-101

Dresselhaus, E.C., Meffert, M.K., 2019. Cellular Specificity of NF-κB Function in the Nervous System. Front. Immunol. 10. https://doi.org/10.3389/fimmu.2019.01043

Du, W., Hua, F., Li, X., Zhang, J., Li, S., Wang, Weichao, Zhou, J., Wang, Weimin, Liao, P., Yan, Y., Li, G., Wei, S., Grove, S., Vatan, L., Zgodziński, W., Majewski, M., Wallner, G., Chen, H., Kryczek, I., Fang, J.-Y., Zou, W., 2021. Loss of Optineurin Drives Cancer Immune Evasion via Palmitoylation-Dependent IFNGR1 Lysosomal Sorting and Degradation. Cancer Discovery 11, 1826–1843. https://doi.org/10.1158/2159-8290.CD-20-1571

Duan, L., Zaepfel, B.L., Aksenova, V., Dasso, M., Rothstein, J.D., Kalab, P., Hayes, L.R., 2022. Nuclear RNA binding regulates TDP-43 nuclear localization and passive nuclear export. Cell Reports 40, 111106. https://doi.org/10.1016/j.celrep.2022.111106

Dutta, K., Thammisetty, S.S., Boutej, H., Bareil, C., Julien, J.-P., 2020. Mitigation of ALS Pathology by Neuron-Specific Inhibition of Nuclear Factor Kappa B Signaling. J. Neurosci. 40, 5137–5154. https://doi.org/10.1523/JNEUROSCI.0536-20.2020

Ebnet, K., Brown, K.D., Siebenlist, U.K., Simon, M.M., Shaw, S., 1997. Borrelia burgdorferi activates nuclear factor-kappa B and is a potent inducer of chemokine and adhesion molecule gene expression in endothelial cells and fibroblasts. J. Immunol. 158, 3285–3292.

Ederle, H., Funk, C., Abou-Ajram, C., Hutten, S., Funk, E.B.E., Kehlenbach, R.H., Bailer, S.M., Dormann, D., 2018. Nuclear egress of TDP-43 and FUS occurs independently of Exportin-1/CRM1. Sci Rep 8. https://doi.org/10.1038/s41598-018-25007-5

Eleftherianos, I., More, K., Spivack, S., Paulin, E., Khojandi, A., Shukla, S., 2014. Nitric Oxide Levels Regulate the Immune Response of Drosophila melanogaster Reference

Laboratory Strains to Bacterial Infections. Infect Immun 82, 4169–4181. https://doi.org/10.1128/IAI.02318-14

Ellis, B.L., Hirsch, M.L., Barker, J.C., Connelly, J.P., Steininger, R.J., Porteus, M.H., 2013. A survey of ex vivo/in vitro transduction efficiency of mammalian primary cells and cell lines with Nine natural adeno-associated virus (AAV1-9) and one engineered adeno-associated virus serotype. Virology Journal 10, 74. https://doi.org/10.1186/1743-422X-10-74

Engelhardt, J.I., Tajti, J., Appel, S.H., 1993. Lymphocytic Infiltrates in the Spinal Cord in Amyotrophic Lateral Sclerosis. Arch Neurol 50, 30–36. https://doi.org/10.1001/archneur.1993.00540010026013

Estes, P.S., Boehringer, A., Zwick, R., Tang, J.E., Grigsby, B., Zarnescu, D.C., 2011. Wild-type and A315T mutant TDP-43 exert differential neurotoxicity in a Drosophila model of ALS. Human Molecular Genetics 20, 2308–2321. https://doi.org/10.1093/hmg/ddr124

Fakhoury, M., 2018. Microglia and Astrocytes in Alzheimer's Disease: Implications for Therapy. Curr Neuropharmacol 16, 508–518. https://doi.org/10.2174/1570159X15666170720095240

Fang, F., Kwee, L.C., Allen, K.D., Umbach, D.M., Ye, W., Watson, M., Keller, J., Oddone, E.Z., Sandler, D.P., Schmidt, S., Kamel, F., 2010. Association between blood lead and the risk of amyotrophic lateral sclerosis. Am. J. Epidemiol. 171, 1126–1133. https://doi.org/10.1093/aje/kwq063

Floare, M.-L., Allen, S.P., 2020. Why TDP-43? Why Not? Mechanisms of Metabolic Dysfunction in Amyotrophic Lateral Sclerosis. J Exp Neurosci 15, 2633105520957302. https://doi.org/10.1177/2633105520957302

Fomin, V., Richard, P., Hoque, M., Li, C., Gu, Z., Fissore-O'Leary, M., Tian, B., Prives, C., Manley, J.L., 2018. The C9ORF72 gene, implicated in ALS/FTD, encodes a protein that functions in control of endothelin and glutamate signaling. Molecular and Cellular Biology. https://doi.org/10.1128/MCB.00155-18

Frakes, A.E., Ferraiuolo, L., Haidet-Phillips, A.M., Schmelzer, L., Braun, L., Miranda, C.J., Ladner, K.J., Bevan, A.K., Foust, K.D., Godbout, J.P., Popovich, P.G., Guttridge, D.C., Kaspar, B.K., 2014. Microglia induce motor neuron death via the classical NF-κB pathway in amyotrophic lateral sclerosis. Neuron 81, 1009–1023. https://doi.org/10.1016/j.neuron.2014.01.013

François-Moutal, L., Perez-Miller, S., Scott, D.D., Miranda, V.G., Mollasalehi, N., Khanna, M., 2019. Structural Insights Into TDP-43 and Effects of Post-translational Modifications. Frontiers in Molecular Neuroscience 12.

Gargano, J.W., Martin, I., Bhandari, P., Grotewiel, M.S., 2005. Rapid iterative negative geotaxis (RING): a new method for assessing age-related locomotor decline in Drosophila. Exp Gerontol 40, 386–395. https://doi.org/10.1016/j.exger.2005.02.005

Geloso, M.C., Corvino, V., Marchese, E., Serrano, A., Michetti, F., D'Ambrosi, N., 2017. The Dual Role of Microglia in ALS: Mechanisms and Therapeutic Approaches. Front Aging Neurosci 9. https://doi.org/10.3389/fnagi.2017.00242

Gerbino, V., Kaunga, E., Ye, J., Canzio, D., O'Keeffe, S., Rudnick, N.D., Guarnieri, P., Lutz, C.M., Maniatis, T., 2020. The Loss of TBK1 Kinase Activity in Motor Neurons or in All Cell Types Differentially Impacts ALS Disease Progression in SOD1 Mice. Neuron 106, 789-805.e5. https://doi.org/10.1016/j.neuron.2020.03.005

Gerondakis, S., Siebenlist, U., 2010. Roles of the NF-κB Pathway in Lymphocyte Development and Function. Cold Spring Harb Perspect Biol 2, a000182. https://doi.org/10.1101/cshperspect.a000182

Ghosh, M., Yang, Y., Rothstein, J.D., Robinson, M.B., 2011. Nuclear Factor-κB Contributes to Neuron-Dependent Induction of Glutamate Transporter-1 Expression in Astrocytes. J. Neurosci. 31, 9159–9169. https://doi.org/10.1523/JNEUROSCI.0302-11.2011

Gilmore, T.D., Wolenski, F.S., 2012. NF-κB: where did it come from and why? Immunological Reviews 246, 14–35. https://doi.org/10.1111/j.1600-065X.2012.01096.x

Giovannoni, F., Quintana, F.J., 2020. The Role of Astrocytes in CNS Inflammation. Trends in Immunology 41, 805–819. https://doi.org/10.1016/j.it.2020.07.007

Gorgoni, B., Zhao, Y.-B., Krishnan, J., Stansfield, I., 2019. Destabilization of Eukaryote mRNAs by 5′ Proximal Stop Codons Can Occur Independently of the Nonsense-Mediated mRNA Decay Pathway. Cells 8, 800. https://doi.org/10.3390/cells8080800

Grassano, M., Brodini, G., Marco, G.D., Casale, F., Fuda, G., Salamone, P., Brunetti, M., Sbaiz, L., Gallone, S., Cugnasco, P., Bombaci, A., Vasta, R., Manera, U., Canosa, A., Moglia, C., Calvo, A., Traynor, B.J., Chio, A., 2022. Phenotype Analysis of Fused in Sarcoma Mutations in Amyotrophic Lateral Sclerosis. Neurology Genetics 8. https://doi.org/10.1212/NXG.0000000000200011

Green, K.M., Linsalata, A.E., Todd, P.K., 2016. RAN translation—what makes it run? Brain Res 1647, 30–42. https://doi.org/10.1016/j.brainres.2016.04.003

Guerrini, L., Molteni, A., Wirth, T., Kistler, B., Blasi, F., 1997. Glutamate-Dependent Activation of NF-κB During Mouse Cerebellum Development. J. Neurosci. 17, 6057–6063. https://doi.org/10.1523/JNEUROSCI.17-16-06057.1997

Gurney, M.E., Pu, H., Chiu, A.Y., Dal Canto, M.C., Polchow, C.Y., Alexander, D.D., Caliendo, J., Hentati, A., Kwon, Y.W., Deng, H.X., 1994. Motor neuron degeneration in mice that express a human Cu,Zn superoxide dismutase mutation. Science 264, 1772–1775. https://doi.org/10.1126/science.8209258

Guttenplan, K.A., Weigel, M.K., Adler, D.I., Couthouis, J., Liddelow, S.A., Gitler, A.D., Barres, B.A., 2020. Knockout of reactive astrocyte activating factors slows disease progression in an ALS mouse model. Nature Communications 11, 3753. https://doi.org/10.1038/s41467-020-17514-9

Hall, E.D., Oostveen, J.A., Gurney, M.E., 1998. Relationship of microglial and astrocytic activation to disease onset and progression in a transgenic model of familial ALS. Glia 23, 249–256. https://doi.org/10.1002/(SICI)1098-1136(199807)23:3<249::AID-GLIA7>3.0.CO;2-#

Halperin, J.J., Kaplan, G.P., Brazinsky, S., Tsai, T.F., Cheng, T., Ironside, A., Wu, P., Delfiner, J., Golightly, M., Brown, R.H., 1990. Immunologic reactivity against Borrelia burgdorferi in patients with motor neuron disease. Arch. Neurol. 47, 586–594.

Hänsel, Y., Ackerl, M., Stanek, G., 1995. [ALS-like sequelae in chronic neuroborreliosis]. Wien Med Wochenschr 145, 186–188.

Hassani, A., Corboy, J.R., Al-Salam, S., Khan, G., 2018. Epstein-Barr virus is present in the brain of most cases of multiple sclerosis and may engage more than just B cells. PLoS One 13, e0192109. https://doi.org/10.1371/journal.pone.0192109

Hatzipetros, T., Bogdanik, L.P., Tassinari, V.R., Kidd, J.D., Moreno, A.J., Davis, C., Osborne, M., Austin, A., Vieira, F.G., Lutz, C., Perrin, S., 2014. C57BL/6J congenic Prp-TDP43A315T mice develop progressive neurodegeneration in the myenteric plexus of the colon without exhibiting key features of ALS. Brain Research, RNA Metabolism 2013 1584, 59–72. https://doi.org/10.1016/j.brainres.2013.10.013

Hellerbrand, C., Jobin, C., Iimuro, Y., Licato, L., Sartor, R.B., Brenner, D.A., 1998. Inhibition of NFkappaB in activated rat hepatic stellate cells by proteasome inhibitors

and an IkappaB super-repressor. Hepatology 27, 1285–1295.
https://doi.org/10.1002/hep.510270514

Henkel, J.S., Beers, D.R., Siklós, L., Appel, S.H., 2006. The chemokine MCP-1 and the
dendritic and myeloid cells it attracts are increased in the mSOD1 mouse model of
ALS. Mol Cell Neurosci 31, 427–437. https://doi.org/10.1016/j.mcn.2005.10.016

Henkel, J.S., Beers, D.R., Zhao, W., Appel, S.H., 2009. Microglia in ALS: The Good, The
Bad, and The Resting. J Neuroimmune Pharmacol 4, 389–398.
https://doi.org/10.1007/s11481-009-9171-5

Herz, J., Johnson, K.R., McGavern, D.B., 2015. Therapeutic antiviral T cells
noncytopathically clear persistently infected microglia after conversion into antigen-
presenting cells. J Exp Med 212, 1153–1169. https://doi.org/10.1084/jem.20142047

Hetru, C., Hoffmann, J.A., 2009. NF-κB in the Immune Response of Drosophila. Cold Spring
Harb Perspect Biol 1. https://doi.org/10.1101/cshperspect.a000232

Hill, J.M., Zhao, Y., Clement, C., Neumann, D.M., Lukiw, W.J., 2009. HSV-1 infection of
human brain cells induces miRNA-146a and Alzheimer-type inflammatory signaling.
Neuroreport 20, 1500–1505. https://doi.org/10.1097/WNR.0b013e3283329c05

Huang, C., Zhou, H., Tong, J., Chen, H., Liu, Y.-J., Wang, D., Wei, X., Xia, X.-G., 2011.
FUS Transgenic Rats Develop the Phenotypes of Amyotrophic Lateral Sclerosis and
Frontotemporal Lobar Degeneration. PLOS Genetics 7, e1002011.
https://doi.org/10.1371/journal.pgen.1002011

Huisman, M.H.B., Seelen, M., de Jong, S.W., Dorresteijn, K.R.I.S., van Doormaal, P.T.C.,
van der Kooi, A.J., de Visser, M., Schelhaas, H.J., van den Berg, L.H., Veldink, J.H.,
2013. Lifetime physical activity and the risk of amyotrophic lateral sclerosis. J.
Neurol. Neurosurg. Psychiatry 84, 976–981. https://doi.org/10.1136/jnnp-2012-
304724

Ishigaki, S., Sobue, G., 2018. Importance of Functional Loss of FUS in FTLD/ALS. Front
Mol Biosci 5, 44. https://doi.org/10.3389/fmolb.2018.00044

Ito, Y., Ofengeim, D., Najafov, A., Das, S., Saberi, S., Li, Y., Hitomi, J., Zhu, H., Chen, H.,
Mayo, L., Geng, J., Amin, P., DeWitt, J.P., Mookhtiar, A.K., Florez, M., Ouchida,
A.T., Fan, J., Pasparakis, M., Kelliher, M.A., Ravits, J., Yuan, J., 2016. RIPK1
mediates axonal degeneration by promoting inflammation and necroptosis in ALS.
Science 353, 603–608. https://doi.org/10.1126/science.aaf6803

Jäckel, S., Summerer, A.K., Thömmes, C.M., Pan, X., Voigt, A., Schulz, J.B., Rasse, T.M., Dormann, D., Haass, C., Kahle, P.J., 2015. Nuclear import factor transportin and arginine methyltransferase 1 modify FUS neurotoxicity in Drosophila. Neurobiology of Disease 74, 76–88. https://doi.org/10.1016/j.nbd.2014.11.003

Jara, J.H., Gautam, M., Kocak, N., Xie, E.F., Mao, Q., Bigio, E.H., Özdinler, P.H., 2019. MCP1-CCR2 and neuroinflammation in the ALS motor cortex with TDP-43 pathology. Journal of Neuroinflammation 16, 196. https://doi.org/10.1186/s12974-019-1589-y

Jer-Cherng Chang, David B. Morton*, 2017. Drosophila lines with mutant and wild type human TDP-43 replacing the endogenous gene reveals phosphorylation and ubiquitination in mutant lines in the absence of viability or lifespan defects. https://doi.org/10.1371/journal.pone.0180828

Jin, M., Günther, R., Akgün, K., Hermann, A., Ziemssen, T., 2020. Peripheral proinflammatory Th1/Th17 immune cell shift is linked to disease severity in amyotrophic lateral sclerosis. Scientific Reports 10, 5941. https://doi.org/10.1038/s41598-020-62756-8

Jurga, A.M., Paleczna, M., Kuter, K.Z., 2020. Overview of General and Discriminating Markers of Differential Microglia Phenotypes. Frontiers in Cellular Neuroscience 14.

Kabashi, E., Bercier, V., Lissouba, A., Liao, M., Brustein, E., Rouleau, G.A., Drapeau, P., 2011. FUS and TARDBP but Not SOD1 Interact in Genetic Models of Amyotrophic Lateral Sclerosis. PLOS Genetics 7, e1002214. https://doi.org/10.1371/journal.pgen.1002214

Kabashi, E., Valdmanis, P.N., Dion, P., Spiegelman, D., McConkey, B.J., Velde, C.V., Bouchard, J.-P., Lacomblez, L., Pochigaeva, K., Salachas, F., Pradat, P.-F., Camu, W., Meininger, V., Dupre, N., Rouleau, G.A., 2008. TARDBP mutations in individuals with sporadic and familial amyotrophic lateral sclerosis. Nat Genet 40, 572–574. https://doi.org/10.1038/ng.132

Källstig, E., McCabe, B.D., Schneider, B.L., 2021. The Links between ALS and NF-κB. International Journal of Molecular Sciences 22, 3875. https://doi.org/10.3390/ijms22083875

Kamada, M., Izumi, Y., Ayaki, T., Nakamura, M., Kagawa, S., Kudo, E., Sako, W., Maruyama, H., Nishida, Y., Kawakami, H., Ito, H., Kaji, R., 2014. Clinicopathologic

features of autosomal recessive amyotrophic lateral sclerosis associated with optineurin mutation. Neuropathology 34, 64–70. https://doi.org/10.1111/neup.12051

Kashyap, S., Sarkar, M., 2010. Mycoplasma pneumonia: Clinical features and management. Lung India 27, 75–85. https://doi.org/10.4103/0970-2113.63611

Kassed, C.A., Herkenham, M., 2004. NF-κB p50-deficient mice show reduced anxiety-like behaviors in tests of exploratory drive and anxiety. Behavioural Brain Research 154, 577–584. https://doi.org/10.1016/j.bbr.2004.03.026

Kaufman, T.C., 2017. A Short History and Description of Drosophila melanogaster Classical Genetics: Chromosome Aberrations, Forward Genetic Screens, and the Nature of Mutations. Genetics 206, 665–689. https://doi.org/10.1534/genetics.117.199950

Kaur, S.J., McKeown, S.R., Rashid, S., 2016. Mutant SOD1 mediated pathogenesis of Amyotrophic Lateral Sclerosis. Gene 577, 109–118. https://doi.org/10.1016/j.gene.2015.11.049

Khalfallah, Y., Kuta, R., Grasmuck, C., Prat, A., Durham, H.D., Vande Velde, C., 2018. TDP-43 regulation of stress granule dynamics in neurodegenerative disease-relevant cell types. Scientific Reports 8, 7551. https://doi.org/10.1038/s41598-018-25767-0

Khor, S., Cai, D., 2020. Control of lifespan and survival by Drosophila NF-κB signaling through neuroendocrine cells and neuroblasts. Aging (Albany NY) 12, 24604–24622. https://doi.org/10.18632/aging.104196

Kim, C.-H., Paik, D., Rus, F., Silverman, N., 2014. The Caspase-8 Homolog Dredd Cleaves Imd and Relish but Is Not Inhibited by p35. J Biol Chem 289, 20092–20101. https://doi.org/10.1074/jbc.M113.544841

Kim, S.H., Shanware, N.P., Bowler, M.J., Tibbetts, R.S., 2010. Amyotrophic Lateral Sclerosis-associated Proteins TDP-43 and FUS/TLS Function in a Common Biochemical Complex to Co-regulate HDAC6 mRNA*,. Journal of Biological Chemistry 285, 34097–34105. https://doi.org/10.1074/jbc.M110.154831

Kino, Y., Washizu, C., Kurosawa, M., Yamada, M., Miyazaki, H., Akagi, T., Hashikawa, T., Doi, H., Takumi, T., Hicks, G.G., Hattori, N., Shimogori, T., Nukina, N., 2015. FUS/TLS deficiency causes behavioral and pathological abnormalities distinct from amyotrophic lateral sclerosis. Acta Neuropathologica Communications 3, 24. https://doi.org/10.1186/s40478-015-0202-6

Koski, L., Ronnevi, C., Berntsson, E., Wärmländer, S.K.T.S., Roos, P.M., 2021. Metals in ALS TDP-43 Pathology. Int J Mol Sci 22, 12193. https://doi.org/10.3390/ijms222212193

Kounatidis, I., Chtarbanova, S., Cao, Y., Hayne, M., Jayanth, D., Ganetzky, B., Ligoxygakis, P., 2017. NF-κB Immunity in the Brain Determines Fly Lifespan in Healthy Aging and Age-Related Neurodegeneration. Cell Rep 19, 836–848. https://doi.org/10.1016/j.celrep.2017.04.007

Kratsovnik, E., Bromberg, Y., Sperling, O., Zoref-Shani, E., 2005. Oxidative stress activates transcription factor NF-kB-mediated protective signaling in primary rat neuronal cultures. J Mol Neurosci 26, 27–32. https://doi.org/10.1385/jmn:26:1:027

Kuhle, J., Lindberg, R.L.P., Regeniter, A., Mehling, M., Steck, A.J., Kappos, L., Czaplinski, A., 2009. Increased levels of inflammatory chemokines in amyotrophic lateral sclerosis. Eur J Neurol 16, 771–774. https://doi.org/10.1111/j.1468-1331.2009.02560.x

Kumar, D.R., Aslinia, F., Yale, S.H., Mazza, J.J., 2011. Jean-Martin Charcot: The Father of Neurology. Clinical Medicine & Research 9, 46. https://doi.org/10.3121/cmr.2009.883

Kuroda, M., Sok, J., Webb, L., Baechtold, H., Urano, F., Yin, Y., Chung, P., de Rooij, D.G., Akhmedov, A., Ashley, T., Ron, D., 2000. Male sterility and enhanced radiation sensitivity in TLS−/− mice. The EMBO Journal 19, 453–462. https://doi.org/10.1093/emboj/19.3.453

Kyrargyri, V., Vega-Flores, G., Gruart, A., Delgado-García, J.M., Probert, L., 2015. Differential contributions of microglial and neuronal IKKβ to synaptic plasticity and associative learning in alert behaving mice. Glia 63, 549–566. https://doi.org/10.1002/glia.22756

Lanson, N.A., Jr, Maltare, A., King, H., Smith, R., Kim, J.H., Taylor, J.P., Lloyd, T.E., Pandey, U.B., 2011. A Drosophila model of FUS-related neurodegeneration reveals genetic interaction between FUS and TDP-43. Human Molecular Genetics 20, 2510–2523. https://doi.org/10.1093/hmg/ddr150

Lanson, N.A., Pandey, U.B., 2012. FUS-related proteinopathies: Lessons from animal models. Brain Research, RNA-Binding Proteins in Neurological Disease 1462, 44–60. https://doi.org/10.1016/j.brainres.2012.01.039

Lee, Shinrye, Kim, S., Kang, H.-Y., Lim, H.R., Kwon, Y., Jo, M., Jeon, Y.-M., Kim, S.R., Kim, K., Ha, C.M., Lee, Seongsoo, Kim, H.-J., 2020. The overexpression of TDP-43 in astrocytes causes neurodegeneration via a PTP1B-mediated inflammatory response. J Neuroinflammation 17. https://doi.org/10.1186/s12974-020-01963-6

Li, Y., Ray, P., Rao, E.J., Shi, C., Guo, W., Chen, X., Woodruff, E.A., Fushimi, K., Wu, J.Y., 2010. A Drosophila model for TDP-43 proteinopathy. Proceedings of the National Academy of Sciences 107, 3169–3174. https://doi.org/10.1073/pnas.0913602107

Liddelow, S.A., Barres, B.A., 2017. Reactive Astrocytes: Production, Function, and Therapeutic Potential. Immunity 46, 957–967. https://doi.org/10.1016/j.immuni.2017.06.006

Liddelow, S.A., Guttenplan, K.A., Clarke, L.E., Bennett, F.C., Bohlen, C.J., Schirmer, L., Bennett, M.L., Münch, A.E., Chung, W.-S., Peterson, T.C., Wilton, D.K., Frouin, A., Napier, B.A., Panicker, N., Kumar, M., Buckwalter, M.S., Rowitch, D.H., Dawson, V.L., Dawson, T.M., Stevens, B., Barres, B.A., 2017. Neurotoxic reactive astrocytes are induced by activated microglia. Nature 541, 481–487. https://doi.org/10.1038/nature21029

Lin, Y., Jamison, S., Lin, W., 2012. Interferon-γ Activates Nuclear Factor-κ B in Oligodendrocytes through a Process Mediated by the Unfolded Protein Response. PLoS One 7, e36408. https://doi.org/10.1371/journal.pone.0036408

Lindsley, D.L., Roote, J., Kennison, J.A., 2013. Anent the Genomics of Spermatogenesis in Drosophila melanogaster. PLOS ONE 8, e55915. https://doi.org/10.1371/journal.pone.0055915

Liu, J., Gao, L., Zang, D., 2015. Elevated Levels of IFN-γ in CSF and Serum of Patients with Amyotrophic Lateral Sclerosis. PLoS One 10, e0136937. https://doi.org/10.1371/journal.pone.0136937

Liu, J., Wang, F., 2017. Role of Neuroinflammation in Amyotrophic Lateral Sclerosis: Cellular Mechanisms and Therapeutic Implications. Front Immunol 8, 1005. https://doi.org/10.3389/fimmu.2017.01005

Liu, T., Zhang, L., Joo, D., Sun, S.-C., 2017. NF-κB signaling in inflammation. Signal Transduction and Targeted Therapy 2, 1–9. https://doi.org/10.1038/sigtrans.2017.23

Liu, X., Berry, C.T., Ruthel, G., Madara, J.J., MacGillivray, K., Gray, C.M., Madge, L.A., McCorkell, K.A., Beiting, D.P., Hershberg, U., May, M.J., Freedman, B.D., 2016. T Cell Receptor-induced Nuclear Factor κB (NF-κB) Signaling and Transcriptional

Activation Are Regulated by STIM1- and Orai1-mediated Calcium Entry *. Journal of Biological Chemistry 291, 8440–8452. https://doi.org/10.1074/jbc.M115.713008

Liu, Y., Gordesky-Gold, B., Leney-Greene, M., Weinbren, N.L., Tudor, M., Cherry, S., 2018. Inflammation-induced STING-dependent autophagy restricts Zika virus infection in the Drosophila brain. Cell Host Microbe 24, 57-68.e3. https://doi.org/10.1016/j.chom.2018.05.022

Liu, Y.-C., Chiang, P.-M., Tsai, K.-J., 2013. Disease Animal Models of TDP-43 Proteinopathy and Their Pre-Clinical Applications. Int J Mol Sci 14, 20079–20111. https://doi.org/10.3390/ijms141020079

Liu, Y.-Z., Wang, Y.-X., Jiang, C.-L., 2017. Inflammation: The Common Pathway of Stress-Related Diseases. Front Hum Neurosci 11. https://doi.org/10.3389/fnhum.2017.00316

Liu-Yesucevitz, L., Bilgutay, A., Zhang, Y.-J., Vanderwyde, T., Citro, A., Mehta, T., Zaarur, N., McKee, A., Bowser, R., Sherman, M., Petrucelli, L., Wolozin, B., 2010. Tar DNA Binding Protein-43 (TDP-43) Associates with Stress Granules: Analysis of Cultured Cells and Pathological Brain Tissue. PLOS ONE 5, e13250. https://doi.org/10.1371/journal.pone.0013250

Logroscino, G., Traynor, B.J., Hardiman, O., Chiò, A., Mitchell, D., Swingler, R.J., Millul, A., Benn, E., Beghi, E., EURALS, 2010. Incidence of amyotrophic lateral sclerosis in Europe. J. Neurol. Neurosurg. Psychiatry 81, 385–390. https://doi.org/10.1136/jnnp.2009.183525

Logunov, D.I., Shchebliakov, D.V., Zubkova, O.V., Shmarov, M.M., Rakovskaia, I.V., Gintsburg, L.A., Gudkov, A.V., Naroditskiĭ, B.S., 2009. [Lipid-associated membrane lipopeptides of M. arginini activate NF-kB by interacting with TLR2/1, TLR2/6, and TLR2/CD14]. Mol. Gen. Mikrobiol. Virusol. 25–28.

López-Erauskin, J., Tadokoro, T., Baughn, M.W., Myers, B., McAlonis-Downes, M., Chillon-Marinas, C., Asiaban, J.N., Artates, J., Bui, A.T., Vetto, A.P., Lee, S.K., Le, A.V., Sun, Y., Jambeau, M., Boubaker, J., Swing, D., Qiu, J., Hicks, G.G., Ouyang, Z., Fu, X.-D., Tessarollo, L., Ling, S.-C., Parone, P.A., Shaw, C.E., Marsala, M., Lagier-Tourenne, C., Cleveland, D.W., Cruz, S.D., 2018. ALS/FTD-Linked Mutation in FUS Suppresses Intra-axonal Protein Synthesis and Drives Disease Without Nuclear Loss-of-Function of FUS. Neuron 100, 816-830.e7. https://doi.org/10.1016/j.neuron.2018.09.044

Lutz, C., 2018. Mouse models of ALS: Past, present and future. Brain Research, RNA Metabolism in Neurological Disease 2018 1693, 1–10. https://doi.org/10.1016/j.brainres.2018.03.024

Maes, M.E., Colombo, G., Schulz, R., Siegert, S., 2019. Targeting microglia with lentivirus and AAV: Recent advances and remaining challenges. Neurosci Lett 707, 134310. https://doi.org/10.1016/j.neulet.2019.134310

Maier, A., Deigendesch, N., Müller, K., Weishaupt, J.H., Krannich, A., Röhle, R., Meissner, F., Molawi, K., Münch, C., Holm, T., Meyer, R., Meyer, T., Zychlinsky, A., 2015. Interleukin-1 Antagonist Anakinra in Amyotrophic Lateral Sclerosis--A Pilot Study. PLoS One 10, e0139684. https://doi.org/10.1371/journal.pone.0139684

Markovinovic, A., Cimbro, R., Ljutic, T., Kriz, J., Rogelj, B., Munitic, I., 2017. Optineurin in amyotrophic lateral sclerosis: Multifunctional adaptor protein at the crossroads of different neuroprotective mechanisms. Prog. Neurobiol. 154, 1–20. https://doi.org/10.1016/j.pneurobio.2017.04.005

Martorana, F., Foti, M., Virtuoso, A., Gaglio, D., Aprea, F., Latronico, T., Rossano, R., Riccio, P., Papa, M., Alberghina, L., Colangelo, A.M., 2019. Differential Modulation of NF-κB in Neurons and Astrocytes Underlies Neuroprotection and Antigliosis Activity of Natural Antioxidant Molecules [WWW Document]. Oxidative Medicine and Cellular Longevity. https://doi.org/10.1155/2019/8056904

Masaki, K., Sonobe, Y., Ghadge, G., Pytel, P., Roos, R.P., 2019. TDP-43 proteinopathy in Theiler's murine encephalomyelitis virus infection. PLOS Pathogens 15, e1007574. https://doi.org/10.1371/journal.ppat.1007574

Mathiesen, S.N., Lock, J.L., Schoderboeck, L., Abraham, W.C., Hughes, S.M., 2020. CNS Transduction Benefits of AAV-PHP.eB over AAV9 Are Dependent on Administration Route and Mouse Strain. Molecular Therapy - Methods & Clinical Development 19, 447–458. https://doi.org/10.1016/j.omtm.2020.10.011

McCambridge, M., Stinson, M.J., 2020. Advances in chronic traumatic encephalopathy. JAAPA 33, 39–42. https://doi.org/10.1097/01.JAA.0000654008.48462.01

McCauley, M.E., O'Rourke, J.G., Yáñez, A., Markman, J.L., Ho, R., Wang, X., Chen, S., Lall, D., Jin, M., Muhammad, A.K.M.G., Bell, S., Landeros, J., Valencia, V., Harms, M., Arditi, M., Jefferies, C., Baloh, R.H., 2020. C9orf72 in myeloid cells suppresses STING-induced inflammation. Nature 585, 96–101. https://doi.org/10.1038/s41586-020-2625-x

Meffert, M.K., Baltimore, D., 2005. Physiological functions for brain NF-kappaB. Trends Neurosci. 28, 37–43. https://doi.org/10.1016/j.tins.2004.11.002

Meffert, M.K., Chang, J.M., Wiltgen, B.J., Fanselow, M.S., Baltimore, D., 2003. NF-kappa B functions in synaptic signaling and behavior. Nat. Neurosci. 6, 1072–1078. https://doi.org/10.1038/nn1110

Mejzini, R., Flynn, L.L., Pitout, I.L., Fletcher, S., Wilton, S.D., Akkari, P.A., 2019. ALS Genetics, Mechanisms, and Therapeutics: Where Are We Now? Front Neurosci 13, 1310. https://doi.org/10.3389/fnins.2019.01310

Menon, P., Vucic, S., 2021. The Upper Motor Neuron—Improved Knowledge from ALS and Related Clinical Disorders. Brain Sci 11, 958. https://doi.org/10.3390/brainsci11080958

Mettang, M., Reichel, S.N., Lattke, M., Palmer, A., Abaei, A., Rasche, V., Huber-Lang, M., Baumann, B., Wirth, T., 2018. IKK2/NF-κB signaling protects neurons after traumatic brain injury. FASEB J 32, 1916–1932. https://doi.org/10.1096/fj.201700826R

Miller, R.G., Block, G., Katz, J.S., Barohn, R.J., Gopalakrishnan, V., Cudkowicz, M., Zhang, J.R., McGrath, M.S., Ludington, E., Appel, S.H., Azhir, A., 2015. Randomized phase 2 trial of NP001–a novel immune regulator: Safety and early efficacy in ALS. Neurol Neuroimmunol Neuroinflamm 2, e100. https://doi.org/10.1212/NXI.0000000000000100

Miller, S.C., Huang, R., Sakamuru, S., Shukla, S.J., Attene-Ramos, M.S., Shinn, P., Van Leer, D., Leister, W., Austin, C.P., Xia, M., 2010. Identification of Known Drugs that Act as Inhibitors of NF-κB Signaling and their Mechanism of Action. Biochem Pharmacol 79, 1272–1280. https://doi.org/10.1016/j.bcp.2009.12.021

Miller, T.M., Cudkowicz, M.E., Genge, A., Shaw, P.J., Sobue, G., Bucelli, R.C., Chiò, A., Van Damme, P., Ludolph, A.C., Glass, J.D., Andrews, J.A., Babu, S., Benatar, M., McDermott, C.J., Cochrane, T., Chary, S., Chew, S., Zhu, H., Wu, F., Nestorov, I., Graham, D., Sun, P., McNeill, M., Fanning, L., Ferguson, T.A., Fradette, S., 2022. Trial of Antisense Oligonucleotide Tofersen for SOD1 ALS. New England Journal of Medicine 387, 1099–1110. https://doi.org/10.1056/NEJMoa2204705

Mishra, P.-S., Dhull, D.K., Nalini, A., Vijayalakshmi, K., Sathyaprabha, T.N., Alladi, P.A., Raju, T.R., 2016. Astroglia acquires a toxic neuroinflammatory role in response to the

cerebrospinal fluid from amyotrophic lateral sclerosis patients. Journal of
Neuroinflammation 13, 212. https://doi.org/10.1186/s12974-016-0698-0

Mitchell, J.C., McGoldrick, P., Vance, C., Hortobagyi, T., Sreedharan, J., Rogelj, B., Tudor,
E.L., Smith, B.N., Klasen, C., Miller, C.C.J., Cooper, J.D., Greensmith, L., Shaw,
C.E., 2013. Overexpression of human wild-type FUS causes progressive motor
neuron degeneration in an age- and dose-dependent fashion. Acta Neuropathol 125,
273–288. https://doi.org/10.1007/s00401-012-1043-z

Mizwicki, M.T., Fiala, M., Magpantay, L., Aziz, N., Sayre, J., Liu, G., Siani, A., Chan, D.,
Martinez-Maza, O., Chattopadhyay, M., Cava, A.L., 2012. Tocilizumab attenuates
inflammation in ALS patients through inhibition of IL6 receptor signaling. Am J
Neurodegener Dis 1, 305–315.

Morgan, S., Orrell, R.W., 2016. Pathogenesis of amyotrophic lateral sclerosis. Br. Med. Bull.
119, 87–98. https://doi.org/10.1093/bmb/ldw026

Morgan, T.H., 1910. SEX LIMITED INHERITANCE IN DROSOPHILA. Science 32, 120–
122. https://doi.org/10.1126/science.32.812.120

Morris, M.C., Gilliam, E.A., Li, L., 2015. Innate Immune Programing by Endotoxin and Its
Pathological Consequences. Front Immunol 5.
https://doi.org/10.3389/fimmu.2014.00680

Nakaya, T., Maragkakis, M., 2018. Amyotrophic Lateral Sclerosis associated FUS mutation
shortens mitochondria and induces neurotoxicity. Sci Rep 8, 15575.
https://doi.org/10.1038/s41598-018-33964-0

Nguyen, H.P., Van Broeckhoven, C., van der Zee, J., 2018. ALS Genes in the Genomic Era
and their Implications for FTD. Trends in Genetics 34, 404–423.
https://doi.org/10.1016/j.tig.2018.03.001

Nicolson, G.L., 2008. Chronic Bacterial and Viral Infections in Neurodegenerative and
Neurobehavioral Diseases. Lab Med 39, 291–299.
https://doi.org/10.1309/96M3BWYP42L11BFU

Nicolson, G.L., Nasralla, M.Y., Haier, J., Pomfret, J., 2002. High frequency of systemic
mycoplasmal infections in Gulf War veterans and civilians with Amyotrophic Lateral
Sclerosis (ALS). J Clin Neurosci 9, 525–529.

Niu, C., Zhang, J., Gao, F., Yang, L., Jia, M., Zhu, H., Gong, W., 2012. FUS-
NLS/Transportin 1 Complex Structure Provides Insights into the Nuclear Targeting

Mechanism of FUS and the Implications in ALS. PLOS ONE 7, e47056.
https://doi.org/10.1371/journal.pone.0047056

Nivon, M., Fort, L., Muller, P., Richet, E., Simon, S., Guey, B., Fournier, M., Arrigo, A.-P.,
Hetz, C., Atkin, J.D., Kretz-Remy, C., 2016. NFκB is a central regulator of protein
quality control in response to protein aggregation stresses via autophagy modulation.
MBoC 27, 1712–1727. https://doi.org/10.1091/mbc.e15-12-0835

Nolan, M., Talbot, K., Ansorge, O., 2016. Pathogenesis of FUS-associated ALS and FTD:
insights from rodent models. Acta Neuropathologica Communications 4, 99.
https://doi.org/10.1186/s40478-016-0358-8

Nonaka, M., Chen, X.H., Pierce, J.E., Leoni, M.J., McIntosh, T.K., Wolf, J.A., Smith, D.H.,
1999. Prolonged activation of NF-kappaB following traumatic brain injury in rats. J.
Neurotrauma 16, 1023–1034. https://doi.org/10.1089/neu.1999.16.1023

Oeckinghaus, A., Ghosh, S., 2009. The NF-κB Family of Transcription Factors and Its
Regulation. Cold Spring Harb Perspect Biol 1.
https://doi.org/10.1101/cshperspect.a000034

Oikawa, K., Odero, G.L., Platt, E., Neuendorff, M., Hatherell, A., Bernstein, M.J., Albensi,
B.C., 2012. NF-κB p50 subunit knockout impairs late LTP and alters long term
memory in the mouse hippocampus. BMC Neurosci 13, 45.
https://doi.org/10.1186/1471-2202-13-45

O'Rourke, J.G., Bogdanik, L., Yáñez, A., Lall, D., Wolf, A.J., Muhammad, A.K.M.G., Ho,
R., Carmona, S., Vit, J.P., Zarrow, J., Kim, K.J., Bell, S., Harms, M.B., Miller, T.M.,
Dangler, C.A., Underhill, D.M., Goodridge, H.S., Lutz, C.M., Baloh, R.H., 2016.
C9orf72 is required for proper macrophage and microglial function in mice. Science
351, 1324–1329. https://doi.org/10.1126/science.aaf1064

Oskarsson, B., Horton, D.K., Mitsumoto, H., 2015. Potential Environmental Factors in
Amyotrophic Lateral Sclerosis. Neurol Clin 33, 877–888.
https://doi.org/10.1016/j.ncl.2015.07.009

Otsmane, B., Aebischer, J., Moumen, A., Raoul, C., 2014. Cerebrospinal fluid-targeted
delivery of neutralizing anti-IFNγ antibody delays motor decline in an ALS mouse
model. NeuroReport 25, 49–54. https://doi.org/10.1097/WNR.0000000000000043

Ouali Alami, N., Schurr, C., Olde Heuvel, F., Tang, L., Li, Q., Tasdogan, A., Kimbara, A.,
Nettekoven, M., Ottaviani, G., Raposo, C., Röver, S., Rogers-Evans, M.,
Rothenhäusler, B., Ullmer, C., Fingerle, J., Grether, U., Knuesel, I., Boeckers, T.M.,

Ludolph, A., Wirth, T., Roselli, F., Baumann, B., 2018. NF-κB activation in astrocytes drives a stage-specific beneficial neuroimmunological response in ALS. EMBO J 37. https://doi.org/10.15252/embj.201798697

Paganoni, S., Macklin, E.A., Hendrix, S., Berry, J.D., Elliott, M.A., Maiser, S., Karam, C., Caress, J.B., Owegi, M.A., Quick, A., Wymer, J., Goutman, S.A., Heitzman, D., Heiman-Patterson, T., Jackson, C.E., Quinn, C., Rothstein, J.D., Kasarskis, E.J., Katz, J., Jenkins, L., Ladha, S., Miller, T.M., Scelsa, S.N., Vu, T.H., Fournier, C.N., Glass, J.D., Johnson, K.M., Swenson, A., Goyal, N.A., Pattee, G.L., Andres, P.L., Babu, S., Chase, M., Dagostino, D., Dickson, S.P., Ellison, N., Hall, M., Hendrix, K., Kittle, G., McGovern, M., Ostrow, J., Pothier, L., Randall, R., Shefner, J.M., Sherman, A.V., Tustison, E., Vigneswaran, P., Walker, J., Yu, H., Chan, J., Wittes, J., Cohen, J., Klee, J., Leslie, K., Tanzi, R.E., Gilbert, W., Yeramian, P.D., Schoenfeld, D., Cudkowicz, M.E., 2020. Trial of Sodium Phenylbutyrate-Taurursodiol for Amyotrophic Lateral Sclerosis. N Engl J Med 383, 919–930. https://doi.org/10.1056/NEJMoa1916945

Phifer-Rixey, M., Nachman, M.W., 2015. Insights into mammalian biology from the wild house mouse Mus musculus. eLife 4, e05959. https://doi.org/10.7554/eLife.05959

Picher-Martel, V., Dutta, K., Phaneuf, D., Sobue, G., Julien, J.-P., 2015. Ubiquilin-2 drives NF-κB activity and cytosolic TDP-43 aggregation in neuronal cells. Molecular Brain 8, 71. https://doi.org/10.1186/s13041-015-0162-6

Poloni, M., Facchetti, D., Mai, R., Micheli, A., Agnoletti, L., Francolini, G., Mora, G., Camana, C., Mazzini, L., Bachetti, T., 2000. Circulating levels of tumour necrosis factor-α and its soluble receptors are increased in the blood of patients with amyotrophic lateral sclerosis. Neuroscience Letters 287, 211–214. https://doi.org/10.1016/S0304-3940(00)01177-0

Polymenidou, M., Lagier-Tourenne, C., Hutt, K.R., Huelga, S.C., Moran, J., Liang, T.Y., Ling, S.-C., Sun, E., Wancewicz, E., Mazur, C., Kordasiewicz, H., Sedaghat, Y., Donohue, J.P., Shiue, L., Bennett, C.F., Yeo, G.W., Cleveland, D.W., 2011. Long pre-mRNA depletion and RNA missplicing contribute to neuronal vulnerability from loss of TDP-43. Nat Neurosci 14, 459–468. https://doi.org/10.1038/nn.2779

Pomerantz, J.L., Baltimore, D., 1999. NF-kappaB activation by a signaling complex containing TRAF2, TANK and TBK1, a novel IKK-related kinase. EMBO J 18, 6694–6704. https://doi.org/10.1093/emboj/18.23.6694

Ponath, G., Park, C., Pitt, D., 2018. The Role of Astrocytes in Multiple Sclerosis. Frontiers in Immunology 9. https://doi.org/10.3389/fimmu.2018.00217

Pozniak, P.D., White, M.K., Khalili, K., 2014. TNF-α/NF-κB signaling in the CNS: possible connection to EPHB2. J Neuroimmune Pharmacol 9, 133–141. https://doi.org/10.1007/s11481-013-9517-x

Prell, T., Lautenschläger, J., Weidemann, L., Ruhmer, J., Witte, O.W., Grosskreutz, J., 2014. Endoplasmic reticulum stress is accompanied by activation of NF-κB in amyotrophic lateral sclerosis. Journal of Neuroimmunology 270, 29–36. https://doi.org/10.1016/j.jneuroim.2014.03.005

Prinz, M., Priller, J., 2017. The role of peripheral immune cells in the CNS in steady state and disease. Nat Neurosci 20, 136–144. https://doi.org/10.1038/nn.4475

Qin, L., Wu, X., Block, M.L., Liu, Y., Breese, G.R., Hong, J.-S., Knapp, D.J., Crews, F.T., 2007. Systemic LPS causes chronic neuroinflammation and progressive neurodegeneration. Glia 55, 453–462. https://doi.org/10.1002/glia.20467

Qiu, H., Lee, S., Shang, Y., Wang, W.-Y., Au, K.F., Kamiya, S., Barmada, S.J., Finkbeiner, S., Lui, H., Carlton, C.E., Tang, A.A., Oldham, M.C., Wang, H., Shorter, J., Filiano, A.J., Roberson, E.D., Tourtellotte, W.G., Chen, B., Tsai, L.-H., Huang, E.J., 2014. ALS-associated mutation FUS-R521C causes DNA damage and RNA splicing defects. J. Clin. Invest. 124, 981–999. https://doi.org/10.1172/JCI72723

Raoul, C., Estévez, A.G., Nishimune, H., Cleveland, D.W., deLapeyrière, O., Henderson, C.E., Haase, G., Pettmann, B., 2002. Motoneuron Death Triggered by a Specific Pathway Downstream of Fas: Potentiation by ALS-Linked SOD1 Mutations. Neuron 35, 1067–1083. https://doi.org/10.1016/S0896-6273(02)00905-4

Rath, D., Amlinger, L., Rath, A., Lundgren, M., 2015. The CRISPR-Cas immune system: Biology, mechanisms and applications. Biochimie, Special Issue: Regulatory RNAs 117, 119–128. https://doi.org/10.1016/j.biochi.2015.03.025

Redman, M., King, A., Watson, C., King, D., 2016. What is CRISPR/Cas9? Arch Dis Child Educ Pract Ed 101, 213–215. https://doi.org/10.1136/archdischild-2016-310459

Renton, A.E., Chiò, A., Traynor, B.J., 2014. State of play in amyotrophic lateral sclerosis genetics. Nat. Neurosci. 17, 17–23. https://doi.org/10.1038/nn.3584

Rinkenbaugh, A.L., Baldwin, A.S., 2016. The NF-κB Pathway and Cancer Stem Cells. Cells 5. https://doi.org/10.3390/cells5020016

Ripps, M.E., Huntley, G.W., Hof, P.R., Morrison, J.H., Gordon, J.W., 1995. Transgenic mice expressing an altered murine superoxide dismutase gene provide an animal model of amyotrophic lateral sclerosis. Proc Natl Acad Sci U S A 92, 689–693. https://doi.org/10.1073/pnas.92.3.689

Rochat, C., Bernard-Marissal, N., Pradervand, S., Perrin, F.E., Raoul, C., Aebischer, P., Schneider, B.L., 2021. Expression of a miRNA targeting mutated SOD1 in astrocytes induces motoneuron plasticity and improves neuromuscular function in ALS mice. bioRxiv 2021.01.08.425706. https://doi.org/10.1101/2021.01.08.425706

Roche, P.A., Furuta, K., 2015. The ins and outs of MHC class II-mediated antigen processing and presentation. Nat Rev Immunol 15, 203–216. https://doi.org/10.1038/nri3818

Rolland, P., Madjd, Z., Durrant, L., Ellis, I.O., Layfield, R., Spendlove, I., 2007. The ubiquitin-binding protein p62 is expressed in breast cancers showing features of aggressive disease. Endocrine-Related Cancer 14, 73–80. https://doi.org/10.1677/erc.1.01312

Rowland, L., Shneider, N., 2001. Amyotrophic Lateral Sclerosis. The New England journal of medicine 344, 1688–700. https://doi.org/10.1056/NEJM200105313442207

Ryan, T.A., Tumbarello, D.A., 2018. Optineurin: A Coordinator of Membrane-Associated Cargo Trafficking and Autophagy. Front Immunol 9, 1024. https://doi.org/10.3389/fimmu.2018.01024

Sacht, G., Märten, A., Deiters, U., Süssmuth, R., Jung, G., Wingender, E., Mühlradt, P.F., 1998. Activation of nuclear factor-kappaB in macrophages by mycoplasmal lipopeptides. Eur J Immunol 28, 4207–4212. https://doi.org/10.1002/(SICI)1521-4141(199812)28:12<4207::AID-IMMU4207>3.0.CO;2-R

Saeed, M., Yang, Y., Deng, H.-X., Hung, W.-Y., Siddique, N., Dellefave, L., Gellera, C., Andersen, P.M., Siddique, T., 2009. Age and founder effect of SOD1 A4V mutation causing ALS. Neurology 72, 1634–1639. https://doi.org/10.1212/01.wnl.0000343509.76828.2a

Şahin, A., Held, A., Bredvik, K., Major, P., Achilli, T.-M., Kerson, A.G., Wharton, K., Stilwell, G., Reenan, R., 2017. Human SOD1 ALS Mutations in a Drosophila Knock-In Model Cause Severe Phenotypes and Reveal Dosage-Sensitive Gain- and Loss-of-Function Components. Genetics 205, 707–723. https://doi.org/10.1534/genetics.116.190850

Sako, W., Ito, H., Yoshida, M., Koizumi, H., Kamada, M., Fujita, K., Hashizume, Y., Izumi, Y., Kaji, R., 2012. Nuclear factor κ B expression in patients with sporadic amyotrophic lateral sclerosis and hereditary amyotrophic lateral sclerosis with optineurin mutations. Clin Neuropathol 31, 418–423. https://doi.org/10.5414/NP300493

Salminen, T.S., Vale, P.F., 2020. Drosophila as a Model System to Investigate the Effects of Mitochondrial Variation on Innate Immunity. Frontiers in Immunology 11.

Salvagno, C., Cubillos-Ruiz, J.R., 2021. Optineurin Guards IFNγ Signaling in Cancer Cells. Cancer Discovery 11, 1623–1625. https://doi.org/10.1158/2159-8290.CD-21-0362

Schirmeier, S., Klämbt, C., 2015. The Drosophila blood-brain barrier as interface between neurons and hemolymph. Mechanisms of Development, Neurovascular unit 138, 50–55. https://doi.org/10.1016/j.mod.2015.06.002

Schuman, E.M., Madison, D.V., 1994. Nitric oxide and synaptic function. Annu. Rev. Neurosci. 17, 153–183. https://doi.org/10.1146/annurev.ne.17.030194.001101

Seelen, M., van Doormaal, P.T.C., Visser, A.E., Huisman, M.H.B., Roozekrans, M.H.J., de Jong, S.W., van der Kooi, A.J., de Visser, M., Voermans, N.C., Veldink, J.H., van den Berg, L.H., 2014. Prior medical conditions and the risk of amyotrophic lateral sclerosis. J Neurol 261, 1949–1956. https://doi.org/10.1007/s00415-014-7445-1

Sen, R., Baltimore, D., 1986. Multiple nuclear factors interact with the immunoglobulin enhancer sequences. Cell 46, 705–716. https://doi.org/10.1016/0092-8674(86)90346-6

Sharma, A., Lyashchenko, A.K., Lu, L., Nasrabady, S.E., Elmaleh, M., Mendelsohn, M., Nemes, A., Tapia, J.C., Mentis, G.Z., Shneider, N.A., 2016. ALS-associated mutant FUS induces selective motor neuron degeneration through toxic gain of function. Nat Commun 7, 10465. https://doi.org/10.1038/ncomms10465

Shelkovnikova, T.A., An, H., Skelt, L., Tregoning, J.S., Humphreys, I.R., Buchman, V.L., 2019. Antiviral Immune Response as a Trigger of FUS Proteinopathy in Amyotrophic Lateral Sclerosis. Cell Rep 29, 4496-4508.e4. https://doi.org/10.1016/j.celrep.2019.11.094

Shenouda, M., Xiao, S., MacNair, L., Lau, A., Robertson, J., 2022. A C-Terminally Truncated TDP-43 Splice Isoform Exhibits Neuronal Specific Cytoplasmic Aggregation and Contributes to TDP-43 Pathology in ALS. Frontiers in Neuroscience 16.

Sherri, N., Salloum, N., Mouawad, C., Haidar-Ahmad, N., Shirinian, M., Rahal, E.A., 2018. Epstein-Barr Virus DNA Enhances Diptericin Expression and Increases Hemocyte Numbers in Drosophila melanogaster via the Immune Deficiency Pathway. Frontiers in Microbiology 9.

Shih, V.F.-S., Tsui, R., Caldwell, A., Hoffmann, A., 2011. A single NFκB system for both canonical and non-canonical signaling. Cell Res 21, 86–102. https://doi.org/10.1038/cr.2010.161

Silva, D.F., Candeias, E., Esteves, A.R., Magalhães, J.D., Ferreira, I.L., Nunes-Costa, D., Rego, A.C., Empadinhas, N., Cardoso, S.M., 2020. Microbial BMAA elicits mitochondrial dysfunction, innate immunity activation, and Alzheimer's disease features in cortical neurons. Journal of Neuroinflammation 17, 332. https://doi.org/10.1186/s12974-020-02004-y

Slowicka, K., van Loo, G., 2018. Optineurin Functions for Optimal Immunity. Front Immunol 9. https://doi.org/10.3389/fimmu.2018.00769

Sreedharan, J., Blair, I.P., Tripathi, V.B., Hu, X., Vance, C., Rogelj, B., Ackerley, S., Durnall, J.C., Williams, K.L., Buratti, E., Baralle, F., de Belleroche, J., Mitchell, J.D., Leigh, P.N., Al-Chalabi, A., Miller, C.C., Nicholson, G., Shaw, C.E., 2008. TDP-43 Mutations in Familial and Sporadic Amyotrophic Lateral Sclerosis. Science 319, 1668–1672. https://doi.org/10.1126/science.1154584

Stallings, N.R., Puttaparthi, K., Dowling, K.J., Luther, C.M., Burns, D.K., Davis, K., Elliott, J.L., 2013. TDP-43, an ALS Linked Protein, Regulates Fat Deposition and Glucose Homeostasis. PLOS ONE 8, e71793. https://doi.org/10.1371/journal.pone.0071793

Steward, R., 1987. Dorsal, an embryonic polarity gene in Drosophila, is homologous to the vertebrate proto-oncogene, c-rel. Science 238, 692–694. https://doi.org/10.1126/science.3118464

Stolow, D.T., Haynes, S.R., 1995. Cabeza, a Drosophila gene encoding a novel RNA binding protein, shares homology with EWS and TLS, two genes involved in human sarcoma formation. Nucleic Acids Res 23, 835–843.

Stommel, E.W., Cohen, J.A., Fadul, C.E., Cogbill, C.H., Graber, D.J., Kingman, L., Mackenzie, T., Channon Smith, J.Y., Harris, B.T., 2009. Efficacy of thalidomide for the treatment of amyotrophic lateral sclerosis: A phase II open label clinical trial. Amyotrophic Lateral Sclerosis 10, 393–404. https://doi.org/10.3109/17482960802709416

Streit, L., Kuhn, T., Vomhof, T., Bopp, V., Ludolph, A.C., Weishaupt, J.H., Gebhardt, J.C.M., Michaelis, J., Danzer, K.M., 2022. Stress induced TDP-43 mobility loss independent of stress granules. Nat Commun 13, 5480. https://doi.org/10.1038/s41467-022-32939-0

Suescun, J., Chandra, S., Schiess, M.C., 2019. Chapter 13 - The Role of Neuroinflammation in Neurodegenerative Disorders, in: Actor, J.K., Smith, K.C. (Eds.), Translational Inflammation, Perspectives in Translational Cell Biology. Academic Press, pp. 241–267. https://doi.org/10.1016/B978-0-12-813832-8.00013-3

Suk, T.R., Rousseaux, M.W.C., 2020. The role of TDP-43 mislocalization in amyotrophic lateral sclerosis. Molecular Neurodegeneration 15, 45. https://doi.org/10.1186/s13024-020-00397-1

Sun, S.-C., 2017. The non-canonical NF-κB pathway in immunity and inflammation. Nature reviews. Immunology 17, 545. https://doi.org/10.1038/nri.2017.52

Sun, S.-C., 2011. Non-canonical NF-κB signaling pathway. Cell Res 21, 71–85. https://doi.org/10.1038/cr.2010.177

Swanson, L.C., Trujillo, E.A., Thiede, G.H., Katzenberger, R.J., Shishkova, E., Coon, J.J., Ganetzky, B., Wassarman, D.A., 2020. Survival Following Traumatic Brain Injury in Drosophila Is Increased by Heterozygosity for a Mutation of the NF-κB Innate Immune Response Transcription Factor Relish. Genetics 216, 1117–1136. https://doi.org/10.1534/genetics.120.303776

Swarup, V., Phaneuf, D., Dupré, N., Petri, S., Strong, M., Kriz, J., Julien, J.-P., 2011. Deregulation of TDP-43 in amyotrophic lateral sclerosis triggers nuclear factor κB–mediated pathogenic pathways. J Exp Med 208, 2429–2447. https://doi.org/10.1084/jem.20111313

Sweeney, S.E., Mo, L., Firestein, G.S., 2007. Antiviral gene expression in rheumatoid arthritis: Role of IKKε and interferon regulatory factor 3. Arthritis & Rheumatism 56, 743–752. https://doi.org/10.1002/art.22421

Tolwinski, N.S., 2017. Introduction: Drosophila—A Model System for Developmental Biology. J Dev Biol 5. https://doi.org/10.3390/jdb5030009

Tortarolo, M., Vallarola, A., Lidonnici, D., Battaglia, E., Gensano, F., Spaltro, G., Fiordaliso, F., Corbelli, A., Garetto, S., Martini, E., Pasetto, L., Kallikourdis, M., Bonetto, V., Bendotti, C., 2015. Lack of TNF-alpha receptor type 2 protects motor neurons in a cellular model of amyotrophic lateral sclerosis and in mutant SOD1 mice but does not

affect disease progression. Journal of Neurochemistry 135, 109–124. https://doi.org/10.1111/jnc.13154

Toth, R.P., Atkin, J.D., 2018. Dysfunction of Optineurin in Amyotrophic Lateral Sclerosis and Glaucoma. Frontiers in Immunology 9, 1017. https://doi.org/10.3389/fimmu.2018.01017

Troost, D., van den Oord, J.J., de Jong, J.M., Swaab, D.F., 1989. Lymphocytic infiltration in the spinal cord of patients with amyotrophic lateral sclerosis. Clin Neuropathol 8, 289–294.

Turner, M.R., Cagnin, A., Turkheimer, F.E., Miller, C.C.J., Shaw, C.E., Brooks, D.J., Leigh, P.N., Banati, R.B., 2004. Evidence of widespread cerebral microglial activation in amyotrophic lateral sclerosis: an [11C](R)-PK11195 positron emission tomography study. Neurobiol Dis 15, 601–609. https://doi.org/10.1016/j.nbd.2003.12.012

Tusco, R., Jacomin, A.-C., Jain, A., Penman, B.S., Larsen, K.B., Johansen, T., Nezis, I.P., 2017. Kenny mediates selective autophagic degradation of the IKK complex to control innate immune responses. Nat Commun 8, 1264. https://doi.org/10.1038/s41467-017-01287-9

Uddin, Md.S., Kabir, Md.T., Mamun, A.A., Sarwar, Md.S., Nasrin, F., Emran, T.B., Alanazi, I.S., Rauf, A., Albadrani, G.M., Sayed, A.A., Mousa, S.A., Abdel-Daim, M.M., 2021. Natural Small Molecules Targeting NF-κB Signaling in Glioblastoma. Front Pharmacol 12, 703761. https://doi.org/10.3389/fphar.2021.703761

Ugolini, G., Raoul, C., Ferri, A., Haenggeli, C., Yamamoto, Y., Salaün, D., Henderson, C.E., Kato, A.C., Pettmann, B., Hueber, A.-O., 2003. Fas/Tumor Necrosis Factor Receptor Death Signaling Is Required for Axotomy-Induced Death of Motoneurons In Vivo. J. Neurosci. 23, 8526–8531. https://doi.org/10.1523/JNEUROSCI.23-24-08526.2003

Uranishi, H., Tetsuka, T., Yamashita, M., Asamitsu, K., Shimizu, M., Itoh, M., Okamoto, T., 2001. Involvement of the Pro-oncoprotein TLS (Translocated in Liposarcoma) in Nuclear Factor-κB p65-mediated Transcription as a Coactivator. J. Biol. Chem. 276, 13395–13401. https://doi.org/10.1074/jbc.M011176200

Uysal, Hi., Bilge, U., İlhanli, N., Gromicho, M., Grosskreutz, J., Kuzma-Kozakiewicz, M., Pinto, S., Petri, S., Szacka, K., Nieporecki, K., De Carvalho, M., 2021. ALS and fertility: does ALS affect number of children patients have? Amyotrophic Lateral Sclerosis and Frontotemporal Degeneration 22, 94–100. https://doi.org/10.1080/21678421.2020.1813313

Valanne, S., Wang, J.-H., Rämet, M., 2011. The Drosophila Toll Signaling Pathway. The Journal of Immunology 186, 649–656. https://doi.org/10.4049/jimmunol.1002302

Valbuena, G.N., Tortarolo, M., Bendotti, C., Cantoni, L., Keun, H.C., 2017. Altered Metabolic Profiles Associate with Toxicity in SOD1G93A Astrocyte-Neuron Co-Cultures. Sci Rep 7, 50. https://doi.org/10.1038/s41598-017-00072-4

Vance, C., Scotter, E.L., Nishimura, A.L., Troakes, C., Mitchell, J.C., Kathe, C., Urwin, H., Manser, C., Miller, C.C., Hortobágyi, T., Dragunow, M., Rogelj, B., Shaw, C.E., 2013. ALS mutant FUS disrupts nuclear localization and sequesters wild-type FUS within cytoplasmic stress granules. Hum Mol Genet 22, 2676–2688. https://doi.org/10.1093/hmg/ddt117

Vandamme, T.F., 2014. Use of rodents as models of human diseases. J Pharm Bioallied Sci 6, 2–9. https://doi.org/10.4103/0975-7406.124301

Vanneste, J., Vercruysse, T., Boeynaems, S., Sicart, A., Van Damme, P., Daelemans, D., Van Den Bosch, L., 2019. C9orf72-generated poly-GR and poly-PR do not directly interfere with nucleocytoplasmic transport. Scientific Reports 9, 15728. https://doi.org/10.1038/s41598-019-52035-6

Voigt, A., Herholz, D., Fiesel, F.C., Kaur, K., Müller, D., Karsten, P., Weber, S.S., Kahle, P.J., Marquardt, T., Schulz, J.B., 2010. TDP-43-Mediated Neuron Loss In Vivo Requires RNA-Binding Activity. PLOS ONE 5, e12247. https://doi.org/10.1371/journal.pone.0012247

Waibel, S., Neumann, M., Rabe, M., Meyer, T., Ludolph, A.C., 2010. Novel missense and truncating mutations in FUS/TLS in familial ALS. Neurology 75, 815–817. https://doi.org/10.1212/WNL.0b013e3181f07e26

Wang, J.-W., Brent, J.R., Tomlinson, A., Shneider, N.A., McCabe, B.D., 2011. The ALS-associated proteins FUS and TDP-43 function together to affect Drosophila locomotion and life span. J. Clin. Invest. 121, 4118–4126. https://doi.org/10.1172/JCI57883

Wang, T., Zhang, X., Li, J.J., 2002. The role of NF-κB in the regulation of cell stress responses. International Immunopharmacology 2, 1509–1520. https://doi.org/10.1016/S1567-5769(02)00058-9

Watson, M.R., Lagow, R.D., Xu, K., Zhang, B., Bonini, N.M., 2008. A Drosophila Model for Amyotrophic Lateral Sclerosis Reveals Motor Neuron Damage by Human SOD1. J. Biol. Chem. 283, 24972–24981. https://doi.org/10.1074/jbc.M804817200

White, M.A., Kim, E., Duffy, A., Adalbert, R., Phillips, B.U., Peters, O.M., Stephenson, J., Yang, S., Massenzio, F., Lin, Z., Andrews, S., Segonds-Pichon, A., Metterville, J., Saksida, L.M., Mead, R., Ribchester, R.R., Barhomi, Y., Serre, T., Coleman, M.P., Fallon, J.R., Bussey, T.J., Brown, R.H., Sreedharan, J., 2018. TDP-43 gains function due to perturbed autoregulation in a Tardbp knock-in mouse model of ALS-FTD. Nat Neurosci 21, 552–563. https://doi.org/10.1038/s41593-018-0113-5

Wijesekera, L.C., Leigh, P.N., 2009. Amyotrophic lateral sclerosis. Orphanet J Rare Dis 4, 3. https://doi.org/10.1186/1750-1172-4-3

Wils, H., Kleinberger, G., Janssens, J., Pereson, S., Joris, G., Cuijt, I., Smits, V., Ceuterick-de Groote, C., Van Broeckhoven, C., Kumar-Singh, S., 2010. TDP-43 transgenic mice develop spastic paralysis and neuronal inclusions characteristic of ALS and frontotemporal lobar degeneration. Proceedings of the National Academy of Sciences 107, 3858–3863. https://doi.org/10.1073/pnas.0912417107

Winkler, B., Funke, D., Benmimoun, B., Spéder, P., Rey, S., Logan, M.A., Klämbt, C., 2021. Brain inflammation triggers macrophage invasion across the blood-brain barrier in Drosophila during pupal stages. Science Advances 7, eabh0050. https://doi.org/10.1126/sciadv.abh0050

Winton, M.J., Van Deerlin, V.M., Kwong, L.K., Yuan, W., Wood, E.M., Yu, C.-E., Schellenberg, G.D., Rademakers, R., Caselli, R., Karydas, A., Trojanowski, J.Q., Miller, B.L., Lee, V.M.-Y., 2008. A90V TDP-43 variant results in the aberrant localization of TDP-43 in vitro. FEBS Lett 582, 2252–2256. https://doi.org/10.1016/j.febslet.2008.05.024

Wobst, H.J., Wesolowski, S.S., Chadchankar, J., Delsing, L., Jacobsen, S., Mukherjee, J., Deeb, T.Z., Dunlop, J., Brandon, N.J., Moss, S.J., 2017. Cytoplasmic Relocalization of TAR DNA-Binding Protein 43 Is Not Sufficient to Reproduce Cellular Pathologies Associated with ALS In vitro. Front Mol Neurosci 10, 46. https://doi.org/10.3389/fnmol.2017.00046

Wolf, Y., Shemer, A., Levy-Efrati, L., Gross, M., Kim, J.-S., Engel, A., David, E., Chappell-Maor, L., Grozovski, J., Rotkopf, R., Biton, I., Eilam-Altstadter, R., Jung, S., 2018. Microglial MHC class II is dispensable for experimental autoimmune encephalomyelitis and cuprizone-induced demyelination. European Journal of Immunology 48, 1308–1318. https://doi.org/10.1002/eji.201847540

Wong, P.C., Pardo, C.A., Borchelt, D.R., Lee, M.K., Copeland, N.G., Jenkins, N.A., Sisodia, S.S., Cleveland, D.W., Price, D.L., 1995. An adverse property of a familial ALS-linked SOD1 mutation causes motor neuron disease characterized by vacuolar degeneration of mitochondria. Neuron 14, 1105–1116. https://doi.org/10.1016/0896-6273(95)90259-7

Wu, S.-C., Cao, Z.-S., Chang, K.-M., Juang, J.-L., 2017. Intestinal microbial dysbiosis aggravates the progression of Alzheimer's disease in Drosophila. Nat Commun 8, 24. https://doi.org/10.1038/s41467-017-00040-6

Xu, Y.-F., Gendron, T.F., Zhang, Y.-J., Lin, W.-L., D'Alton, S., Sheng, H., Casey, M.C., Tong, J., Knight, J., Yu, X., Rademakers, R., Boylan, K., Hutton, M., McGowan, E., Dickson, D.W., Lewis, J., Petrucelli, L., 2010. Wild-Type Human TDP-43 Expression Causes TDP-43 Phosphorylation, Mitochondrial Aggregation, Motor Deficits, and Early Mortality in Transgenic Mice. J Neurosci 30, 10851–10859. https://doi.org/10.1523/JNEUROSCI.1630-10.2010

Xu, Y.-F., Zhang, Y.-J., Lin, W.-L., Cao, X., Stetler, C., Dickson, D.W., Lewis, J., Petrucelli, L., 2011. Expression of mutant TDP-43 induces neuronal dysfunction in transgenic mice. Molecular Neurodegeneration 6, 73. https://doi.org/10.1186/1750-1326-6-73

Xue, Y.C., Ruller, C.M., Fung, G., Mohamud, Y., Deng, H., Liu, H., Zhang, J., Feuer, R., Luo, H., 2018. Enteroviral Infection Leads to Transactive Response DNA-Binding Protein 43 Pathology in Vivo. The American Journal of Pathology 188, 2853–2862. https://doi.org/10.1016/j.ajpath.2018.08.013

Yamanaka, K., Chun, S.J., Boillee, S., Fujimori-Tonou, N., Yamashita, H., Gutmann, D.H., Takahashi, R., Misawa, H., Cleveland, D.W., 2008. Astrocytes as determinants of disease progression in inherited ALS. Nat Neurosci 11, 251–253. https://doi.org/10.1038/nn2047

Yin, J., Valin, K.L., Dixon, M.L., Leavenworth, J.W., 2017. The Role of Microglia and Macrophages in CNS Homeostasis, Autoimmunity, and Cancer. J Immunol Res 2017, 5150678. https://doi.org/10.1155/2017/5150678

Ying, H., Yue, B.Y.J.T., 2012. Chapter five - Cellular and Molecular Biology of Optineurin, in: Jeon, K.W. (Ed.), International Review of Cell and Molecular Biology. Academic Press, pp. 223–258. https://doi.org/10.1016/B978-0-12-394305-7.00005-7

Yu, B., Pamphlett, R., 2017. Environmental insults: critical triggers for amyotrophic lateral sclerosis. Translational Neurodegeneration 6, 15. https://doi.org/10.1186/s40035-017-0087-3

Yu, C.-H., Davidson, S., Harapas, C.R., Hilton, J.B., Mlodzianoski, M.J., Laohamonthonkul, P., Louis, C., Low, R.R.J., Moecking, J., De Nardo, D., Balka, K.R., Calleja, D.J., Moghaddas, F., Ni, E., McLean, C.A., Samson, A.L., Tyebji, S., Tonkin, C.J., Bye, C.R., Turner, B.J., Pepin, G., Gantier, M.P., Rogers, K.L., McArthur, K., Crouch, P.J., Masters, S.L., 2020. TDP-43 Triggers Mitochondrial DNA Release via mPTP to Activate cGAS/STING in ALS. Cell 183, 636-649.e18. https://doi.org/10.1016/j.cell.2020.09.020

Zakaria, R., Wan Yaacob, W.M., Othman, Z., Long, I., Ahmad, A.H., Al-Rahbi, B., 2017. Lipopolysaccharide-induced memory impairment in rats: a model of Alzheimer's disease. Physiol Res 66, 553–565. https://doi.org/10.33549/physiolres.933480

Zambon, R.A., Nandakumar, M., Vakharia, V.N., Wu, L.P., 2005. The Toll pathway is important for an antiviral response in Drosophila. Proceedings of the National Academy of Sciences 102, 7257–7262. https://doi.org/10.1073/pnas.0409181102

Zamudio, F., Loon, A.R., Smeltzer, S., Benyamine, K., Navalpur Shanmugam, N.K., Stewart, N.J.F., Lee, D.C., Nash, K., Selenica, M.-L.B., 2020. TDP-43 mediated blood-brain barrier permeability and leukocyte infiltration promote neurodegeneration in a low-grade systemic inflammation mouse model. Journal of Neuroinflammation 17, 283. https://doi.org/10.1186/s12974-020-01952-9

Zarei, S., Carr, K., Reiley, L., Diaz, K., Guerra, O., Altamirano, P.F., Pagani, W., Lodin, D., Orozco, G., Chinea, A., 2015. A comprehensive review of amyotrophic lateral sclerosis. Surg Neurol Int 6. https://doi.org/10.4103/2152-7806.169561

Zarnegar, B.J., Wang, Y., Mahoney, D.J., Dempsey, P.W., Cheung, H.H., He, J., Shiba, T., Yang, X., Yeh, W., Mak, T.W., Korneluk, R.G., Cheng, G., 2008. Activation of noncanonical NF-κB requires coordinated assembly of a regulatory complex of the adaptors cIAP1, cIAP2, TRAF2, TRAF3 and the kinase NIK. Nat Immunol 9, 1371–1378. https://doi.org/10.1038/ni.1676

Zhan, L., Xie, Q., Tibbetts, R.S., 2015. Opposing roles of p38 and JNK in a Drosophila model of TDP-43 proteinopathy reveal oxidative stress and innate immunity as pathogenic components of neurodegeneration. Hum Mol Genet 24, 757–772. https://doi.org/10.1093/hmg/ddu493

Zhang, J., Luo, J., Chen, J., Dai, J., Montell, C., 2020. The Role of Y Chromosome Genes in Male Fertility in Drosophila melanogaster. Genetics 215, 623–633. https://doi.org/10.1534/genetics.120.303324

Zhang, Q., Lenardo, M.J., Baltimore, D., 2017. 30 Years of NF-κB: A Blossoming of Relevance to Human Pathobiology. Cell 168, 37–57. https://doi.org/10.1016/j.cell.2016.12.012

Zhang, R., Miller, R.G., Gascon, R., Champion, S., Katz, J., Lancero, M., Narvaez, A., Honrada, R., Ruvalcaba, D., McGrath, M.S., 2009. Circulating endotoxin and systemic immune activation in sporadic Amyotrophic Lateral Sclerosis (sALS). J Neuroimmunol 206, 121–124. https://doi.org/10.1016/j.jneuroim.2008.09.017

Zhang, Y., Reichel, J.M., Han, C., Zuniga-Hertz, J.P., Cai, D., 2017. Astrocytic Process Plasticity and IKKβ/NF-κB in Central Control of Blood Glucose, Blood Pressure, and Body Weight. Cell Metabolism 25, 1091-1102.e4. https://doi.org/10.1016/j.cmet.2017.04.002

Zheng, H., Yang, X., Xi, Y., 2016. Fat body remodeling and homeostasis control in Drosophila. Life Sciences 167, 22–31. https://doi.org/10.1016/j.lfs.2016.10.019

Zhu, L., Fukunaga, R., 2021. RNA-binding protein Maca is crucial for gigantic male fertility factor gene expression, spermatogenesis, and male fertility, in Drosophila. PLoS Genet 17, e1009655. https://doi.org/10.1371/journal.pgen.1009655

Zou, J.Y., Crews, F.T., 2005. TNF alpha potentiates glutamate neurotoxicity by inhibiting glutamate uptake in organotypic brain slice cultures: neuroprotection by NF kappa B inhibition. Brain Res 1034, 11–24. https://doi.org/10.1016/j.brainres.2004.11.014

9

Chapter 9 - Annexes

- -

9.1 Challenges of gene editing techniques

9.1.1 Introduction

Genome editing is a common method used to modify organisms and cell lines in order to study both fundamental sciences and diseases. Among the methods that exist are PhiC31 integrase technology and the CRISPR/Cas9 system, both of which will be explained further in this annex.

When studying genes in *Drosophila melanogaster*, the PhiC31 integration system has been widely used. PhiC31 is a bacteriophage that uses an integrase enzyme to insert its genes into its host. The integrase mediates recombination between a phage attachment (attP) and a bacterial attachment site (attB). By inserting attB or attP sites in fly genomes, injection of plasmids containing genes surrounded by attB or attP sites can enable insertion of genes-of-interest into host genomes in the presence of PhiC31 integrase.

Another commonly used genome engineering technology in *Drosophila melanogaster*, but also in other organisms and cell lines, is the CRISPR/Cas9 system, based on the adaptive immune system used in bacteria to protect against bacteriophage infection (Rath et al., 2015). The bacterial genome contains a so-called CRISPR locus, which comprises many short repeated sequences with unique sequence spacers in between. The spacers stem from different phages that have previously infected the bacteria, and when a new phage is present, the CRISPR locus is transcribed. The spacers are processed into mature crRNA, and by using this crRNA as a guide, the Cas proteins can recognize the phage DNA and cut it. This has been adapted to use in genome editing by designing guide RNAs that target a specific gene and using the Cas9 protein to make a cut and enable integration of a gene-of-interest. The

system has received wide interest thanks to its potential to change mutated genes and correct genetic disorders (Redman et al., 2016). However, there are some limitations to the technology, including potential off-target activity.

In this annex, I will present some of the challenges we faced when using PhiC31 integrase and CRISPR/Cas9 gene editing in our experiments. The aim is to highlight the importance of verifying the correct insertion, deletion, or mutation of the gene-of-interest when applying gene editing techniques.

9.1.2 Results

Using PhiC31 to replace hFUS in a fly line previously generated using CRISPR/Cas9

When creating the humanized FUS *Drosophila* lines, see chapter one, we faced a few challenges along the way. Originally, instead of creating separate CRISPR/Cas9 lines for hFUS wild-type and each of the ALS mutants, we aimed to first generate the hFUS wild-type line, including PhiC31 attP sites before the hFUS wild-type gene and after the dsRed cassette. This would enable replacement of hFUS wild-type - p10 3'UTR - dsRed cassette with hFUS wild-type or ALS mutant - p10 3'UTR, effectively creating ALS mutants and removing the dsRed cassette simultaneously (figure 1). Therefore, hFUS wild-type and ALS mutants were separately cloned into different donor plasmids, with each hFUS gene being followed by a p10 3'UTR. The donor plasmids were then injected into the embryos of the original hFUS wild-type fly line, together with PhiC31 integrase, and the dsRed-negative *Drosophila*, which should have the successful gene replacement, were selected.

However, when collecting the progeny of the fly lines not expressing dsRed, no *Drosophila* of the correct genotypes eclosed. Since we were aware, from the original hFUS wild-type fly line, that at least the hFUS wild-type should rescue Caz-/- and eclose into adults, we suspect the PhiC31 exchange did not happen as planned. It is possible that the hFUS wild-type - p10 3'UTR – dsRed was excised, but the hFUS wild-type or ALS mutant - p10 3'UTR was not properly inserted, creating Caz-/- *Drosophila* that could not eclose. To further improve this technique for future use, it may be necessary to include a GFP cassette in the donor plasmid that can then be selected for, ensuring that all the selected flies have the inserted gene.

Figure 9-1. PhiC31 integrase used to insert hFUS ALS mutations
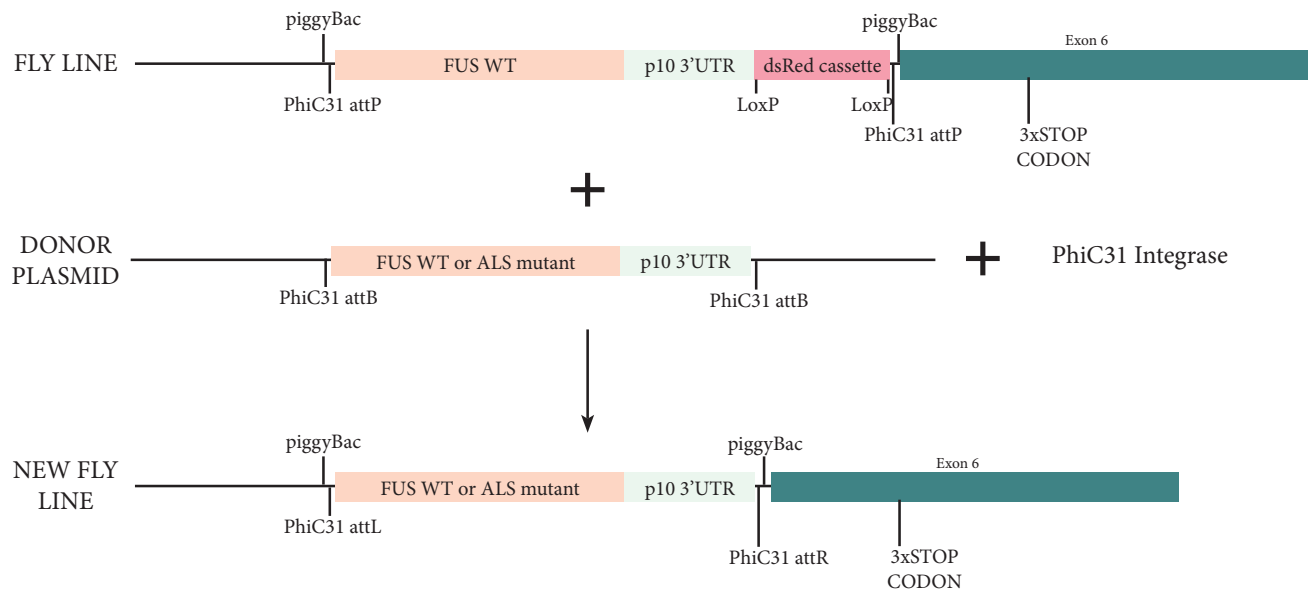
Figure 1: The aim was to use PhiC31 integrase technology to insert hFUS ALS mutants and remove the dsRed cassette. hFUS wild-type or ALS mutant, including the p10 3'UTR but without the dsRed cassette, replaces the hFUS wild-type - p10 3'UTR - dsRed cassette. Therefore, flies are created with hFUS wild-type or mutant, missing the dsRed cassette, without needing to create another CRISPR/Cas9 fly line.

CRISPR/Cas9 insertion may not cause deletion of endogenous gene

Due to the complications of using the PhiC31 integrase to replace the hFUS wild-type gene with mutants, we instead made separate CRISPR/Cas9 constructs for each of the hFUS mutants. The injection of the DNA into fly embryos was performed by Genetivision Corporation (USA), and for each fly line, three different copies of the fly line were sent to us. The fly lines were sequenced to ensure the correct insertion of the gene, and subsequently western blot was performed to ensure expression of hFUS and deletion of Caz. In the western blot, however, for two of the hFUS R495X lines (line 1 and line 3), we observed the absence of hFUS expression and the presence of endogenous Caz expression, suggesting that the gene was not properly inserted (figure 2A). Still, the dsRed was visibly expressed in the flies, and the sequencing confirmed the insertion of the hFUS gene, making it possible that the hFUS gene was inserted without deletion of Caz. It remains unclear why the hFUS gene is not being expressed.

CRISPR/Cas9 insertion can cause expression of both endogenous gene and inserted gene

When making the humanized TDP-43 *Drosophila* lines using CRISPR/Cas9, we also encountered some issues. After injection of the CRISPR/Cas9 plasmids into fly embryos by Genetivision Corporation (USA), we received back 3 copies of each hTDP-43 genotype. The lines were sequenced and the correct insertion of the gene was confirmed. When analyzed through western blot, however, we observed expression of both the human TDP-43 protein and the fly TBPH protein in all the hTDP-43 wild-type lines and one of the hTDP-43 G287S lines (see example of the hTDP-43 wild-type lines in figure 2B). From this we drew the conclusion that while hTDP-43 gene was inserted, the endogenous *tbph* gene was reinserted or duplicated, causing the presence of both in the genome. Through repeated injection of the CRISPR/Cas9 plasmid DNA in the fly embryos we were able to identify lines expressing only hTDP-43 to use in our study.

Figure 9-2. The gene-of-interest is inserted but the endogenous gene is not lost
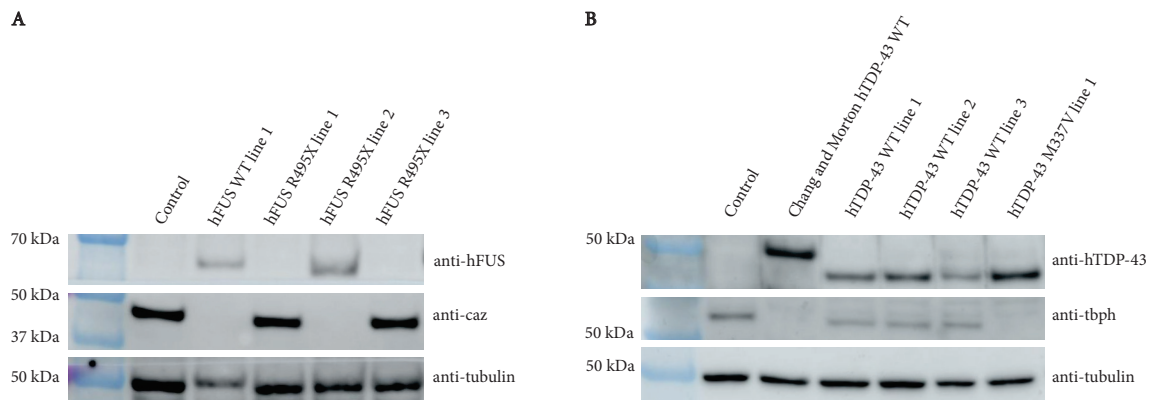
Figure 2: We discovered that during insertion, it is possible that the gene-of-interest is inserted but the endogenous gene is not lost. (A) A western blot of the hFUS wild-type line, as well as three of the hFUS R495X lines, that we created using CRISPR/Cas9. In the hFUS R495X mutants 1 and 3, only the Caz protein is expressed despite integration of the hFUS sequence. (B) A western blot depicting three of the hTDP-43 wild-type lines, and one of the hTDP-43 M337V lines, that we created using CRISPR/Cas9. Also included is a positive control using Chang and Morton's hTDP-43 wild-type line, which shows a slightly heavier band due to the protein being attached to a FLAG tag. Note the expression of both hTDP-43 and TBPH in hTDP-43 lines 1, 2 and 3.

9.1.3 Discussion

In this annex, we have identified some of the problems that may occur using the PhiC31 integrase system and CRISPR/Cas9 technology. While both techniques enable varied and useful genome editing, it is important to verify protein expression and correct insertion. The PhiC31 integrase system is often used in *Drosophila* gene editing to insert exogenous genes. In our study, we aimed to combine it with an already-made CRISPR/Cas9 humanized FUS fly, by injecting said fly with a donor plasmid containing PhiC31 attB sites. However, we observed what we assume to be an excision of the gene-of-interest without insertion of the donor plasmid DNA. It could be that the insertion of the donor plasmid DNA occurs at a very low rate, and that by including a GFP cassette in the donor plasmid it would be easier to identify the *Drosophila* with an integrated donor gene.

CRISPR/Cas9 is a novel and well-used technology to insert exogenous genes into organisms and cell lines. While it greatly increases the gene editing possibilities, there are some known challenges, such as the possibility of off-targets. When creating the humanized FUS and TDP-43 *Drosophila*, we discovered another potential difficulty of using CRISPR/Cas9 to replace an endogenous gene: reinsertion or duplication of the endogenous gene causing the presence of both genes in the genome. It is unclear how exactly this happens, but seems to be a response of the organism in order to ensure survival. It highlights the importance of always verifying the expression of the gene-of-interest and the absence of any potential gene that is being replaced.

9.1.4 Conclusion

In conclusion, we experienced challenges both when using PhiC31 integrase technology in a CRISPR/Cas9 edited *Drosophila*, as well as during CRISPR/Cas9 replacement of a *Drosophila* gene with a human gene. We conclude that there are still yet to be discovered effects of gene editing, and that experiments verifying the intended gene edits are of grave importance.

Curriculum Vitae
Emma Källstig

Molecular neurobiologist

E-mail
emma.kallstig@gmail.com

Date of birth
1994-06-27

Nationality
Swedish

Address
Chemin des côtes 66
1020 Renens
Switzerland

Tel.
+41 (0)78 726 38 81

Languages
Swedish   fluent (native)
English   fluent
French   B1 written and
           spoken

References
References available upon
request.

PROJECTS

2017-ongoing — **Using CRISPR/Cas9 technology to model Amyotrophic lateral sclerosis (ALS) in *Drosophila melanogaster*, and investigating the role of the NF-κB pathway in those models**
Position: Doctoral assistant. Supervisor: Prof. Brian McCabe, Laboratory of Neural Genetics and Disease, EPFL, Switzerland.
- Using CRISPR/Cas9 technology to create humanized *Drosophila melanogaster* ALS models
- Studying the effect of the NF-κB immune pathway activation on ALS models through fly genetics
- Using bacterial infection of flies to activate the NF-κB pathway
- Analyzing the effects through neuromuscular junction immunohistochemistry, lifespan studies, and motor behavior assays

2017-ongoing — **Inhibition of the NF-κB pathway in an ALS mouse model through AAV-mediated gene therapy**
Position: Doctoral assistant. Supervisor: Dr. Bernard Schneider, Bertarelli Foundation Gene Therapy Core Facility, EPFL, Switzerland.
- Creation of adeno-associated viruses (AAVs) expressing NF-κB inhibitors in a tissue-specific manner
- Treatment of ALS model mice with the AAV viruses through intracerebroventricular injection
- Studying the effect of the treatment on motor behavior and electrical neuromuscular function through rotarod, swimming tank assay, and compound muscle action potential measurements

2016-2017 — **Knockout of Hsp70 co-chaperone DNAJB1 in HEK293 cells overexpressing α-synuclein to investigate the effects on α-synuclein aggregation**
Position: Master student, continued by an internship. Supervisor: Dr. Christian Hansen, Molecular Neurobiology research group, Lund University, Sweden.
- HEK293 cell line work, transfection, and Western Blots using cell lysate
- Immunocytochemistry

2016-2017 — **Studying the effect of conditional dopaminergic knockout of the Unfolded Protein Response protein Ire1 in a Parkinson's disease mouse model**
Position: Master student. Supervisor: Dr. Christian Hansen, Molecular Neurobiology research group, Lund University, Sweden.
- Induced an Ire1 knockout in a Parkinson's disease mouse model via the Cre-Lox method
- Used the behavioral tests open field assay and rotarod to investigate the effects of the Ire1 knockout on motor symptoms

2015 **Comparing oxidative stress levels in the plasma of migrating and non-migrating blackbirds**
Position: Bachelor student. Supervisor: Dr. Caroline Isaksson, Laboratory of Evolutionary Ecology, Lund University, Sweden.

- Used the Ferric reducing antioxidant power (FRAP) assay to measure the overall non-enzymatic antioxidant potential of the plasma
- Analyzed the level of the oxidative stress marker malondialdehyde through coupled gas chromatography and electron ionization mass spectrometry

EDUCATION

2017-ongoing Doctoral Assistant specializing in neuroscience, École Polytechnique Fédérale de Lausanne, Switzerland
- Including being a teaching assistant for bachelor and master students

2015-2017 Master of Science in Molecular Biology, Lund University, Sweden

2012-2015 Bachelor of Science in Molecular Biology, Lund University, Sweden
- One year of exchange studies at University of California, Los Angeles, USA (major: neuroscience)

TECHNICAL SKILLS

Laboratory techniques: Molecular cloning, *in vivo* mouse experiments (including intracerebroventricular injection, behavioral studies, dissection) *in vivo Drosophila melanogaster* experiments (fly pushing and genetics, dissection, behavioral experiments), cell culture, immunohistochemistry.

Informatics: Adobe InDesign, Zotero, ImageJ.

PROFESSIONAL CERTIFICATES

- Laboratory Animal Science for Researchers course, Lund University, 2016 (practical and theoretical course for experimental work with mice)

- Réseau des animaleries lémaniques – RESAL, Université de Lausanne, 2018 (a practical and theoretical course in certifying for experimental work with mice according to the Swiss guidelines)

- Introduction to Python: Absolute beginner and Introduction to Python: Fundamentals

PUBLICATIONS

- Rochat, C. Bernard-Marissal, N**., Källstig, E**., Pradervand, S., Perrin, FE., Aebischer, P., Raoul, C., Schneider, BL. 2022. Astrocyte-targeting RNA interference against mutated superoxide dismutase 1 induces motoneuron plasticity and protects fast-fatigable motor units in a mouse model of amyotrophic lateral sclerosis. Glia 70(5).

- **Källstig, E.**, McCabe BD., Schneider BL. 2021. The Links between ALS and NF-kappaB. Int. J. Mol. Sci. 22(8), 3875.

- Laversenne, V., Nazeeruddin, S., **Källstig, E**., Colin, P., Voize, C., Schneider, BL. 2020. Anti-Aβ antibodies bound to neuritic plaques enhance microglia activity and mitigate tau pathology. Acta Neuropathologica Communications 8 (1).

- Aprile, F., **Källstig, E.**, Limorenko, G., Vendruscolo, M., Ron, D., Hansen, C. 2017. The molecular chaperones DNAJB6 and Hsp70 cooperate to suppress α-synuclein aggregation. Scientific reports 7 (9039).

- Eikenaar, C., **Källstig, E.**, Andersson, M., Herrera-Dueñas, A., Isaksson, C. 2017. Oxidative Challenges of Avian Migration: A Comparative Field Study on a Partial Migrant. Physiological and Biochemical Zoology 90 (2).